1975

Properties Of Lung Surfactant And Its Interaction With Bronchographic Agents

Friedrich Samuel Schuerch

PROPERTIES OF LUNG SURFACTANT AND ITS INTERACTION WITH BRONCHOGRAPHIC AGENTS

by

Friedrich Samuel Schürch
Department of Biophysics

Submitted in partial fulfillment
of the requirements for the degree of
Doctor of Philosophy

Faculty of Graduate Studies
The University of Western Ontario
London, Ontario
January, 1975

ABSTRACT

Interaction of bronchographic agents with lung surfactant was investigated to determine if the signs and symptoms of atelectasis known to develop in patients post bronchogram within minutes of the introduction of the contrast material were due to interference of these agents with the surfactant.

Two indirect methods were used: a) Surface tray experiments with extracts of lung surfactant, and b) an investigation of pressure-volume characteristics of excised rabbit lungs before and after bronchography.

For the surface tray experiments, a system of reference had to be developed. Properties of films from lung lavage, from fractionated foam, and finally from synthetic dipalmitoyl phosphatidyl choline (DPPC) were studied at the air-liquid interface. The minimum surface tensions of lung surfactant films were found to be dependent on cycling speed and temperature. At 37°C, minimum surface tensions below 5 mN/m could be produced only by increasing the speed closer to physiological frequencies, e.g. 8 cycles/minute. Results from fractionated surfactant foam were more consistent than the ones from fluid from lung lavage.

Experiments with mixtures of synthetic DPPC and unsaturated phosphatidyl cholines demonstrated that the ratio of saturated to unsaturated PC determined the minimum surface tension for a given cycling speed and temperature.

Hysteresis loops of lung surfactant show a plateau between 22 and 25 mN/m. Plateaux could be reproduced by mixed films from synthetic DPPC and other phospholipids (unsaturated PC or saturated PG). The plateau level of mixed films was dependent on the mixing ratio. The bigger the ratio of DPPC to unsaturated PC or PG (saturated), the lower were the plateau level and the minimum surface tension.

The conclusion was that surfactant plateaux are due to separation of components and squeezing out of molecules other than saturated PC. Minimum surface tensions of lung surfactant films below the plateau level are very likely due to saturated PC.

The bronchographic agents Dionosil Oily and Aqueous, Hytrast and tantalum powder were investigated for their interaction with lung surfactant. The effects of particles and of peanut oil, the suspension medium in Dionosil Oily, were studied separately. If particles or peanut oil were added to surfactant or DPPC films, the surface properties were altered. Particles or peanut oil prevent the surface

tension from reaching relatively low values. The range from near zero surface tension up to the plateau level (22 - 25 mN/m) was the most affected.

Dionosil Oily and peanut oil entered the alveoli readily. Microatelectasis in sections of the lung was related to the presence of Dionosil Oily or peanut oil. Characteristics of pressure-volume diagrams of excised lungs were significantly altered by Dionosil Oily or peanut oil.

Dionosil Aqueous, Hytrast and tantalum powder could generally not be found in histological sections. However, Dionosil Aqueous and Hytrast seemed to obstruct the airways.

The final conclusion is that Dionosil Oily reduces the surface activity of lung surfactant in situ. There is strong evidence that the suspension medium, peanut oil, is responsible for the interaction with surfactant, although an effect of particles cannot be excluded.

ACKNOWLEDGEMENTS

I wish to express my gratitude to Dr. Margot P. Roach for her generous help and advice throughout the course of this work. Many thanks are due to Dr. Fred Possmayer for his invaluable help in biochemistry. He willingly provided laboratory space and gave impetus to various aspects of this thesis.

I extend my appreciation to those who enhanced the progress of this work in many ways, especially to the people of the Biophysics Department. I would like to mention by name Mrs. Dorothy Elston and Mr. Livio Rigutto for their kind assistance with technical problems and Mrs. Vera Jordan for her encouraging greetings in the early hours of the morning. I am greatful to Dr. L. N. Johnson for use of his instruments and Mr. Christian Rupp for technical assistance.

Mrs. Eleonore Swann prepared the histological sections, Mr. Bill Rigg built some of the apparatus. Mrs. Susan Bright, Mr. Patrick Shum and Mr. Ken Bocking worked as summer students on related projects. Many thanks to all these persons.

Nicht zuletzt möchte ich meiner Frau Ruth ganz herzlich danken für die lange Geduldsprobe und das sorgfältige Ausführen der Schreibarbeiten.

Samuel Schürch

Department of Biophysics,
The University of Western Ontario
January 31, 1975

This work was supported in part by the James Picker Foundation on the recommendation of the Committee on Radiology NAS-NRC, and by the Ontario Thoracic Society.

The author wishes to express his indebtedness to these organizations.

TABLE OF CONTENTS

LIST OF FIGURES

LIST OF TABLES

LIST OF APPENDICES

PREFACE

The objective of this thesis is to determine the effect of various bronchographic agents on lung surfactant.

In the first part, films of lung alveolar surfactant and related synthetic phospholipids are studied. The influence of cycling speed and temperature on hysteresis loops and the hysteresis effect itself are investigated. Various methods of preparation of the extracted surfactant and its composition are discussed.

In part two, interactions of lung alveolar surfactant and contrast media used in bronchography, are studied. The influence of the contrast media was examined by surface tray experiments and by pressure-volume tests on excised rabbit lungs. Finally, the relationship of the two approaches are compared.

PART I

PROPERTIES OF LUNG ALVEOLAR SURFACTANT AND RELATED SYNTHETIC COMPONENTS AT THE AIR-LIQUID INTERFACE

CHAPTER 1

LUNG ALVEOLAR SURFACTANT - HISTORICAL BACKGROUND

1.1 Terminology

We have adopted the terminology used in Scarpelli's book: "The Surfactant System of the Lung" (1968).

The alveolar lining layer is an acellular lining layer and covers the surface of the epithelial cells of the alveoli as a continuous film. The major part of the lining layer is some 5 to 20 nm thick, but it can reach 1 to 3 μm where deep clefts must be smoothed out or where a macrophage is present. The uppermost part, facing the air, is about 2 to 3 nm thick and is called the surface film of the lining layer (Weibel, 1970/1971, p. 56). The surface film consists of surface active molecules (surfactants).

The hypophase is the "bulk" phase of the lining layer below the surface film.

The surfactant system of the lung consists of the chemical constituents of the lining layer.

The surfactant is used synonymously with "the surfactant system of the lung".

1.2 Physiology

In 1929, Karl von Neergaard observed differences in the pressure-volume characteristics of isolated air-filled lungs as compared to fluid-filled lungs. He concluded there must be an alveolar coating with a surface tension lower than that of other physiological fluids. Von Neergaard's work received little attention until Pattle (1955) discovered the extraordinary stability of bubbles from lung foam. He suggested that the lining films of pulmonary bubbles came from the alveolar surface directly, and therefore, their physical properties represented the characteristics of the alveolar lining film in situ. Pattle concluded that the stability of the bubbles obtained from extracts of normal lungs is a function of the near zero surface tension produced by potent surface active agents in the lining layer.

Clements (1957) pioneered surface tray studies to test the surface activity of material from the alveolar lining layer. He found that periodically compressed and expanded films showed variable surface tension with the lowest value about 10 mN/m at 20% film area. His studies demonstrated also that the compression and expansion part of the surface tension area characteristics showed a "hysteresis effect". Clements and his co-workers (1958, 1961, 1962) formulated a theory about alveolar stability on the basis of their surface tray model studies. The assumptions were that the alveolar surface is analogous

to the surface of the liquid extract and that the alveolar surface area changes directly with the alveolar volume. The stability theory states that as the area decreases during deflation of the lung, the surface tension falls toward zero.

1.3 Chemistry and organization

Since the early experiments by Pattle and Clements, the main question has been: are the pulmonary surfactants lipoproteins or phospholipids? Pattle (1965) concluded from his investigations and those by Klaus et al. (1961) that surfactant is a lipoprotein, rich in phospholipid. In several papers, such as these of Abrams (1966) and Galdston et al. (1969), the isolation of a specific lipoprotein was reported. This view was challenged in several papers by Scarpelli and his co-workers, e.g. Scarpelli et al. (1967), Scarpelli et al. (1970). Scarpelli does not deny that proteins are present in the hypophase, but states that all the surface activity is in a purified lipid fraction.

In the last few years attention has been given to possible contamination from the blood. Protein found in alveolar washings was attributed to leakage from the blood system. Hurst et al. (1973), Reifenrath et al. (1973a).

Briefly, there is no definite answer yet for the question "what is surfactant". However, there is wide agreement that the surface activity of the surfactant

resides in the phospholipids, mainly in saturated dipalmitoyl phosphatidyl choline.

In recent papers, some associations of lipid and protein are discussed. Frosolone et al. (1970), King et al. (1972), II., Colacicco et al. (1973).

Surfactant may exist as relatively large lipid-protein particles, about the size of mitochondria. They would function as a surface store and periodically release the phospholipid fraction required for the film of the interface.

CHAPTER 2

OUTLINE OF THE PROBLEMS

2.1 Dynamic properties of lung surfactant films

The characteristics of normal surfactant were defined from the work of Clements and his group (1958, 1961, 1962). If preparations of surfactant are placed on a surface tray and the films periodically compressed and expanded, a minimum surface tension below 10 to 15 mN/m should develop at about 20% film area. The curves show a typical hysteresis effect. (For the preparation methods, see Scarpelli, 1968, pp. 54-76). These criteria have been used in many studies. However, the experiments were usually done at room temperature and at cycling speeds far below physiological frequencies.

In order to have a reliable reference system, the influence of temperature, speed and lecithin content on the minumum surface tension was investigated.

We found that characteristics of hysteresis loops are very dependent on the way the lung extracts are treated prior to the surface tray experiments. Therefore, preparation methods had to be developed and standardized.

2.2 Properties of films from synthetic dipalmitoyl phosphatidyl choline (DPPC)

According to the literature, mainly phospholipids are responsible for the surface activity of the alveolar lining layer. The most important factor is saturated DPPC. However, there is a controversy about the ability of DPPC films to produce surface tensions below about 5 mN/m at 37°C, and about the behaviour on repeated cycling. The structure of these films at near zero surface tension and the mechanism responsible for the hysteresis effect are not well understood.

2.3 Stability of phospholipid films

Factors which interfere with film stability were investigated. Is it unsaturation in the carbohydrate chains or is it the chain length itself? There is also a controversy about the influence of protein on the stability and reproducibility of phospholipid films.

2.4 Plateau of lung alveolar surfactant hysteresis loops

Surface tension area characteristics of surfactant films demonstrate a typical plateau at about 23 to 25 mN/m. We will show that the characteristics of this plateau can be reproduced by mixed films from phospholipids.

CHAPTER 3

SURFACE FILMS

3.1 Introduction

The boundary region between two adjacent bulk phases is called an "interface". When one of the phases is a gas or a vapour, the term "surface" is commonly used. Here we are interested in the liquid-gas interface.

3.2 Surface tension and surface energy

Consider a drop of a liquid in equilibrium with its vapour in the absence of external forces. The drop spontaneously takes the form of a sphere, the shape with the minimum surface to volume ratio. In order to increase the surface area of the drop, work has to be done. Therefore, it can be seen that the surface molecules are in a state of higher potential energy than the molecules in the bulk phase. This is explained in part by the fact that surface molecules have fewer nearest neighbours, and consequently fewer intermolecular interactions than bulk molecules.

There is a free energy change associated with an isothermal, reversible formation of a liquid surface. The presence of unbalanced forces acting on the surface molecules leads to the concept of surface tension. For a plane interface, surface tension is defined as the

force acting parallel to the surface perpendicular to a line of unit length anywhere in the surface.

3.3 Thermodynamic treatment of a surface

In a real system, there is a finite distance across an interface. The properties gradually change from those of one adjacent bulk phase to those of the other. One way of treating a surface is to consider it as a phase which is distinct from the bulk phases and which has a finite thickness and volume. This treatment was developed by Guggenheim (1933), pp. 160-181. A short description of Guggenheim's method can be found in Adam (1968), pp. 404-409.

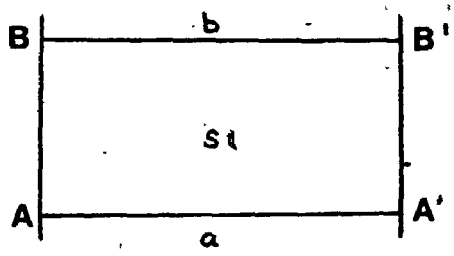

In the figure above, the regions a and b are homogeneous bulk phases, separated by the surface phase s. All changes in properties from a to b take place in the region between AA' and BB'. In Guggenheim's concept, the surface

phase is a definite region of matter, with its own volume, entropy, energy and other properties. For the Gibbs' treatment, see Adam (1968), pp. 106-113.

Here, we will adopt Guggenheim's concept. Properties concerning the surface phase alone will be denoted by a superscript s. The work done by the system in increasing the volume in one of the bulk phases by dV is pdV where p is the pressure in that bulk phase. The work done by increasing the volume of the surface phase by dV^s and its area by dA, is:

$$pdV^s - \gamma dA$$

where γ is the surface tension.

3.4. Thermodynamic functions for the surface phase

If E^s = total internal energy of the surface phase for an area A,

S^s = entropy of the surface phase,

N_i^s = number of moles (or molecules) of species i in the surface phase

A = surface area

μ_i = chemical potential of species i in the surface phase, then

dE^s will be:

$$dE^s = TdS^s + \gamma dA - pdV^s + \sum_i \mu_i \, dN_i^s \qquad (3.1)$$

N.B.: In thermodynamic equilibrium, the chemical potentials of the two bulk phases and the surface phase are equal: $\mu^a = \mu^b = \mu^s$,

this explains the missing index s on μ_i.

3.5 Thermodynamic equilibrium

For a closed system, the entropy assumes a maximum. Since experiments are usually not done in isolated systems, rather at constant pressure and constant temperature, or at constant volume and temperature, the thermodynamic equilibrium is characterized by extreme values of the following functions:

3.5.1 The Helmholtz free energy (F)

Definition: $F = E - TS$ (3.2)

where E = internal energy,

S = entropy,

T = absolute temperature.

$dF = dE - d(TS)$ and with (3.1), for the surface phase follows:

$$dF^S = \gamma dA - pdV^S - S^S dT + \sum_i \mu_i dN_i^S \qquad (3.3)$$

F^S is a function of A, V^S, T, N_i^S.

If these quantities are given, the condition for equilibrium is:

$dF^S = 0$, and F^S becomes a minimum.

From (3.3) we see that the surface tension is now defined as:

$$\gamma = \left(\frac{\partial F^S}{\partial A}\right), \quad (V^S, T, N_i^S \text{ are constant}) \qquad (3.4)$$

Therefore, the surface tension is the Helmholtz free energy per unit area, at constant T, V^S, N_i^S. If we have adsorption of molecules at the interface, the N_i^S are no longer constant and (3.4) does not hold.

3.5.2 The Gibbs' free energy, or the free enthalpy (G)

Definition: $G = E + pV - TS$ (3.5)

$dG = dE + d(pV) - d(TS)$

with (3.1) and for the surface phase:

$$dG^S = \gamma dA + V^S dp - S^S dT + \sum_i \mu_i dN_i^S \quad (3.6)$$

G^S is a function of A, p, T, N_i^S.

If these quantities are given, the condition for equilibrium is:

$dG^S = 0$, and G^S becomes a minimum.

The definition of the surface tension follows from (3.6):

$$\gamma = \left(\frac{\partial G^S}{\partial A}\right), \text{ (p, T, } N_i^S \text{ are constant)} \quad (3.7)$$

Therefore, the surface tension can be defined as well as the Gibbs' free energy per unit area, at constant T, p, N_i^S. Both definitions are suitable for our experimental set-up, since we work at constant temperature and constant pressure. In the case of an insoluble monolayer, V^S and N_i^S are assumed to be constant.

3.6 Properties of insoluble monolayers

3.6.1 Substances which form an insoluble monolayer

A substance with a proper polar group, called "hydrophilic" and a relatively large nonpolar portion, called "hydrophobic" can form a monolayer on water. This type of molecule is also called "amphiphilic". The polar group favours solubility in water, the hydrophobic carbohydrate chains prevent it. The balance between them determines whether a molecule will form an insoluble

monolayer. See Gaines (1966), p. 136 for details.

3.6.2 State of a monolayer

In three dimensions, substances can be gaseous, liquid or solid. In a monolayer, the different degrees of molecular interactions between the surface molecules and the subphase can result in several more distinct phases, which have no analogue in three dimensions.

Figure 1 shows a surface pressure-area diagram with the main possible states. We are using the terminology introduced by Adam (1968), pp. 39-70. A good description can also be found in Gaines (1966), pp. 156-188.

a) The gaseous state is characterized by negligible interaction between the molecules, and is realized only for relatively large areas per molecule, from several hundred $Å^2$/molecule up to several thousand $Å^2$/molecule. The hydrocarbon tails are in random motion and may be in contact with the water. This state can be described by the ideal gas equation in two dimensions:

$$\pi A = \kappa T \qquad (3.1)$$

where π = surface pressure (mN/m)

A = area per molecule (m^2/molecule)

κ = 1.3805×10^{-23} Joule/degree

T = absolute temperature

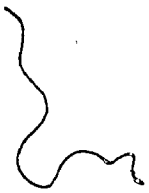

Figure 1: States of a monolayer

(for details see text)

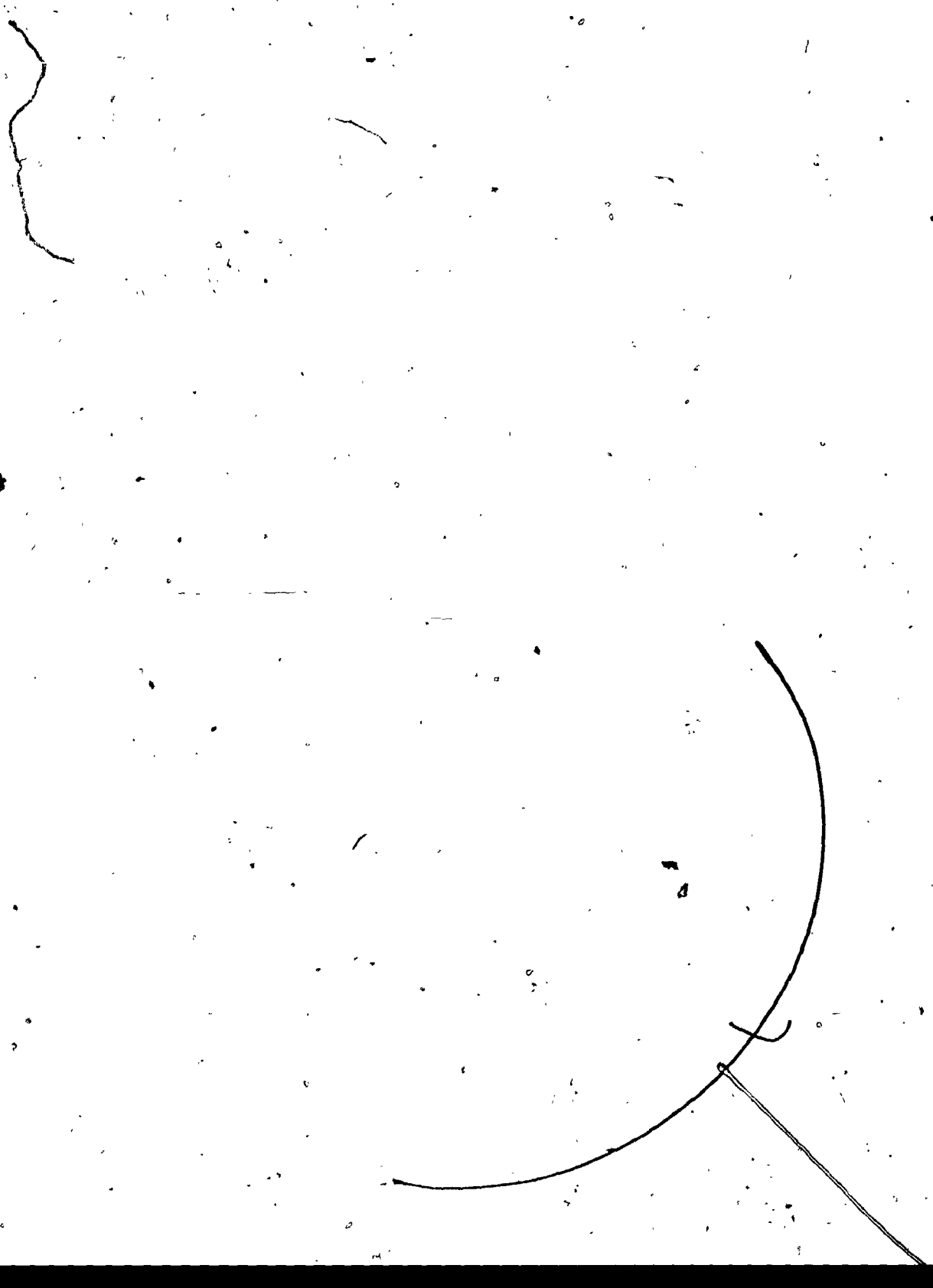

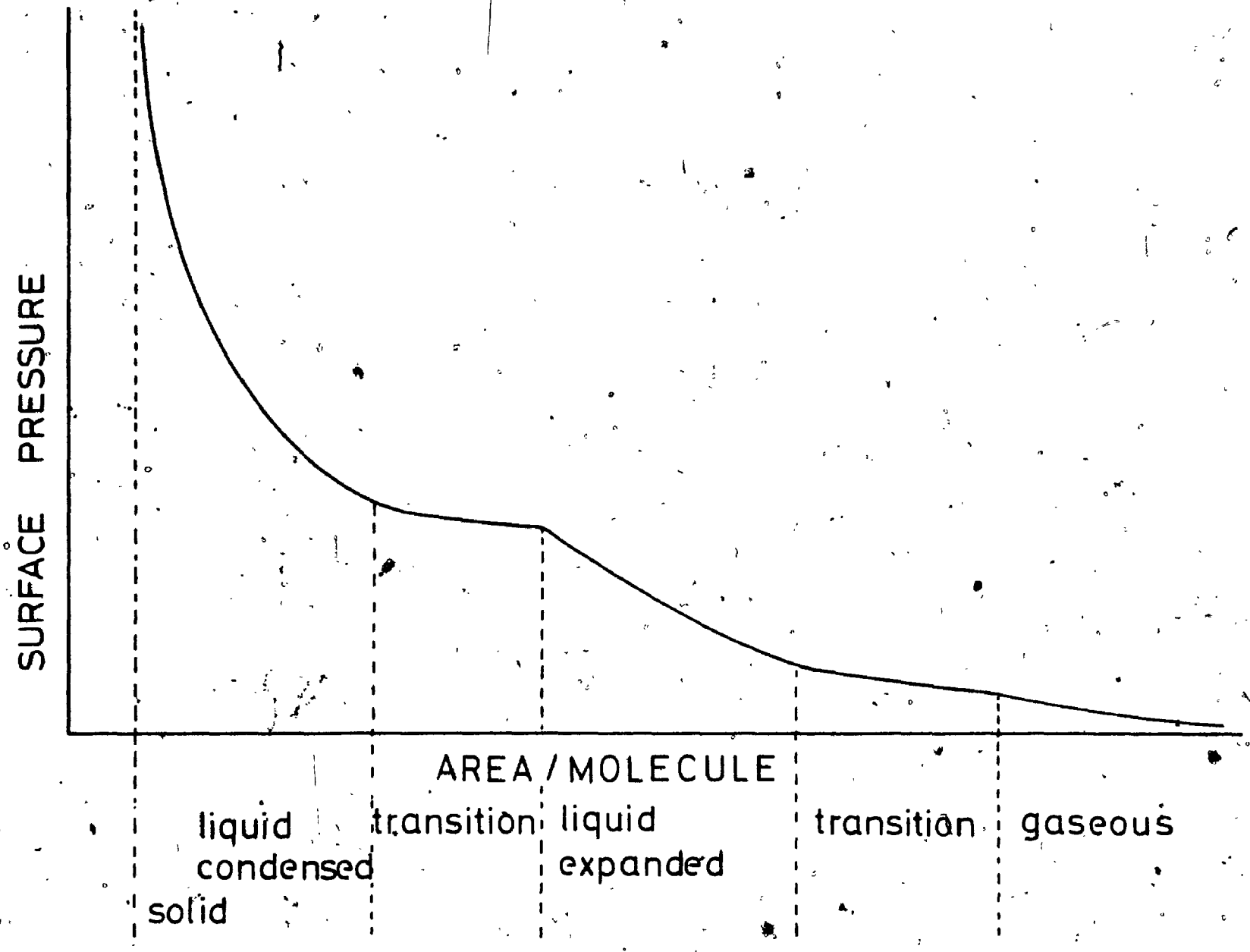
SURFACE PRESSURE
AREA / MOLECULE
solid
liquid condensed
transition
liquid expanded
transition
gaseous

b) At higher compression a transition occurs into the liquid expanded state. The chains are still in random motion but they are progressively lifted from the surface. The area per molecule, for a molecule with two hydrocarbon tails may be about 100 $Å^2$.

c) At still higher compressions, the side chains are more and more vertically oriented. The hydrophilic end groups are closely packed but possibly still hydrated. This state is called liquid condensed.

d) On further increase in pressure, the water molecules between the polar heads are squeezed out and the hydrocarbon chains are organized parallel to each other and most closely packed. This state is called condensed or solid.

Once the limiting area per molecule is obtained, further compression will change the monolayer into a three dimensional structure and the monolayer collapses. Several proposals for the description for the liquid expanded state can be found in the literature. They are of the Van der Waal's type. However, a detailed quantitative interpretation has not yet been achieved. See Gaines (1966), pp. 167-172.

3.6.3 Quantities used in monolayer studies

See Gaines (1966), pp. 140-156.

"Equilibrium spreading pressure" is the pressure, where the monolayer is in thermodynamic equilibrium with the stable bulk phases. If spread with a solvent, after evaporation, the monolayer is not necessarily in equilibrium, and may be called metastable.

Collapse pressure is the highest pressure to which a monolayer can be compressed without detectable expulsion of molecules to form a new phase.

Area of final collapse is the absolute minimum area into which the molecules can be crowded. We will use this area synonymously with the "limiting area of the molecule" in the monolayer.

Since the aim is to investigate dynamic properties of periodically compressed and expanded films, our monolayer systems will not be in the thermodynamic equilibrium. However, we will define a "quasi equilibrium state".

3.6.4 The surface pressure π

In monolayer experiments, the film is usually confined by a moveable barrier on one side and by the surface tray on the other sides. The barrier functions as the semipermeable membrane of the three dimensional analogue to osmotic pressure (Adam, 1968, p. 22).

As already pointed out in 3.5, for an insoluble monolayer, either the Helmholtz free energy or the Gibbs'

free energy are suitable to define the surface tension.

The change of the Helmholtz free energy for the surface phase with film forming molecules and water molecules is:

$$dF_f^s = -S_f^s\,dT + \gamma dA + \mu_f dN_f + \mu_w dN_w \qquad (3.2)$$

where: "s" = surface phase

"f" = film

"w" = water in the surface with film molecules

For the surface phase with water alone we have:

$$dF_o^s = -S_o^s\,dT + \gamma_o dA + \mu_o dN_o . \qquad (3.3)$$

where: "o" = water surface only, and

μ_o = μ_w for equilibrium.

By subtraction of equation (3.3) from equation (3.2), we get:

$$dF_f^s - dF_o^s = (S_o^s - S_f^s)dT + (\gamma - \gamma_o)dA + \mu_f dN_f + \mu_w(dN_w - dN_o)$$

With $dF_f^s - dF_o^s = dF_f$

$S_o^s - S_f^s = S_f$

$\gamma_o - \gamma_f = \pi$ (surface pressure)

The Helmholtz free energy change for the film is then:

$$dF_f = -S_f dT - \pi dA + \mu_f dN_f + \mu_w(dN_w - dN_o)$$

For an insoluble monolayer dN_f, dN_w and dN_o are assumed to be negligible. Thus we can write:

$$dF_f = -S_f dT - \pi dA \qquad (3.4)$$

For references see Becker (1964), pp. 50-57, Guggenheim (1933), pp. 160-181, Motomura (1967).

3.7 Surface potential

The potential difference between a point in the bulk of a solution and a point in the bulk gaseous phase above the solution is modified by the presence of a monomolecular layer at the surface. The potential difference due to this modification relative to the potential difference across the "clean" surface is called the surface potential of the monolayer ΔV, (Gaines, 1966, p. 18).

3.7.1 The surface volta potential χ^s

χ^s originates from the presence of oriented dipoles in a surface phase. Two contributions are to be considered:

a) χ_1^s: due to polarized atoms or molecules (molecular dipoles)

b) χ_2^s: due to dipoles formed by segregation of particles e.g. ions, of opposite charge in a direction normal to the surface (ionic double layer).

$$\chi^s = \chi_1^s + \chi_2^s \qquad (3.6)$$

The first term, χ_1^s, is usually related to the following model: An array of surface dipoles is equivalent to the two plates of a charged capacitor. The two plates are separated by the distance d, normal to the surface, between the two charges of the dipole.

The potential difference across a parallel plate capacitor with charge Q, the area of a plate A, and the distance between the plates d, is:

$$U = \frac{1}{\varepsilon} \frac{Qd}{A} \qquad (3.7)$$

where ε is the permittivity of the medium. In a vacuum, $\varepsilon = \varepsilon_o$, the vacuum permittivity. (For an alternate model see Appendix II).

We put $Q = mq$, where m = number of charges, and q = a unit charge. Then we substitute $a\cos\theta$ for d, where a = distance between the two charges of the dipole and θ is the angle between the dipole axis and the normal to the plane. The potential difference becomes:

$$U = \frac{1}{\varepsilon} \frac{mq}{A} a\cos\theta = \chi_1^s$$

where $qa\cos\theta = p_n$ = normal component of the dipole moment. The potential difference due to the dipole layer is then:

$$\chi_1^s = \frac{1}{\varepsilon} N p_n \qquad (3.8)$$

with ε = permittivity of the medium (C/Vm)

N = m/A, number of dipoles per unit area ($1/m^2$)

p_n = $p\cos\theta$, normal component of the dipole moment (Cm)

3.7.2 Surface potential of an insoluble monolayer

Changes in the molecular dipole potential χ_1^s can be measured, provided the ionic double layer potential χ_2^s remains constant. The surface potential is then defined as

$$\Delta V = \frac{1}{\epsilon} \Delta(Np_n) \qquad (3.9)$$

This equation is commonly used to interpret surface potentials produced by spreading of insoluble monolayers at the air-water interface. Generally, both the ionic double layer and the molecular dipole potentials will contribute to the total potential difference across an interface, and the assumption of χ_1^s and χ_2^s being independent is an oversimplification. For further reading and comments see Gaines (1966), pp. 188-192 and Aveyard et al. (1973), pp. 31-57.

In this study, we measured the surface potential of dipalmitoyl phosphatidyl choline, a zwitterionic molecule. Colacicco (1971) points out that this molecule is a neutral phospholipid between pH 4 and 9. The assumption of independence of χ_1^s and χ_2^s might therefore be justified.

In (3.8), ϵ is usually taken as ϵ_o, the vacuum permittivity.

3.8 Surface tension - area measurements

3.8.1 The Langmuir-Wilhelmy method

This method was used to record surface tension as a function of periodically compressed and expanded films. Description of the set-up can be found in any book about experimental surface chemistry.

3.8.2 Apparatus

We used:

1. The *Cahn dynamic surface tension accessory
2. The Cahn electrobalance RTL
3. A Hewlett Packard X-Y recorder, Model 7005B

Ten cycling speeds can be chosen, according to the gear position, between 1/12 cycle/min and 12 cycles/min. The speed - time characteristic is approximately sinusoidal. The maximum area between the teflon blades was 50.0 cm^2, the minimum area 12.5 cm^2, corresponding to 100% and 25% relative area. The accuracy of the reading of the surface tension was better than $\pm$ 1 mN/m.

3.8.3 Constant temperature bath

Water from a constant temperature bath could be circulated around the trough, which was immersed in water. Stabilization of the temperature of the liquid content of the trough was better than $\pm$ 0.5°C.

3.8.4 The sensor

A platinum plate of 1 cm width and approximately 6 µm thickness was used. It was mounted and adjusted to touch the liquid surface. Buoyancy effects could be neglected. The platinum plate was cleaned frequently with 20% chromic acid and flamed thoroughly prior to each experiment.

*Cahn Division, Ventron Instruments Corp., Jefferson St., Paramount, California 90723

On repeated cycling, expecially in the expansion part, the platinum plate produced wrong readings (see Appendix IX). This was particularly true for films from synthetic phospholipids, but not for lung surfactant. Continuous loops from phospholipid monolayers were recorded with a strip of filter paper as sensor. The output signal was calibrated with the platinum plate.

3.8.5 The teflon trough

The trough had to be cleaned very carefully prior to each experiment by rubbing with a solution of detergent (Fisher Sparkleen), followed by 20% chromic acid. The tray was then rinsed with running tap water, then with methanol and finally with light petroleum which dried quickly. Cleaning of the trough proved to be the biggest single problem since contamination had to be avoided.

3.8.6 Leakage

Leakage between the teflon wipers and the wall of the trough was a very serious problem, especially at relatively low cycling speeds, below 2 cycles/min and at temperatures above 30°C. The original Cahn surface tray set-up had to be modified.

3.8.7 Modification: the rhombic trough

Four metal plates were connected by hinges. Metal pins, coated with teflon tubing were put through the hinges in order to support an endless teflon ribbon. The

Figure 2a:

1. Electrometer
2. Electrobalance
3. Surface tray
4. X-Y recorders
5. Constant temperature bath

Figure 2b:

1. Ionizing air electrode
2. Rhombus-shaped barrier
3. Surface tension sensor (platinum)
4. Electrobalance

123 -(2)


4

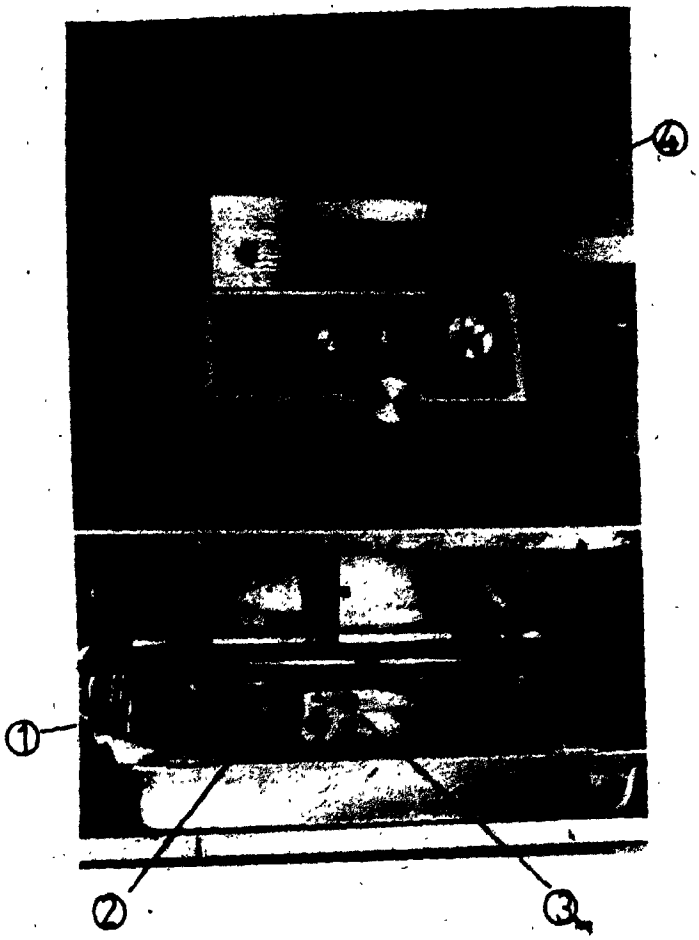
4
1
2
3

teflon ribbon was made from plumbing tape and the ends were "welded" together with hot tweezers. The ribbon was replaced after each experiment with surfactant or protein.

Two different rhombic frames were made, the larger one at 15 cm side length was used for the lipid monolayer studies. The alveolar surfactant experiments were done with the smaller one, of 7 cm side length. Pyrex glass trays were chosen according to the size of the rhombic frames. Cleaning of the modified apparatus was no problem with chromic acid. With the rhombus-shaped trough, leaks were eliminated completely. However, there was the disadvantage of a nonlinear change of the area (Appendix I). Some of the experiments at higher cycling speeds (above about 2 cycles/min) could still be done with the old system. But the results were compared and checked with those from the modified apparatus.

3.9 Surface potential measurements

3.9.1. Method

The air gap above the film was ionized with a gold plated electrode. The α-source, *Americium 241, of a total activity of 20 microcuries, is built into the head of the air electrode. The resistance of the air gap (about 0.5 cm) was approximately 10^{10} Ohms. The electrode in the subphase was a silver wire coated with silver chloride. The circuit

*Americium 241, sealed source for surface tension studies Model A 1011. Nuclear Radiation Developments, 360 Eddystone Ave., Downsview, Ontario.

is shown schematically below:

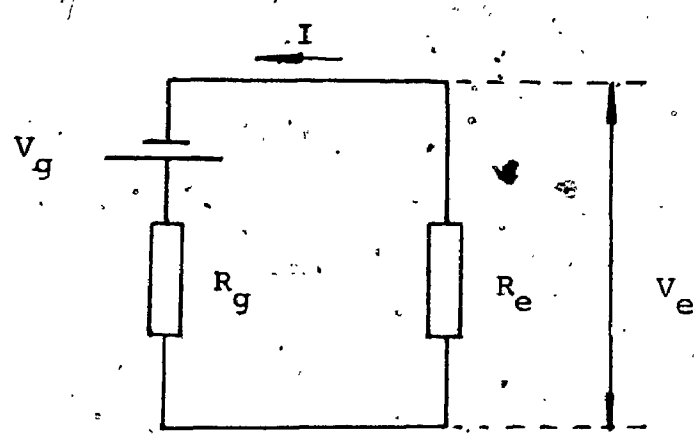

V_g: Potential difference between the air electrode, Am 241, and the subphase Ag-AgCl electrode

R_g: Gap resistance

R_e: Input impedance of the electrometer

V_e: Voltage recorded

Applying Kirchhoff's law:

$$V_g - R_g I - R_e I = 0$$

$$V_g = I(R_g + R_e)$$

If $R_g \ll R_e$, then $V_g \simeq IR_e = V_e$

If R_g, the gap resistance, is much smaller than the input impedance, R_e, of the electrometer, then we have:

$V_g \simeq V_e$. In our case: $R_g \simeq 10^{10}$ Ohms

$R_e \simeq 10^{14}$ Ohms

The electrometer was a *Corning Model 101 digital instrument with an analogue output for the X-Y recorder and an input impedance greater than 10^{14} Ohms.

3.9.2 Stability of the baseline potential

The surface potential of the subphase solution (baseline potential) was an excellent test for contamination. The slightest contamination of the 0.9% NaCl solution produced a relatively large increase of the baseline potential, even if the surface tension stayed constant. The surface was considered "clean" if the baseline potential changed less than 10 mV for reduction of the surface area to 25%. The drift of the baseline potential could be avoided by properly "aging" the air electrode. Prior to the spreading of the film, the electrode was mounted above the NaCl solution and left for at least three hours. The surface was then swept with filterpaper and test runs were recorded for stability of the baseline potential. Only after all of these precautionary measures, the monolayers were spread.

*Corning Glass Works, Laboratory Products Dept., Scientific Instruments, Medfield, Mass. 02052, U.S.A.

CHAPTER 4

DYNAMIC PROPERTIES OF LUNG SURFACTANT FILMS RELATED TO PHOSPHOLIPID CONTENT

4.1 Materials and methods

4.1.1 Extraction

White rabbits of 2 to 3.5 kg were anaesthetized with an intraperitoneal injection of 30 to 40 ml of 20% urethane solution. The trachea was then exposed and cannulated and the chest opened. Four gentle lavages, each with 40 ml of 0.9% NaCl solution (pH 6.4 to 7.1), were done. Each volume of saline was injected and withdrawn three times before being collected in an ice-cooled flask. The total lung wash of about 150 to 160 ml was then centrifuged at 800 g and about 3°C for 20 min for sedimentation of the cellular material. The supernatant was the basic material for all surface tray experiments.

4.1.2 Preparation

The surface tray experiments were done with the following preparations:

a) The cell-free material was emptied directly into the trough and aged for at least two hours prior to the experiments. Since the capacity of the teflon trough was about 100 ml, we obtained only one trough filling per

rabbit lavage.

b) The cell-free material was centrifuged at 27,000 g and 3°C for 30 min. The white pellet was dissolved in as little chloroform : methanol (1 : 1, by vol.) as possible, and 100% (by vol.) n-hexane added. The supernatant was then placed into the trough and dissolved material of the white pellet spread on the surface until the surface tension was below 30 mN/m. Spreading had to be done slowly, drop by drop, allowing time for evaporation of the solvents. With this technique, about four surface trays could be prepared from each rabbit lavage.

c) The cell-free material was fractionated in a glass column. Clean air from a steel cylinder passed through the liquid and produced a dense foam. The effect of the fractionation could be observed directly, as the foam on the top of the pipe was very dense and the bubbles appeared to be of uniform size. Foam from lower parts of the column clearly had a less uniform distribution of bubble size. Big bubbles burst before they were able to reach the top of the glass pipe. The stable foam from the top was then collected and saline added to increase the volume about four times. The fractionation was repeated about four to five times. At the end of the process there were two qualities of foam: no. 1, from the top of the column and no. 2, from the lower parts.

Since the foam could not be used directly in the surface tray, because the bubbles would just sit on top of the saline surface, it had to be desiccated at about 37°C. Before the foam was completely dry, a little distilled water which had been boiled previously, was added. The rest of the bubbles disappeared then by diffusion into the airless water. This preparation was then spread drop by drop with a syringe on top of the saline in the surface tray, until the surface tension was below 50 mN/m. Two to four surface trays could be prepared from each rabbit.

4.1.3 The content of phosphatidyl choline (PC)

From the total lung wash of about 150 to 160 ml; 30 to 50 ml were diverted for lipid analysis. The cell-free material was freeze dried; the lipids were then extracted by chloroform : methanol (1 : 1, by vol.), and washed three times with 0.9% saline (2-phase system), in order to remove proteins. The lipids were then spotted on a plate coated with silica gel. (Thin layer chromatography, TLC). A schematic presentation of the method can be found in Appendix III. The phosphorus assay was done according to Rouser et al. (1963).

4.2 Results

4.2.1 Preparation of the surfactant

Hysteresis curves of surfactant prepared according to the methods described in 4.1.2 were examined.

Most of the changes regarding extreme values of surface tension and reproducibility of consecutive curves occurred in the first series of ten loops. The following curves could not be distinguished from each other in most cases. The long term development over a series of a hundred or more curves will be discussed later. Loop no. 10 of the first series was therefore taken as the reference for the influence of the investigated factors.

Results from the preparations according to 4.1.2 a) and b), were comparable with respect to the shape, the reproducibility of the curves and to the extreme values of the surface tension. However, about one third of the lung lavages showed a minimum surface tension of about 20 mN/m at 37°C and 8 cycles/min. This value is considered as too high relative to "normal" values of 15 mN/m and less. Contamination from the blood might have been the reason for relatively high minimum surface tensions.

The top quality foam no. 1 of the third method (4.1.2 c) produced the most reproducible hysteresis loops and minimum surface tensions as low as the "best" preparations of the first two methods. Spreading of the films could be more standardized. Foam suspended in water was spread on the surface until the tension at constant maximum area was about 50 mN/m. After an "aging" time of approximately three hours, the surface tension was usually below 30 mN/m and periodic compression and expansion of

the film was started. The second quality foam, no. 2, demonstrated constantly higher minimum surface tensions and consecutive loops were less reproducible.

4.2.2 Temperature- and speed dependence of cell-free ~~lung alveolar~~ surfactant

The preparation was according to method a) of 4.1.2.

a) Influence of temperature at a constant cycling speed of 2 cycles/min

Figure 3 shows photographs of original tracings. At 23°C, the minimum surface tension of loop no. 10 is below 10 mN/m. At 37°C, the minimum surface tension is approximately 18 mN/m. Both series show a marked plateau at about 23 mN/m.

b) Effect of cycling speed at constant temperature

In Figure 4, at 2 cycles/min, the minimum surface tension is about 15 mN/m, at 8 cycles/min approximately 10 mN/m.

In Tables I and II, the data of fifteen independent experiments are summarized. According to 4.1.2 a), cell-free lung lavage of fifteen rabbits was obtained and for each sample the minimum surface tension of loop no. 10 was determined. Small sampling theory with a paired variate analysis was used to test the statistical significance of the difference between the minimum surface tensions. At a 1% level of significance, with the t-test we conclude:

1. From Table I:

The minimum surface tension at 37°C is significantly higher than at 23°C, for the constant speed of 8 cycles/min.

2. From Table II:

The minimum surface tension at 8 cycles/min is significantly lower than at 2 cycles/min, for 37°C.

4.2.3 Effect of speed on the minimum surface tension of foam fraction 1

The preparation was according to method c) of 4.1. In Table III the data of seven independent experiments are summarized. Unfortunately, the sample size is only about half the size of Tables I and II. But the minimum surface tensions at 2 cycles/min and at 8 cycles/min seem to be considerably lower than for the unfractionated preparations of Tables I and II. Again, there is a significant difference between the minimum surface tensions due to the speed effect (1% level).

4.2.4 Amount of phosphatidyl choline (lecithin) - minimum surface tension. Regression and correlation

For each sample of Table I, the amount of total phosphatidyl choline, m_{pc}, (saturated and unsaturated) was determined. The minimum surface tensions at 8 cycles/min and the corresponding amounts of phosphatidyl choline were then analyzed by linear regression and correlation, at 37°C and 22°C.

For the regression line:

33•(2)

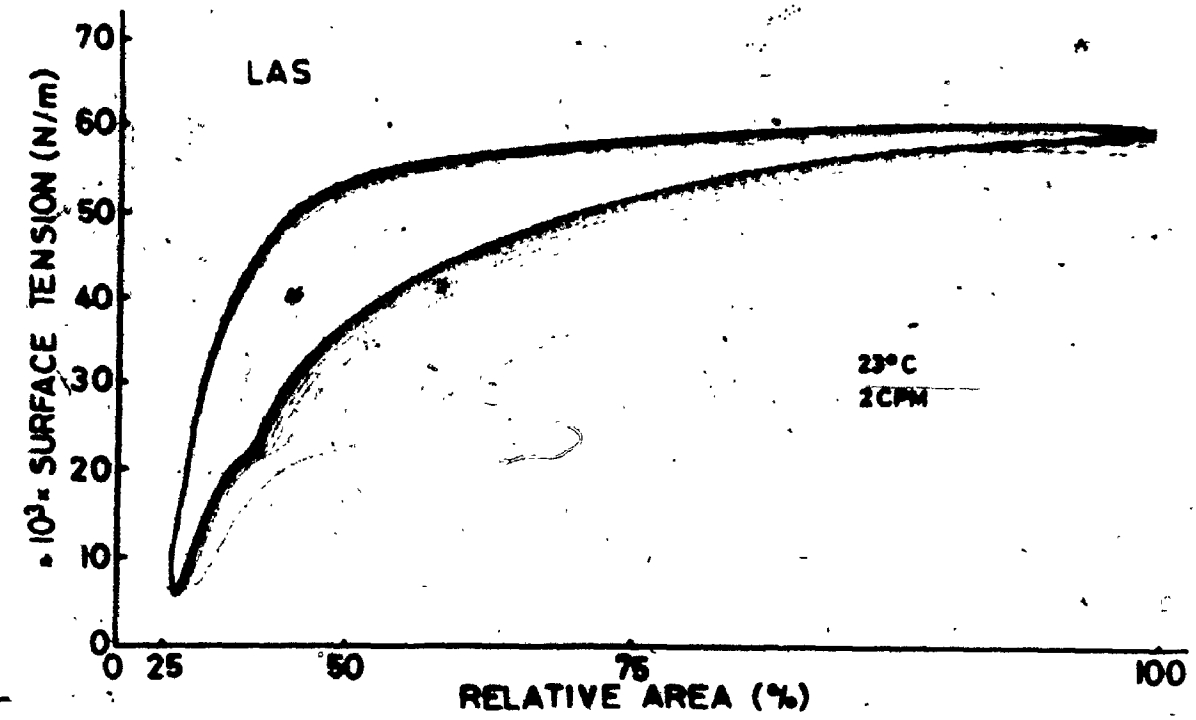
LAS
10^3 × SURFACE TENSION (N/m)
70
60
50
40
30
20
10
0
0
25
50
75
100
RELATIVE AREA (%)
23°C
2CPM

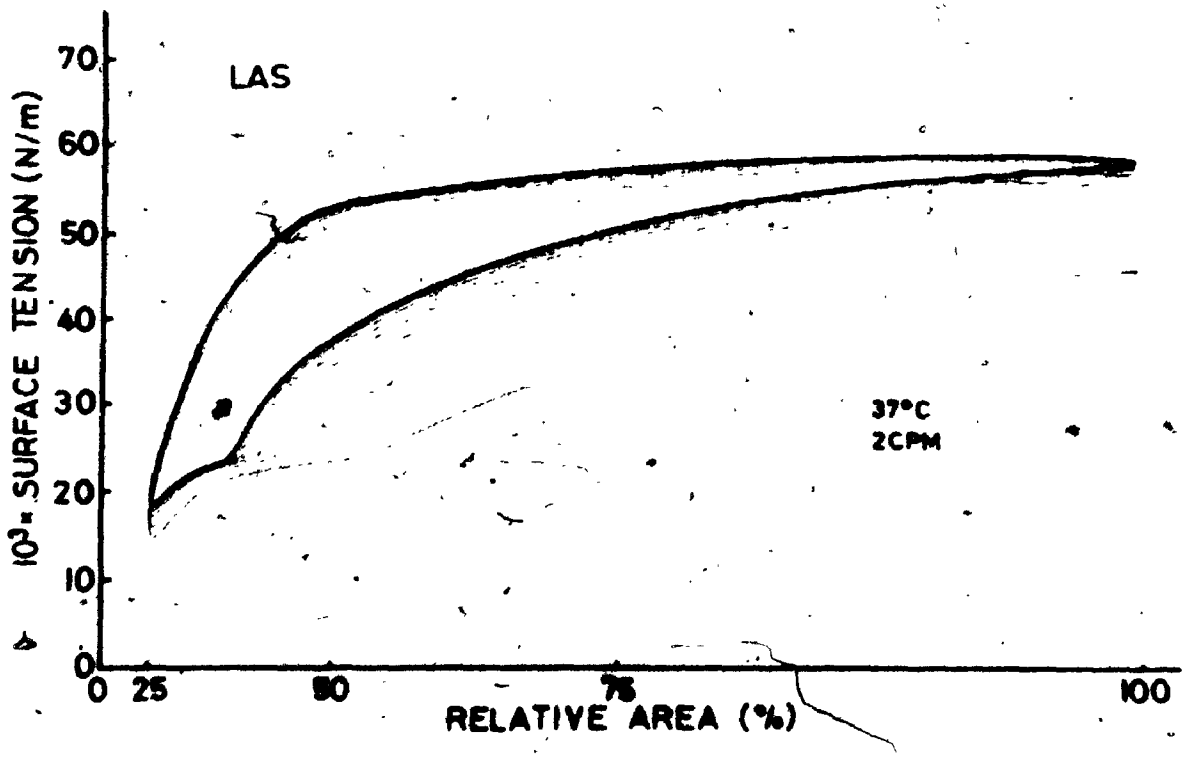
LAS
10^3 × SURFACE TENSION (N/m)
70
60
50
40
30
20
10
0
0
25
50
75
100
RELATIVE AREA (%)
37°C
2CPM

Figure 4: Speed dependence of hysteresis loops from lung alveolar surfactant (LAS)

Original tracings of ten consecutive curves

The loops go clockwise.

Figure 4a: Temperature: 37 ± 0.5°C

Speed: 2 cycles/min

Figure 4b: Temperature: 37 ± 0.5°C

Speed: 8 cycles/min

Note: The minimum surface tension of loop no. 10 at 2 cycles/min is about 15 mN/m, at 8 cycles/min about 1.0 mN/m.

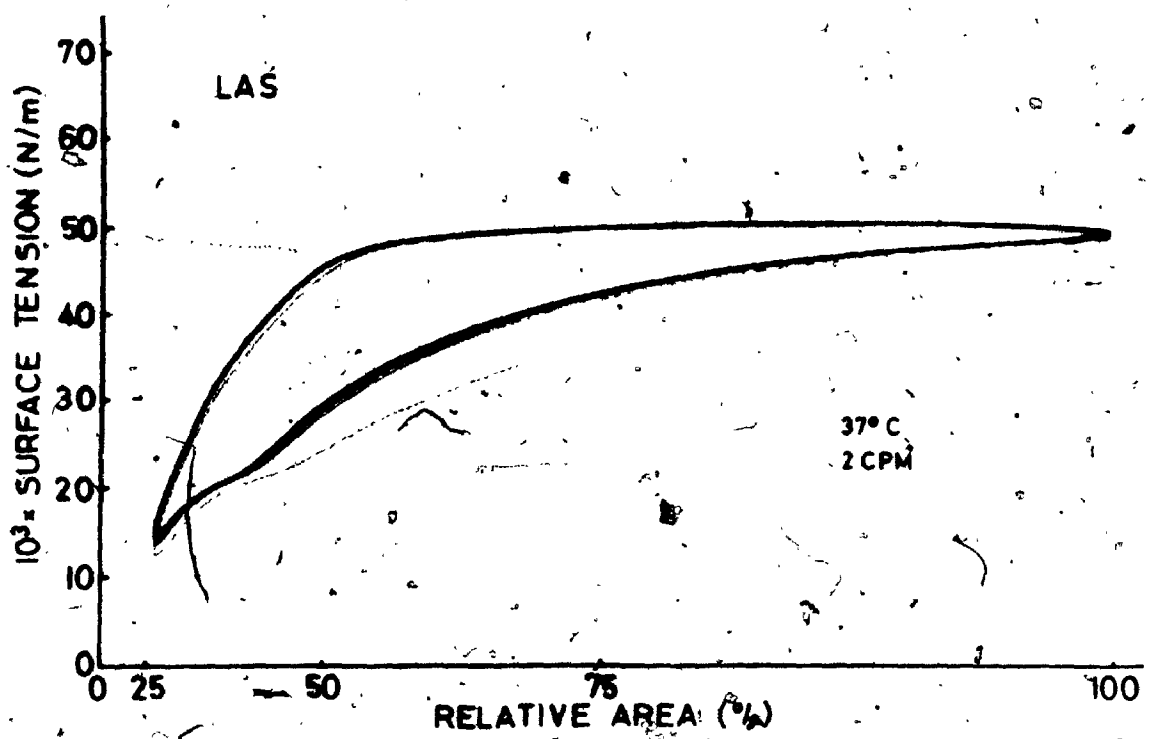
LAS
10^3 × SURFACE TENSION (N/m)
70
60
50
40
30
20
10
0
0
25
50
75
100
RELATIVE AREA (%)
37° C
2 CPM

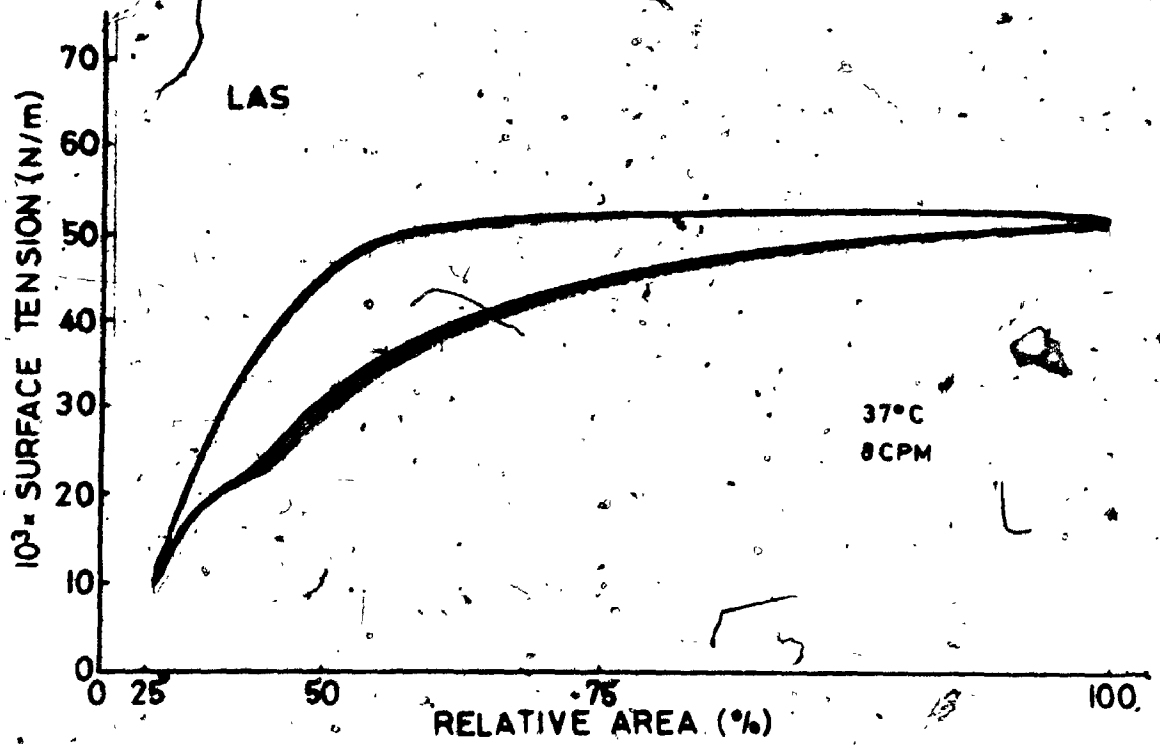
LAS
10^3 × SURFACE TENSION (N/m)
70
60
50
40
30
20
10
0
0
25
50
75
100
RELATIVE AREA (%)
37°C
8 CPM

TABLE I

EFFECT OF TEMPERATURE AND PHOSPHATIDYL CONTENT ON THE MINIMUM SURFACE TENSION OF LUNG ALVEOLAR SURFACTANT AT 8 CYCLES/MIN

	Surface tension ± 0.5 (mN/m)		PC content (m_{pc}) ± 8% (mg)
Sample no.	22 ± 0.5°C	37 ± 0.5°C	
1	10.2	21.4	1.86
2	10.8	24.2	1.92
3	7.80	22.4	3.92
4	6.40	24.3	3.14
5	7.10	25.4	3.40
6	6.40	16.6	7.62
7	5.20	16.1	7.76
8	6.80	14.7	8.18
9	2.00	8.40	9.38
10	3.50	9.80	10.2
11	3.20	5.50	13.6
12	2.50	8.10	10.2
13	9.60	21.2	3.78
14	9.60	21.5	3.68
15	5.50	16.8	6.24
MEAN	6.40	17.1	$p < 0.01$ not paired
± S.E.	2.92	6.57	$p < 0.005$ paired

m_{pc} is the amount of PC in a sample (one trough filling), in milligrams.

Note: The surfactant was prepared according to 4.1.2 a).

TABLE II

EFFECT OF SPEED ON THE MINIMUM SURFACE TENSION OF LUNG ALVEOLAR SURFACTANT AT (37 ± 0.5)°C

Sample no.	Surface tension ± 0.5 (mN/m) 2 cycles/min	8 cycles/min
1	23.8	21.4
2	24.0	24.2
3	23.1	22.4
4	24.5	24.3
5	24.2	25.4
6	22.0	16.6
7	23.2	16.1
8	20.3	14.7
9	15.4	8.40
10	15.0	9.80
11	13.6	5.50
12	17.7	8.10
13	19.6	12.2
14	23.3	21.5
15	21.2	16.8
MEAN	20.7	16.5
± S.E.	3.67	6.58

$p < 0.05$ not paired

$p < 0.01$ paired

TABLE III

EFFECT OF SPEED ON THE MINIMUM SURFACE TENSION OF FOAM FRACTION 1 OF LUNG ALVEOLAR SURFACTANT, AT 37°C

	Surface tension ± 0.5 mN/m	
Sample no.	2 cycles/min	8 cycles/min
1	18.0	14.9
2	12.1	8.70
3	11.6	9.00
4	9.80	3.60
5	10.4	5.70
6	11.2	6.00
7	13.3	8.40
MEAN	12.3	8.00
± S.E.	2.74	3.60

$p < 0.01$ not paired

$p < 0.005$ paired.

$$\gamma = A + Bm_{pc},$$

the following quantities are calculated: at 22°C (Figure 5a)

$$A = 11.02 \text{ mN/m}$$

$$B = - 0.73 \text{ mN/m·mg}$$

Standard error of estimate, S.E.E.

$$\text{S.E.E.} = 1.28 \text{ mN/m}$$

Correlation coefficient, r

$$r = - 0.89$$

With 95% confidence limits of - 0.69 and - 0.97 for the correlation coefficient of the population. At 37°C, (Figure 5b):

$$A = 28.32 \text{ mN/m}$$

$$B = - 1.78 \text{ mN/m·mg}$$

$$\text{S.E.E.} = 1.84 \text{ mN/m}$$

$$r = - 0.95$$

With 95% confidence limits of - 0.87 and - 0.98 for the correlation coefficient of the population.

Thus the amount of lecithin in the sample appears to determine the minimum surface tension.

4.2.5 Development of hysteresis loops of lung alveolar surfactant on repeated cycling

Several hundred continuous loops were recorded with a speed of 8 cycles/min at room temperature and 37°C. Regardless of the method of preparation (see 4.1.2), the minimum surface tension rose up to the plateau level at about 23 mN/m. At this level, the curves seemed to be stationary, at least for more than several hundred further successive cycles. At 22°C a much longer cycling time was required

Figure 5: Regression lines with standard error of estimate of minimum surface tension and amount of phosphatidyl choline (lecithin). (See Table I).
The surfactant was prepared according to 4.1.2 a).

Figure 5a: Standard error of estimate

S.E.E. = 1.28 mN/m

Correlation coefficient

r = 0.89

95% confidence limits

- 0.69 and - 0.97

Figure 5b: S.E.E. = 1.84 mN/m

r = - 0.95

95% confidence limits

- 0.87 and - 0.98

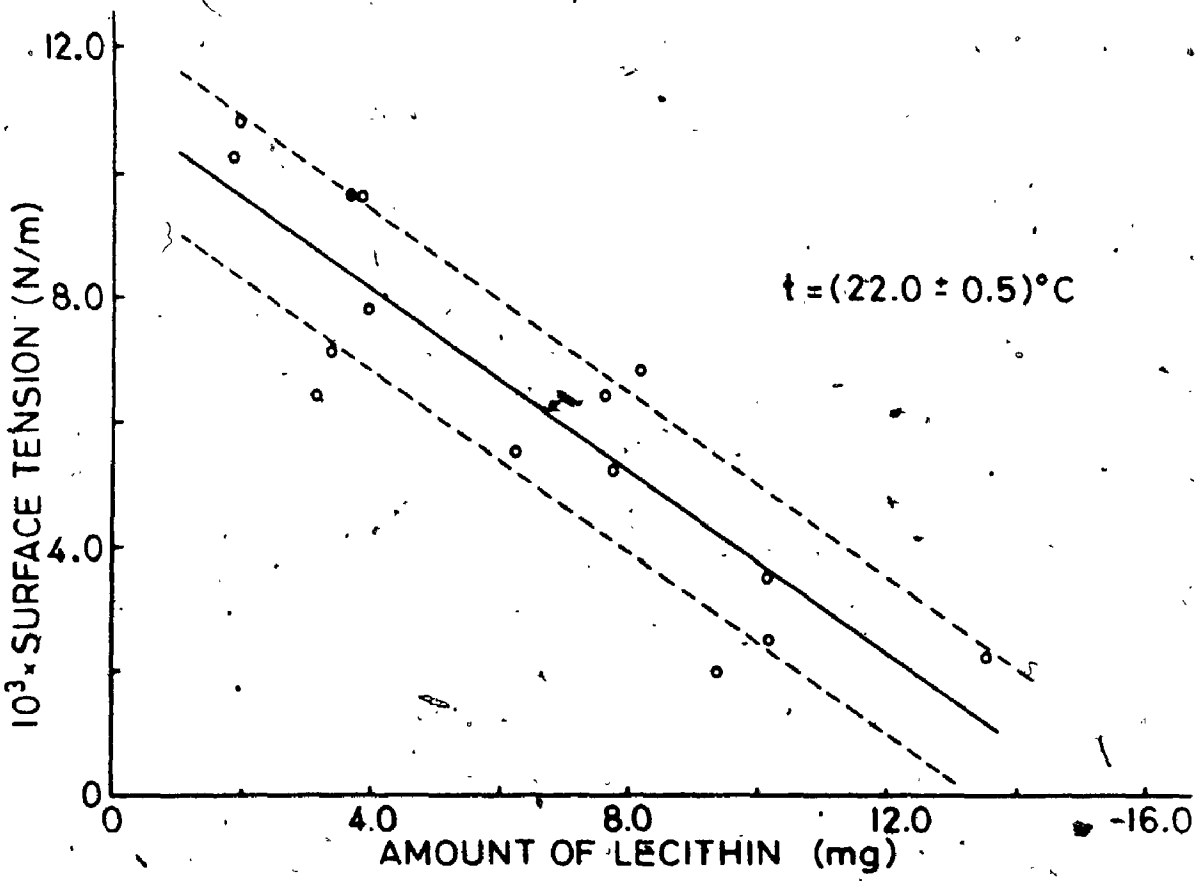
12.0
8.0
4.0
0
10^3 × SURFACE TENSION (N/m)
t = (22.0 ± 0.5)°C
0
4.0
8.0
12.0
16.0
AMOUNT OF LECITHIN (mg)

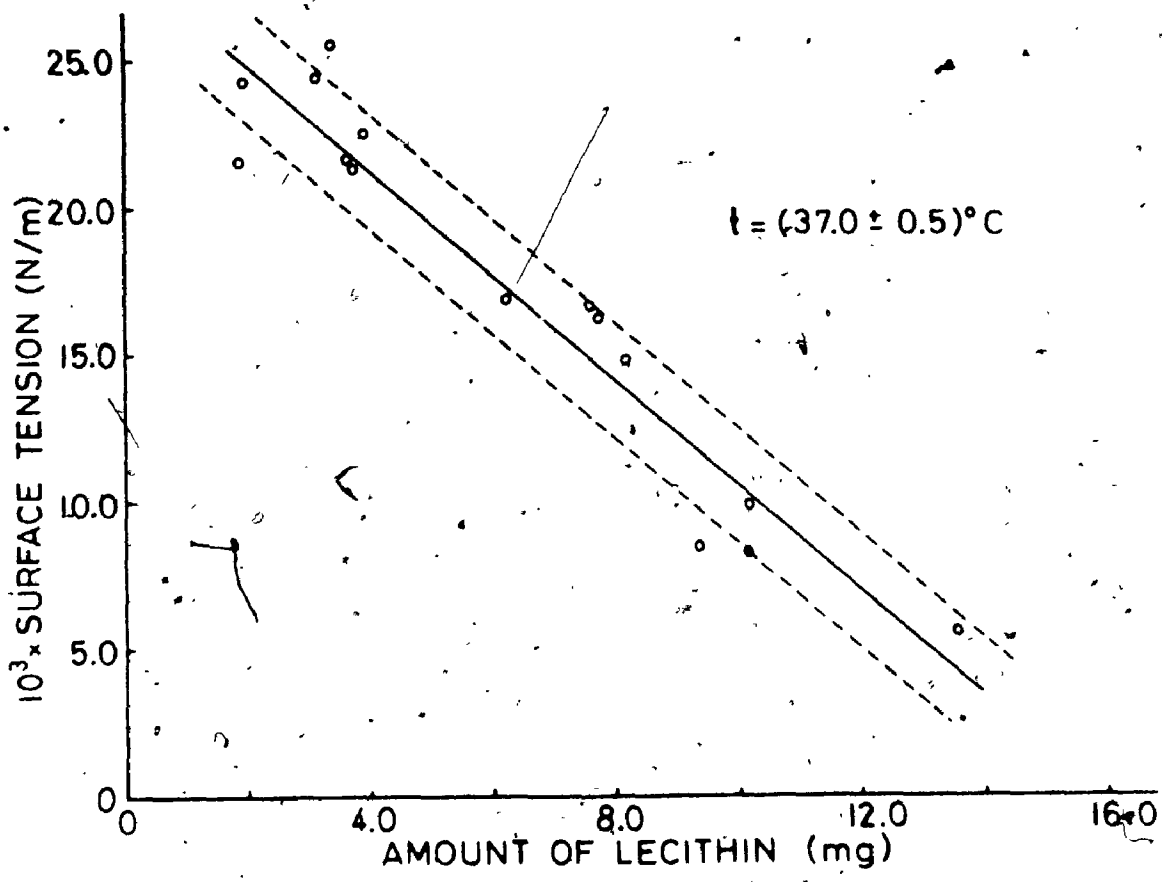
25.0
20.0
15.0
10.0
5.0
0
10^3 × SURFACE TENSION (N/m)
t = (37.0 ± 0.5)° C
0
4.0
8.0
12.0
16.0
AMOUNT OF LECITHIN (mg)

to produce this "stationary state", than at 37°C.

The long term development was dependent on the way the surfactant was prepared. Hysteresis curves from the cell-free unfractionated preparation reached the stationary state at 22°C with loop no. 50 to no. 100, and at 37°C with loop no. 10 to no. 30. Hysteresis curves from foam fraction no. 1 rose to the stationary state only after more than 600 continuous cycles at 22°C, and after more than 200 cycles at 37°C (see Figure 6).

4.3 Summary

From these experiments, we conclude that cycling speed and temperature play interdependent roles on the stability of surface tension-area loops of lung surfactant. The method of preparation, cycling speed and temperature, all determine when the films become stable. In addition, the lecithin content appears to determine the minimum surface tension. Thus the lipid fraction of lung surfactant will be studied next.

Figure 6: Development of hysteresis loops from lung alveolar surfactant, foam fraction 1, on continuous and successive cycling.

The curves go clockwise.

Figure 6a: Loop no. 10 demonstrated the plateau at about 23 mN/m.

Figure 6b: Loop no. 200 represents the stationary state, with the minimum surface tension at the plateau level of about 23 mN/m.

The following curves, up to no. 1000, did not show a measurable increase of the minimum surface tension.

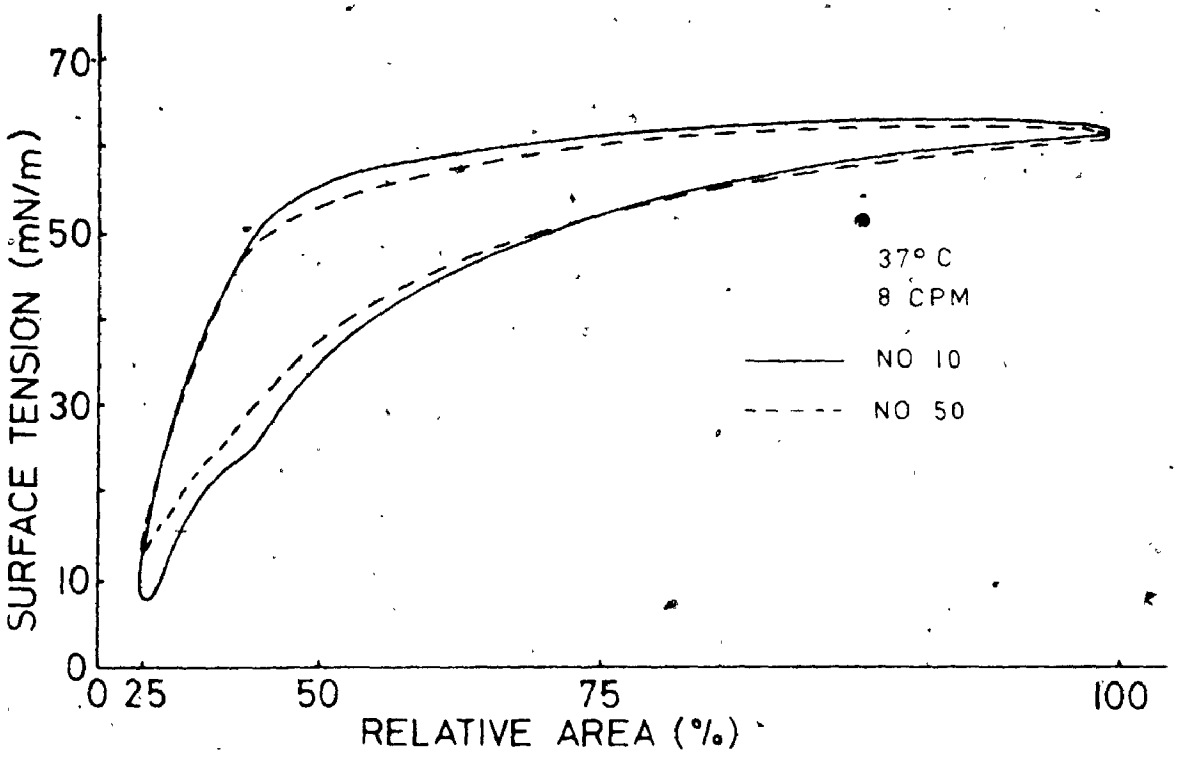
70
50
30
10
0
SURFACE TENSION (mN/m)
0 25
50
75
100
RELATIVE AREA (%)
37° C
8 CPM
NO 10
NO 50

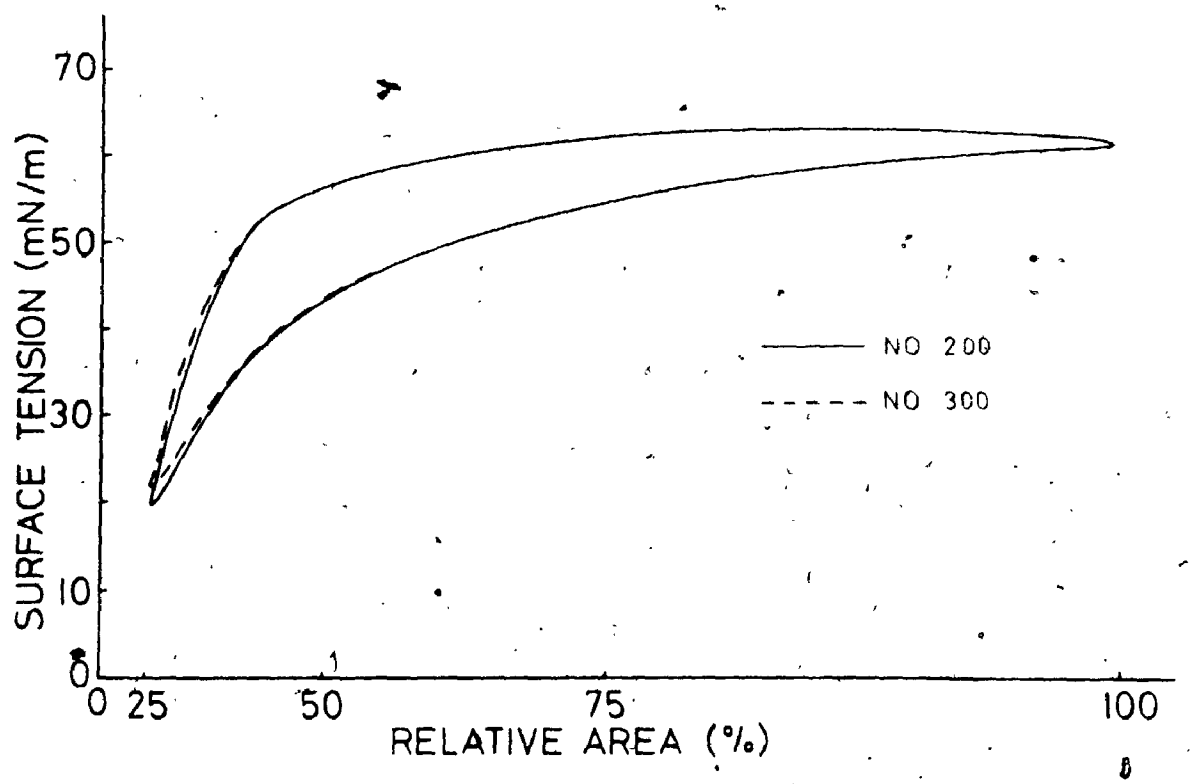
70
50
30
10
0
SURFACE TENSION (mN/m)
0 25
50
75
100
RELATIVE AREA (%)
NO 200
NO 300

CHAPTER 5

PROPERTIES OF THE LIPID FRACTION OF LUNG SURFACTANT

5.1 Methods

Extraction of the lipid fraction and its analysis by thin layer chromatography have been described in 4.1.3.

For the surface tray studies, the concentration of the lipid solution was compared with a standard solution of 2 mg/ml of dipalmitoyl phosphatidyl choline (DPPC). If equal amounts of the solutions lowered the surface tension by the same order of magnitude, we assumed the lipid concentration of the lipid fraction to be about 2 mg/ml, otherwise it was adjusted by evaporation or dilution. For easier spreading of the films, usually we added n-hexane to make a final solution of chloroform : methanol : n-hexane (1 : 1 : 1, by vol.), with a lipid concentration of about 2 mg/ml. The monolayers were then spread at maximum area and to produce a surface tension of about 30 mN/m.

Approximately 3 to 5 min were allowed for the solvents to evaporate before the cycling was started.

5.2 Results

5.2.1 Phospholipid composition of rabbit lung surfactant

The results are summarized in Table IV. Figure 7 demonstrates the separation of the various phospholipids by thin layer chromatography. The dominant factor is phosphatidyl choline (PC), with over 80% of the total phospholipid content. Phosphatidyl glycerol (PG), counts for about 10% and phosphatidyl serine and phosphatidyl inositol combined for approximately 5%. Only about 4% of the total surfactant phospholipid is phosphatidyl ethanolamine (PE). It seems to be a much more important factor in the lung tissue (Figure 7).

5.2.2 Surface tray studies

a) Quality of the extract

Figure 8a shows the series of the first ten curves of a film formed by the lipid fraction of foam no. 1, (see 4.1.2 c). The initial surface tension at maximum area is below 30 mN/m, the minimum value possible for static conditions. It could not be decreased further by excessive spreading of film material. The loops demonstrate the typical plateau like surfactant curves, at about 23 to 25 mN/m.

Figure 8b shows the first ten curves of a film from the lipid fraction of foam no. 2. It demonstrates how fractionation affects the development of the hysteresis loops and the minimum surface tension.

TABLE IV

PHOSPHOLIPID COMPOSITION OF ~~RABBIT~~ LUNG ALVEOLAR SURFACTANT

Phospholipid	% of total phospholipid MEAN ± S.E.	Range %	No. of samples
phosphatidyl choline (PC)	82 ± 5.1	76-91	21
phosphatidyl glycerol (PG)	9.2 ± 2.4	7.5-11.6	8
phosphatidyl ethanolamine (PE)	4.0 ± 1.5	3.4-5.0	21
phosphatidyl serine (PS) + phosphatidyl inositol (PI)	5.5 ± 1.0	4.7-6.8	20

Other phospholipids such as lysophosphatidyl choline sphingomyelin, phosphatidyl dimethyl ethanolamine may also be present, but these are negligible quantitatively.

For each sample, the phospholipids were measured three to four times.

For comparison, from Pfleger et al. (1971)

Lipid composition of dog lung alveolar surfactant

Phospholipid	% of total phospholipid
PC	74
PG	10
PE	4
PI	3
PS	2
LPC + Sphingomyelin	5

Figure 7: Separation of the phospholipids from rabbit lung alveolar surfactant and from rabbit lung tissue (whole lung) by thin layer chromatography.

N	Neutral lipids
PG	Phosphatidyl glycerol
PE	Phosphatidyl ethanolamine
PS	Phosphatidyl serine
PI	Phosphatidyl inositol
PC	Phosphatidyl choline
SPHING	Sphingomyelin
LPC	Lyso phosphatidyl choline

Note: PE seems to be an important factor in whole lung tissue, but not in alveolar wash.

The lipid analysis was done by Mr. Patrick Shum.

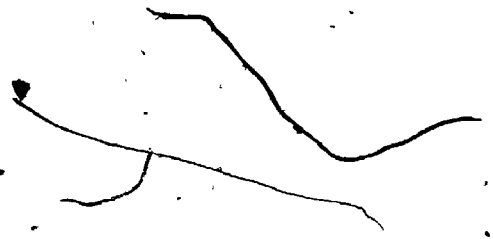

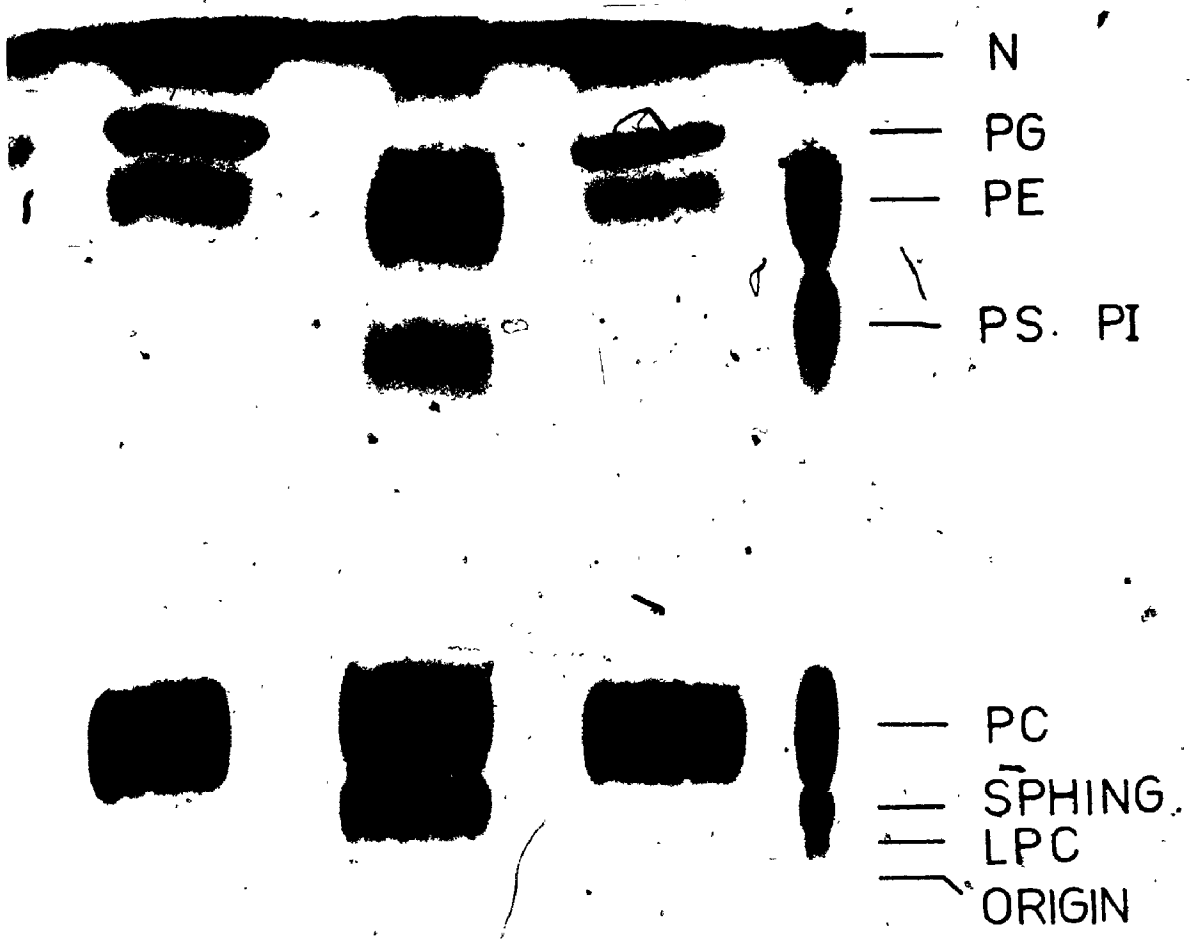
N
PG
PE
PS. PI
PC
SPHING.
LPC
ORIGIN
ALVEOLAR WASH
LUNG TISSUE
ALVEOLAR WASH
MARKERS

Figure 8: Effect of the foam quality on the minimum surface tension of the first ten curves.

The curves go clockwise.

The films were spread from the lipid extract of foam no. 1 and 2 (4.1.2.c).

Figure 8a: The minimum surface tension of loop no. 10 is about 5 mN/m for the lipid fraction of foam no. 1.

Figure 8b: The minimum surface tension of loop no. 10 is about 23 mN/m for the lipid fraction of foam no. 2.

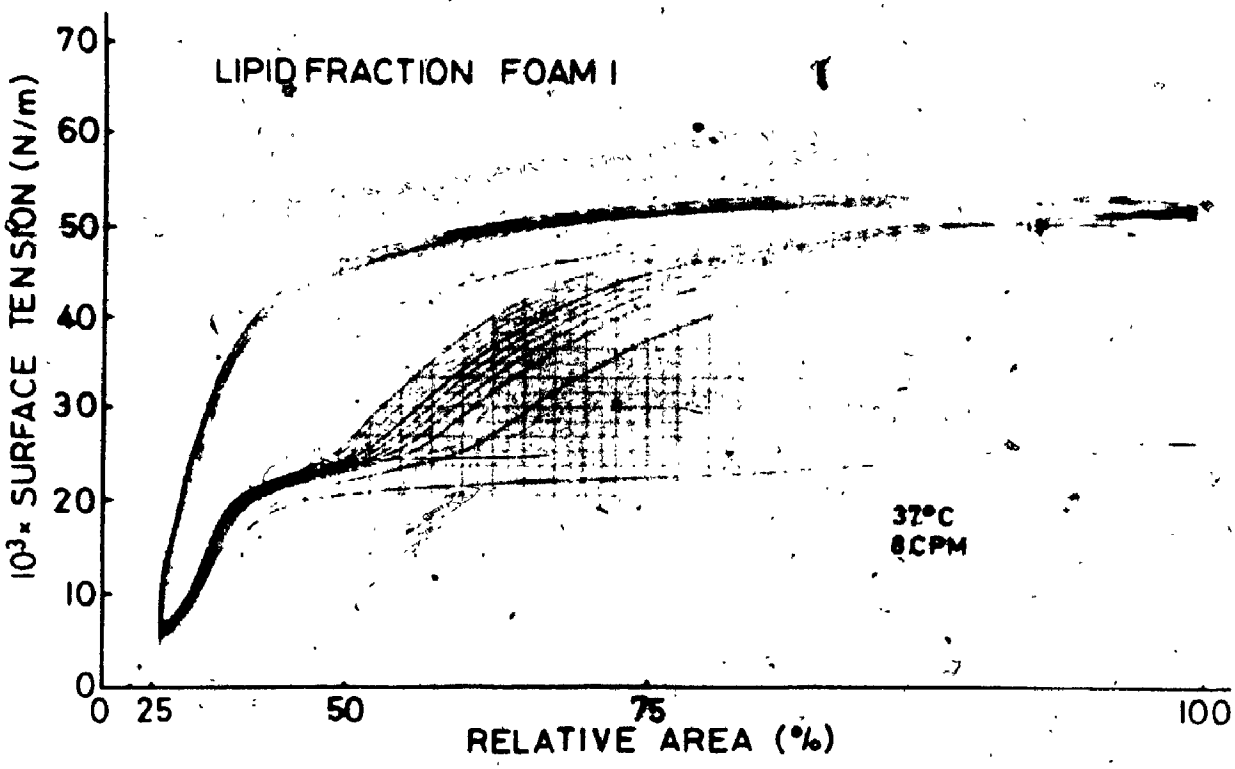
LIPID FRACTION FOAM I
10^3 × SURFACE TENSION (N/m)
70
60
50
40
30
20
10
0
0
25
50
75
100
RELATIVE AREA (%)
37°C
8 CPM

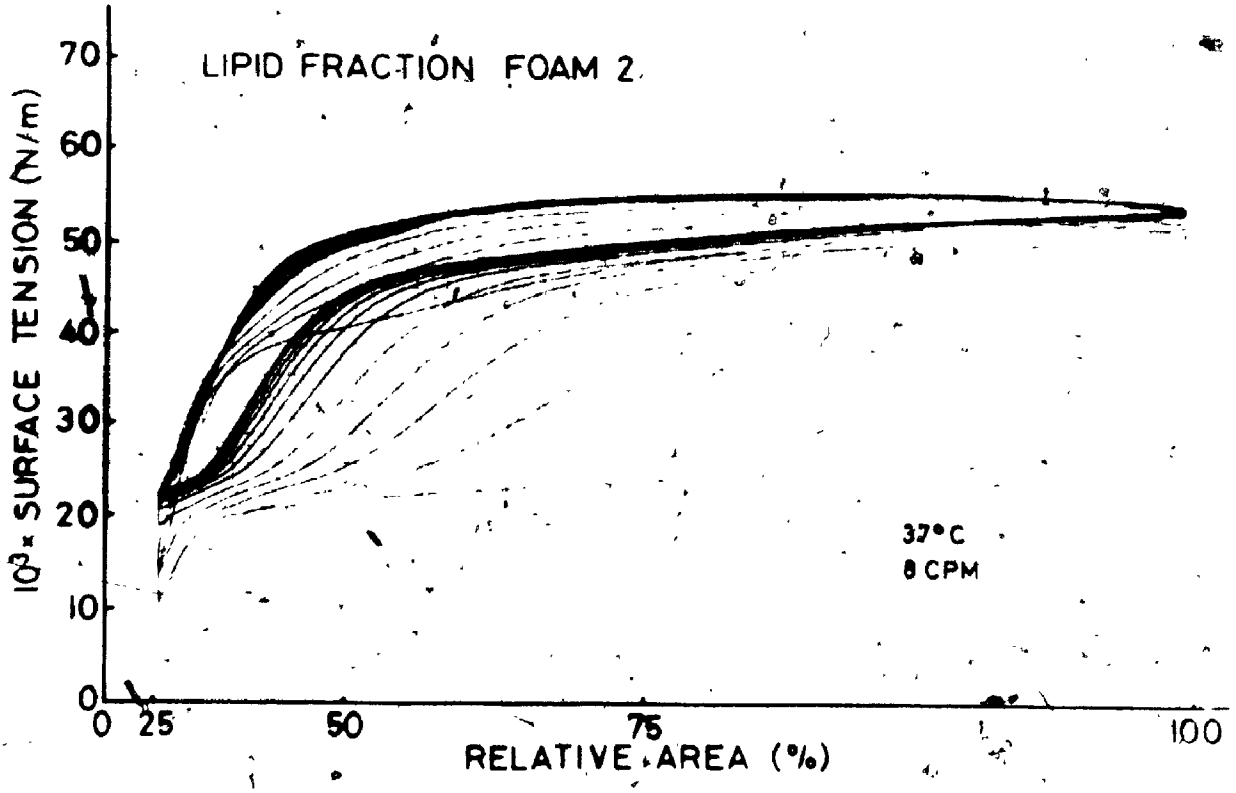
LIPID FRACTION FOAM 2
10^3 × SURFACE TENSION (N/m)
70
60
50
40
30
20
10
0
0
25
50
75
100
RELATIVE AREA (%)
37°C
8 CPM

b) Influence of protein (Figure 9)

Even relatively large amounts of albumin in the subphase have no effect on the minimum surface tension. For Figure 9b, the same film material as for Figure 9a was used, except that the subphase contained approximately 3.5 mg/ml of albumin bovine. The protein decreases only the maximum surface tension. It will be shown later that albumin does not interfere with the development of large series (several hundred curves) of hysteresis loops from synthetic dipalmitoyl phosphatidyl choline.

c) Speed effect

Figure 10 illustrates the influence of the cycling speed on films from the lipid fraction of foam no. 1 (4.1.2 c).

No. 10 of the first ten curves are drawn. At 1/12 cycle/min, the minimum surface tension was about 18 mN/m, at 4/3 cycle/min about 9 mN/m and at 2 cycles/min about 2 mN/m (not shown on Figure 10).

5.3 Summary

1) Lipid fraction

Films from the lipid fraction of foam no. 1 produce lower minimum surface tensions and more reproducible hysteresis loops than the ones from the lipid fraction of foam no. 2.

The speed effect is similar to the one observed on surfactant films. Albumin in the subphase has no effect on the minimum surface tension and on the reproducibility of consecutive curves.

2) Phospholipid composition of rabbit lung surfactant

Unfractionated lung surfactant contains more than 80% PC, about 9% PG and 5% PS or PI.

Figure 9: Effect of albumin on hysteresis loops from the lipid fraction of foam no. 1

Figure 9a: Lipid fraction only

Figure 9b: Approximately 3.5 mg/ml of albumin bovine in the subphase

Note: The presence of albumin in the subphase has no effect on the minimum surface tension, the plateau level and reproducibility of consecutive curves. Only the maximum surface tension seems to be affected.

2 5

OF/DE

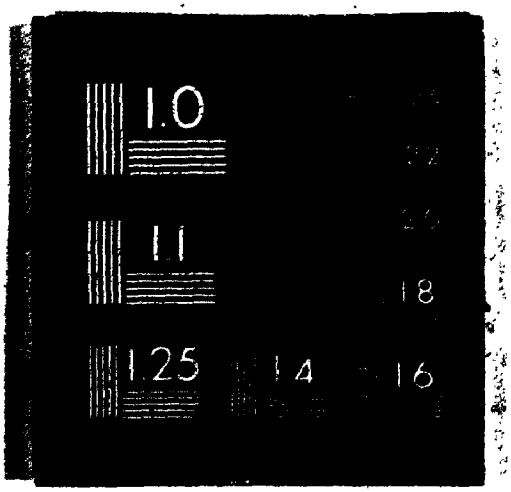

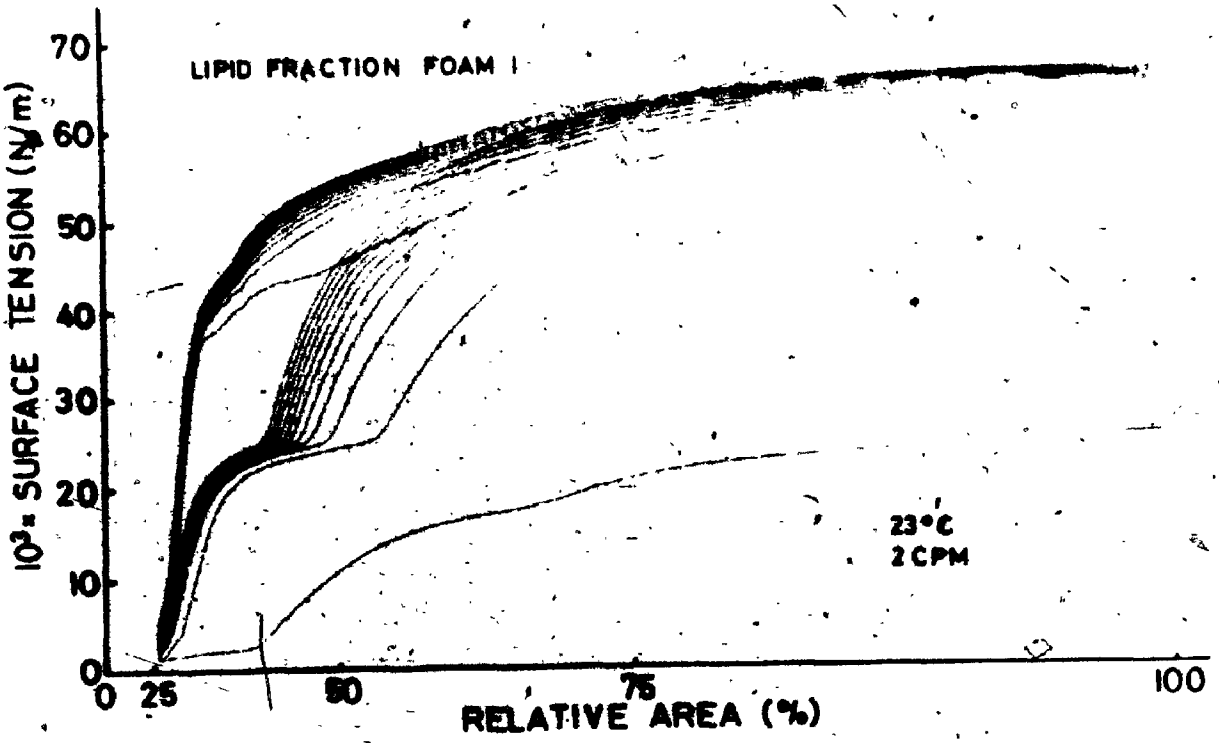
LIPID FRACTION FOAM I
10^3 × SURFACE TENSION (N/m)
70
60
50
40
30
20
10
0
0
25
50
75
100
RELATIVE AREA (%)
23°C
2 CPM

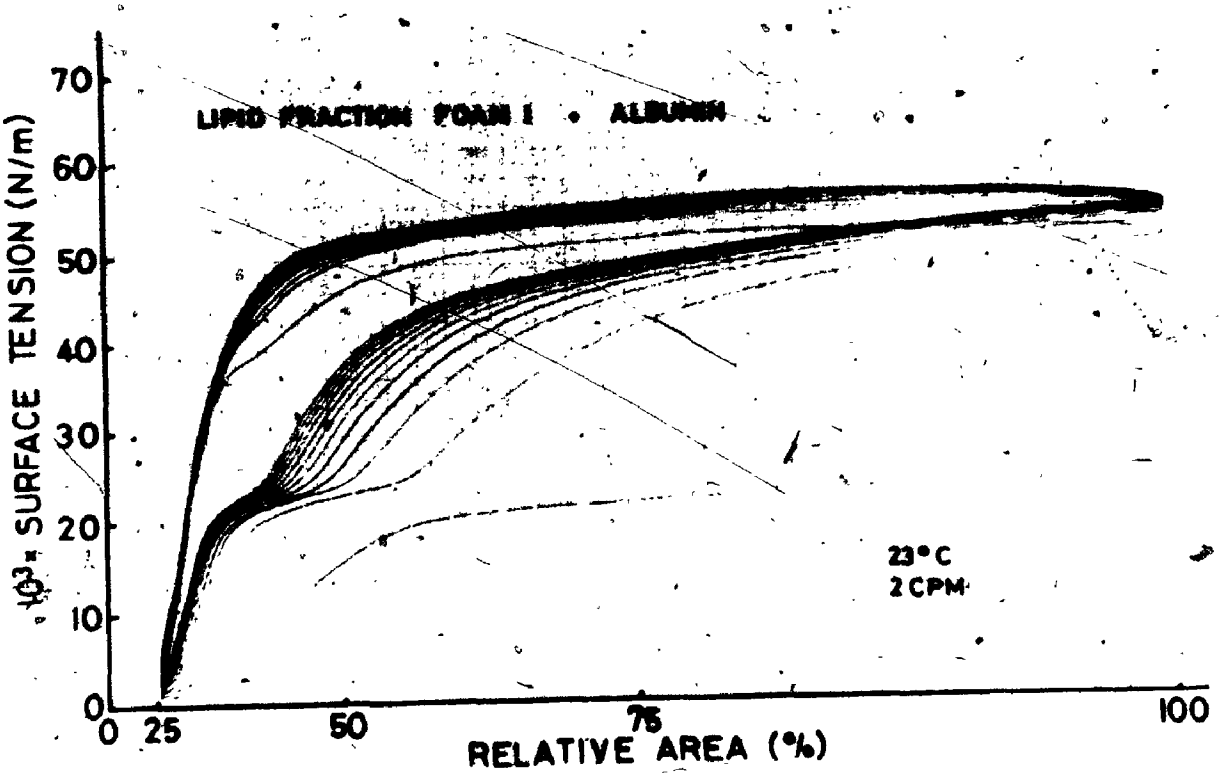
LIPID FRACTION FOAM I • ALBUMIN
10^3 × SURFACE TENSION (N/m)
70
60
50
40
30
20
10
0
0
25
50
75
100
RELATIVE AREA (%)
23°C
2 CPM

Figure 10: Speed effect on films from the lipid fraction of foam no. 1. At 1/12 cycle/min, the minimum surface tension is about 18 mN/m, at 4/3 cycle/min about 9 mN/m.

No. 10 of the first series of ten curves is shown.

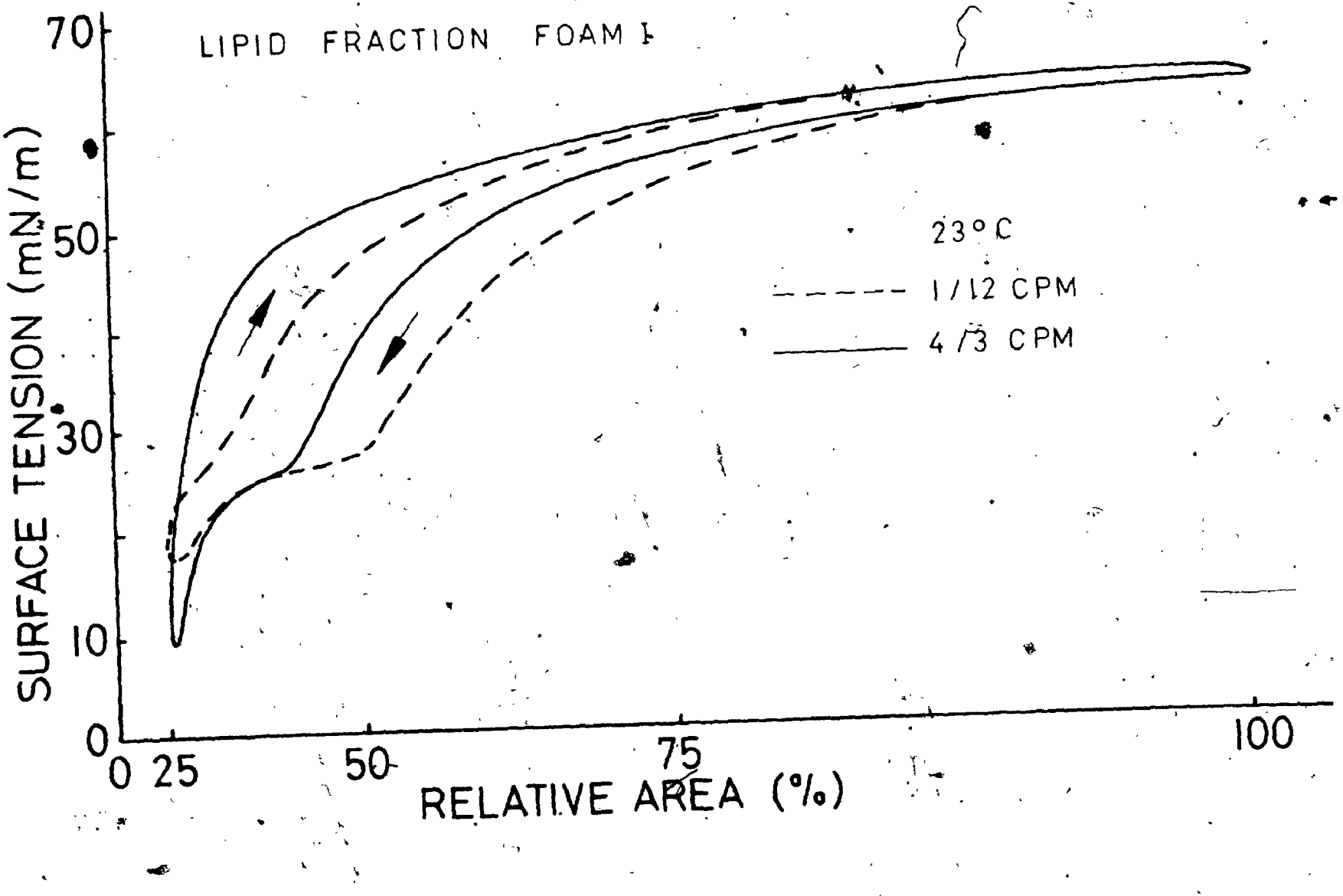
LIPID FRACTION FOAM I
SURFACE TENSION (mN/m)
70
50
30
10
0
0 25
50
75
100
RELATIVE AREA (%)
23° C
1/12 CPM
4/3 CPM

50-(2)

CHAPTER 6

DISCUSSION OF CHAPTERS 4 AND 5

6.1 Preparation of the films

A wide variety of methods are described in the literature. Scarpelli (1968, Chapter 4) points out that standardization of extraction of the surfactant and preparation of the film is an empirical process for a particular laboratory. However, centrifugation between 300 g and 1000 g for sedimentation of the cellular material is a common initial procedure.

Since "aging" of the cell-free material (4.1.2 a) was important with respect to low minimum surface tension and reproducibility on repeated cycling, we conclude a time dependent organization of the film. Molecules which interact most strongly with each other at the interface, produce the lowest free energy per unit area. It is therefore reasonable to allow an "aging" time until no further detectable decrease of the surface tension can be observed under static conditions. Scarpelli (1968, p. 67) suggests 15 min to one hour before compression of the surface is begun. We found a time of one hour usually too short and prefered an aging time of up to three hours.

Even foam 1, from the top of the fractionation column had to be "aged" more than one hour until no further

decrease of the surface tension occurred. The static minimum surface tension was then approximately 25 mN/m, the value obtained from synthetic lecithin films.

The fact that monolayers of the lipid fraction alone demonstrate a surface activity very similar to that of lavage surfactant, suggests that protein is not an important factor of the surface film itself. However, it may be an important component of particles in the subphase.

Reifenrath et al. (1973a) report that albumin decreases the ability of lecithin films to reduce surface tension regardless of the protein being in the surface film or in the subphase. Without exception, we did not find any interference with the minimum surface tension of monolayers from the lipid fraction. Albumin in concentrations up to 5 mg/ml in the subphase affected only the maximum surface tension. Also, there was no measurable effect due to albumin on the development of hysteresis loops with repeated cycling.

6.2 Temperature and speed dependence

Variations of temperature between 22°C and 38°C are reported to have no influence on surface properties of surfactant (Avery et al. 1959). Not much attention has been given to the influence of speed on the surface tension-area diagram. It was assumed that cycling frequencies from as low as one cycle per hour up to 14

cycles/min have no significant effect on the hysteresis loops (Scarpelli, 1968, p. 67). However, Frosolone et al. (1970) found that about five times as much surfactant material had to be applied on a surface with a 28 min cycle as with a 3 min cycle in order to get a surface tension of 12 mN/m. Protein or lipid components other than lecithin are suggested by these authors to be the reason for the dynamic effect.

From our study, we conclude that the minimum surface tension at 37°C is significantly higher than at 22°C, leaving the speed and the amount of film material constant. This was found to be true for crude lung lavage material, for the foam fraction 1, and for the lipid fraction. The experiments with protein suggest that the speed dependence cannot be attributed to the presence of albumin in the system. We will show later that lipid components other than lecithin are very likely responsible for the speed effect. But we will also demonstrate that dynamic effects for pure DPPC films in the temperature range from 22°C up to about 40°C and from 1/12 cycle/min up to 8 cycles/min are negligible.

6.3. Development of hysteresis loops on repeated cycling

Slama et al. (1973) used a bubble method for large series, up to several thousand, continuous cycles. Their "Equilibrium area surface tension diagram" corresponds

to our "stationary" hysteresis loop. Generally, our findings agree with theirs, except that the minimum surface tension of our stationary state is about (3 - 5)mN/m higher, at the plateau level, (23 - 25 mN/m). They did not mention the typical plateau of the surface tension-area diagram to which the minimum surface tension rises with time.

6.4 Phospholipid composition of rabbit alveolar surfactant

We found that over 80% of the total surfactant phospholipid was PC. Frosolono et al. (1970) reported the corresponding number to be 76% in dog lung surfactant, with 54% DPPC. Toshima et al. (1972) found 68% PC in the total phospholipid content of rat surfactant.

The second most abundant component was PG, which made up more than 9% of the total phospholipid. This agrees well with the finding of Pfleger et al. (1972), who reported 9% of the total surfactant phospholipid to be PG. They found only 2% PG in the phospholipid content of whole lung tissue. Like PC, PG seems to be strategically located and it may be an important factor of the surfactant. For further information on the phospholipid content see Toshima et al. (1972), Pfleger et al. (1971), Frosolono et al. (1970).

6.5 Regression and correlation

The good correlation between the lecithin content (total lecithin, saturated and unsaturated), and the

minimum surface tension supports the importance of this component. The results were obtained in spite of our crude washing technique and therefore uncontrolled "contamination" by protein and other factors (Hurst et al., 1973, Reifenrath et al., 1973a).

No relationship between the maximum surface tension and the lecithin content could be detected. This suggests components of surface active material other than lecithin determine the maximum surface tension.

Plateaux of curves from lung alveolar surfactant or of the lipid fraction, regardless of the preparation, are not measurably dependent on cycling speed and temperature.

Surfactant samples with a relatively low lecithin content showed a minimum surface tension at about the plateau level, between 22 and 25 mN/m, even at 8 cycles/min and room temperature.

6.6 Summary

Cell-free crude lung lavage material from rabbits was compared with foam fractions and with the lipid extract of the same lavage.

1) Surface tension-area diagrams from cell-free preparations were found to be temperature- and speed dependent. At 37°C, surface tensions below 10 mN/m were possible only

by increasing the cycling speed to values closer to physiological frequencies, e.g. 8 cycles/min.

2) Foam from the top of the fractionation column produced more consistent results than the unfractionated cell-free lung wash; the minimum surface tension was lower and there was less change between successive loops.

3) Characteristics of surfactant hysteresis curves, minimum surface tension, plateau and change on successive cycling could be reproduced by the lipid fraction alone.

4) Albumin, up to relatively high concentrations in the hypophase, had no measurable effect on the minimum surface tension of films from the lipid extract.

5) After series of about a hundred to a thousand continuous cycles, the surface tension-area diagram reached a "stationary state" at the plateau level of about (23 - 25)mN/m. This process is dependent on temperature and on the quality of the foam fraction, but not on cycling speed.

6) The good correlation between the lecithin content and the minimum surface tension, in spite of "uncontrolled contamination" of the lavage material, supported the importance of lecithin.

7) More than 80% of the total phospholipid was found to be phosphatidyl choline (PC). About 9% of the total

phospholipid was phosphatidyl glycerol (PG).

CHAPTER 7

SYNTHETIC COMPONENTS RELATED TO LUNG ALVEOLAR SURFACTANT

7.1 Introduction

Recently, a good selection of pure synthetic phospholipids has become available. Cadenhead (1970), p. 175, points out that a better understanding of the properties of extracted natural phospholipid mixtures is now possible by comparison with those of selected synthetics. In Table V some important phospholipids can be found. Their stereospecific and common names are given.

7.1.1 Non polar lipid

Reifenrath (1973) reported that cholesterol may be an important factor of surfactant, at least in rat lungs: his estimated ratio of cholesterol to phosphatidyl choline is between 1 : 5 and 1 : 15.

Frosolono et al. (1970) found cholesterol to be about 11% of the total surfactant lipids from dog lungs. Pfleger et al. (1971) estimated between 10% and 16% of cholesterol in total surfactant lipids from dog lungs.

7.1.2 Phospholipids

Galdston et al. (1969) reported that about 90% of the total surfactant lipids are phospholipids in rabbit lungs. Pfleger et al. (1971) gave the corresponding number

to be 80%, for dog lungs.

We have already presented our findings regarding the phospholipid composition of rabbit alveolar wash in 5.2.1. Over 80% of the total phospholipid content was PC, about 9% was PG, and approximately 5% was PS and PI combined. In Table VI, the structures of PC, PG and PS are shown.

7.1.3 Fatty acid distribution

Detailed information about the fatty acid distribution of total surfactant phospholipids can be found in Frosolono et al. (1970), Pfleger et al. (1971), Toshima et al. (1972), Galdston et al. (1969).

Palmitic acid (C16 : 0), is the most important factor in all the phospholipids. Pfleger et al. (1971) found approximately 60% palmitic acid in both, PC and PG.

It is interesting to note that there are relatively large portions of (C18 : 0) and of the one unsaturated compound (C18 : 1). There are only trace amounts of fatty acids with less than fourteen carbon atoms in a chain. Galdston et al. (1969) found about 10% of (C16 : 1), 29% of (C18 : 1), and 14% of (C18 : 2) of the total fatty acids in rabbit lung surfactant.

7.2 Properties at the air-liquid interface

7.2.1 Introduction

In the following, characteristics of films from synthetic DPPC or PC (C16 : 0), PG (C16 : 0), PS (C16 : 0) were investigated. The influence of unsaturation and chain length on the dynamic properties of DPPC layers were studied.

The behaviour of DPPC films in presence of albumin was described.

7.2.2 Materials and methods

The apparatus has been described in 3.8.

Lipids

Synthetic lipids were purchased from *Serdary Research Laboratories. All solvents were of spectroscopic grade. The lipids were usually dissolved in chloroform. N-hexane was then added with a little propanol as a spreading agent. The concentrations were 2 mg/ml if not otherwise specified. For problems with spreading solutions, see Munden et al. (1973a). DPPC was dissolved in chloroform : propanol : n-hexane (1 : 1 : 8, by vol.).

The solutions were stored at about 5°C and renewed every other day. The chemicals were not further purified. However, the lecithin was periodically tested for purity

---

*Serdary Research Laboratories, 1643 Kathryn Dr., London, Ontario, N6G 2R7

TABLE V

SYNTHETIC PHOSPHOLIPIDS, NOMENCLATURE

Stereospecific name	common names	Abbreviations
L-1,2 dilauroyl-sn-glycerol-3-phosphatidyl choline	L-3-phosphatidyl choline dilauroyl (C12:0)	PC (C12:0)
L-1,2 dimyristoyl-sn-glycerol-3-phosphatidyl choline	L-3-phosphatidyl choline dimyristoyl (C14:0)	PC (C14:0)
L-1,2 dipalmitoyl-sn-glycerol-3-phosphatidyl choline	L-3-phosphatidyl choline dipalmitoyl (C16:0) (dipalmitoyl lecithin)	PC (C16:0) or DPPC
L-1,2 distearoyl-sn-glycerol-3-phosphatidyl choline	L-3-phosphatidyl choline distearoyl (C18:0)	PC (C18:0)
L-1,2 dioleoyl-sn-glycerol-3-phosphatidyl choline	L-3-phosphatidyl choline dioleoyl (C18:1)	PC (C18:0)
L-1,2 dilinolenoyl-sn-glycerol-3-phosphatidyl choline	L-3-phosphatidyl choline dilinolenoyl (C18:3)	PC (C18:3)
L-1,2 dipalmitoyl-sn-glycerol-3-phosphatidyl glycerol	L-3-phosphatidyl glycerol dipalmitoyl (C16:0)	PG (C16:0)
L-1,2 dipalmitoyl-sn-glycerol-3-phosphatidyl serine	L-3-phosphatidyl serine dipalmitoyl (C16:0)	PS (C16:0)
L-1,2 dipalmitoyl-sn-glycerol-3-phosphatidic acid	L-3-phosphatidic acid dipalmitoyl (C16:0)	

TABLE VI

STRUCTURE OF THREE PHOSPHOLIPIDS

PC : Phosphatidyl choline

PG : Phosphatidyl glycerol

PS : Phosphatidyl serine

Note: R_1 and R_2 represent the hydrocarbon chains.

PC

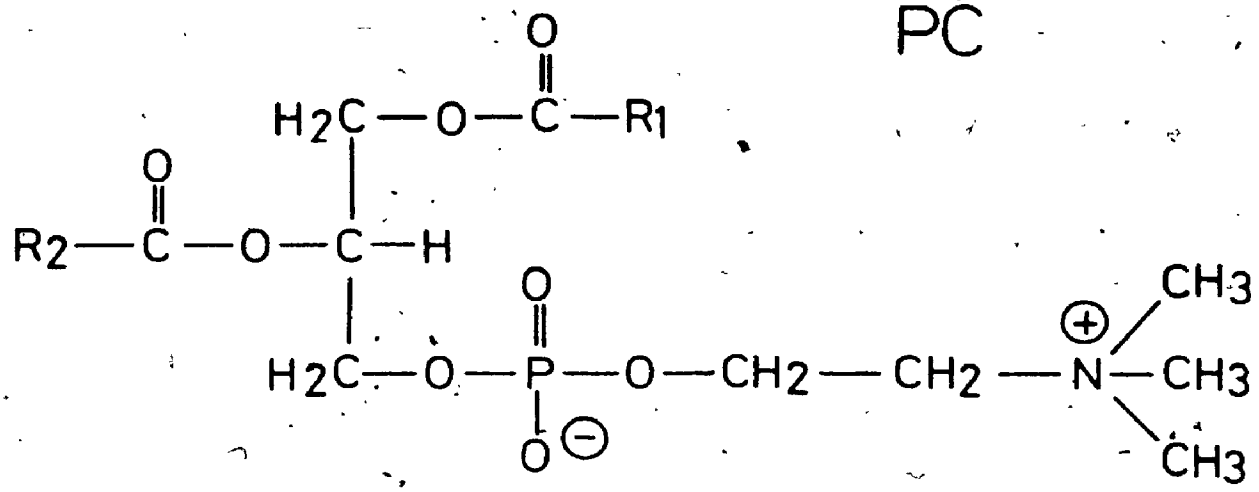

PG

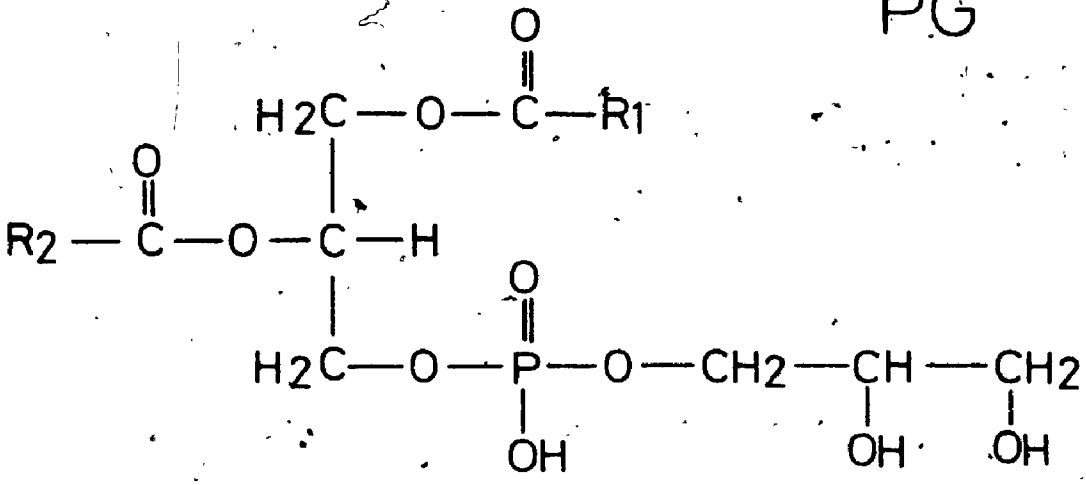

PS

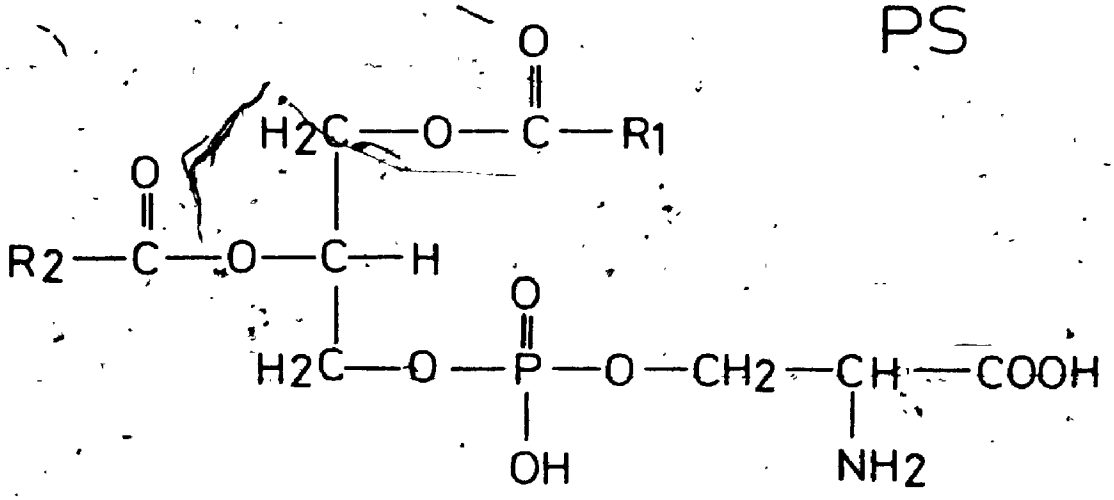

by thin layer chromatography.

The films were spread with a 10 µl Hamilton microsyringe (± 0.1 µl), on a solution of 0.9% NaCl (pH 6.4 - 7.1). The solvents were allowed to evaporate for two to five minutes. The water was double distilled in pyrex glass. Further cleaning of the saline surface was found to be necessary. When the rectangular trough was used, the surface between the two teflon blades was swept several times at minimum area with filter paper until the change of the baseline potential (see 3.9.2) was less than 10 mV for a reduction of the film area to 25%.

When the rhombic trough was used, the surface was cleaned at minimum surface area by aspiration with a pipette.

7.2.3 Experiments with L-1,2 dipalmitoyl-sn-glycerol-3-phosphatidyl choline (PC (C16 : 0) or DPPC)

a) Phase transitions

Figure 11a shows the surface tension-area, Figure 11b the surface potential-area diagrams. The curves were recorded simultaneously and continuously with a cycling speed of 1/12 cycle/min. The experiments were done with the rectangular trough and then repeated with the rhombic tray, in order to check for possible artifacts introduced by leakage. The diagrams are drawn on the basis of at least four independent runs. At maximum film area, the area per

Figure 11: Surface tension-area and surface potential-area characteristics of DPPC films. The curves were recorded simultaneously. The cycling speed was 1/12 cycle/min. Two curves are shown, the upper one for 22 ± 0.5°C (unbroken line), the lower one for 37 ± 0.5°C (broken line).

Figure 11a: Surface tension-area characteristics

S : Point of inflexion, corresponding to $(43 \pm 2)10^{-20}$ m^2/molecule, the limiting area of the DPPC monolayer.

P : Point in about the middle of the transition plateau from the liquid expanded to the liquid condensed state.

Figure 11b: Surface potential-area characteristics

P': This point corresponds to P in Figure 11a. The curves demonstrate two linear parts, separated by a marked change of the slope at P'.

Q : Maximum surface potential. Q does not correspond to S (limiting area).

Note: The area axis is linear.

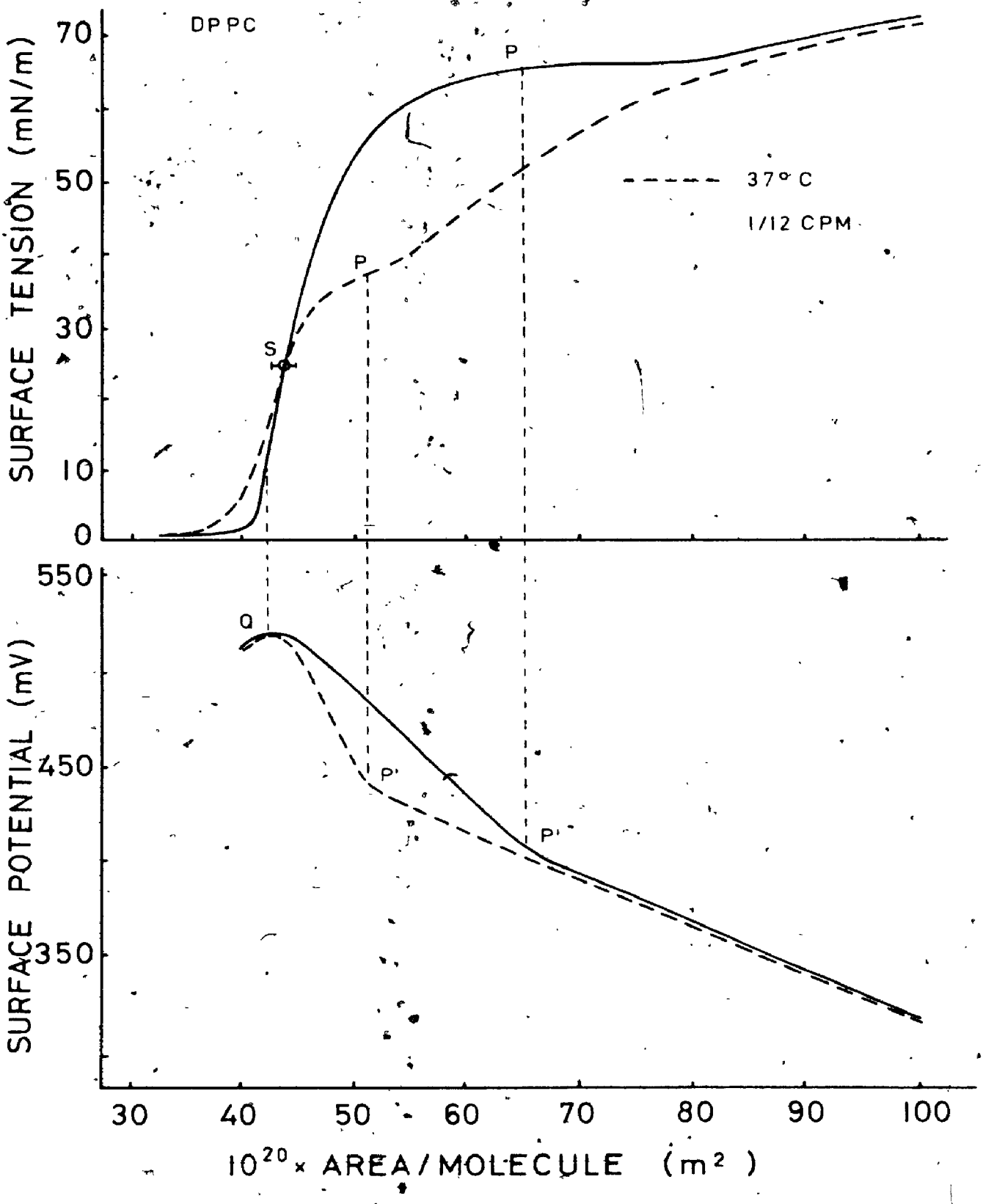
DPPC
SURFACE TENSION (mN/m)
70
50
30
10
0
P
P
S
37° C
1/12 CPM
SURFACE POTENTIAL (mV)
550
450
350
Q
P'
P'
30
40
50
60
70
80
90
100
10^20 × AREA / MOLECULE (m²)

molecule was chosen to be 100 x 10^{-20} m^2 (100 $Å^2$) and the amount of lecithin to be spread was calculated accordingly. The phase transitions from the liquid expanded to the condensed state agree with earlier results (Phillips et al., 1968, Villalonga, 1968). The surface tension-area characteristics show a point of inflexion S, corresponding to (43 ± 2)10^{-20} m^2/molecule (MEAN ± S.E., eight independent experiments), as the limiting area of the molecule in the monolayer.

The surface potential-area diagrams demonstrate two linear parts, separated by a marked change of the slope in P'. This change of slope corresponds approximately to point P in the middle of the transition zone from the liquid expanded to the liquid condensed state in the surface tension curve.

The maximum surface potential, Q, is reached beyond the limiting area, but does not correspond to the smallest possible value of the surface tension.

b) <u>The quasi equilibrium state</u>

Figure 12 represents a surface tension-area diagram at 37°C ± 0.5°C. In order to investigate the time dependent behaviour, the movement of the rhombic tray was stopped at various points and the surface tension recorded as a function of time. Short of the limiting area, at about 25 mN/m, the rise of the surface tension in the first minute after

Figure 12: Surface tension-time characteristics of a DPPC film after stop at various levels of surface tension, indicated by the circles.
The curve with the arrow represents the surface tension-area diagram.

Note: At minimum surface tension, about 2 mN/m, the film is in a relatively stable state (see text).

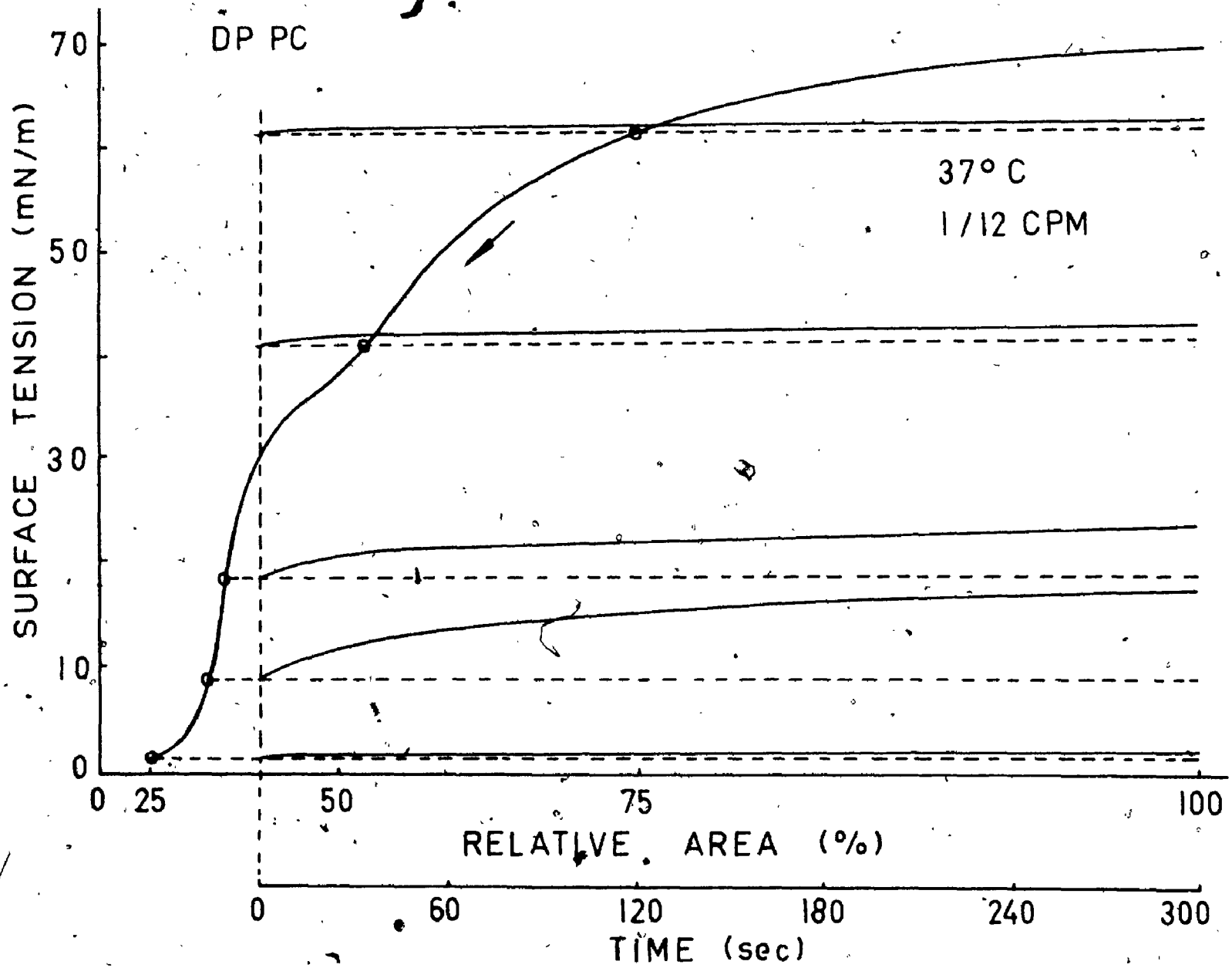
DP PC
37° C
1/12 CPM
SURFACE TENSION (mN/m)
70
50
30
10
0
0
25
50
75
100
RELATIVE AREA (%)
0
60
120
180
240
300
TIME (sec)

the stop was always smaller than 1.0 mN/m, regardless of the temperature, a criterion for stability (Phillips et al., 1968). After the first minute, the surface tension changed less than 0.1 mN/m per minute, indicating a state relatively close to the thermodynamic equilibrium. We are using these criteria to define the "quasi equilibrium state". In order to achieve a true equilibrium, we would have had to fulfill more rigorous conditions, such as an atmosphere saturated with the vapour of the monolayer material.

Below the limiting area, the film is no longer monomolecular, the surface tension rises much faster with time. For a surface tension of 5 to 10 mN/m, we observed the fastest change with time in the first 3 to 5 min after the stop. According to the criteria above, the film is no more in the "quasi equilibrium state".

However, it is very interesting to note that the film, once the minimum surface tension is reached, below 1 mN/m, is again in a much more stable state. The surface tension-time characteristic was observed for at least three hours. Within this time interval, the surface tension rose less than .3 mN/m. Since the film is compressed far beyond the limiting area, it is no longer a monolayer, but rather is characterized by a three dimensional structure which is very stable.

c) Surface potential-area hysteresis

Figure 13 shows the surface tension- and the surface potential-area diagrams of two films. In Figure 13a, the dashed line represents the surface tension-area loop of a monolayer which was spread to produce an initial surface tension of about 65 mN/m. For the unbroken line, more lecithin was spread, the maximum surface tension was initially about 50 mN/m. The expansion part of the unbroken line follows the dashed line; it is therefore omitted in the figure.

Figure 13b corresponds to the upper curve of 13a, Figure 13c to the lower curve of 13a.

The surface potential-area characteristics reach a first maximum in the compression part of the curve. Again, it is demonstrated that this maximum does not correspond to the minimum surface tension. After the first maximum, the surface potential decreases and follows then a horizontal part, corresponding with the horizontal section at minimum surface tension in Figure 13a. In the expansion phase, a second maximum of the surface potential is reached.

For Figure 14 much more lecithin was spread in order to produce the minimum possible surface tension, about 25 mN/m, at maximum trough area and for static conditions. Therefore, the film was already condensed

Figure 13: Surface tension- and surface potential-area diagrams of two films of different initial concentrations.

Figure 13a: The expansion part of the unbroken line follows the same path as the broken line.

Figure 13b: The dashed line corresponds to the upper curve of 13a.

Figure 13c: The unbroken line corresponds to the unbroken curve of 13a.

The surface potential-area loop demonstrates hysteresis and two maxima, the first in the compression part, the second in the expansion part of the curve.

Note: The maximum surface potential does not correspond to the minimum surface tension.

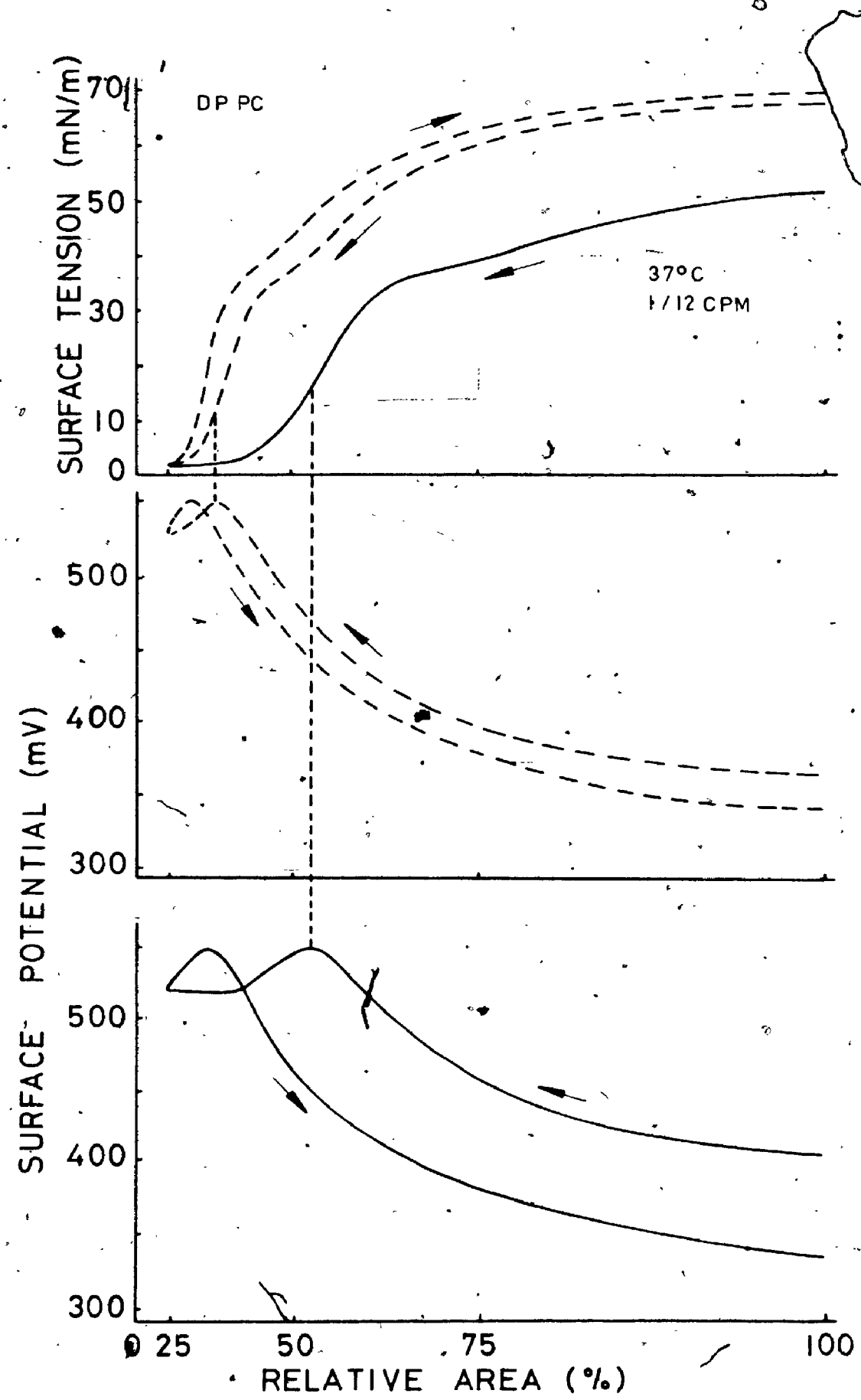
DP PC
37°C
1/12 CPM
SURFACE TENSION (mN/m)
70
50
30
10
0
500
400
300
SURFACE POTENTIAL (mV)
500
400
300
0
25
50
75
100
RELATIVE AREA (%)

Figure 14:

-------- surface tension- and

———— surface potential-area

hysteresis loops, simultaneously recorded

Compression was started from a condensed state of the film. A relatively large amount of lecithin was spread initially to produce the lowest minimum surface tension for static conditions, about 25 mN/m.

Note: The first maximum of the surface potential-area curve is relatively flat, due to the nonlinear area change. The rate of area change is much slower between 100% and 75% film area than between 50% and 25%.

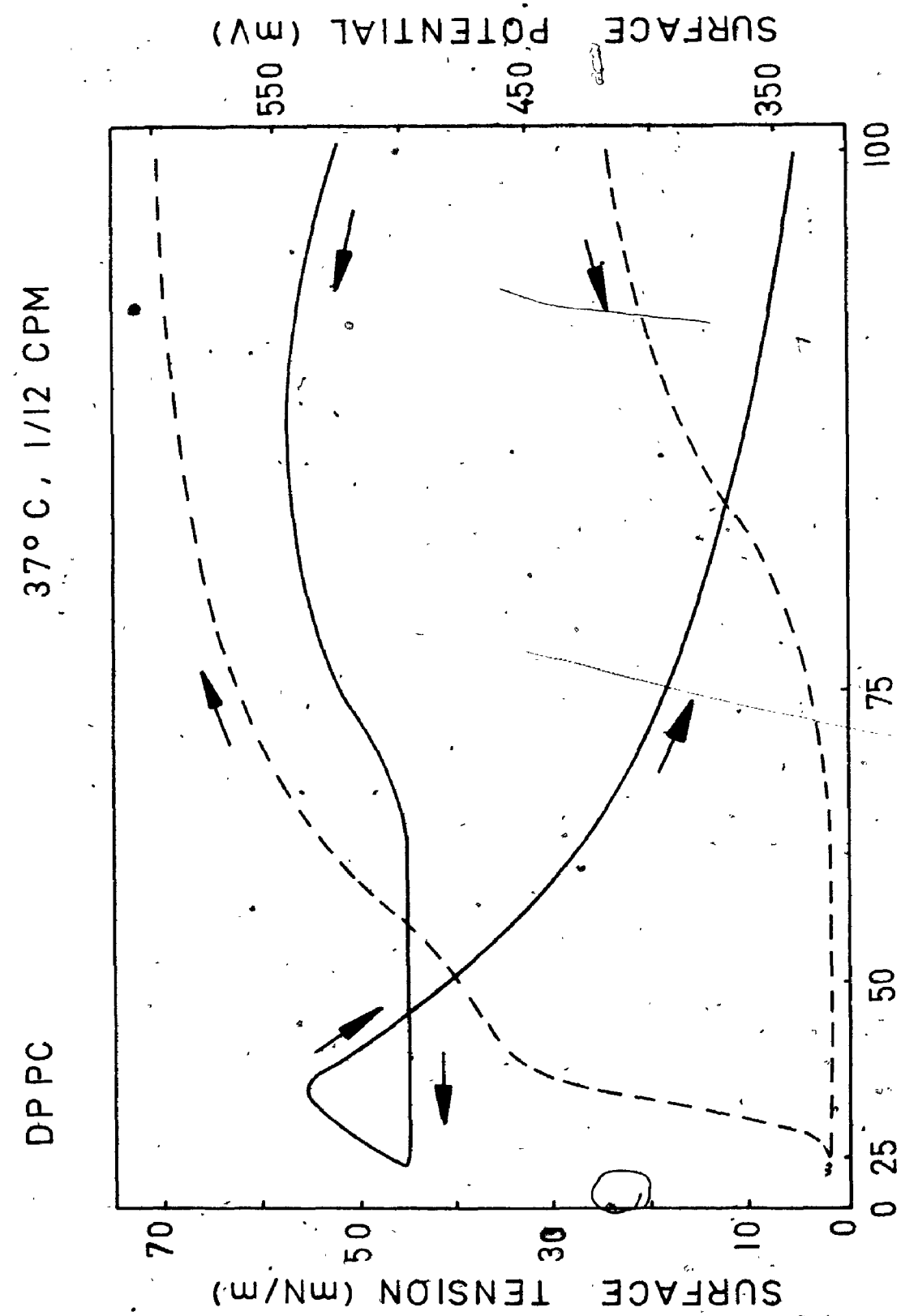
SURFACE POTENTIAL (mV)
550
450
350
100
75
50
25
0
RELATIVE AREA (%)
37° C, 1/12 CPM
DPPC
SURFACE TENSION (mN/m)
70
50
30
10
0

Figure 15: Hysteresis effect due to "loss" of film material during the horizontal part at minimum surface tension. The amount "lost" was determined by respreading the necessary lecithin for reproduction of a particular loop.

Figure 15a: shows three loops with different initial film concentration. The expansion phase of the curves follows an identical path.

Figure 15b: The lecithin quantities which had to be respread were determined six times, the MEAN values ± S.E. are plotted vs. the lengths of the horizontal parts. MP, MP', MP" ... etc.

Note: The experiments were done with the rhombic trough, this explains the greater uncertainty of the area at small areas. The area axis were linearized for the drawings.

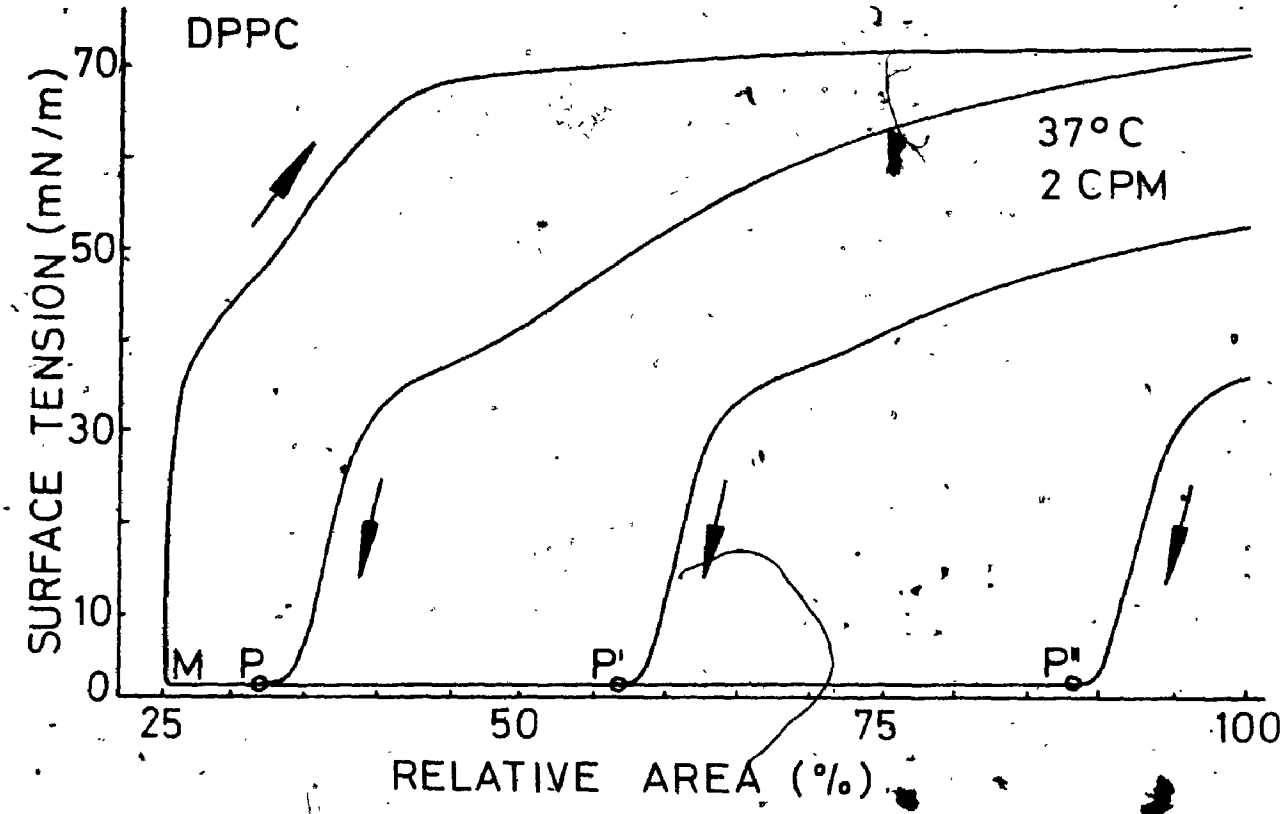
DPPC
37°C
2 CPM
SURFACE TENSION (mN/m)
70
50
30
10
0
M
P
P'
P''
25
50
75
100
RELATIVE AREA (%)

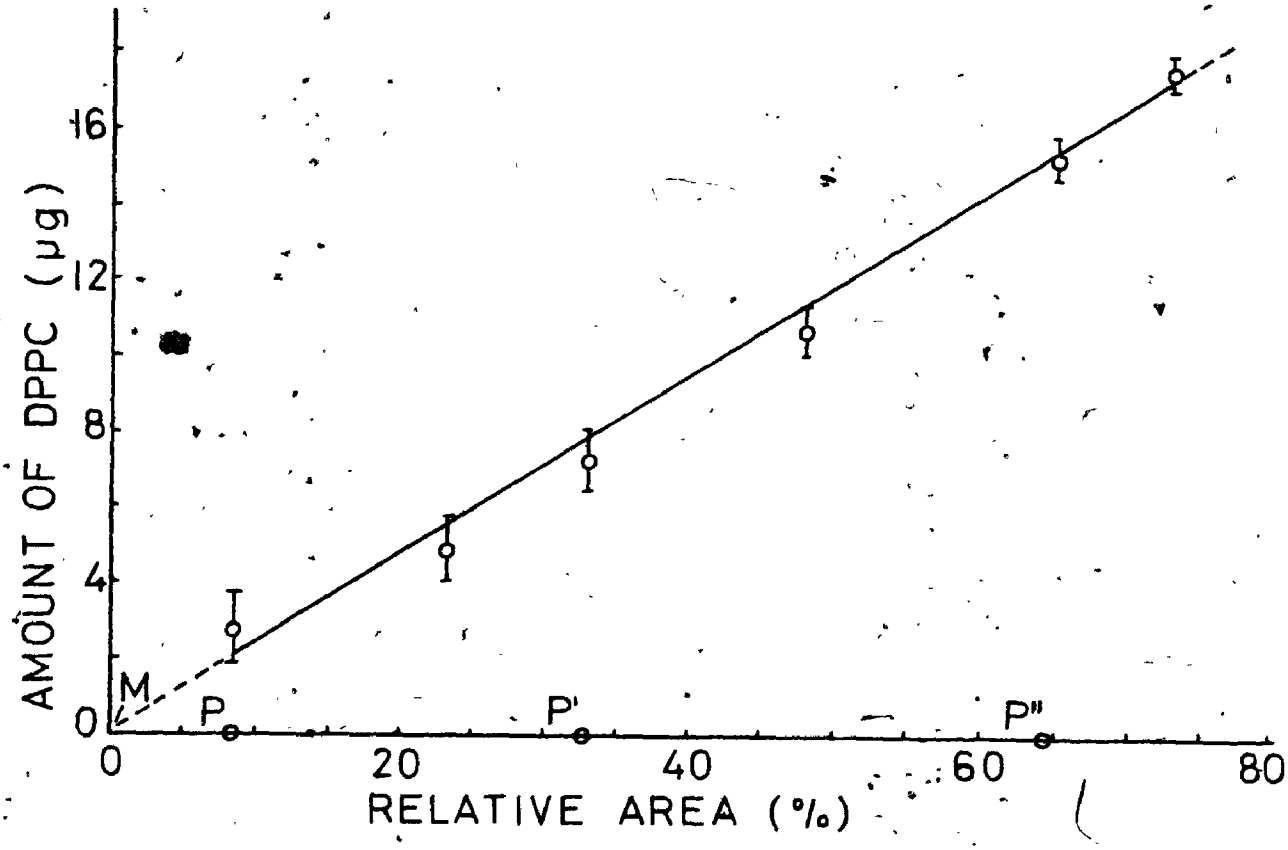
AMOUNT OF DPPC (μg)
16
12
8
4
0
M
P
P'
P''
0
20
40
60
80
RELATIVE AREA (%)

prior to compression. Again, there are two maxima of the surface potential. The horizontal part with the minimum surface tension close to zero corresponds to the horizontal part of the surface potential-area diagram. Upon expansion, the second maximum is reached.

d) Hysteresis and "loss" of film material

Figure 15a shows three curves from films spread to produce different initial surface tensions at maximum trough area. For all diagrams, the expansion parts followed an identical path. In order to reproduce a particular curve, a certain amount of lecithin had to be respread at maximum area, at the end of the expansion part.

In Figure 15b is demonstrated that the "loss" of film material is directly proportional to the horizontal part MP of the surface tension-area diagram, at minimum surface tension. This "loss" was determined by respreading the amount of lecithin necessary to reproduce a specific curve of Figure 15a. In 15b these quantities are plotted against the length of the horizontal parts MP, MP', MP", ... which represent relative film areas. Note, only three curves are shown in Figure 15a.

1. A monolayer with a surface tension of about 72 mN/m required 15 µg of DPPC for the initial spreading. It reached the minimum surface tension of approximately 1 mN/m at (25 to 30)% area. In order to reproduce this loop,

only 0.5 to 1 µg of lecithin had to be respread at 100% area.

2. To reproduce a curve from a highly condensed monolayer with the minimum possible surface tension for static conditions, about 25 mN/m required respreading of 15 - 16 µg of lecithin per cycle.

e) Development upon continuous cycling

For Figure 16, a monolayer was spread at maximum trough area and to produce an initial surface tension of about 55 mN/m. The temperature was 37°C, the film was compressed and expanded continuously at a speed of 2 cycles/min. Loops no. 1, 10 and 200 are shown. Cycling was continued up to loop no. 600. As we have demonstrated in Figure 15, the loss of film material occurs during the horizontal part, at near zero minimum surface tension. Therefore, it is not surprising that the loop areas become smaller and smaller, the horizontal part at minimum surface tension disappears quickly, after three to five curves. However, the minimum surface tension of less than 1 mN/m is maintained for several hundred successive cycles. Only after about 500 curves, a small increase of about 1 to 3 mN/m could be observed.

7.2.4 Discussion

a) Surface tension-area studies

A number of papers have been published about equilibrium properties of lecithin monolayers. (Phillips et al.,

Figure 16: Development of hysteresis loops from DPPC films upon continuous and successive cycling.

Figure 16a: Loop no. 1

Figure 16b: Loop no. 10

Figure 16c: Loop no. 200

Note: Loop no. 600 could not be distinguished from loop no. 200.

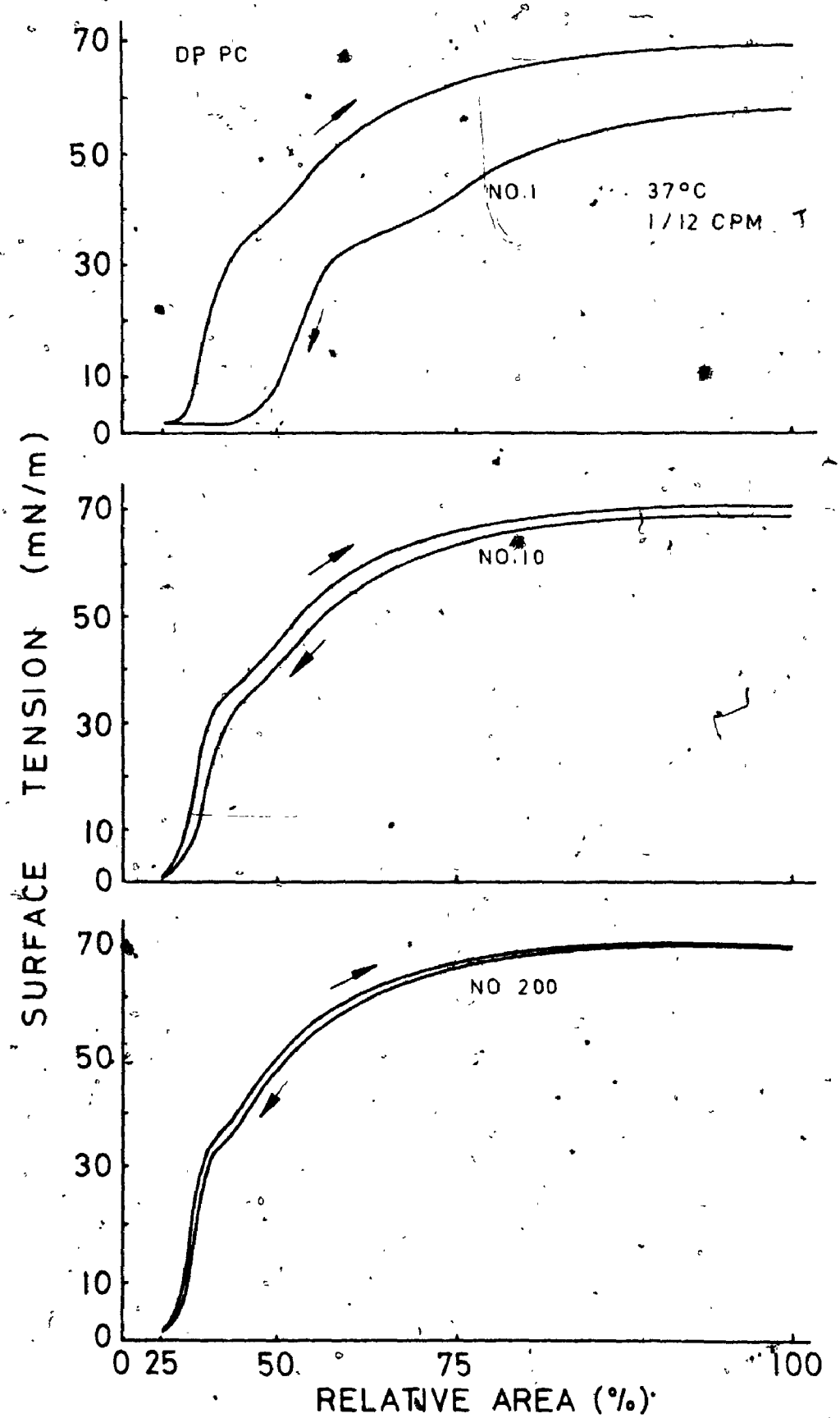
DP PC
NO.1
37°C
1/12 CPM
NO.10
NO 200
70
50
30
10
0
SURFACE TENSION (mN/m)
0 25 50 75 100
RELATIVE AREA (%)

1968, Vilallonga, 1968, Vilallonga et al., 1969, Hayashi et al., 1972). Phillips et al. (1968) pointed out that the marked phase transitions from the liquid expanded to the condensed state are an indication for the purity of the DPPC film material. Since our monolayers demonstrate these transitions clearly and from the good reproducibility of the data, we conclude that the lecithin used was pure. According to the manufacturer, DPPC has a purity better than 99%. We have seen that films from DPPC are stable and in the "quasi equilibrium state", if they are not compressed beyond the limiting area. At the limiting area, the surface tension is approximately 25 mN/m. Since at 25 mN/m the monolayer is most closely packed, a structural change must occur upon further compression. The layer might fold up to a more three dimensional film. (This will be discussed later, see Figure 18).

In Figure 12 we have demonstrated that the film is less stable below 25 mN/m. However, at the minimum possible surface tension, less than 1 mN/m, the films were at least as stable for an arbitrarily chosen time interval of about three hours as in the "quasi equilibrium state", above the limiting area, even at temperatures up to 40°C. Munden and Swarbrick (1973b) report that higher surface pressures were obtainable with lung surfactant than with DPPC. The reason for these findings may be less purified lecithin or leaks from the surface tray, since without exception, our

DPPC films produced lower minimum surface tensions or higher maximum surface pressures than lung surfactant.

b) The hysteresis effect

This effect is due to squeezing out of molecules, mainly at the lowest possible minimum surface tension, below 1 mN/m. This "loss" of film material is characterized by the horizontal part at the bottom of the hysteresis loop. Upon successive cycling by squeezing out of molecules, the compression part comes closer to the expansion part with less and less hysteresis effect. But near zero surface tension is still achieved at minimum film area.

Colacicco et al. (1973), p. 391, demonstrate no. 1 and no. 10 of a series of DPPC curves. Loop no. 10 shows a minimum surface tension of about 12 mN/m. Under no circumstances except in the case of leaks or contamination did the surface tension of a pure DPPC film rise in such a way, for temperatures from 20°C up to 40°C and for the speed range from 1/12 cycle/min to 8 cycles/min.

c) Surface potential-area diagrams

The maximum value of the surface potential in the compression part corresponds to a state of the film just below the limiting area of the molecule, but definitely above the one with the minimum surface tension of less than 1 mN/m. In

$$\Delta V = \frac{1}{\varepsilon} \Delta(Np_n) \qquad (3.8)$$

$p_n = p\cos\theta$ is the vertical component of the dipole moment.

In the literature about surface chemistry, it is assumed that the molecules are more and more vertically oriented during the compression of the film. We would therefore expect a non linear contribution to the surface potential due to this orientation. The permittivity ε is taken as constant and equal to ε_o, the vacuum permittivity. Colacicco (1971) criticizes the capacitor model, since it requires free charges. The dipole layer is a system of neutralized charges.

Our experimental data reveal a linear relationship between the dipole density and the surface potential. The marked change of the slope in P' of Figure 11b could be attributed to a sudden change of the dipole orientation or, what we think as being more likely, a change of the electrical environment of the polar heads. The polar end groups may be hydrated in the liquid expanded state (Kezdy, 1972, p. 137). Upon compression and condensation, the water molecules may be squeezed out, causing a change of the electrical field around the polar heads. Phillips (1972), pp. 159-167, points out that the understanding of the hydration and conformation of the polar head groups are limited and that it is still uncertain how hydration is contributing to the free energy of the monolayer. On the next pages we will describe possible simple mechanisms for the surface tension and surface potential area characteristics.

Figure 17c demonstrates what might happen at P' of Figure 11b. At an area per molecule, short of P', the polar heads are still hydrated, the dipole moments of the water molecules are opposite to the dipole moments of the DPPC molecules. Upon further reduction of the area, the water molecules are squeezed out, the dipole moment per unit area increases and therefore the surface potential increases, resulting in a change of the slope. From equation (3.8) we see that the surface potential is dependent on the number of dipoles per unit area.

Since the maximum surface potential does not correspond to the limiting area of the film, we conclude a higher dipole density upon compression beyond the limiting area.

Figure 18a illustrates the monolayer in the closest packed state, at the limiting area of the molecule. In Figure 18b, the film is folding up and produces a higher dipole density and therefore a bigger surface potential. This might illustrate approximately the situation at maximum surface potential.

In Figure 18c, parts of the layer are pushed into bimolecular structures. There are less dipoles vertically oriented per unit area, which means a lower surface potential. Upon further compression, in Figure 18d, the top parts of Figure 18c are closing in on each other to form

Figure 17: Dipole orientation of the DPPC molecule

Figure 17a: It represents the dipalmitoyl phosphatidyl choline (DPPC) molecule.

Each of the hydrophobic tails contains sixteen carbon atoms. The dipole of the polar head is vertically oriented.

Figure 17b: DPPC molecule, schematically, with vertical orientation of the dipole.

Figure 17c: In the first group, of three molecules, the polar heads are hydrated. The dipoles of the water molecules are opposite to the DPPC dipoles.

The second group demonstrates the situation after squeezing out of the water molecules.

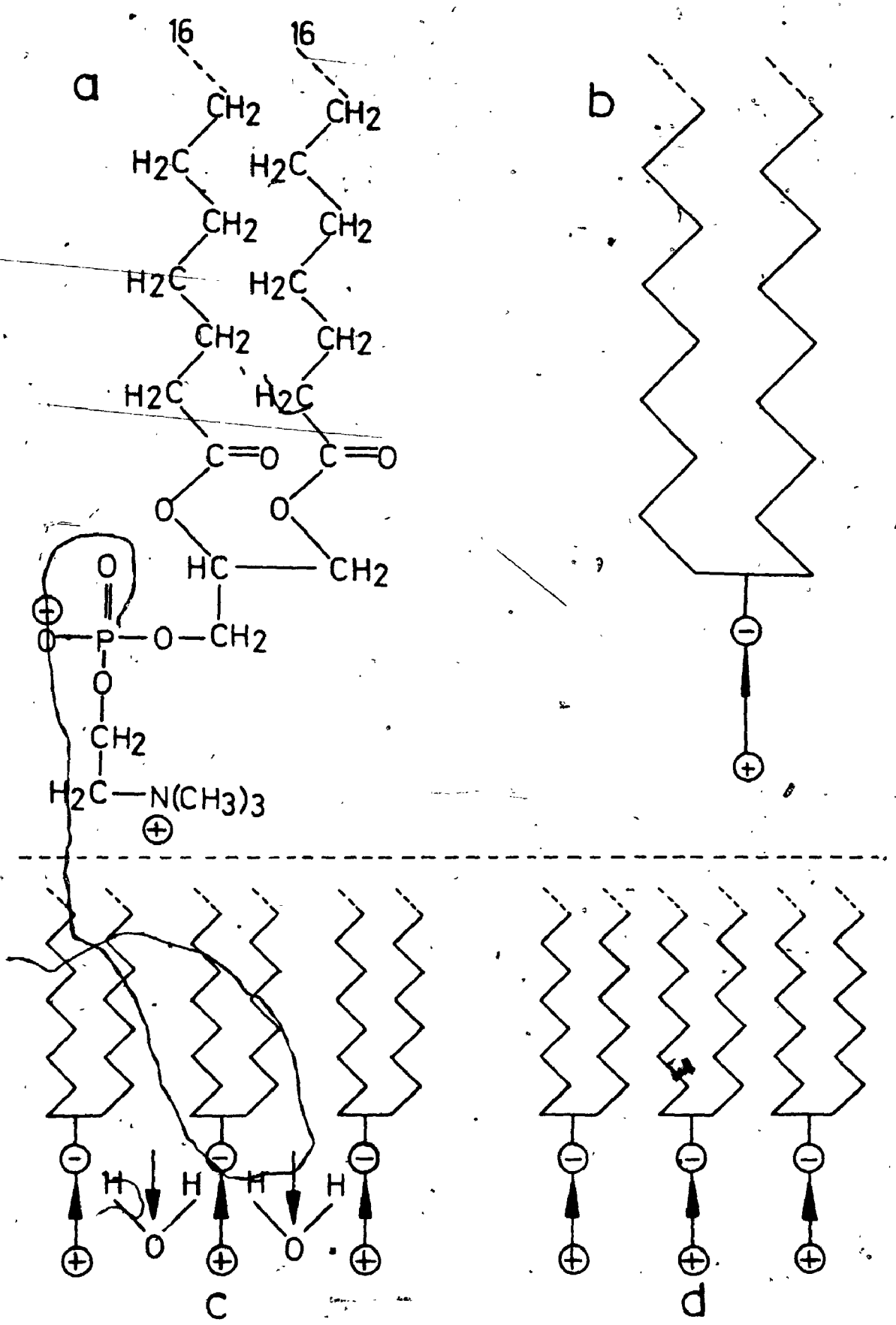
a
16
16
CH2
CH2
H2C
H2C
C=O
C=O
O
O
HC
CH2
O
P
O
CH2
H2C—N(CH3)3
b
H
O
c
d

Figure 18: Compression of the DPPC film (model)

Figure 18a: The DPPC monolayer in the closest packed state, at the limiting area

Figure 18b: Situation after further compression

Figure 18c: On even stronger compression, a three-dimensional structure is being built.

Figure 18d: Micellular structures appear separated from the rebuilt monolayer.

On continuous compression, these micellular bodies are progressively squeezed out and migrate into the subphase.

Note: The maximum surface potential in the compression part corresponds to Figure 17b, where the dipole density is greater than in 17a.

For further comment see text.

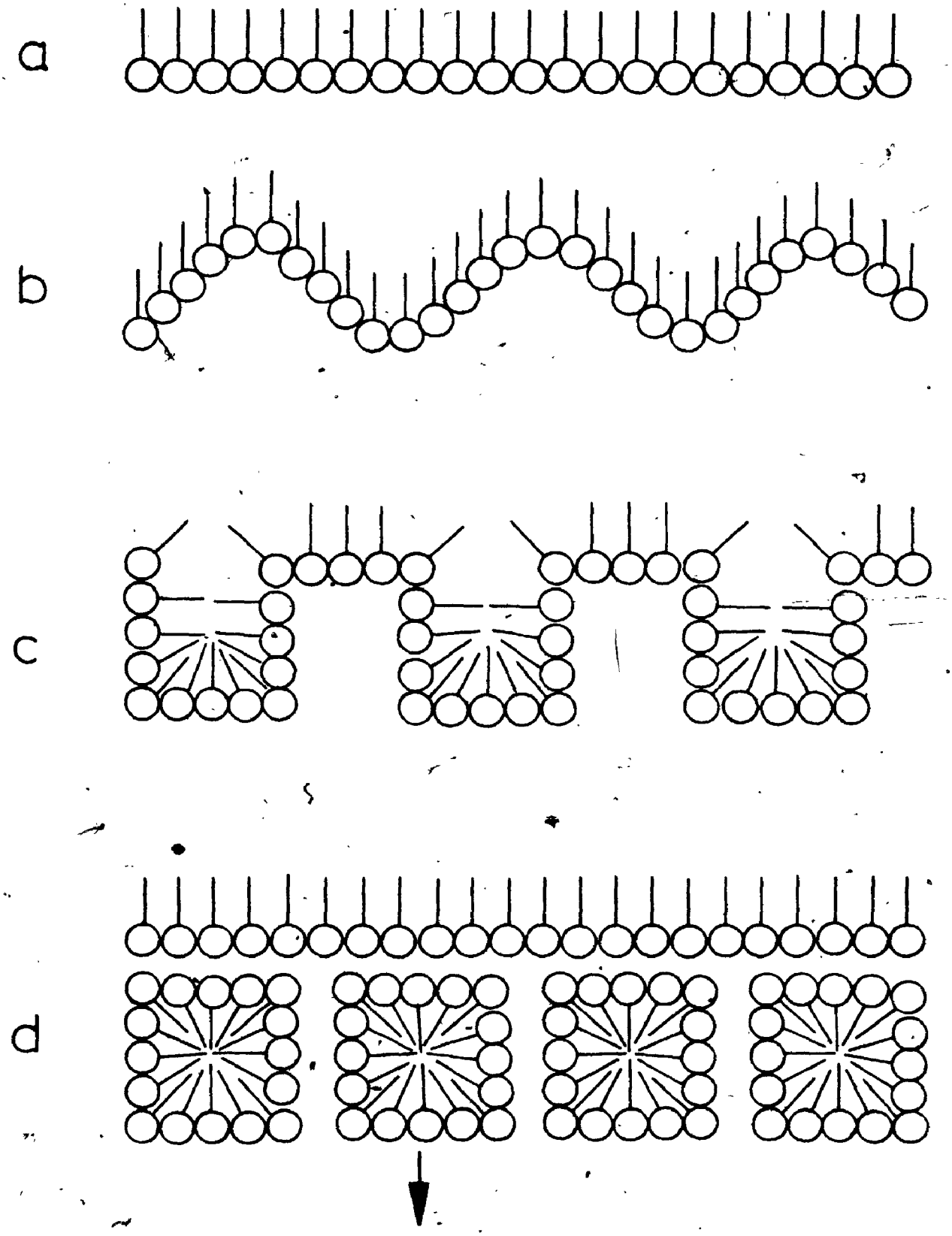
a
b
c
d

again a more or less continuous film. The bimolecular structures are transformed into micellular particles which then are pushed into the subphase. This process corresponds to the horizontal part in the surface potential-area diagram of Figure 14. The surface potential is approximately constant, but not at its maximum value as it is in Figure 18b.

Since there is a second maximum in the expansion part of the surface potential curve, the situation of 18b might be restored when the lateral pressure is released.

7.2.5 Influence of chain length and unsaturation on dynamic properties of phosphatidyl choline films

a) Introduction

The behaviour of lecithin molecules in monolayers are controlled by two mechanisms:

- the short range interaction between methylene groups of adjacent hydrocarbon chains (Van der Waals interaction)
- interaction in the polar region, which depends on many factors, like hydration or electrostatic interaction between ionized groups and the subphase ions. Lecithin is a zwitterion and therefore has no net charge. Between pH 4 and 9 it is a neutral phospholipid, not sensitive to the presence of ions in the subphase (Colacicco, 1971, Hayashi, 1972).

If the hydrocarbon chains are sufficiently long, condensed monolayers will be formed, while shorter chains produce expanded monolayers. Lowering of the temperature can cause the monolayer to become completely condensed, even if it was fully expanded at higher temperatures. Subtracting two methylene groups from each chain of the lecithin molecule, is approximately equivalent to raising the temperature by about 20°C (Phillips et al., 1968, p. 307).

Double bonds between the carbon chains (unsaturation) have an expanding effect. The chains are then less hydrophobic and act against closest possible packing.

b) Results

Figures 19 - 23 illustrate the experiments concerning chain length and unsaturation. The curves were drawn on the basis of at least four independent experiments each. (For comment see the legends to the figures).

7.2.6 Films with phosphatidyl glycerol, PG (C16 : 0) and phosphatidyl serine, PS (C16 : 0)

a) Introduction

These phospholipids have charged polar heads. The behaviour of their films will therefore be much more influenced by pH and the ionic content of the subphase than zwitterionic compounds. The pH of the subphase for all experiments with PG and PS was always between 6.4 and 6.6.

Figure 19: Influence of chain length on surface tension and surface potential-area characteristics, of phosphatidyl choline films.

Figure 19a: The surface tension-area curve of distearoyl PC (C18 : 0) is more condensed than the one from dipalmitoyl PC (C16 : 0), (DPPC).

Figure 19b: The monolayer from dimyristoyl PC (C14 : 0) is more expanded than the monolayers in Figure 19a. The minimum surface tension is about 20 mN/m, considerably higher than for PC (C16 : 0) or PC (C18 : 0). The maximum surface potential is about 450 mV. For PC (C18 : 0) it is approximately 580 mV.

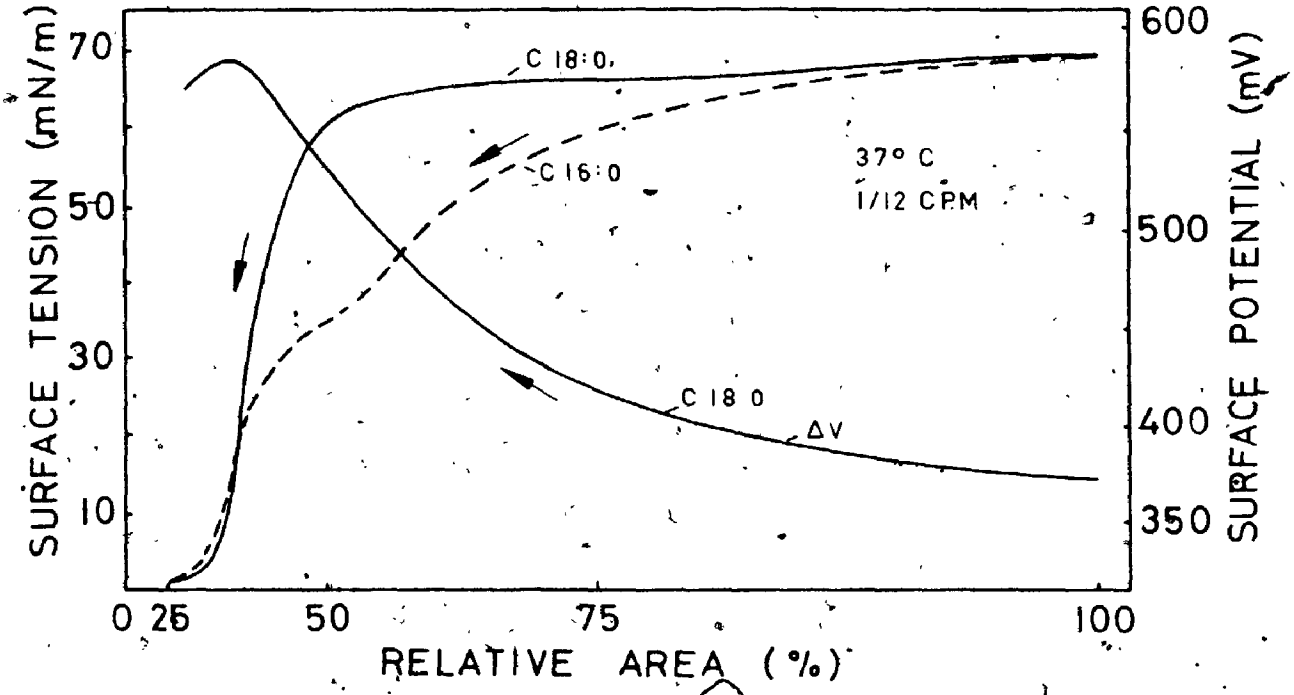
SURFACE TENSION (mN/m)
70
50
30
10
600
500
400
350
SURFACE POTENTIAL (mV)
C 18:0
C 16:0
37° C
1/12 CPM
C 18 0
ΔV
0 25
50
75
100
RELATIVE AREA (%)

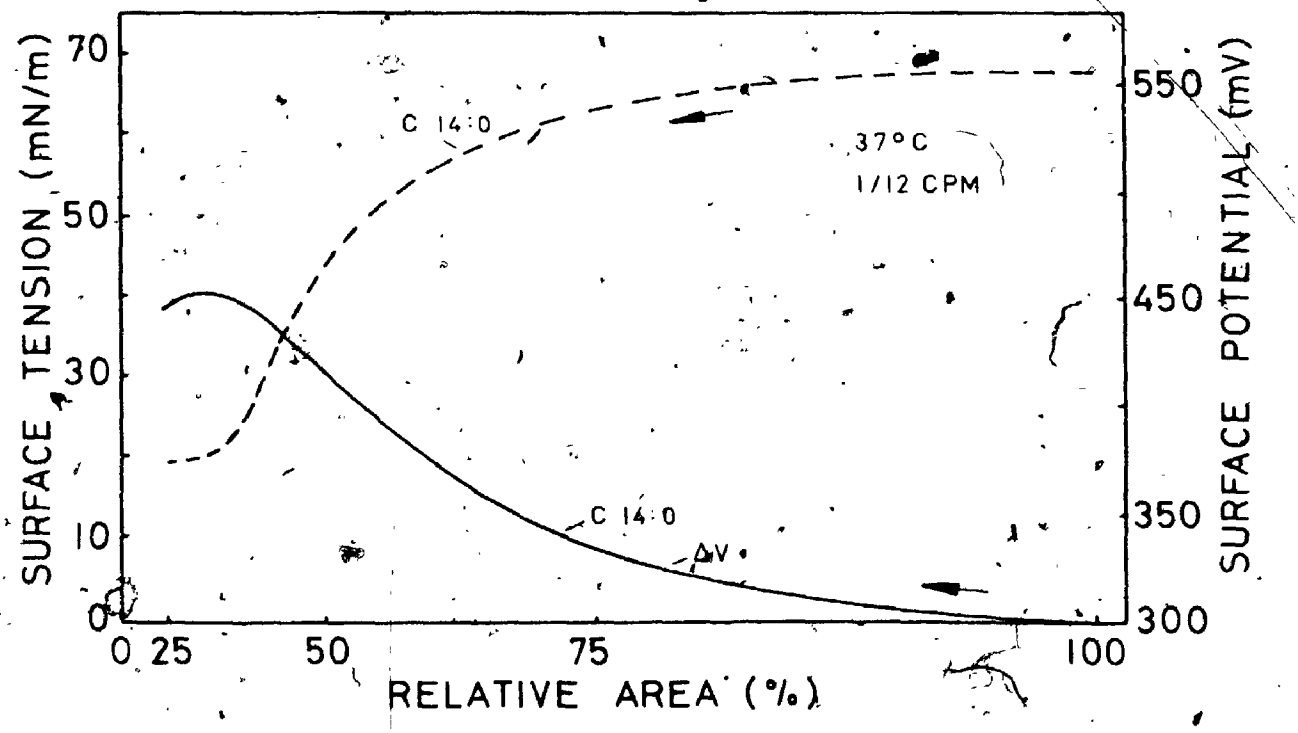
SURFACE TENSION (mN/m)
70
50
30
10
0
550
450
350
300
SURFACE POTENTIAL (mV)
C 14:0
37°C
1/12 CPM
C 14:0
ΔV
0 25
50
75
100
RELATIVE AREA (%)

Figure 20: Films of PC (C14 : 0)

Figure 20a: Single monolayer experiments with dimyristoyl PC (C14 : 0). The minimum surface tension is dependent on the cycling speed; at 1/12 cycle/min, it is about 20 mN/m, at 8 cycles/min about 15 mN/m.

Figure 20b: Development of hysteresis loops on continuous cycling. The film was spread initially at 100% area and to produce a surface tension of about 50 mN/m. Loops no. 2 and no. 50 are shown.

Figure 20c: It represents loop no. 10 of a series of successive curves. The film was spread from a mixture of PC (C16 : 0) : PC (C14 : 0) = 1 : 1, by mass.

Note: A relatively large amount of PC (C14 : 0) in a mixed film with PC (C16 : 0) does not prevent the surface tension from reaching near zero values.

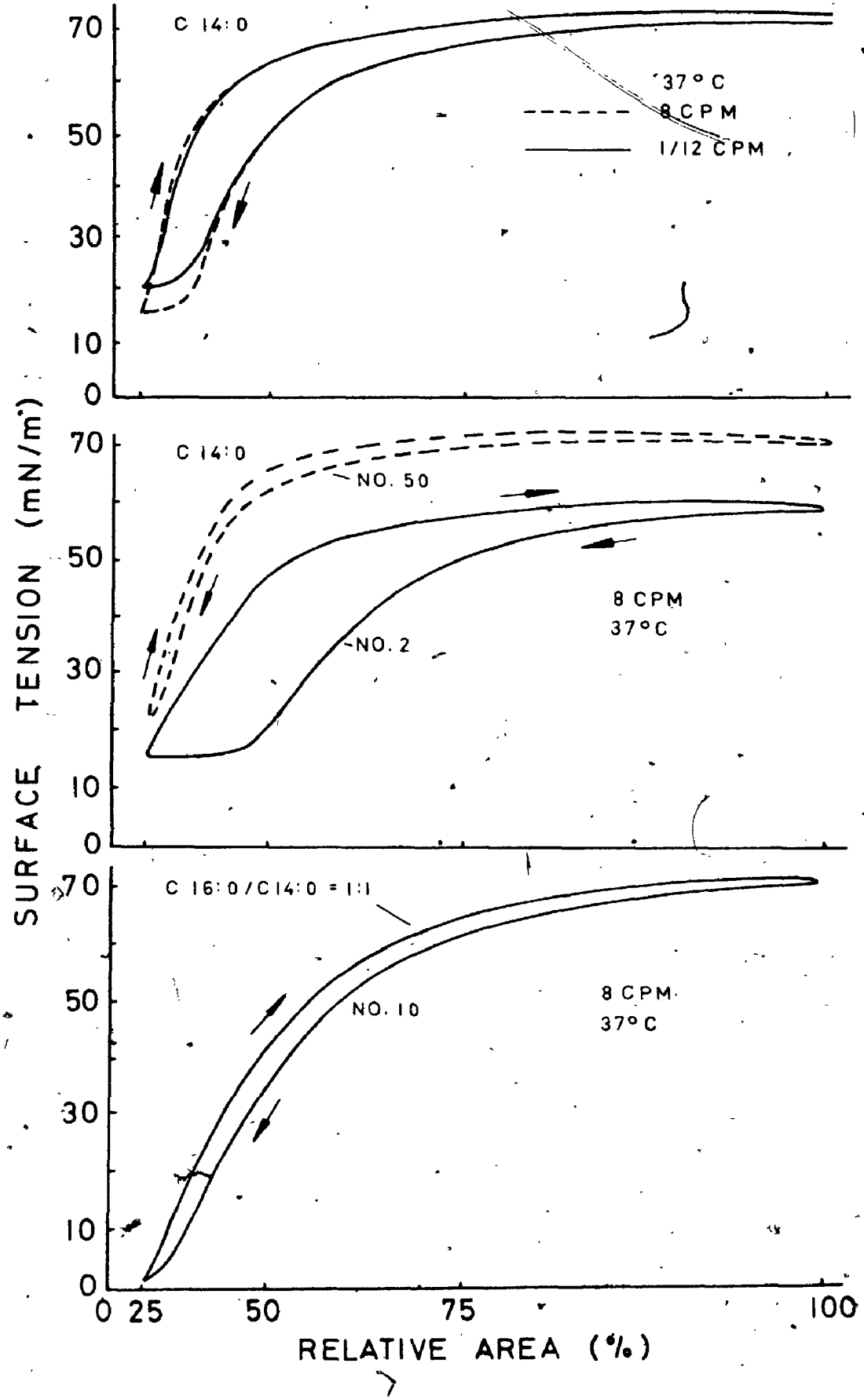
C 14:0
37°C
8 CPM
1/12 CPM
C 14:0
NO. 50
NO. 2
8 CPM
37°C
C 16:0/C14:0 = 1:1
NO. 10
8 CPM
37°C
SURFACE TENSION (mN/m)
RELATIVE AREA (%)
0
10
30
50
70
0 25 50 75 100

Figure 21: Effect of unsaturation on the surface tension- and surface potential-area characteristics.

Figure 21a: The monolayer of PC (C18 : 1) produces a minimum surface tension of about 25 mN/m at 25% area. The minimum surface tension of the saturated PC (C18 : 0) reaches near zero surface tension at minimum film area. The maximum surface potential of PC (C18 : 1) is only about 430 mV, as compared to PC (C18 : 0), with approximately 580 mV (Figure 19a).

Figure 21b: The effect of three double bonds is even more dramatic. The minimum surface tension of the PC (C18 : 3) film is about 33 mN/m. The maximum surface potential is only about 370 mV.

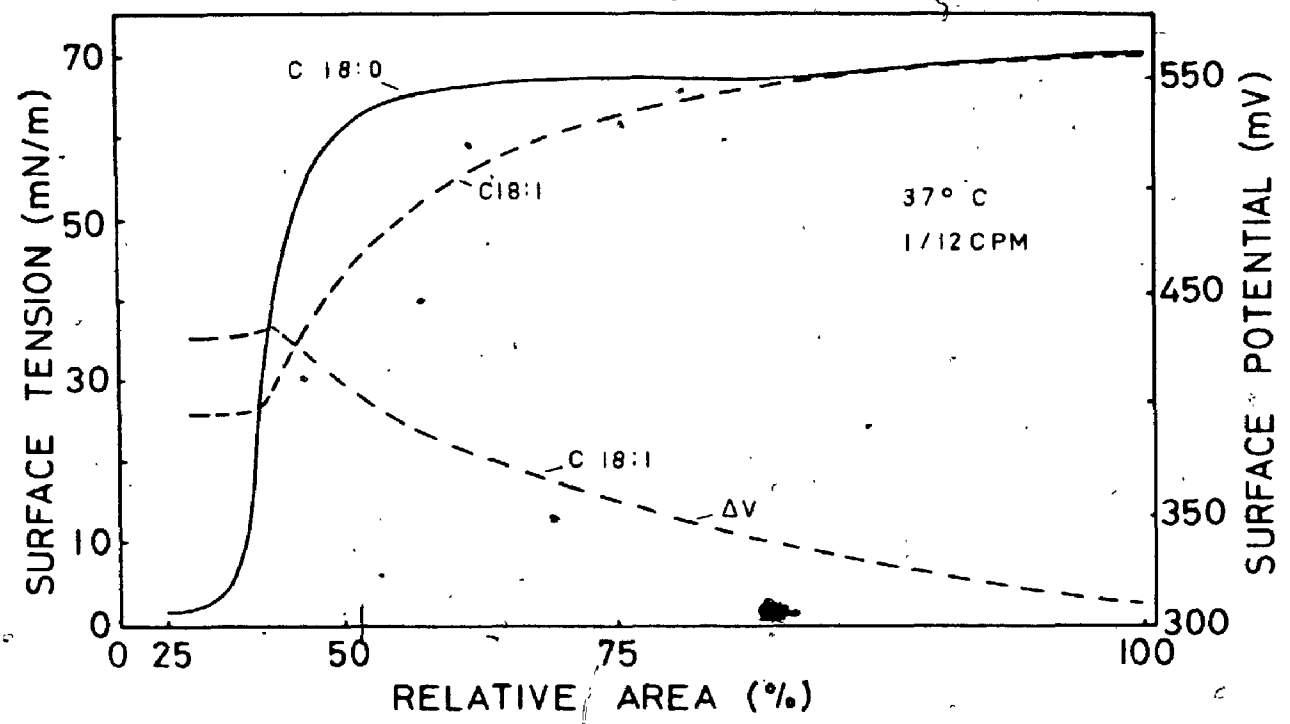
SURFACE TENSION (mN/m)
70
50
30
10
0
C 18:0
C18:1
37° C
1/12 CPM
C 18:1
ΔV
550
450
350
300
SURFACE POTENTIAL (mV)
0 25
50
75
100
RELATIVE AREA (%)

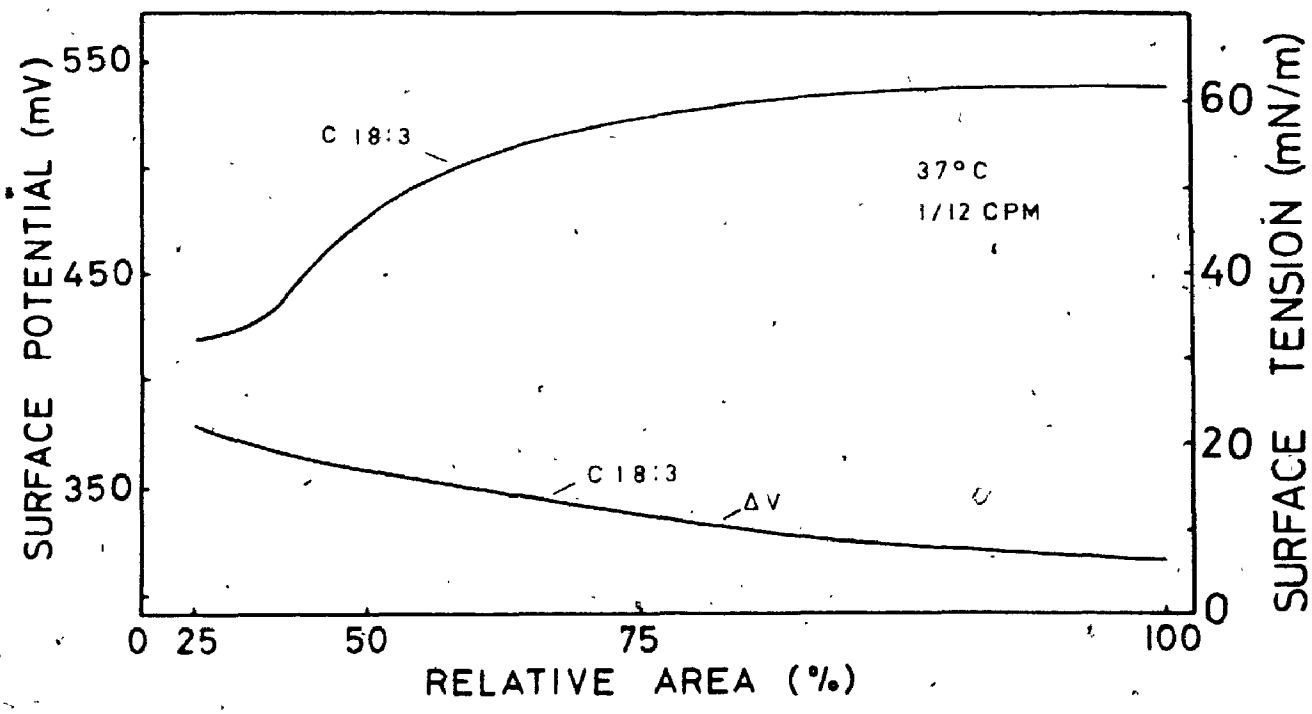
SURFACE POTENTIAL (mV)
550
450
350
C 18:3
37°C
1/12 CPM
C 18:3
ΔV
60
40
20
0
SURFACE TENSION (mN/m)
0 25
50
75
100
RELATIVE AREA (%)

Figure 22: Time dependent behaviour of mixed films

Figure 22a: Surface tension-area characteristic of a mixed film of PC (C18 : 0) and PC (C18 : 3) = 1 : 1, by mass. The compression part of the curve shows a plateau at about 28 mN/m.
In additional experiments cycling was stopped at P and Q and the surface tension was plotted against time.

Figure 22b: Surface tension-area characteristic of a mixed film of PC (C16 : 0) and PC (C18 : 3) = 1 : 1, by mass. The dashed line represents the curve at a speed of 2 cycles/min, the solid line the one at 8 cycles/min. In additional experiments, cycling was stopped at R and S and the surface tension was plotted against time. The figure demonstrates that the minimum surface tension at 8 cycles/min is due to the dynamic behaviour.

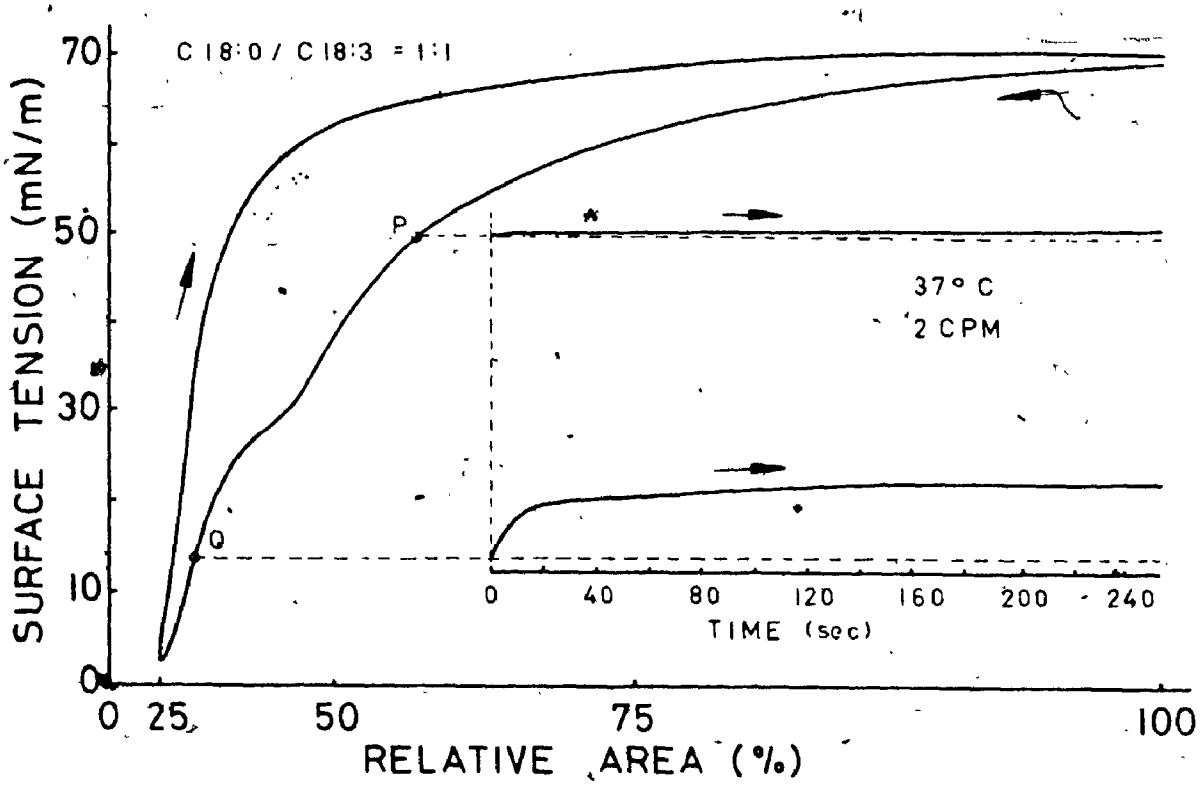
C 18:0 / C 18:3 = 1:1
SURFACE TENSION (mN/m)
70
50
30
10
0
P
Q
37° C
2 CPM
0
40
80
120
160
200
240
TIME (sec)
0
25
50
75
100
RELATIVE AREA (%)

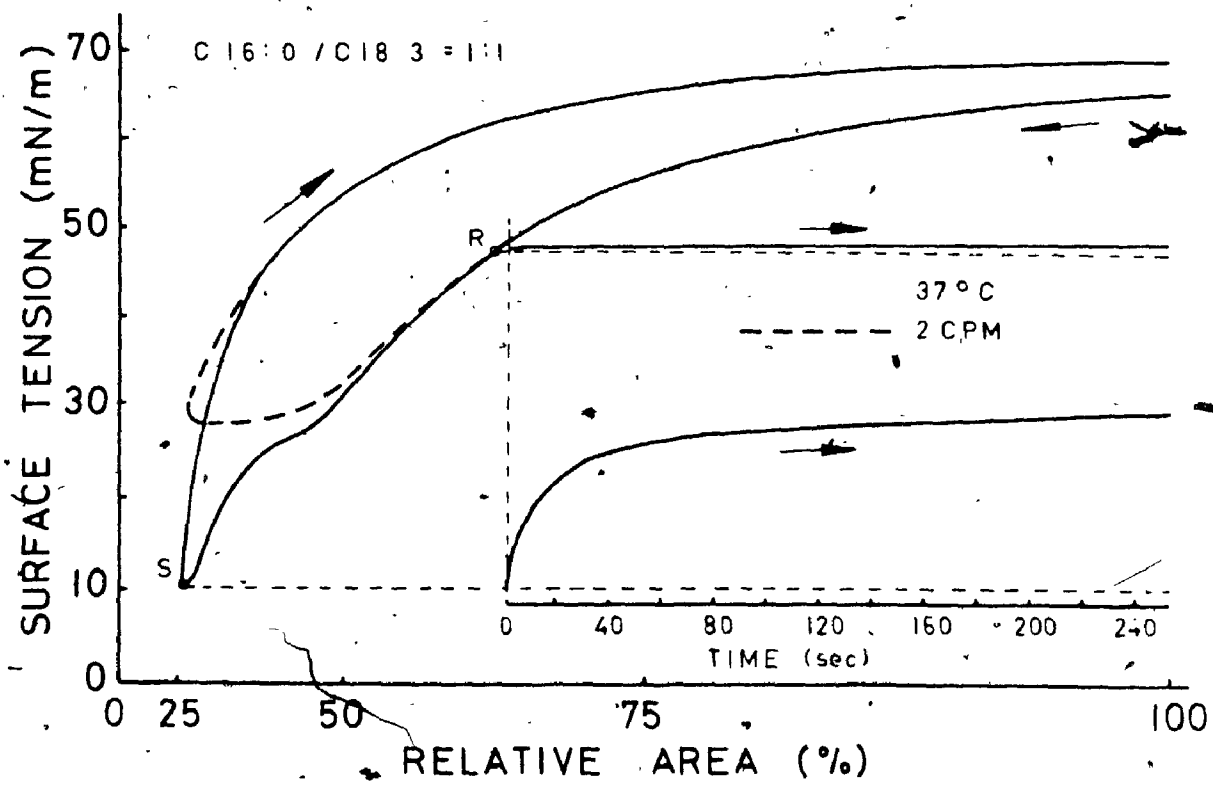
C 16:0 / C 18 3 = 1:1
SURFACE TENSION (mN/m)
70
50
30
10
0
R
S
37° C
2 CPM
0
40
80
120
160
200
240
TIME (sec)
0
25
50
75
100
RELATIVE AREA (%)

Figure 23: Mixed films of various mixing ratios

Figure 23a: Surface tension-area characteristics of monolayers of various mixing ratios (by mass), of PC (C16 : 0) and PC (C18 : 3).

It demonstrates that the minimum surface tension decreases with increasing content of PC (C16 : 0).

Figure 23b: Surface potential-area characteristic of a mixed monolayer of PC (C16 : 0) : PC (C18 : 3) = 8 : 1, by mass.

E indicates the beginning of the separation process. The PC (C18 : 3) molecules are squeezed out in favour of the PC (C16 : 0) molecules, which are then responsible for the further increase of the surface potential. More examples for this separation of components in a mixed film will be demonstrated later.

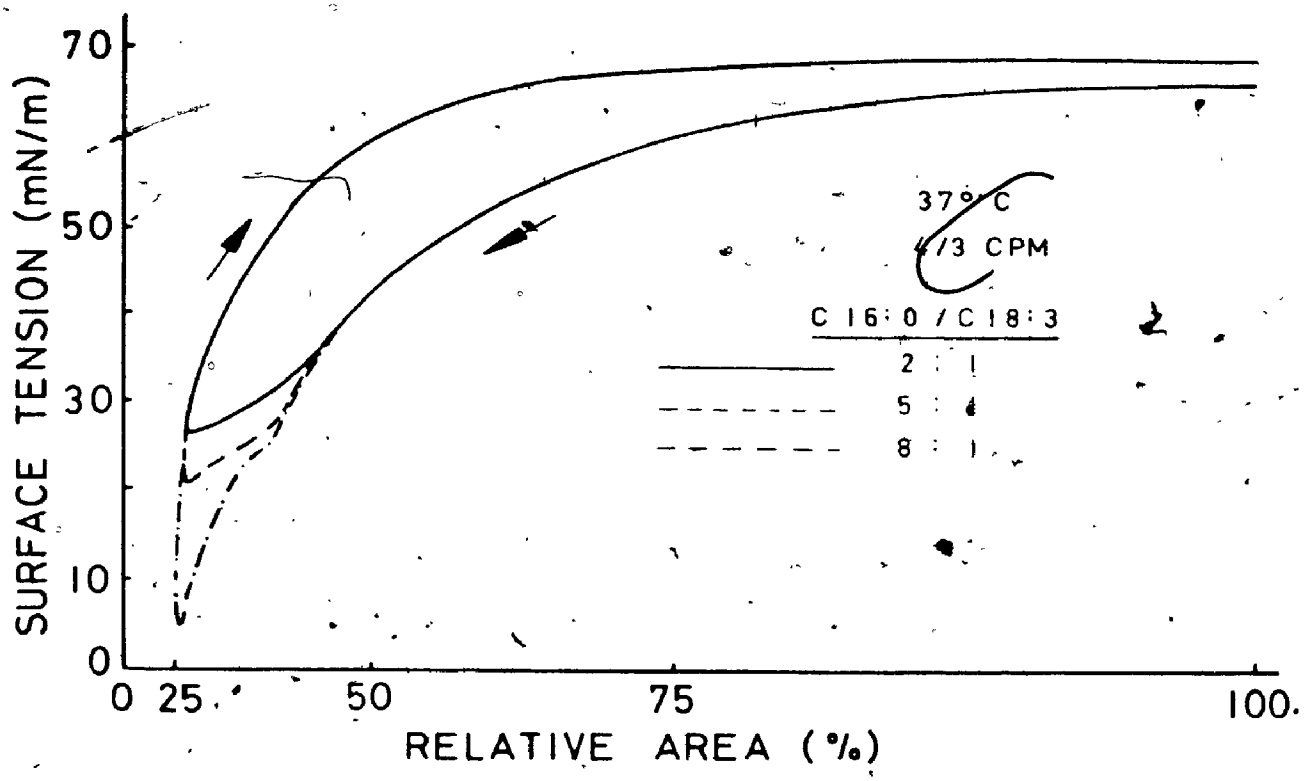
SURFACE TENSION (mN/m)
70
50
30
10
0
0 25 50 75 100
RELATIVE AREA (%)
37° C
4/3 CPM
C 16:0 / C 18:3
2 : 1
5 : 4
8 : 1

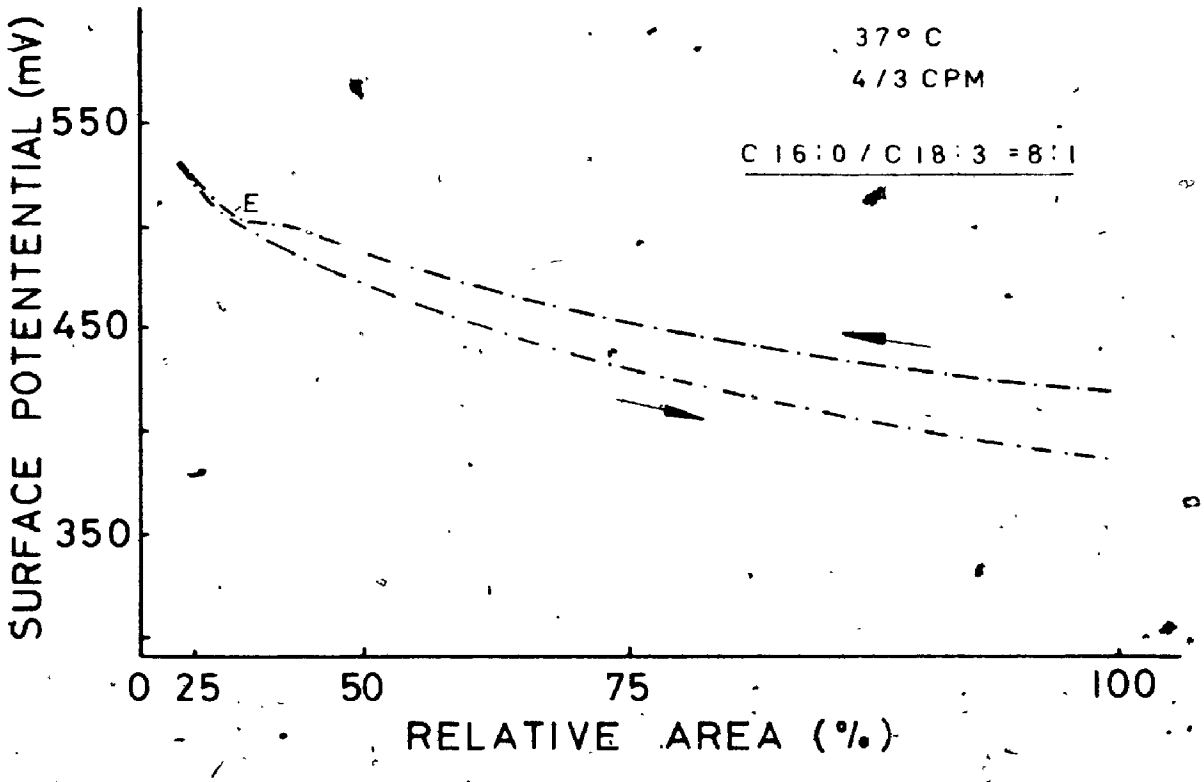
SURFACE POTENTIAL (mV)
550
450
350
0 25 50 75 100
RELATIVE AREA (%)
37° C
4/3 CPM
C 16:0 / C 18:3 = 8:1
E

b) Results

The following figures illustrate experiments with PG and PS. The curves are drawn on the basis of at least four independent experiments.

Figure 24a shows the compression part of a PG (C16 : 0) film. The minimum surface tension is approximately 30 mN/m at 1/12 cycle/min and 37°C. The broken line represents the curve from a PC (C16 : 0) monolayer. For both films, equal amounts (mass) of material were spread at maximum trough area. The PG curve is more expanded than the one from PC. The reason is most likely the different polar head, since the hydrocarbon tails are identical for both molecules. Interactions in the region of the polar head may also be the reason for the higher minimum surface tension.

Figure 24b demonstrates the development of continuously cycled hysteresis loops from a PG (C16 : 0) film. It was spread initially at maximum area and to produce an initial surface tension of about 50 mN/m. Loops no. 2 and 60 are shown on the figure. Due to a dynamic effect, the minimum surface tension is here, with 2 cycles/min about .4 mN/m lower than at 1/12 cycle/min (see Figure 24a).

Figure 25a shows the surface tension-area characteristics of mixed monolayers from PC (C16 : 0) and PG (C16 : 0).

Figure 24: PG films

Figure 24a:

———— The unbroken line shows the compression part of a PG (C16 : 0) monolayer.

-------- The broken line represents the compression part of a PC (C16 : 0) monolayer.

For both layers, equal amounts (mass) of film material was spread at 100% area.

Figure 24b: It demonstrates the development of continuously cycled hysteresis loops, from a PG (C16 : 0) film.

Loops no. 2 and no. 60 are shown.

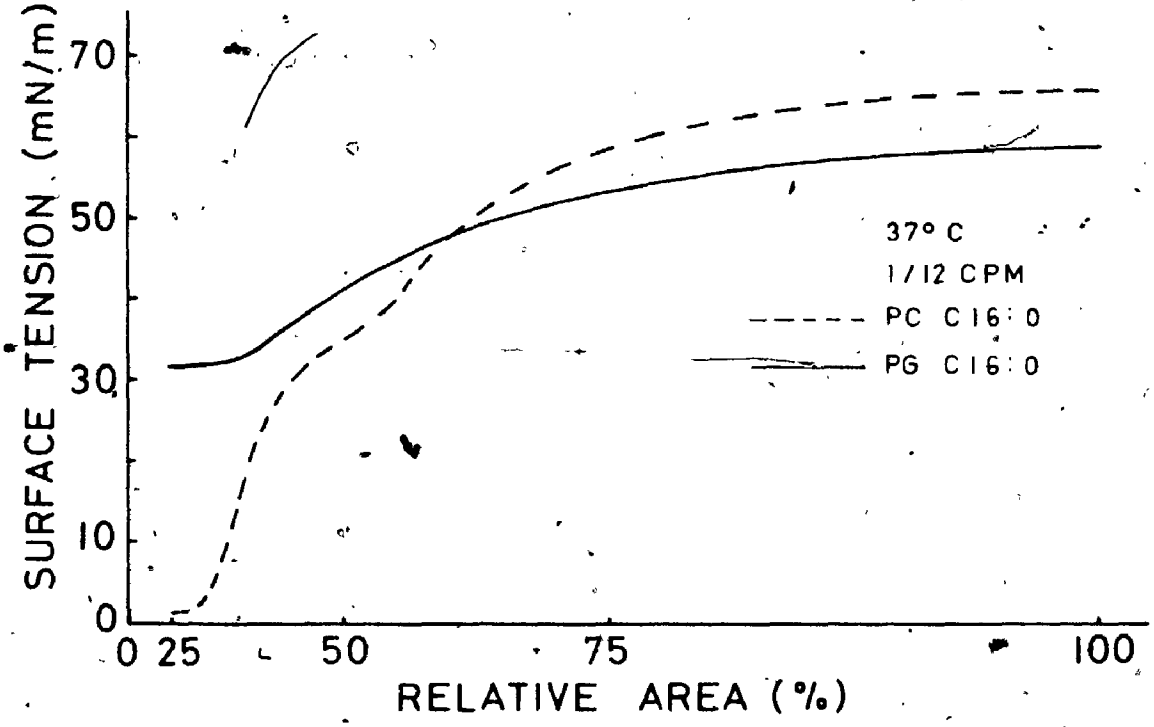
SURFACE TENSION (mN/m)
70
50
30
10
0
0 25
50
75
100
RELATIVE AREA (%)
37° C
1/12 CPM
PC C16:0
PG C16:0

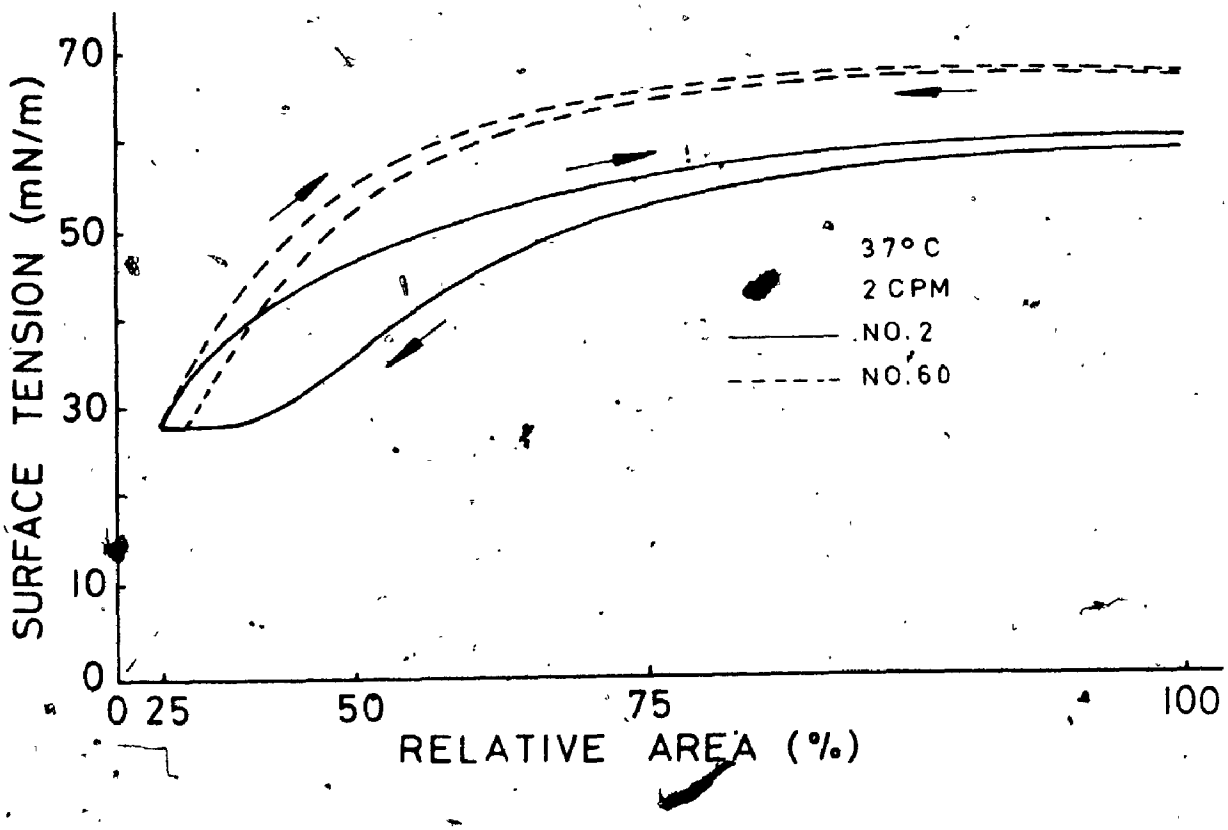
SURFACE TENSION (mN/m)
70
50
30
10
0
0 25
50
75
100
RELATIVE AREA (%)
37° C
2 CPM
NO. 2
NO. 60

The mixing ratio has a great effect on the minimum surface tension and on the plateau of the mixed film. For PC/PG = 1 : 10, by mass, the minimum surface tension is approximately 28 mN/m, the plateau at about 35 mN/m. For PC/PG = 1 : 1, the minimum surface tension is about 1 mN/m, the plateau is approximately at 25 mN/m.

Figure 25b represents the surface potential-area diagrams which were recorded simultaneously with the curves of Figure 25a. The solid line corresponds to the solid line of Figure 25a, the broken line corresponds to the one of Figure 25a. Plateau E illustrates separation of the two components in the mixed film. PG molecules are most likely being squeezed out at the plateau. PC is becoming the dominant factor and is responsible for the further increase of the surface potential. PC is not squeezed out, since there is no horizontal section at near zero surface tension in Figure 25a.

Figure 26 shows about twenty successive cycles from a mixed film of PC (C16 : 0)/PG (C16 : 0) = 1 : 1, by mass. The layer was spread at maximum area and to produce an initial surface tension of about 50 mN/m. The loops demonstrate a marked plateau at approximately 23 mN/m. The plateau is very likely due to a separation of PC and PG molecules in the film that was mixed initially. The PG molecules are squeezed out at the plateau level and the remaining PC molecules cause further decrease

Figure 25: Plateau level of mixed films

Figure 25a: Surface tension area diagrams of mixed films from PC (C16 : 0) and PG (C16 : 0)

For PC/PG = 1 : 10, by mass, the minimum surface tension is about 28 mN/m, the plateau at about 35 mN/m. For PC/PG = 1 : 1, the minimum surface tension is close to zero, the plateau is at about 25 mN/m.

Figure 25b: Surface potential-area curves corresponding to the diagrams of Figure 25a.

Plateau E corresponds to the plateaux in Figure 25a. The reason for the plateau is most likely squeezing out of PG molecules.

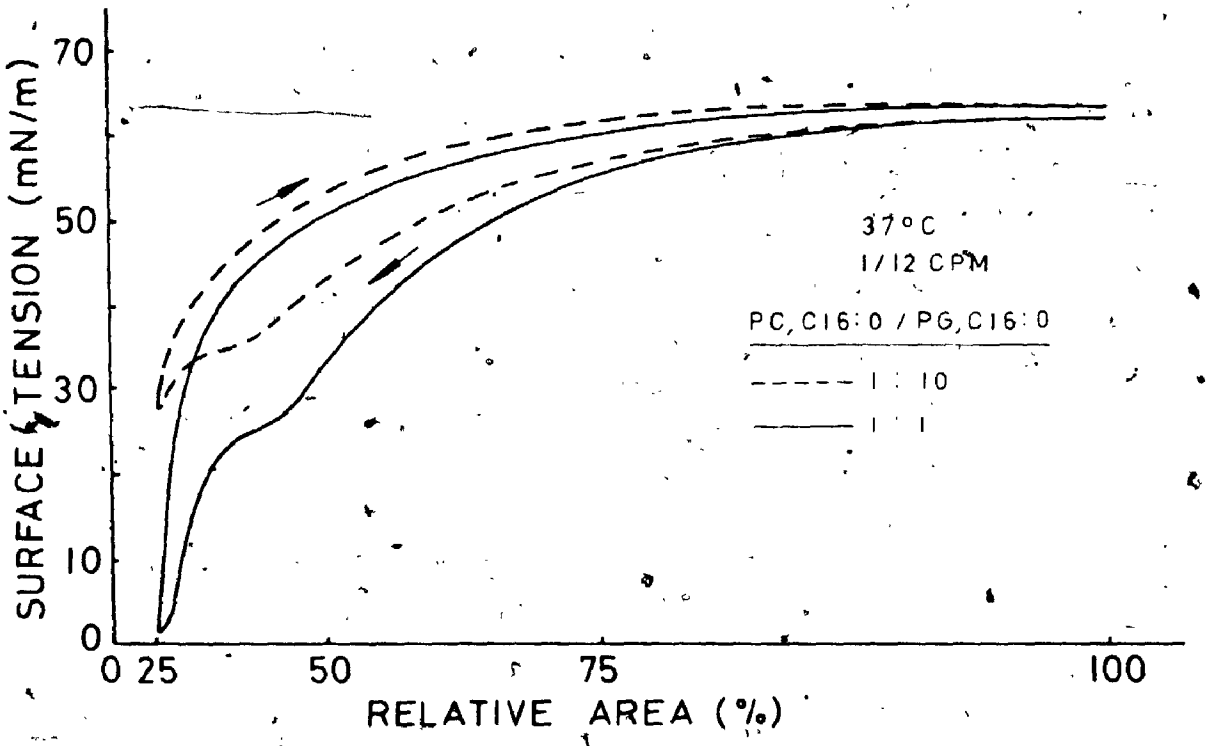
SURFACE TENSION (mN/m)
70
50
30
10
0
0 25
50
75
100
RELATIVE AREA (%)
37°C
1/12 CPM
PC, C16:0 / PG, C16:0
1 : 10
1 : 1

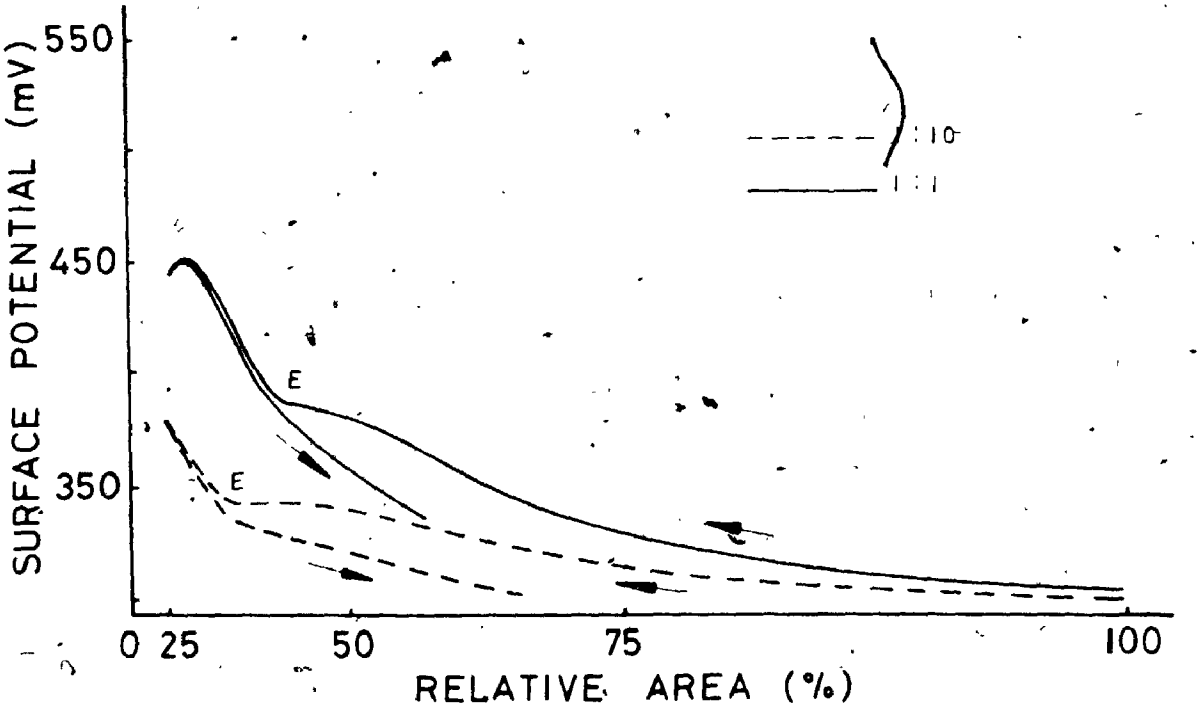
SURFACE POTENTIAL (mV)
550
450
350
0 25
50
75
100
RELATIVE AREA (%)
E
E
1 : 10
1 : 1

Figure 26: Hysteresis loops from a mixed film of PG (C16 : 0)/PC (C16 : 0) = 1 : 1, by mass.
The photograph shows about twenty successive cycles, drawn clockwise.

Note the similarity to lung surfactant hysteresis loops. Plateau, hysteresis and low minimum surface tension are characteristic for lung surfactant loops and for the curves of this figure. The plateau is at about 23 mN/m.

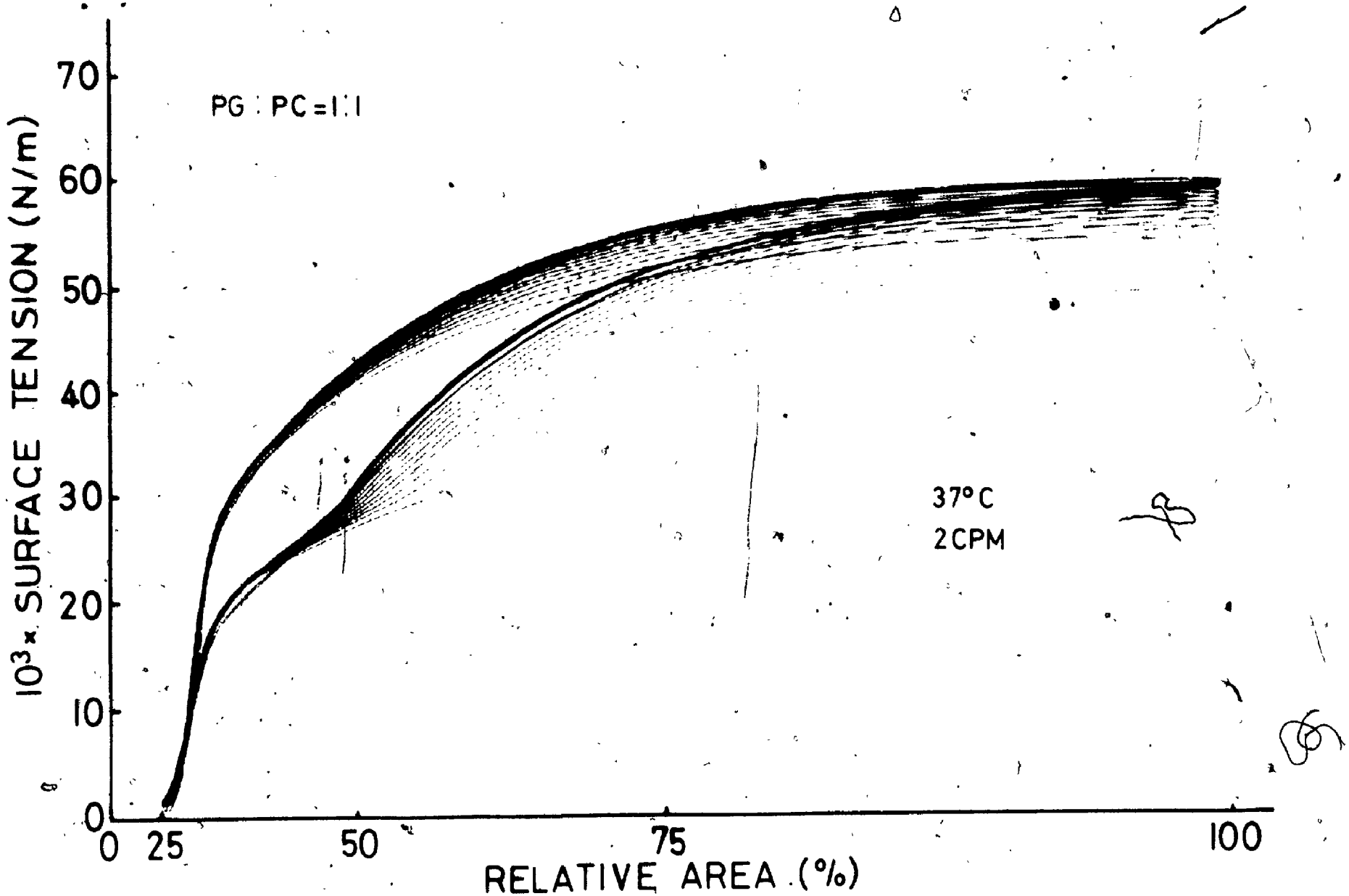
PG : PC = 1 : 1
37°C
2CPM
10^3 × SURFACE TENSION (N/m)
70
60
50
40
30
20
10
0
0
25
50
75
100
RELATIVE AREA (%)

of the surface tension. The loops show more hysteresis than curves from pure PC (C16 : 0). This relatively large hysteresis effect on continuously cycled curves may be due to an exchange mechanism between the subphase and the film. PG molecules, squeezed out at plateau level may re-appear at the surface upon expansion of the film area.

The characteristics of mixed films from PC and PG are very similar to the ones from lung surfactant films. The film of Figure 26 demonstrates a plateau at about the same level (22 - 25)mN/m as curves from lung surfactant. Other characteristics such as low minimum surface tension and hysteresis are typical for both films. (Surfactant and PG/PC).

Phosphatidyl serine, PS (C16 : 0) monolayers produce very similar surface tension- and surface potential-area diagrams to the ones from PG (C16 : 0). The curves are more expanded than the ones from pure PC (C16 : 0).

Figure 27a demonstrates the speed effect on the surface tension-area diagrams of PS (C16 : 0) films. The layers were spread at maximum area and to produce a surface tension of about 60 mN/m. At the slowest speed of 1/12 cycle/min, the minimum surface tension is approximately 28 mN/m, at 2 cpm about 20 mN/m and at 8 cpm about 15 mN/m.

Figure 27b shows curve no. 1 and the loops no. 2 and no. 10 of ten successive cycles from a mixed film of PS (C16 : 0)/PC (C16 : 0) = 1 : 1, by mass. The minimum surface tension is about 1 mN/m, the same as for pure PC (C16 : 0) films. However, there is no plateau like the one produced by mixtures of PG and PC. But similar to PC/PG mixed films, successive loops show more hysteresis than pure PC monolayers.

7.2.7 Influence of some additional agents on films from PC (C16 : 0)

a) Cholesterol

Considerable work has been done on the interaction of cholesterol with various lecithins at the air-liquid interface; see Ghosh et al. (1973). Reifenrath et al. (1973b) investigated surface tension properties of lecithin/cholesterol mixed films with a bubble method. They found that films from mixtures of cholesterol with lecithin in the ratio 1 : 7 do not produce a lower minimum surface tension than about 20 mN/m, regardless of the cycling speed.

We tried mixtures of cholesterol and lecithin in the ratio of 1 : 1, 1 : 2, up to 1 : 10, by mass. The results indicate that for the mixed films 1 : 5, near zero surface tension was again produced at 37°C and 2 cycles/min, but not for mixtures with a higher cholesterol content.

Figure 27: Films with phosphatidyl serine, PS (C16 : 0)

Figure 27a: Speed effect on films of pure PS.
At 8 cycles/min, the minimum surface tension is about 15 mN/m, at 2 cycles/min about 20 mN/m and at 1/12 cycle/min, approximately 28 mN/m.

Figure 27b: Curve no. 1 and the loops no. 2 and no. 10 of ten successive cycles from a mixed film of PS (C16 : 0)/PC (C16 : 0) = 1 : 1, by mass.
The minimum surface tension is close to zero.

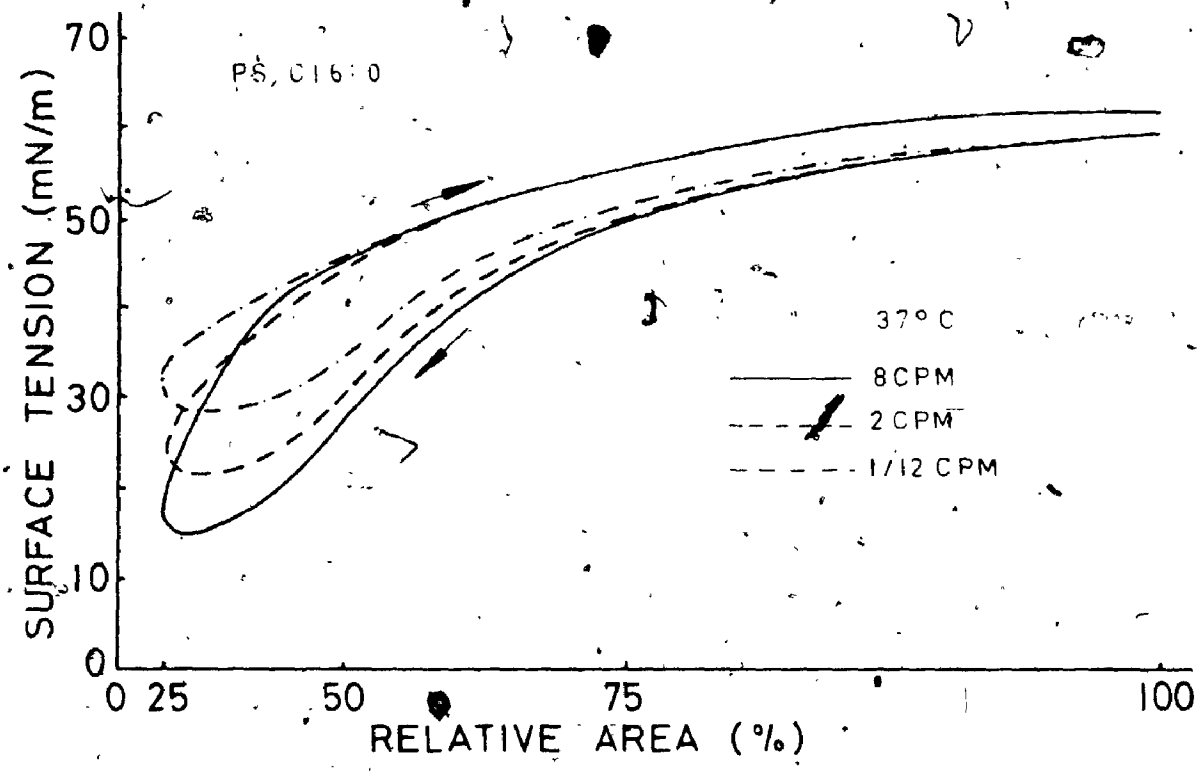
PS, C16:0
SURFACE TENSION (mN/m)
70
50
30
10
0
0 25
50
75
100
RELATIVE AREA (%)
37°C
8CPM
2CPM
1/12 CPM

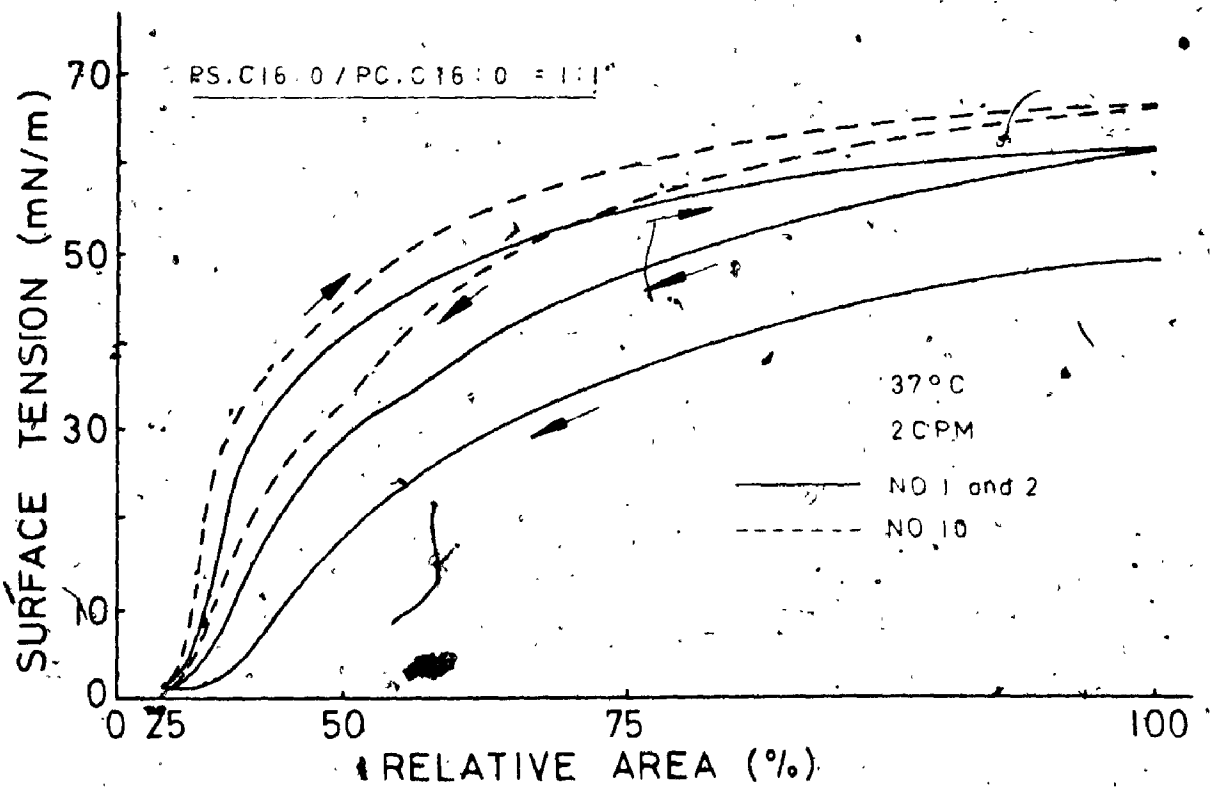
PS.C16:0/PC.C16:0 = 1:1
SURFACE TENSION (mN/m)
70
50
30
10
0
0 25
50
75
100
RELATIVE AREA (%)
37°C
2CPM
NO 1 and 2
NO 10

b) Lyso PC (C16 : 0), phosphatidic acid (C16 : 0), and PE (C16 : 0)

They do not interfere with the ability of PC (C16 : 0) films to reach near zero surface tensions, at least not mixtures up to the ratio of 1 : 1, by mass.

c) Albumin

For Figure 28, 14 µl of an albumin bovine solution, 2 mg/ml, was spread on the 0.9% NaCl surface; the surface tension-area characteristic was recorded at 37°C and 1/12 cycle/min.

In a second experiment, a PC (C16 : 0) monolayer was spread at maximum area and to produce a surface tension of about 70 mN/m. An amount of 14 µl of 2 mg/ml of albumin solution (0.028 mg), was then spread on the lipid monolayer. As expected, the maximum surface tension decreased. The minimum surface tension does not seem to be affected by the presence of protein. For comparison, the surface tension-area curve of a pure PC (C16 : 0) film is also shown.

Figure 29 demonstrates hysteresis loops after about 300 successive cycles. The subphase contained two different amounts of albumin bovine, 0.03 mg/ml for the unbroken curve, 3 mg/ml for the broken line. Both films contained equal amounts of lecithin. The minimum surface tension of the lecithin film is not affected by relatively large amounts of protein in the subphase.

Figure 28: Surface tension- and surface potential-area characteristics of PC (C16 : 0) (DPPC) films in presence of albumin bovine

Figure 28a: Surface-potential-area diagrams

———— DPPC film only

-------- Albumin only

-·-·-·-·- DPPC + Albumin, (0.028 mg spread on the monolayer of DPPC)

Figure 28b: Surface tension-area diagrams recorded simultaneously with the curves of Figure 28a

———— DPPC film only

-------- Albumin only

-·-·-·-·- DPPC + Albumin, (0.028 mg spread on the monolayer of DPPC)

Note: The minimum surface tension of the DPPC film is not affected by the protein.

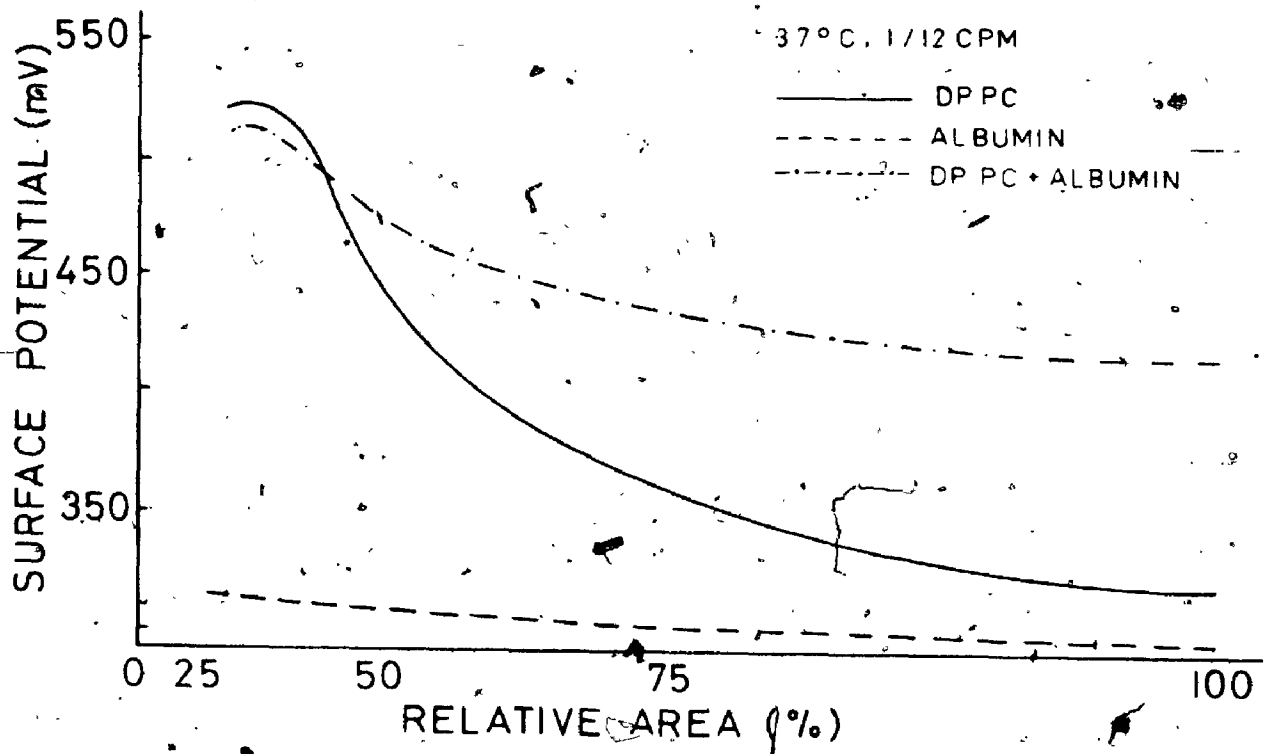
37°C, 1/12 CPM
DP PC
ALBUMIN
DP PC + ALBUMIN
SURFACE POTENTIAL (mV)
550
450
350
0
25
50
75
100
RELATIVE AREA (%)

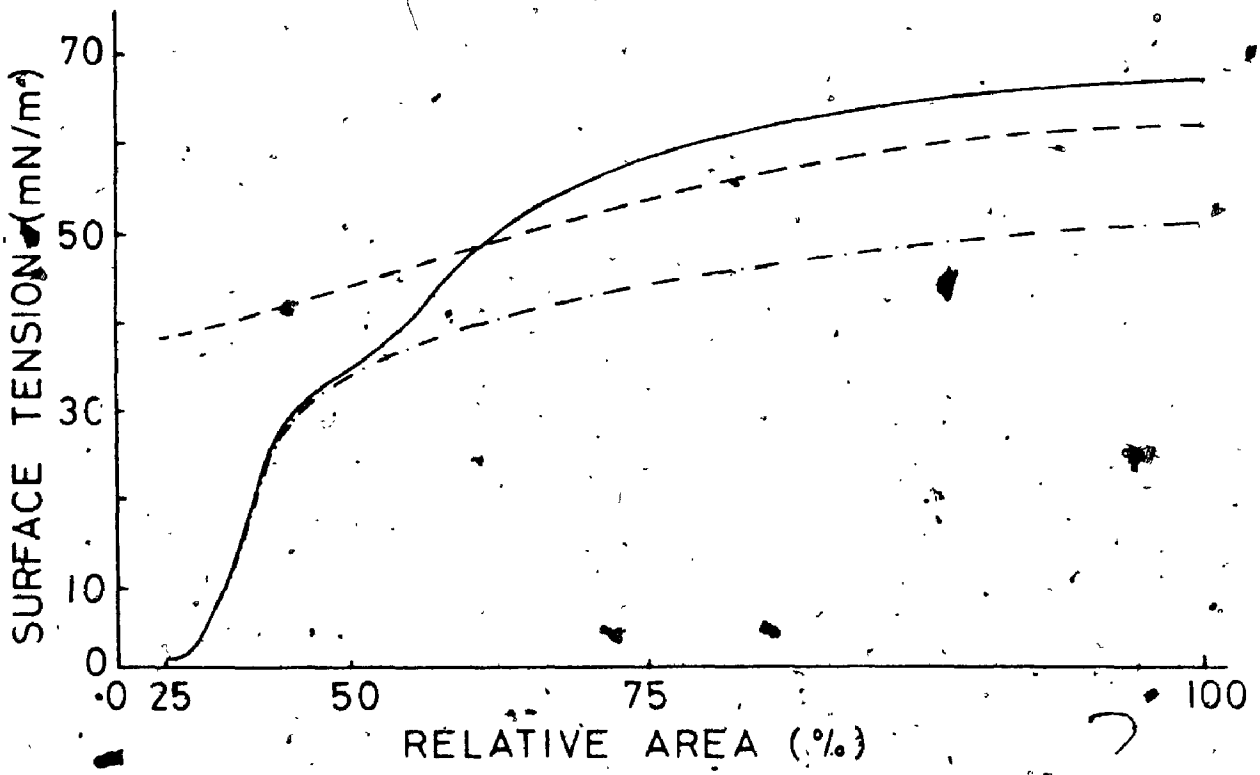
SURFACE TENSION (mN/m)
70
50
30
10
0
0
25
50
75
100
RELATIVE AREA (%)

Figure 29: Surface tension-area characteristics of PC (C16 : 0) films in presence of albumin in the subphase

The curves represent the loops after about 300 successive cycles.

The ability of the lecithin film to reach surface tensions below 5 mN/m is not influenced by relatively large amounts of albumin in the 0.9% NaCl subphase.

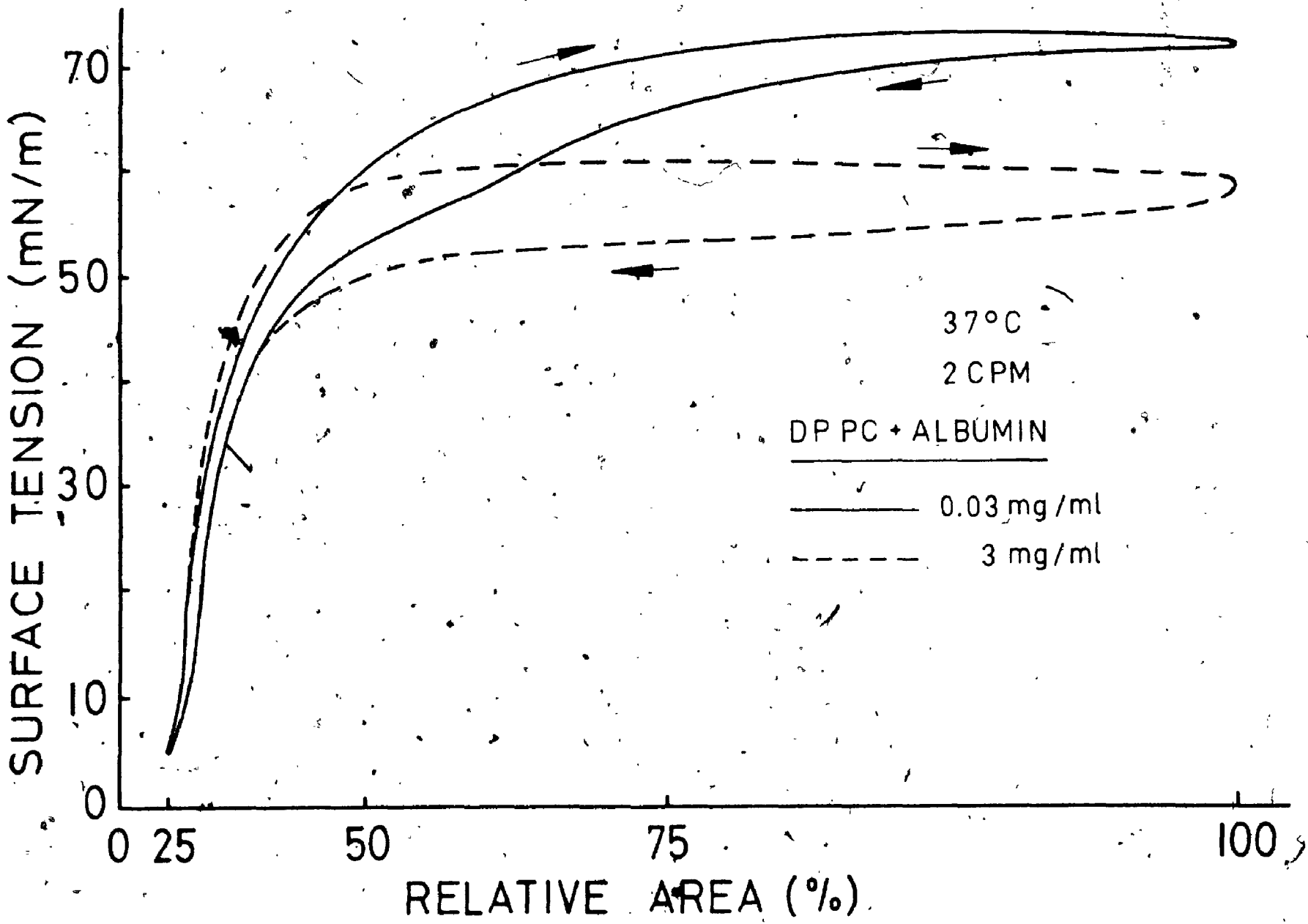
SURFACE TENSION (mN/m)
70
50
30
10
0
0 25
50
75
100
RELATIVE AREA (%)
37°C
2 CPM
DP PC + ALBUMIN
0.03 mg/ml
3 mg/ml

9-8-(2)

The hysteresis effect in the upper part of the graph is due to the albumin, which is squeezed out in the compression phase. Upon expanding of the film, it reappears, preventing the surface tension from rising further.

7.2.8 Separation of components in surface layers from the lipid extract of foam no. 1

In 5.2.2, dynamic properties of films from the lipid extract of foam fraction 1 are described.

Figure 30, curve no. 1, represents the surface tension-area diagram of a film spread at maximum area and to produce a surface tension of about 70 mN/m. For curve no. 2, more film material was spread until the minimum possible surface tension for static conditions, about 25 mN/m, was obtained. For curve no. 3, the process of no. 2 was repeated on the same subsolution.

The results indicate that more and more molecules with stronger surface activity are collected on the surface. The components of the film are separated, and less surface active molecules leave the surface in the compression phase. More strongly interacting molecules remain in the surface film and are then responsible for the further decreasing surface tension.

The molecules remaining in the surface are most probably: PC (C16 : 0) and PC (C18 : 0). Molecules with

Figure 30: Separation of components in surface layers from the lipid extract of foam no. 1

Figure 30a: Surface tension-area characteristics

No. 1 was obtained from a film spread initially to produce a surface tension of 70 mN/m. For no. 2, much more material was spread in order to achieve the lowest minimum surface tension for static conditions, about 25 mN/m. For no. 3, the process of no. 2 was repeated.

Squeezing out of less-surface-active molecules is demonstrated by the successive lower minimum surface tensions, and by the increased hysteresis effect of the surface tension- and surface potential-area diagrams.

Figure 30b: Surface potential-area characteristics, recorded simultaneously with the curves of Figure 30a.

E : Plateau likely due to squeezing out of molecules other than PC.

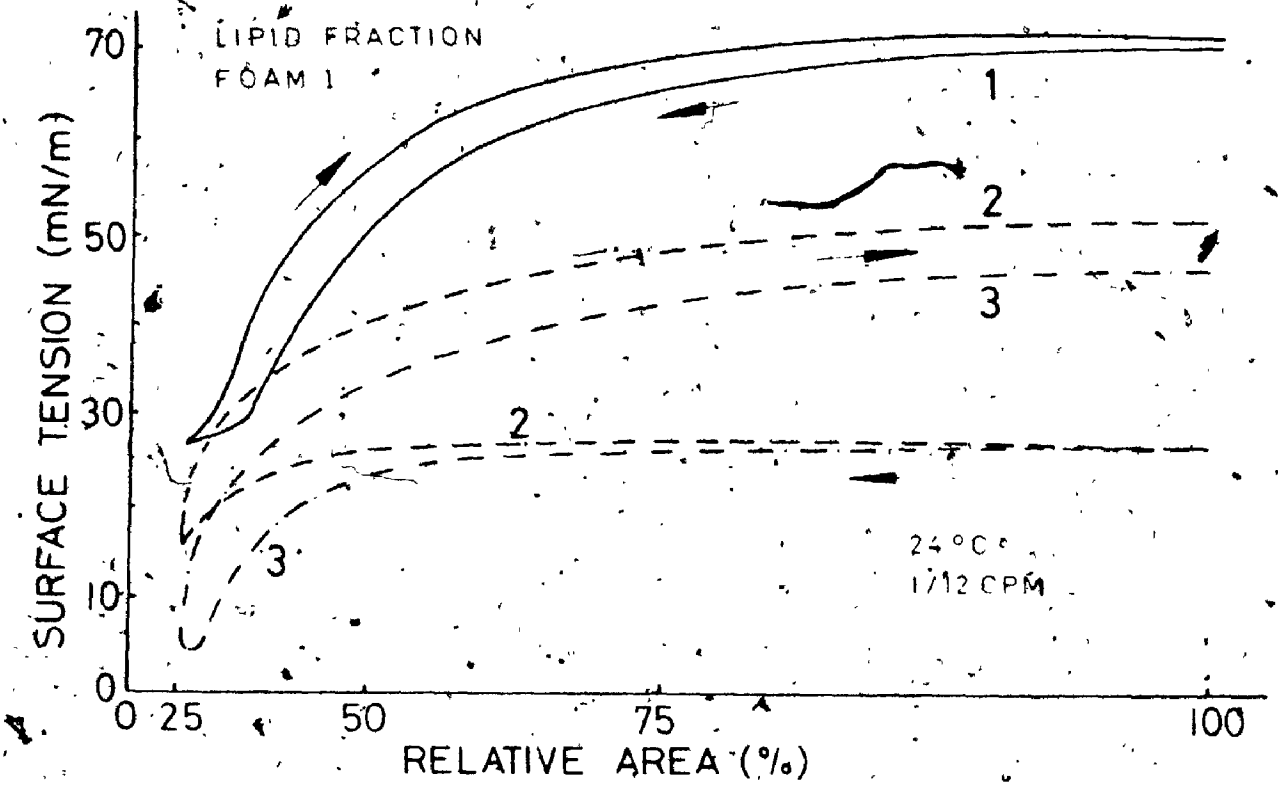
LIPID FRACTION
FOAM 1
SURFACE TENSION (mN/m)
70
50
30
10
0
1
2
3
2
3
24°C
1/12 CPM
0 25 50 75 100
RELATIVE AREA (%)

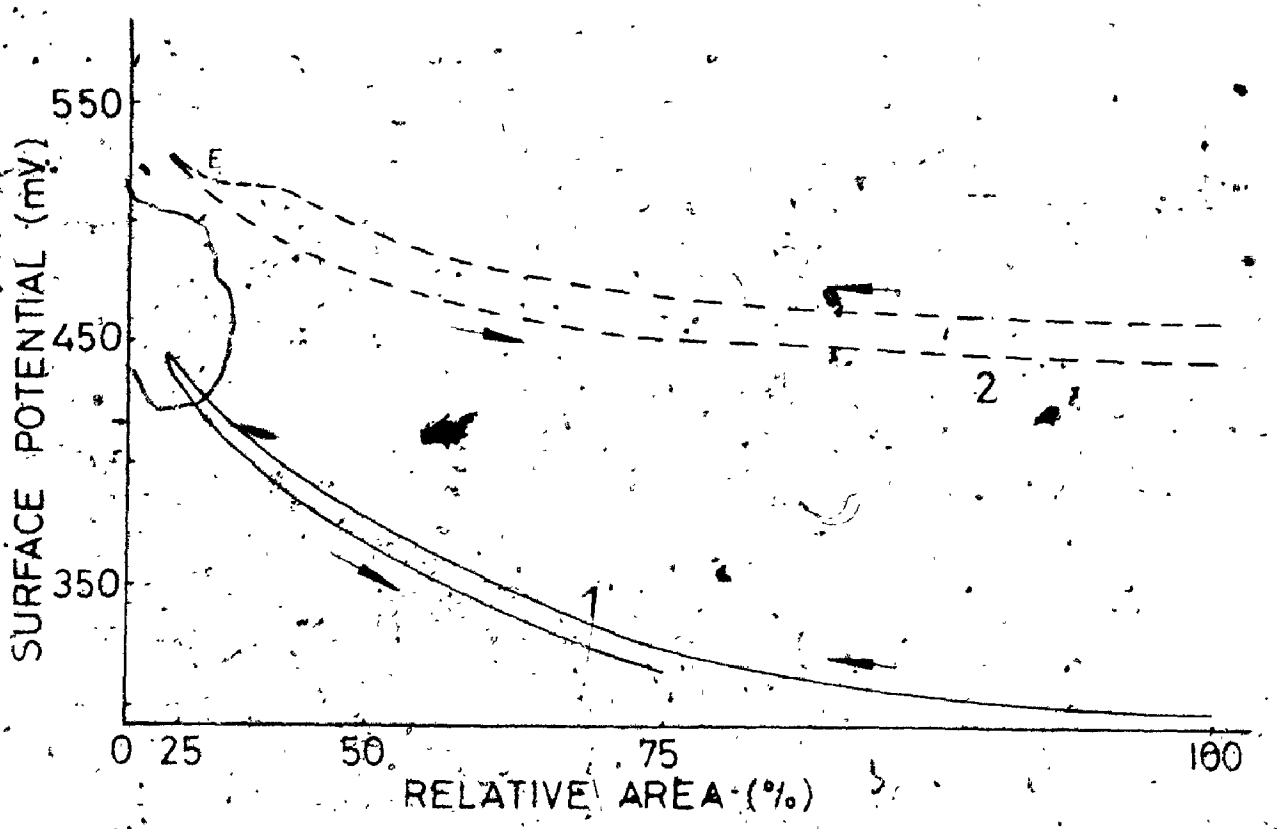
SURFACE POTENTIAL (mV)
550
450
350
E
2
1
0 25 50 75 100
RELATIVE AREA (%)

3 5

OF/DE

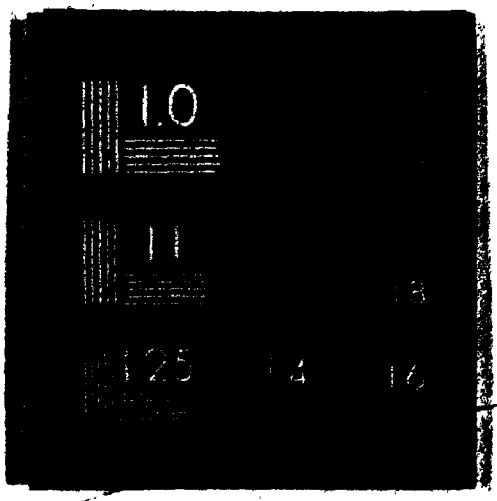

shorter hydrocarbon chains or with double bonds and possibly also PG and PS molecules are squeezed out.

CHAPTER 8

DISCUSSION OF PART I

8.1 Nature of lung alveolar surfactant

The nature of surfactant and its definition, operationally or chemically, will certainly require more work.

From our investigation we cannot say much about the relatively new concept of surfactant being in the form of structured bodies, which are typical for the liquid crystalline phases of phospholipid-water systems. Steim et al. (1969) described surfactant as appearing in the form of micelloids, about 0.3 - 0.5 μm in diameter, containing essentially only a mixture of lipids and almost no protein. Dermer (1970) reported that the "Inclusion bodies" of the alveolar type II cells, show the typical lamellar crystalline phase of a lecithin-water system.

Frosolono et al. (1973) support the postulate that surfactant has the characteristics of bimolecular lamellae with the hydrocarbon chains closely packed, (structured gel). They think the surface active fraction is a "particulate" lipoprotein assembly.

From the fact that "aging" of the surfactant films was necessary, we may conclude that phospholipids are leaving the structured particles in the subphase to form the surface film. We cannot think of protein having any significant role in the film itself, since all the typical characteristics of surfactant hysteresis loops can be reproduced by the lipid extract alone.

8.2 Dipalmitoyl phosphatidyl choline (DPPC)

As Colacicco et al. (1973) point out, DPPC meets the operational criteria of surfactant, such as: near zero surface tension and hysteresis. If we accept near zero surface tension as mandatory we may discuss two types of DPPC films:

A. The monolayer is initially, at 100% area in a highly condensed state with a surface tension below 30 mN/m. A compression of about 10% produces a surface tension below 1 mN/m. On further reduction of the film area, this near zero minimum surface tension is maintained. The curve follows a path parallel to the area axis. During this process, film substance is continuously squeezed out and the "loss" of film material is proportional to the length of the bottom part of the curv- (7.2.3 d).

Since this squeezed out material does not respread on the surface upon reexpansion of the film, at least not

within a time interval of about 15 min, it has probably migrated into the subphase, possibly in form of stable aggregates of micellular structure. For the film type A, we have to consider two cases:

1. the area is reduced very little, about 10%, the minimum surface tension of less than 1 mN/m is obtained just at the end of the compression phase.

2. the area is reduced to about 25% of the initial area, the curve follows a relatively long horizontal path at near zero surface tension.

In the first case, no film material is squeezed out, there is no separation of the compression- and expansion part of the curve (no hysteresis). The maximum surface tension is about 25 - 30 mN/m, the minimum approximately 1 mN/m.

In case two, a relatively large amount of film material is no longer available for the following cycle. In order to restore the initial state of the film, the substance "lost" has to be resupplied at the end of the expansion phase. The curves show a large hysteresis effect.

B. <u>The monolayer is initially, at 100% in the liquid expanded state, with a surface tension above 70 mN/m.</u>

On reduction of the area, the film condenses and produces

near zero surface tension at the end of the compression phase, at about 25% area. As for type A, case 1, almost no substance is squeezed out, since there is no compression at near zero surface tension. The maximum surface tension is above 70 mN/m, the minimum is about 1 mN/m.

In 7.2.3 d), we have seen that continuous cycling of a film type A, case 2, requires a large amount of lecithin per cycle, equivalent to about the material needed for one monolayer of type B.

Alveolar lecithin has a surprisingly short turnover time. Toshima et al. (1972b) found between 5 and 15 hours. Iwainsky et al. (1970) found a biological half life for the time from inorganic phosphorus to lecithin phosphorus to be approximately 6 hours. Although there is a continuous supply of lecithin to the alveolar lining layer, it is unlikely that such large amounts would be needed per cycle, as this occurred in a film of type A, case 2.

8.3 Dynamic properties

The dynamic characteristics of films from lung alveolar surfactant of any investigated preparation must be attributed to other factors than dipalmitoyl lecithin, since pure DPPC monolayers produce near zero surface tension at cycling speeds far below physiological frequencies, even at 40°C. Mixed films from saturated and

unsaturated lecithins demonstrate strong dynamic effects (7.2.5 b). Unsaturation in mixed layers with DPPC influences film stability much more than shorter chain length. Since significant amounts of unsaturated components in lung surfactant are reported in the literature (7.1.3), it is likely that unsaturation is responsible for the dynamic properties of surfactant films. Also, monolayers from phosphatidyl serine, PS (C16 : 0), reveal dependence of the minimum surface tension on the cycling speed. But PS accounts for only about 5% of the surfactant phospholipids. It is therefore probably less important for the dynamic behaviour.

8.4 Plateaux

The characteristic plateau of hysteresis loops from surfactant or from its lipid extract is always found between 22 and 25 mN/m, with no measurable influence of temperature and speed on its level. Since phase transitions in monolayers from DPPC are temperature dependent, at 37°C it occurs at about 35 mN/m, we conclude that surfactant plateaux are not due to phase transitions. We observed plateaux in curves of the following mixed films:

- PC (C18 : 0) with PC (C18 : 1) or PC (C18 : 3)
- DPPC with PC (C18 : 1) or PC (C18 : 3)
- DPPC with PG (C16 : 0).

As is demonstrated in 7.2.6, the plateau level is dependent on the ratio of the components in the mixed layers.

The larger the amount of DPPC relative to PG, the lower is the plateau. Mixed film from PC/PG (1 : 1, by vol.), see Figure 26, showed a plateau at approximately 23 mN/m, the level of the surfactant plateau.

The surface tension- and surface potential area characteristics of mixed films from synthetic components and of layers from the lipid fraction of surfactant, strongly suggest that the plateau of surfactant loops is due to separation of the components. The molecules which are able to interact most strongly and therefore produce a lower minimum potential energy, stay in the surface phase.

8.5 Role of components other than DPPC

We have seen that unsaturation and shorter chain length have an expanding effect on films from DPPC. Mixed layers of DPPC, and PG (C16 : 0) or PS (C16 : 0), are more expanded than pure DPPC films and they show more hysteresis on repeated cycling. If there is no constant influx of substance, hysteresis of pure DPPC films disappears quickly. Since layers with PG (C16 : 0) or PS (C16 : 0) show more hysteresis on repeated cycling, we conclude there must be a faster exchange mechanism between a "store" in the subphase and the film itself. It is reasonable to assume that micellular structures are very likely produced during squeezing out. They are probably

less stable if they contain components with unsaturation or shorter chain length or molecules like PG or PS. Therefore, these agents might facilitate an exchange between the surface film and the structured particles in the subphase.

Cholesterol would have an opposite effect, since it condenses liquid expanded lecithin films (Ghosh et al., 1973). In sufficient concentration it prevents the minimum surface tension from going below about 20 mN/m.

8.6 Lung surfactant and alveolar stability

Consider the dynamic system of the breathing lung in the deflation phase and the alveoli as communicating spherical units. Even if the influence of the surface forces was neglected there would be an "a priori" fluctuation of the size of the alveoli, at a given moment. Laplace's law states:

$$\Delta p = \frac{2\gamma}{r}$$

where γ : Surface tension

r : Radius of a spherical unit

Δp : Pressure difference

We now discuss three cases:

1. the surface tension is constant, independent of the area,

2. the surface tension is below 1 mN/m, close to zero,

3. the surface tension decreases with the area.

In the first case, an uneven distribution of the size of the units is promoted, relatively small alveoli would tend to collapse and blow up the larger ones.

The second case is approximately realized by a condensed DPPC film with near zero surface tension. Since according to Laplace, Δp is close to zero, no further fluctuation of the size of the units would be promoted.

In the third case, the surface tension changes as a function of the area and therefore decreases in the deflation phase.

If the area of the film is reduced sufficiently, near zero surface tension is reached. Again, larger fluctuations of the size of the alveoli are prevented. Unfortunately, there are two great drawbacks for building a valid model:

1. the physical state of the surface film at the beginning of the deflation phase is not known, therefore we do not know the necessary reduction of the area to achieve near zero surface tension.

2. the surface area - volume relationship of the "breathing" alveolus is not yet known.

If the film is indeed initially in a highly condensed state, then the surface area - volume relationship would be of no importance, since a reduction of

about 10% of the area is almost certainly realized during normal deflation. Stability of the lung will be further discussed in Part II.

PART II

INTERFERENCE OF BRONCHOGRAPHIC AGENTS WITH ALVEOLAR SURFACTANT AND WITH DIPALMITOYL PHOSPHATIDYL CHOLINE FILMS

CHAPTER 9

INTRODUCTION

9.1 Outline of the problem

It is known that patients during or shortly after bronchographic examination become acutely short of breath (Christoforidis et al., 1962). This dyspnea appears to be caused by collapse of the alveoli in parts of the lung. Whether the atelectasis is due to the contrast medium plugging the airways or due to inactivating or altering the effect of surfactant is not known.

The present study investigated the hypothesis that bronchographic contrast media caused atelectasis by interacting with lung surfactant and reducing its surface activity. This hypothesis arose when Dr. Margot R. Roach (personal communication) heard that the signs and symptoms of atelectasis in patients post bronchogram developed within minutes of the introduction of the contrast material.

If the hypothesis is correct, the following points have to be verified:

1. the bronchographic agent or its suspension medium alter surface properties of surfactant.

2. the material must be found in parts of the lung

where there is surfactant (alveoli and alveolar ducts).

In order to verify point one, surface tray experiments were done with the agent and, if possible with the suspension medium separately.

To prove point two, histological sections of lungs in which the media had been introduced were examined. Quasi static pressure-volume tests on excised lungs gave further evidence for point one, provided the media had been found in the alveoli or alveolar ducts.

9.2 Experimental approach

a) Studies were done on rabbit lungs into which various roentgenographic agents had been introduced. These investigations involved:

- Radiology to determine where the bronchographic material was positioned
- Gross pathological examination to determine the extent of collapse
- Pressure-volume characteristics to determine if the agent altered the lung properties
- Histological examination to determine the position of contrast material and the uniformity of atelectasis.

b) Surface tray studies

The contrast material or its suspension media

were added to films from rabbit lung surfactant and to films of synthetic dipalmitoyl phosphatidyl choline.

CHAPTER 10

EFFECTS OF BRONCHOGRAPHIC AGENTS ON RABBIT LUNGS

10.1 Materials and methods

a) The fluid contrast media, Dionosil Oily, Dionosil Aqueous and Hytrast as well as tantalum powder (1 µm particles) were used. A detailed description of the chemical and physical properties is found in Appendix IV.

b) White rabbits, male or female (2.5 - 3.5 kg), were anaesthetized with 30 to 60 ml of 20% urethane. The trachea of the rabbit was then exposed and cannulated with a "y"-cannula with an outside diameter 0.5 cm and stem length 5.0 cm.

c) Injection of the fluid contrast media

The rabbit was placed supine on the x-ray table. A 15 cm long polyethylene catheter, inside diameter 0.12 cm, which was attached to a size 18 hypodermic needle was then introduced into the "y"-cannula, and fed into the right bronchus until slight resistance was felt. The right bronchus was entered in about 80% of the experiments. A 1 ml syringe was then used to inject 0.25 ml/kg rabbit of the contrast medium. During the injection, the polyethylene cannula was slowly withdrawn about 3 cm. The agent was hopefully distributed evenly throughout the

lung which had been catheterized.

d) Dose

As mentioned before, 0.25 ml/kg rabbit of contrast medium was introduced into the one lung. The dose was estimated to make it comparable to that used in man. According to the manufacturer, a maximum of about 20 ml of Dionosil Oily is used for a human lung. Assuming a lung capacity of 3000 ml for man and of 100 ml for a rabbit of 3 kg, the volume ratio is approximately one to thirty. Therefore, the dose for a rabbit lung would then be about 0.7 ml.

e) Injection of tantalum powder

Tantalum powder particles have a strong tendency to stick together to form conglomerates. This is especially true for the small particles used in this investigation (1 µm size). A method had to be found to suspend the particles in air. The usual way is to use a powder blower or atomizer. However, the required air flow of 0.2 - 0.5 liter/sec (Nadel et al., 1970, Gamsu et al., 1973), was too high for rabbit lungs, where in our method, a catheter had to be introduced into the one lung, leaving the other one without tantalum as a control. We chose the "fluidized-bed-technique", applied by chemical engineers to suspend particles in air. A description of the apparatus is found in Appendix V. The air flow leaving the polyethylene catheter, inside diameter .12 cm, was 1 to 2 ml/sec. The

amount of tantalum powder injected into the one lung was between 0.03 and 0.07 ml or 0.5 to 1.0 g. This compares with 0.5 to 1.0 ml (Gamsu et al., 1973) or 0.2 to 0.5 ml (Nadel et al., 1970) for human bronchograms.

f) X-rays taken

- one any time post anaesthesia as a control
- one immediately (about 10 sec) post injection of the agent
- several at intervals of 10 min to 20 min for up to two hours post injection.

g) Gross pathological examination

After the x-rays, the animal was sacrificed, the trachea closed off with a clamp, so that the lungs would not collapse when the chest was opened. The heart and lungs were then removed "en bloc", and mounted on the cannula in the flask of the pressure-volume apparatus (see Figure 31). Before and during the pressure-volume tests, photographs were taken to reveal any gross pathology.

h) Pressure-volume recordings

Air was infused at a rate of about 2.4 ml/min with a Harvard Infusion Withdrawal pump. Before the air entered the lung, it was moistened by flowing through a 0.5 m long plexiglass tube that was stuffed with wet gauze. All the experiments were done at room temperature. A small clamp was used to close off one principal bronchus, so that

the pressure-volume curves of the opposite lung could be done. The lung without radiopaque material was called the control lung. The volume change ΔV was measured by integrating the flow of the displaced air which was monitored by a hot wire anemometer (see Figure 31 and Appendix VI). The pressure difference between the atmosphere outside and the intrapulmonary pressure was recorded with a Statham P23 AC pressure transducer. The calibration was done with a water manometer. Both, the pressure and the volume signals were displayed on a Hewlett-Packard X-Y recorder.

i) Selection of the pressure-volume curves.

As an illustration of the procedure followed in this study, several pressure-volume loops are shown in Figure 32a. (Hildebrandt et al., 1966, p. 740). Lungs, initially in the degassed or collapsed state, require a relatively large opening pressure. Here at about 10 cm H_2O, the alveoli begin to open. The almost horizontal part in the inflation phase is due to "recruitement" of the alveoli, characterized by a relatively large dV/dp, the compliance.

Since lungs in this investigation were closed off prior to excision, they were not collapsed, except for the parts with bronchographic agents. Some of these parts showed collapsed areas on gross examination.

Figure 31: Pressure-volume apparatus

1	Water manometer
2	Switch tap
3	Statham P23 AC pressure transducer
4	Glass flask
5	Rabbit lung
6	Plexiglass pipe filled with wet gauze
7	Infusion- withdrawal pump, Harvard apparatus
8	Probe: Tungsten wire mounted in a glass tube (constant temperature anemometer)
9	*Monitor, power supply and variable bridge resistance for constant temperature anemometer Models: 1051-1, 1056, 1053B
10	Integrater (see Appendix VI)
11	X-Y recorder Hewlett Packard

*Thermo System Inc., 2500 North Cleveland Ave., St. Paul, Minnesota 55113, U.S.A.

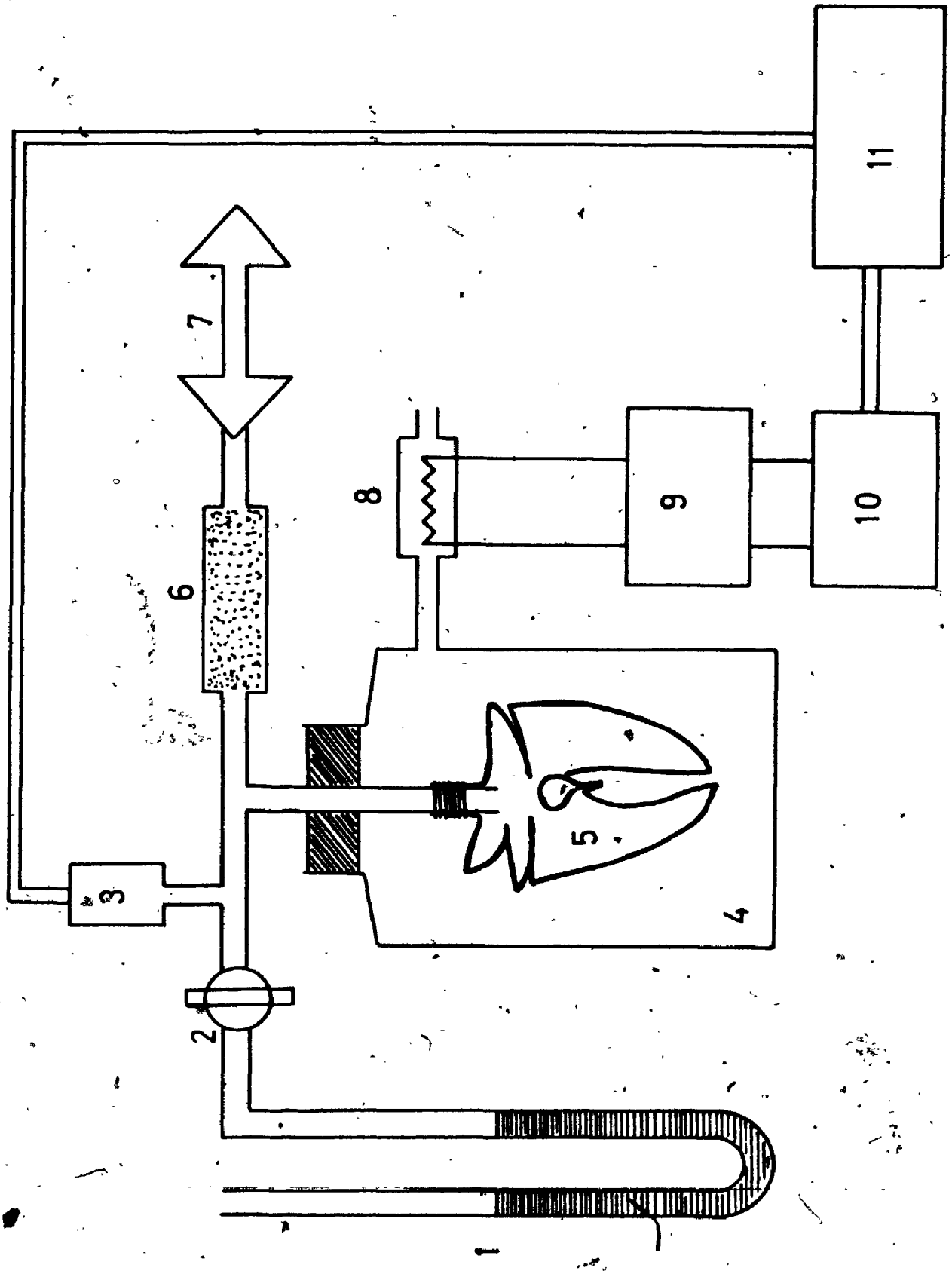
11
7
8
9
10
6
5
3
4
2
1

The first curve of a normal lung has therefore a relatively small opening pressure (no. 1). At the end of the expiration part, at zero pressure, the lungs show trapping of air. The pressure-volume curves do not return to the initial volume at '0'. Usually four to eight successive curves were required until at least three consecutive loops were reproducible within the error range. This state of the pressure-volume characteristic was called "stationary" (Figure 32b). The maximum volume change at 20 cm H_2O pressure was called the "stationary volume change" ΔVs.

k) Histological sections

The trachea of post pressure-volume test lungs were tied at $\Delta p = 0$, with air trapped inside, and the lungs fixed for at least five days in buffered formalin. Since propyliodone, the chemical in Dionosil Oily and Aqueous, and peanut oil are readily dissolved in ethanol, which is usually required in the embedding process, frozen sections had to be done. The thickness of these sections was 10 µm to 15 µm, the stain was Toluidine blue. Control lungs, with no contrast material, Hytrast and tantalum lungs could be prepared the normal way, through alcohol dehydration and paraffin embedding. These sections were between 7 µm and 10 µm. The stain was Toluidine blue too. Hytrast and Dionosil sections were examined with polarized light, which showed the chemicals as optically

Figure 32: Selection of the pressure-volume loops

Figure 32a: The curves, labelled "degassed" and "collapsed" are redrawn from Hildebrandt et al. (1966), p. 740. Our first curve, with origin 0', has a relatively low opening pressure, since the lung was closed off prior to excision.
The expiration part of the loop does not return to 0', which is called air-trapping.

Figure 32b: Loops no. 1 and no. 2 are identical with the ones of Figure 2a.
After four to eight successive curves, the "stationary" loop was obtained: three consecutive curves were reproducible within the error range (Appendix VII).

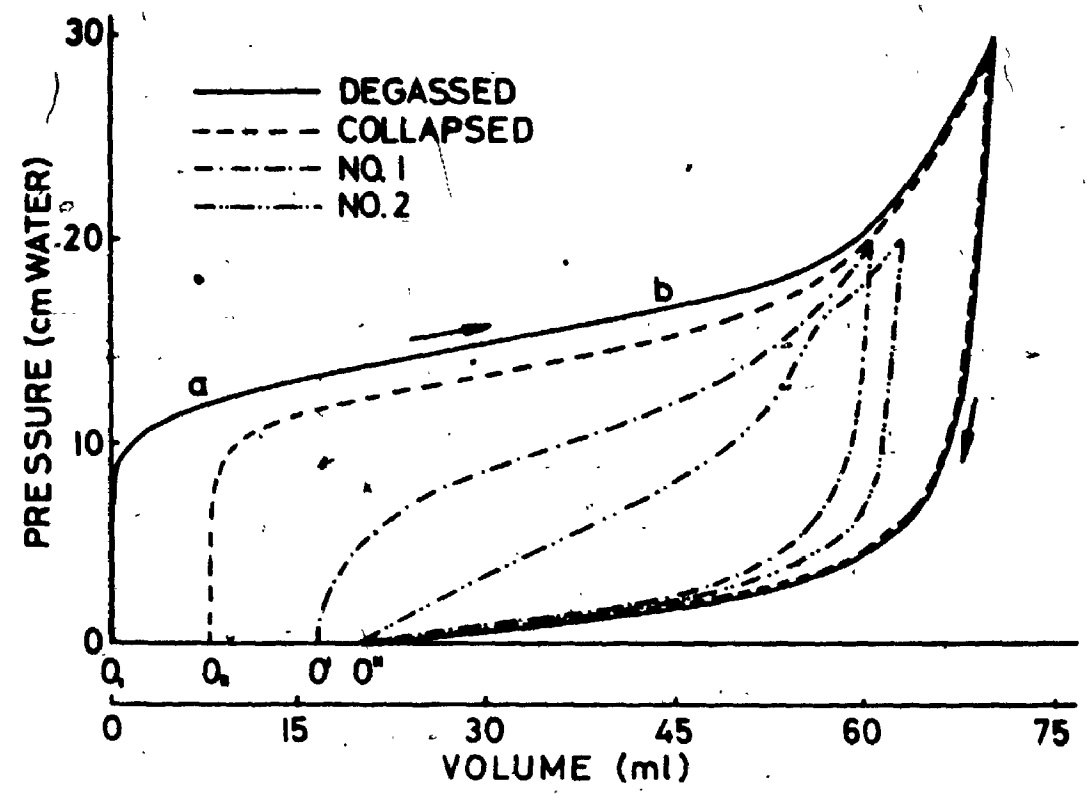
DEGASSED
COLLAPSED
NO. 1
NO. 2
PRESSURE (cm WATER)
30
20
10
0
a
b
0
15
30
45
60
75
VOLUME (ml)

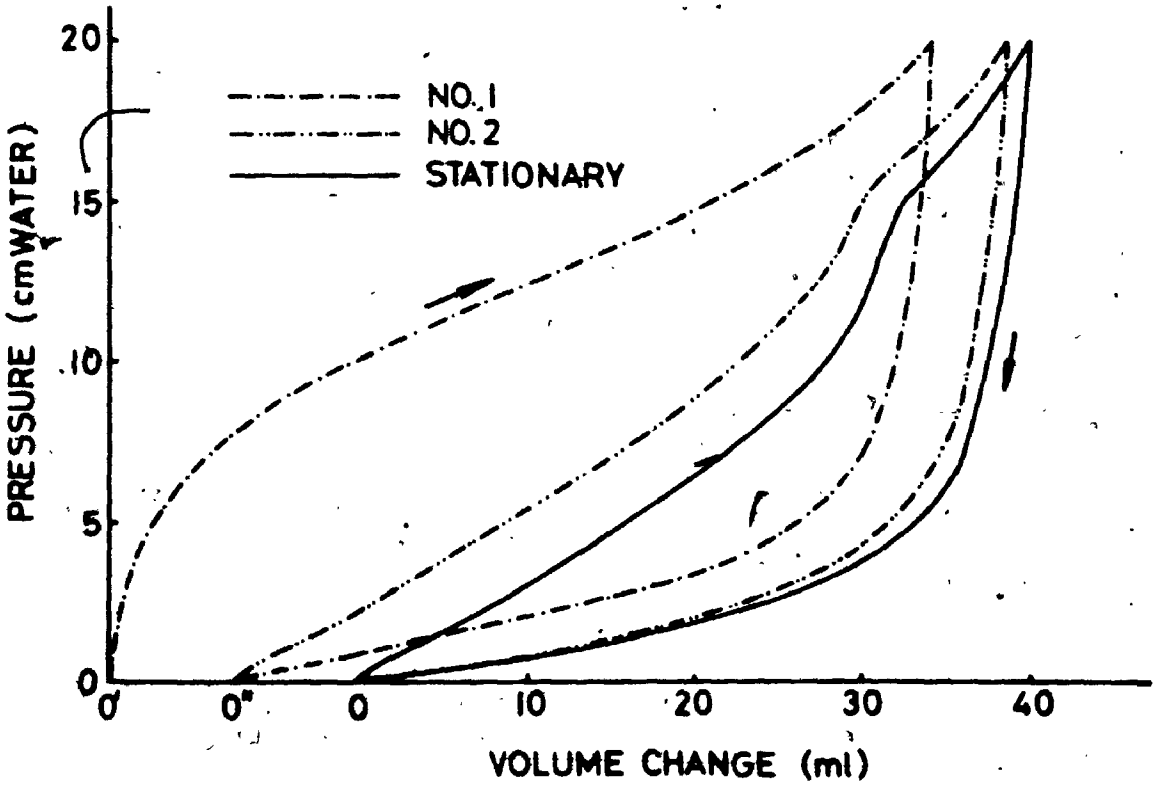
NO. 1
NO. 2
STATIONARY
PRESSURE (cm WATER)
20
15
10
5
0
0'
0"
0
10
20
30
40
VOLUME CHANGE (ml)

active crystals. Tantalum particles and peanut oil droplets could be seen with normal light.

l) "Peanut oil lungs"

In a few experiments, we injected 0.25 ml/kg rabbit of peanut oil into the right lobe of a rabbit lung, using the same technique employed for the bronchographic agents (see 10.1 c). Peanut oil, the suspension medium in Dionosil Oily, reaches the alveoli easily and because of its relatively low viscosity it does not block off the airways.

m) "Saline-rinsed lungs"

In order to remove the surfactant effectively, we rinsed a number of control lungs with 0.9% NaCl solution. The p-V diagrams of the rinsed lungs were then compared with the p-V curves of the same lungs in the normal state.

10.2 Characteristics of the pressure-volume hysteresis loops

Figure 33 demonstrates the stationary curves of a right rabbit lung with Dionosil Oily and of the corresponding left control lung.

a) Inflation

In P_1, at $\frac{p_m}{6} \simeq 3.3$ cm H_2O, the slope of the curve from the right lung is steeper or in other words, the compliance dV/dp is smaller than the corresponding values of the left control lung. It seems that dV/dp is a suitable quantity to destribe changes in the inflation

Figure 33: Stationary loops of a rabbit lung

In the right lung "R" was Dionosil Oily, about 0.8 ml, the left one "L", is the control lung.

P_1: Point of the inflation part, at $\frac{p_m}{6}$ = 3.3 cm H_2O

P_2: Point of the expiration part, at $\frac{p_m}{3}$ = 6.6 cm H_2O

P_3: Point of the expiration part, at $\frac{p_m}{6}$ = 3.3 cm H_2O

Note: p_m = 20 cm H_2O

The scale for the volume change can be shifted horizontally to any desired place.

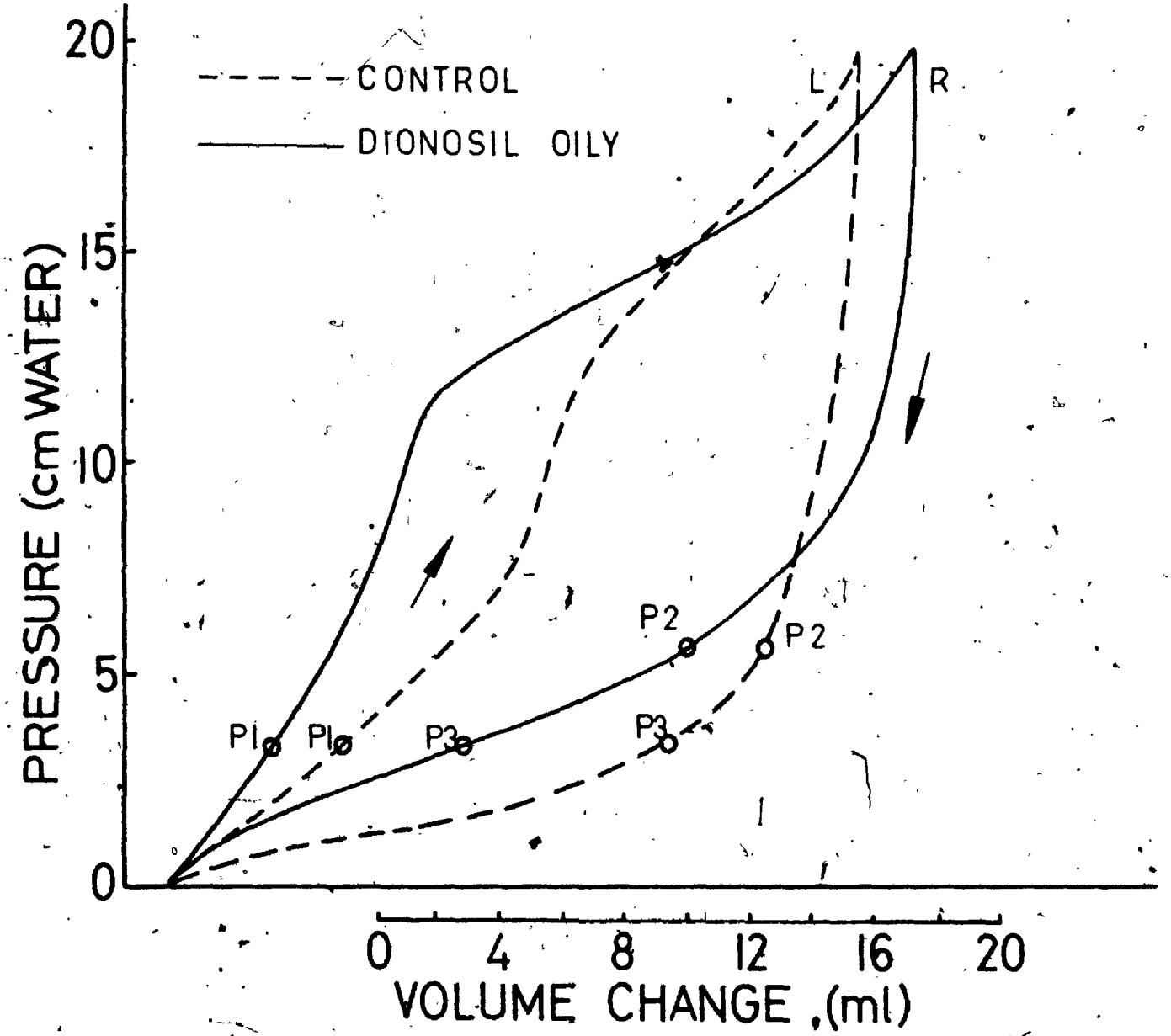
CONTROL
DIONOSIL OILY
L
R
P1
P1
P2
P2
P3
P3
PRESSURE (cm WATER)
0
5
10
15
20
0
4
8
12
16
20
VOLUME CHANGE ,(ml)

123-(2)

part, if taken at a reasonably low pressure. For the lung with Dionosil Oily, more energy is required initially for the inflation process. From the surface tray experiments we will see that clean surfactant films produce lower minimum surface tensions than films contaminated with the peanut oil of Dionosil Oily.

b) Expiration - stability of the lung

In the expiration part, the "peanut oil lung" shows a tendency towards collapse. Below about the pressure of 10 cm H_2O, the "peanut oil lung" retains less air than the normal lung. It is therefore reasonable to develop a factor which expresses in some form retention of air at a relatively low pressure. Clements et al. (1961) define a stability factor for the expiration part of the p-V diagram. This quantity is called the "expansion factor" and is defined as the ratio of the volume retained at p = 5 cm H_2O to the maximum lung volume. A lung with a marked tendency for atelectasis would have a relatively small "expansion factor", on the other hand, if the alveolar structure were stable, the factor would be relatively large.

The stability index "L"

Gruenwald (1963) points out, that the "expansion factor" defined by Clements et al. (1961), gives false values for lungs which trap air irregularly. This was

found to be true for the rabbit lungs used in this study. The meaning of the index "L" is illustrated on Figure 34.

Adaption of "L"

Gruenwald developed the index

$$L = \frac{V_{10} + 2V_5}{2V_{max}}$$

for infant lungs from the perinatal period. However, he states that it can be used for animals, if properly adapted. In the present study ΔV_s, the stationary volume change at p = 20 cm H_2O replaces V_m.

We found also that p_{10} and p_5 were too high for our study. The purpose of the index is to describe retention of air at relatively low pressure. This could be achieved adequately by replacing p_{10} by 1/3 $p_m \approx 6.6$ cm H_2O and p_5 by 1/6 $p_m \approx 3.3$ cm H_2O. (See Table VII).

We are aware of the fact that "stability" could be described in many ways. The reason to choose "L" and to adapt it is that Gruenwald has given some values for rabbits and dogs. He found values for normal dogs to be between 0.9 and 1.2, and for rabbits treated with phosgene gas, below 0.6.

Figure 34: Stability index "L" for the deflation part of the pressure-volume diagram

p_{10} Pressure of 10 cm H_2O

p_5 Pressure of 5 cm H_2O

p_m Maximum pressure

V_5 Volume at p_5

V_{10} Volume at p_{10}

V_m Maximum volume

The deflation curve between P_{10}, P_5 and 0 can be characterized by the areas:

$$A = V_{10} \times \frac{p_5}{2} \quad \text{Triangle } p_5\ P_{10}\ R$$

and $B = V_5 \times p_5$ Rectangle $p_5\ P_5\ V_5\ 0$

A theoretically maximally stable deflation curve would follow the path $P'_{10}\ P'_5\ V_m\ 0$.

The area A + B is then expressed in proportion to the area $P'_{10}\ V_m\ 0$.

L is defined as:

$$L \equiv \frac{V_{10} + 2V_5}{2V_m} \qquad (10.1)$$

The highest possible value of L is 1.5, if

$$V_{10} = V_5 = V_m.$$

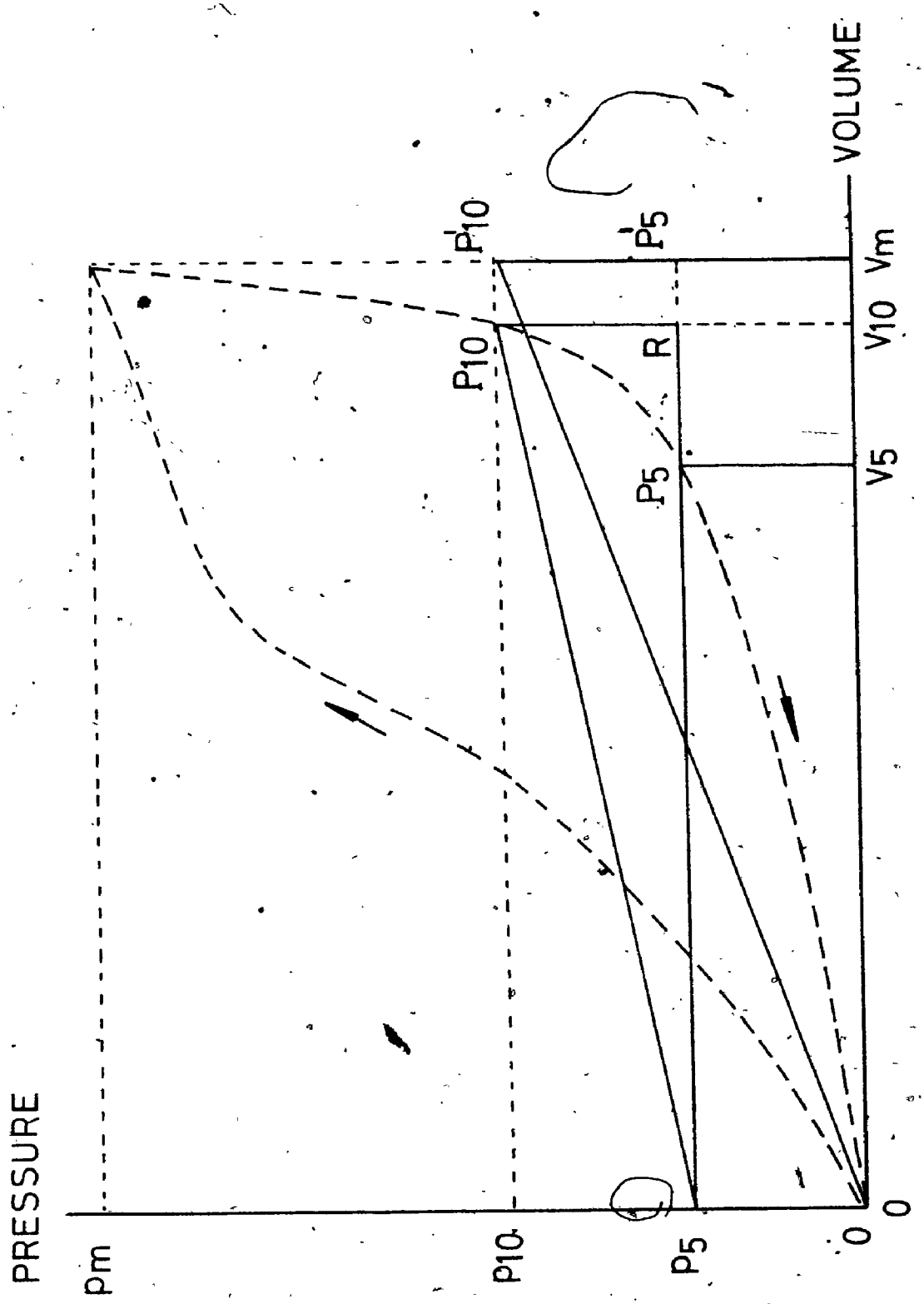
PRESSURE
VOLUME
Pm
P10
P5
0
0
P10
P5
R
V10
Vm
V5

TABLE VII

NOMENCLATURE AND DEFINITIONS

Name and Definition	Symbol	Unit (CGS)
Mass	m	g
Stationary volume change = change of the volume at $\Delta p = 20$ cm H_2O	ΔV_s	ml
Slope in P_1, at $\Delta p = \frac{1}{6} \Delta p_m$ $S_1 = \frac{d}{dV}\left(\Delta p\right)\Delta p_m = 20$ cm H_2O	S_1	cm H_2O/ml
Compliance in P_1, at $\Delta p = \frac{1}{6} \Delta p_m$ $C_1 = \frac{d}{dp}\left(\Delta V\right)$	C_1	
Volume change on expiration in P_2, at $\Delta p = \frac{1}{3} \Delta p_m \cong 6.7$ cm H_2O	ΔV_2	ml
Volume change on expiration in P_2, at $\Delta p = \frac{1}{6} \Delta p_m \cong 3.3$ cm H_2O	ΔV_3	ml
Pressure across the lung: Difference between atmospheric and intrapulmonary pressure	Δp	cm H_2O
Maximum $\Delta p = \Delta p_m = 20$ cm H_2O	Δp_m	cm H_2O
Stability Index $L = \frac{2\Delta V_3 + \Delta V_2}{2\Delta V_s}$ (adapted)	L	
Relative error	R.E.	%

10.3 Results: "Dionosil Oily -","peanut oil -", and "washed out lungs"

10.3.1 Pressure-volume tests

a) Normal lungs

These are lungs with no contrast material in either the left or the right part. A total of nine rabbits were used for control studies. Because of leaks in two lungs, only seven were investigated. The results are in Table VIII. The calculations for the error range can be found in Appendix VII. No trend between the mass of the single lungs and their stationary volume change ΔV_s could be detected (tested by plotting the mass vs. ΔV_s). There was also no relationship between the mass of the rabbit and ΔV_s. It is, however, interesting to note that the ratio of the mass m to the stationary volume change ΔV_s is constant within the error range of about 7%. (with the exception of no. 2). For error estimation see Appendix VII.

This indicates that trapping of air is comparable for a particular pair of lungs. The values $\Delta V_s \times S_l$, or $C_l/\Delta V_s$ for a pair of lungs are comparable and equal within the error range of about 15%. The difficulty arising from the larger right lung could be overcome by taking relative values, such as $C_l/\Delta V_s$ and $m/\Delta V_s$.

The stability indices for a pair of lungs are constant throughout within the error range of 15%. For the standard error of the mean of $C_l/\Delta V_s$ and L, the data

TABLE VIII

NORMAL LUNGS

		m	ΔV_s	$m/\Delta V_s$	S_1	$\Delta V_s S_1$	$C_1/\Delta V_s$	ΔV_2	ΔV_3	L
1	R	14.39	20.0	0.719	0.625	12.5	0.080	17.0	12.0	1.03
	L	10.55	14.5	0.728	1.04	15.1	0.066	13.0	7.50	0.97
2	R	21.50	28.0	0.768	0.520	14.6	0.068	24.0	16.0	1.00
	L	13.42	24.0	0.559	0.685	16.4	0.061	20.0	14.0	1.00
3	R	11.64	17.0	0.685	1.16	19.7	0.051	14.0	8.50	0.91
	L	7.990	13.0	0.615	1.09	14.2	0.070	12.0	9.00	1.15
4	R	8.930	24.0	0.372	0.560	13.4	0.074	21.0	15.0	1.06
	L	8.150	19.0	0.429	0.620	11.8	0.085	16.0	12.0	1.05
5	R	8.580	18.0	0.477	0.830	14.9	0.067	16.0	11.5	1.08
	L	6.560	14.0	0.468	0.750	10.5	0.095	13.0	9.00	1.[illegible]
6	R	10.78	15.0	0.719	0.780	11.7	0.085	15.0	11.5	1.27
	L	6.920	9.50	0.728	1.08	10.3	0.097	8.00	6.50	1.11
7	R	11.52	36.0	0.320	0.340	12.2	0.082	33.0	26.0	1.18
	L	8.630	25.5	0.349	0.528	13.4	0.075	22.0	17.0	1.09
	R.E.(%)	0.5	7.0	8.0						
	MEAN						15.0			15.0
	S.E.						0.075			1.07
							0.0175			0.0918

R: Right lung; L: Left Lung; R.E.: Relative error

from both lungs were used, since there is no significant difference between the means of the right and the left parts ($p > 0.05$). We found also, that for a normal lung the following relation holds (Figure 35 and Table VIII):

$$\frac{m \text{ right}}{\Delta V_{s \text{ right}}} = \frac{m \text{ left}}{\Delta V_{s \text{ left}}} \qquad (10.2)$$

This relation makes it possible to estimate the stationary volume change $\hat{\Delta V}_s$ of the lung with contrast medium (see Table IX), if both masses and ΔV_s of the control lung are known. In column 4 of Table IX, these values $\hat{\Delta V}_s$ are given.

$$\hat{\Delta V}_{s \text{ right}} = \frac{m \text{ right}}{m \text{ left}} \cdot \Delta V_{s \text{ left}} \qquad (10.3)$$

If the contrast medium was in the left lung, $\Delta V_{s \text{ left}}$ was calculated accordingly..

b) Lungs with Dionosil Oily (Table IX)

Without exception, the "Dionosil Lungs" showed large collapsed areas on gross pathological examination. Only after the lungs with Dionosil Oily could be opened completely, the p-V test was done. P-V curves of lungs with collapsed regions would give greatly distorted values and no evaluation of the influence of the agent on the surface activity could be done reliably.

Figure 36 illustrates the procedure followed for the p-V studies. The initially collapsed region (Figure 36a) could be opened up after 5 to 8 runs with pressures

Figure 35: Normal lungs

Stationary loops of the right (R) and the left (L) lung of a normal lung ΔV_s for the right lung is about 25 ml, for the left about 19 ml.

The right lung of a rabbit consists of three lobes, its volume is about 30% bigger than the volume of the left lung, which has only two lobes.

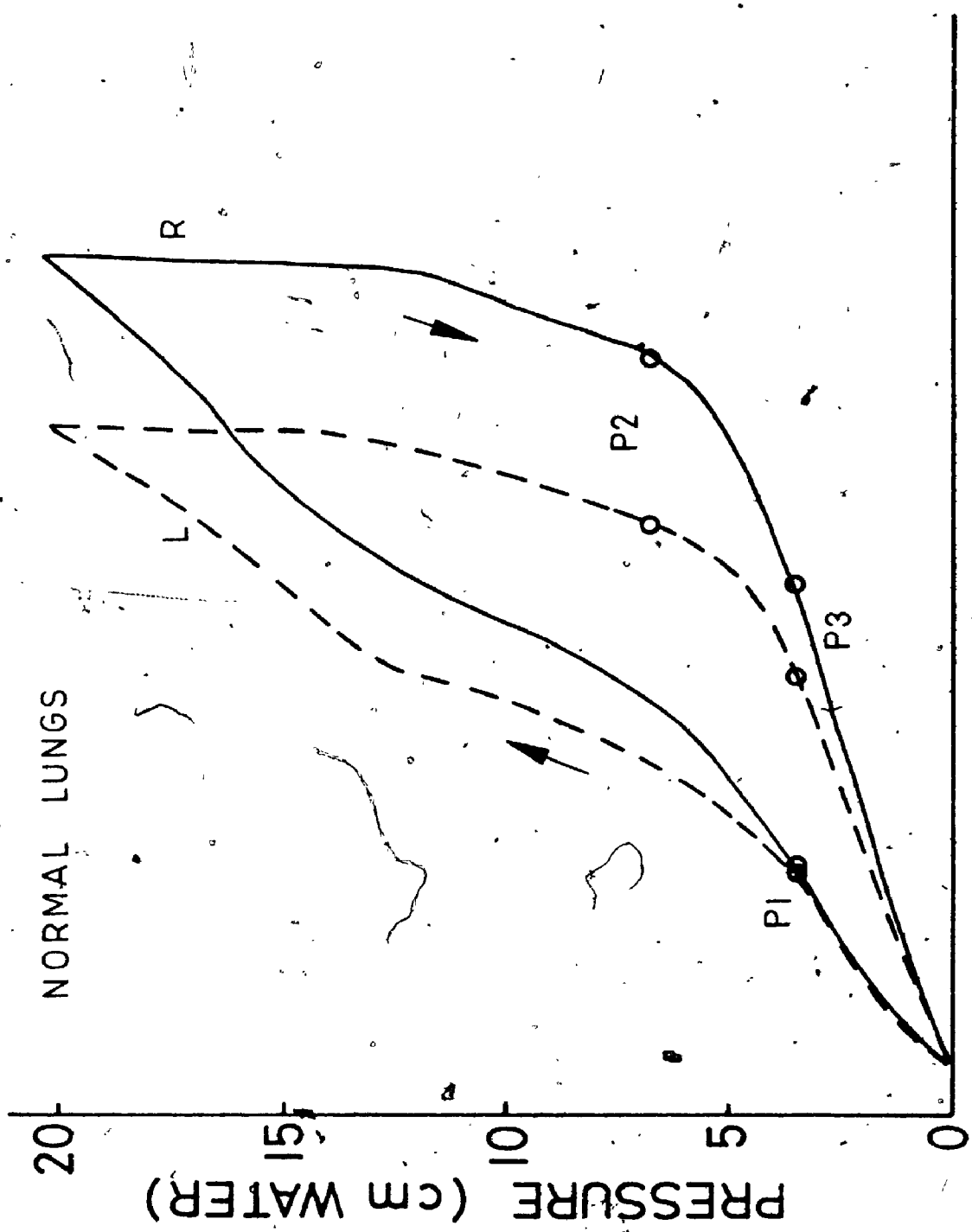
NORMAL LUNGS
R
L
P1
P2
P3
PRESSURE (cm WATER)
20
15
10
5
0
0
4
8
12
16
20
VOLUME CHANGE (ml)

TABLE IX

LUNGS WITH DIONOSIL OILY

In column 4, the calculated values $\hat{\Delta V}_s$, see equation (10.3), agree with the measured quantities ($\pm$ 20%), except for no. 2. This demonstrates that at Δp = 20 cm H_2O, ΔV_s for the Dionosil part has about the value of a normal lung.

The airways do not seem to be blocked by the Dionosil Oily. The x-rays of Dionosil Oily show without exception a diffuse pattern of well spread contrast medium.

In the histological part, we will see, that Dionosil crystals as well as the suspension medium, peanut oil, reach the alveoli.

Note: The agent is in the right lung if not specified otherwise.

TABLE IX

LUNGS WITH DIONOSIL OILY

		m	ΔV_s	$m/\Delta V_s$	$\widehat{\Delta V_s}$	$C_1=\frac{1}{S_1}$	$C_1/\Delta V_s$	$\widehat{C_1/\Delta V_s}$	ΔV_2	ΔV_3	L
1	R	8.370	16.0	0.523		0.700	0.043		13.0	7.00	0.84
	*L	7.120	15.0	0.475	13.6	0.340	0.022	0.025	8.80	4.40	0.58
2	R	10.250	15.0	0.683	21.5	0.340	0.023	0.016	7.70	3.00	0.46
	L	12.38	16.5	0.750		0.860	0.052		14.2	9.70	1.0
3	R	9.390	35.0	0.268	30.4	1.100	0.031	0.036	27.0	15.0	0.81
	L	6.170	20.0	0.308		1.720	0.086		17.7	13.8	1.1
4	R	8.050	26.0	0.309		1.610	0.062		24.0	16.6	1.1
	*L	6.510	22.0	0.296	21.0	0.900	0.041	0.043	15.2	8.0	0.71
5	R	12.76	25.0	0.510		0.640	0.026		18.5	11.2	0.82
	*L	7.840	12.0	0.653	15.4	0.408	0.034	0.026	9.00	5.80	0.86
6	R	11.64	22.5	0.517	24.8	0.420	0.019	0.017	13.5	4.20	0.49
	L	9.150	19.5	0.469		1.12	0.057		17.5	13.4	1.1
7	R	19.74	19.5	1.01	21.2	0.680	0.035	0.032	14.3	7.50	0.75
	L	15.82	17.0	0.931		0.820	0.048		14.7	9.60	1.0
8	R	11.23	17.5	0.642	18.2	0.760	0.043	0.041	12.0	6.00	0.68
	L	9.54	15.5	0.615		0.940	0.061		12.6	10.0	1.1
R.E.(%)		0.5	7.0	8.0			15.0				15.0

R: Right lung; L: Left lung; R.E.: Relative error; *: Agent in left lung

up to 30 cm H_2O (Figure 36d). Figure 37 demonstrates the stationary p-V loops of the lungs of Figure 36. In Figure 38, Dionosil Oily entered the left lung. In Figure 38b, the initially collapsed area is completely expanded; the photograph was taken at $\Delta p = 20$ cm H_2O. Figure 38b, c and d show the same lung at different pressures, in the deflation phase. At $\Delta p = 5$ cm H_2O (Figure 38c) and even more at $\Delta p = 0$ cm H_2O (Figure 38d), the initially collapsed region can be seen again. On inflation, at about $\Delta p = 10$ cm H_2O, the collapsed area is about to disappear again (Figure 38e).

Figure 39 shows x-rays of the lungs of Figure 38. The Dionosil Oily seems to spread out only a few seconds post injection of the agent.

c) Lungs with peanut oil

Peanut oil, the suspension medium of Dionosil Oily, was injected into the right bronchus of four rabbit lungs. The dose was 0.25 ml/kg rabbit. The data and results are summarized in Table X. All of the lungs showed areas of collapse on gross examination, post excision, see Figure 40. However, "opening" of the collapsed regions could be done more easily than with Dionosil Oily. Two to three runs with peak pressures of 20 cm H_2O were usually enough to expand the lung completely. On deflation, below about $p = 10$ cm H_2O, an irregular pattern reappeared, indicating progressive atelectasis (Figure 40c).

Figure 36: Lung with Dionosil Oily

Figure 36a: The lung immediately after excision (seen from the posterior aspect)

A relatively large section of the right lobe with Dionosil Oily is collapsed (see arrow).

Figure 36b: The total lung at $\Delta p = 20$ cm H_2O

Figure 36c: The right lung only, at $\Delta p = 30$ cm H_2O; about 5 to 8 runs with $\Delta p = 30$ cm H_2O were usually necessary to "open" collapsed lobes completely.

Figure 36d: This photograph was taken after completion of the p-v test. The pressure was $\Delta p = 20$ cm H_2O. After this last extension, the lung was closed off at $\Delta p = 0$, ready for fixation in formalin.

Note: Prior to the p-v test, the lung was "opened" completely (see comment for Figure 36c).

At $\Delta p = 0$, prior to fixation, the collapsed region of Figure 36a could again be recognized.

1 3 4•(2)

Figure 37: Stationary loops of the lung of Figure 36

R : right lung with Dionosil Oily

L : left lung: control

Note: The lung with Dionosil Oily demonstrates a bigger slope in P_1 (lower compliance) than the control lung.

The right lung retains much less air at P_3 than the left one.

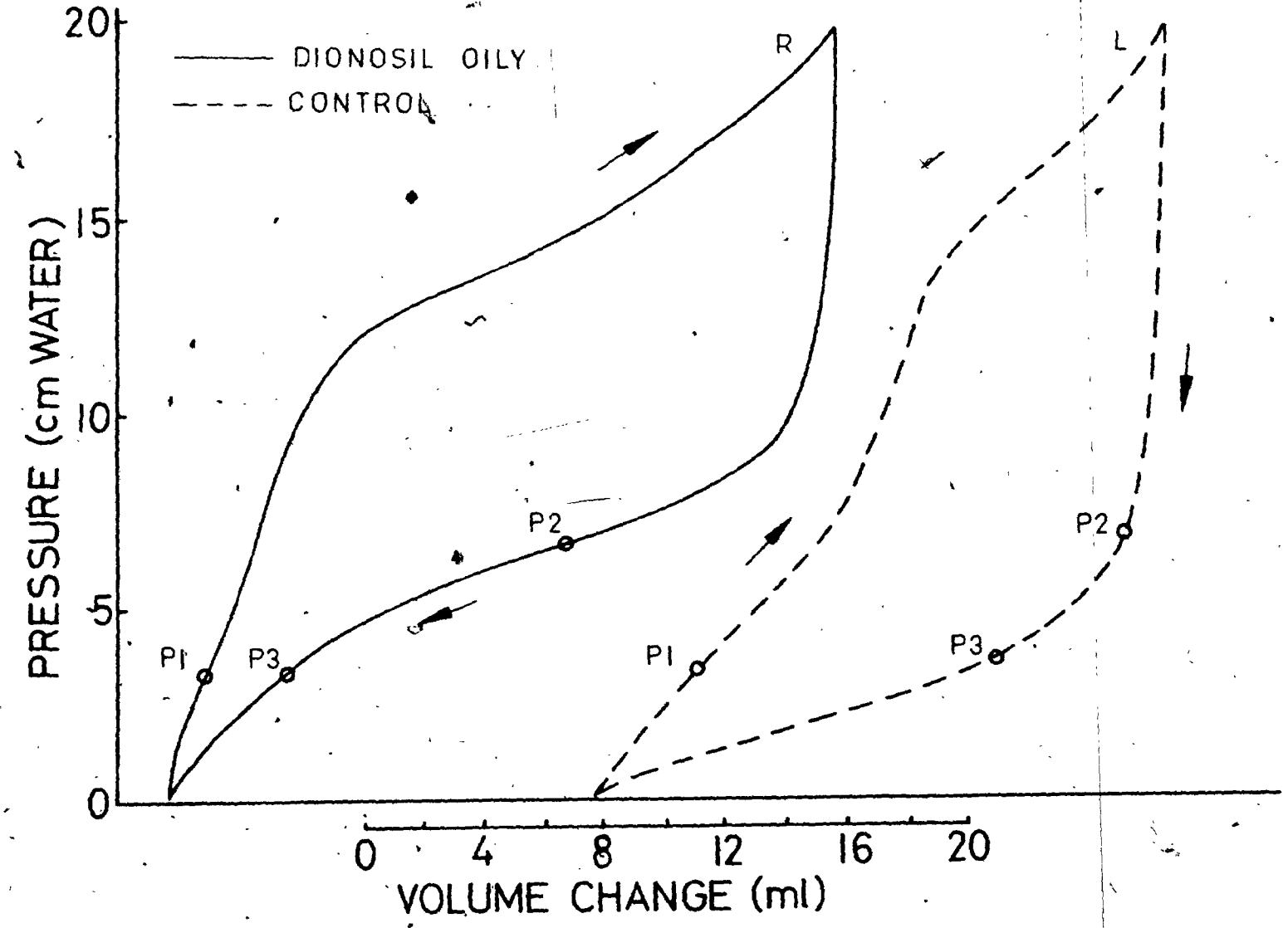
DIONOSIL OILY
CONTROL
R
L
P1
P2
P3
P1
P2
P3
PRESSURE (cm WATER)
0
5
10
15
20
0
4
8
12
16
20
VOLUME CHANGE (ml)

Figure 38: Lung with Dionosil Oily in the left part

Figure 38a: The total lung at the first run post excision, at $\Delta p = 20$ cm H_2O

Figure 38b: The right lung is closed off. The left lung is completely open at $\Delta p = 20$ cm H_2O.

Figure 38c and 38d: The left lung at $\Delta p = 5$ cm H_2O and $\Delta p = 0$ cm H_2O respectively, in the deflation part of the cycle. Below about $\Delta p = 8$ cm H_2O, the collapsed region reappeared.

Figure 38e: Inflation at about $\Delta p = 10$ cm H_2O. The collapsed area is about to disappear again.

136-(2)

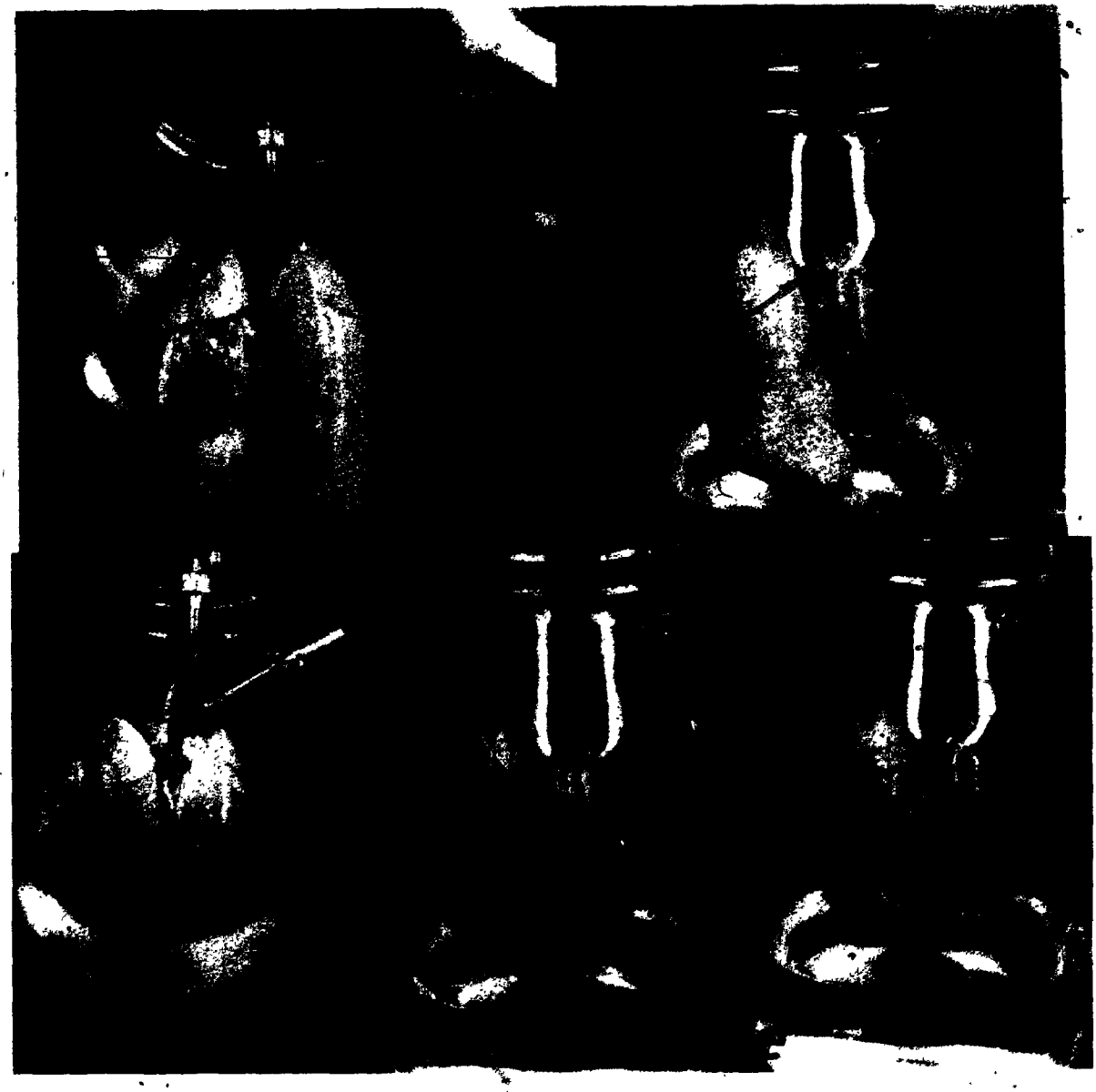

Figure 39: X-rays of the rabbit of Figure 38

The amount of Dionosil Oily was about 0.7 ml. The mass of the rabbit was 2.9 kg.

Figure 39a: It was taken twenty seconds post injection of the medium.

Figure 39b: 12 min post injection

Figure 39c: 60 min post injection

Note: In Figure 39a, the structure of the bronchial tree is still a little recognizable, but no longer in Figures 39b and 39c.

137-(2)

...SERVICE
U.W.O. LONDON.

~~14836~~

14832

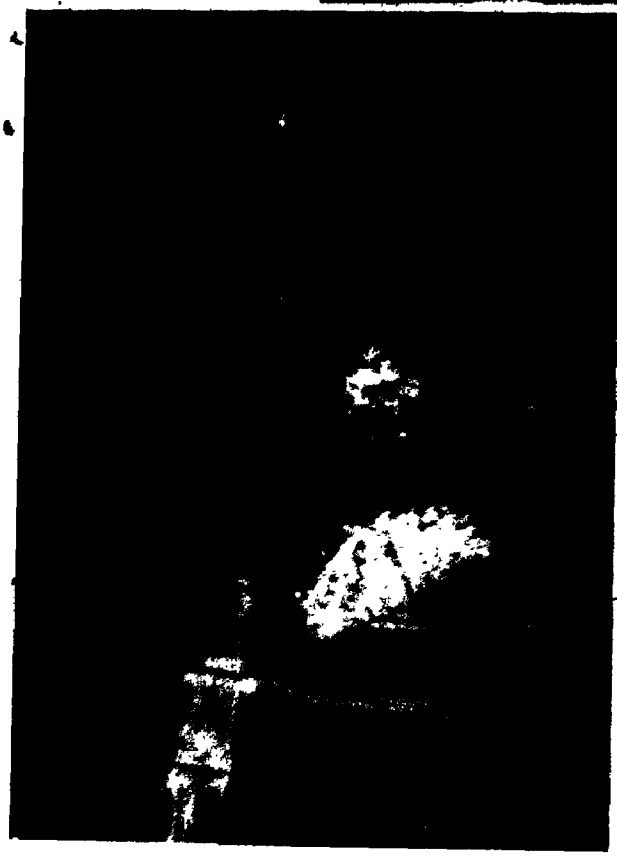

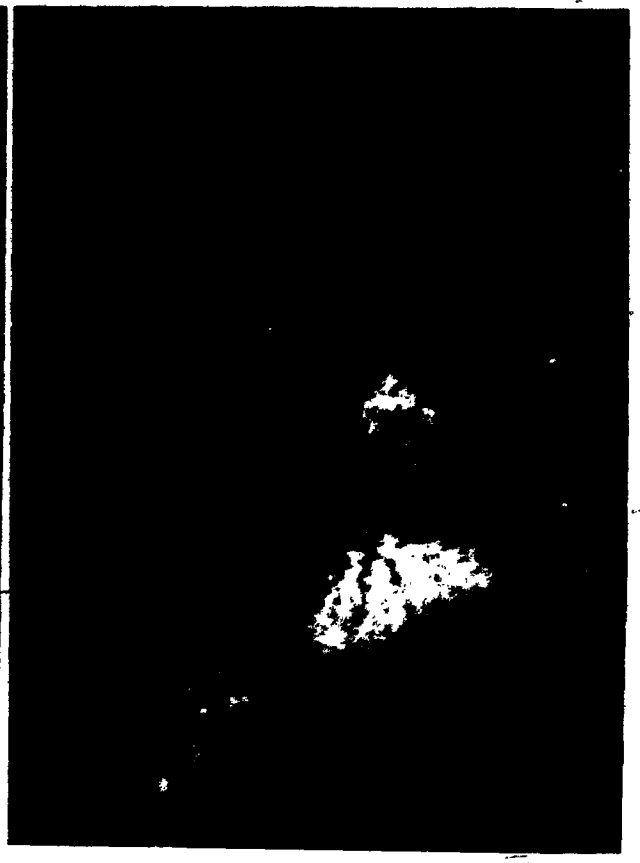

TABLE X

LUNGS WITH PEANUT OIL

		m	ΔV_s	$m/\Delta V_s$	$\widehat{\Delta V}_s$	$C_1=\frac{1}{S_1}$	$C_1/\Delta V_s$	$C_1/\widehat{\Delta V}_s$	ΔV_2	ΔV_3	L
1	R	14.10	35.0	0.403	34.0	0.960	0.027	0.028	28.0	16.0	0.86
	L	8.920	24.0	0.372		1.29	0.054		22.0	19.0	1.25
2	R	7.970	28.0	0.284	25.4	0.460	0.016	0.018	19.0	9.50	0.68
	L	5.040	16.0	0.315		0.900	0.056		13.0	9.00	0.97
3	R	9.890	25.5	0.388	29.3	0.720	0.028	0.024	18.0	11.0	0.78
	L	7.090	21.0	0.338		1.54	0.073		20.0	16.0	1.24
4	R	13.24	29.0	0.463	32.6	0.620	0.021	0.019	20.5	11.8	0.76
	L	9.870	24.0	0.411		1.26	0.052		21.5	18.0	1.19
R.E.(%)		0.5	7.0	8.0			15.0				15.0

R: Right lung; L: Left lung; R.E.: Relative error

Figure 40: "Peanut oil lung"

Figure 40a: Lung post excision. The trachea was closed off prior to opening of the chest.

The rabbit was 3.0 kg. The amount of peanut oil introduced into the right lung was 0.8 - 0.9 ml.

Figure 40b: The total lung expanded at Δp = 20 cm H_2O.

After two to three runs with peak pressures of 20 cm H_2O, the right lung was completely expanded.

Figure 40c: The total lung on deflation, at about Δp = 10 cm H_2O.

The formerly collapsed areas are reappearing as an irregular pattern.

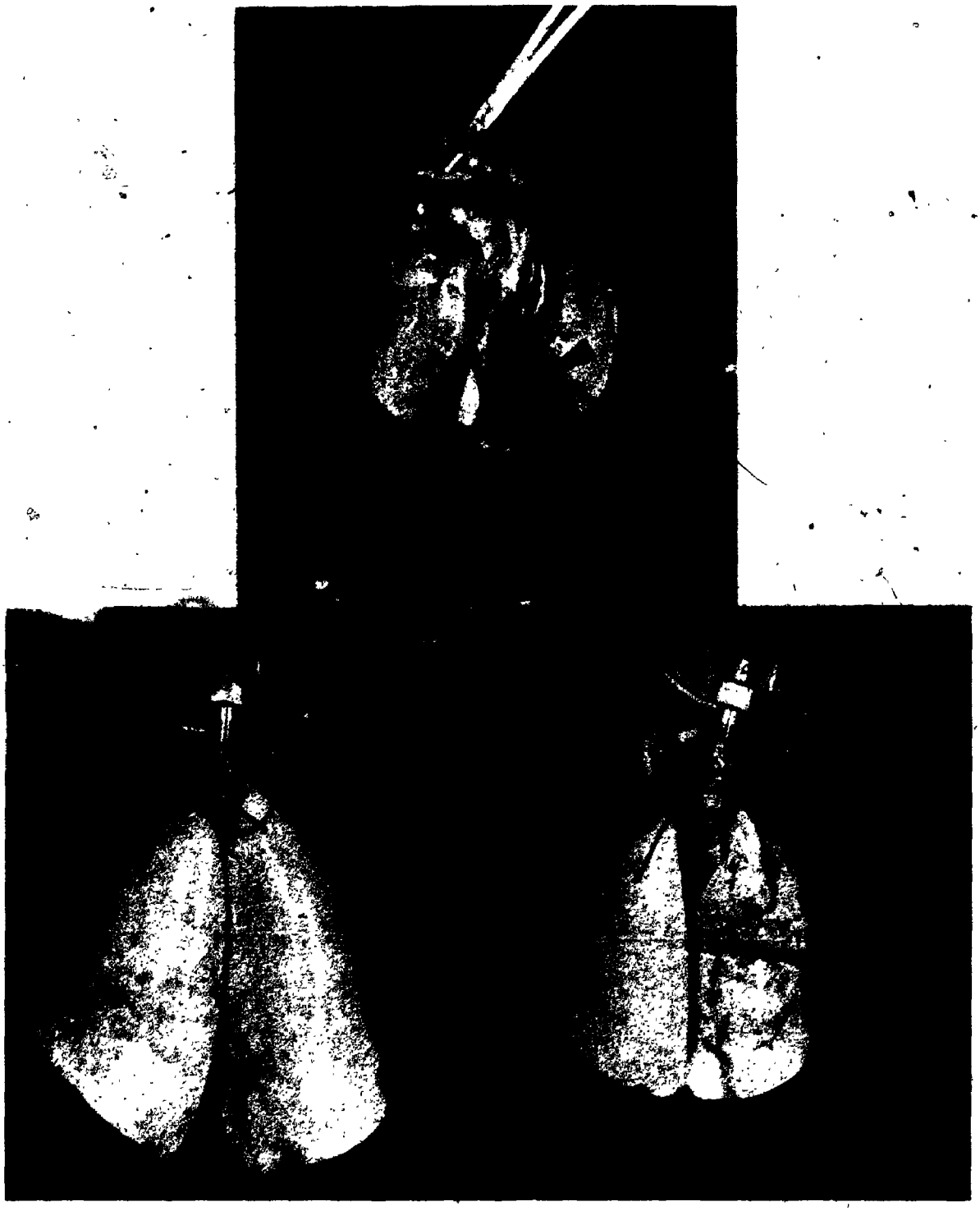

Figure 41 shows stationary p-V loops of a lung with peanut oil in the right part. Again, the slope in P_1 is steeper (smaller compliance) for the right lung than for the control lung. The lung with peanut oil seems to retain less air in the deflation part, at P_3, than the control lung.

d) Lungs rinsed with 0.9% NaCl solution

The right lungs of four of the normal lungs of Table VIII, no. 1, 3, 4, 7, and of an additional lung, were rinsed twice with 30 ml to 40 ml of saline. The purpose was to remove the surfactant and to create an air-saline interface, with a relatively high, constant surface tension. The p-V tests for the normal lung was done with the right lungs too, prior to the rinsing process.

Figure 42 shows the drastically altered characteristics of the p-V curve. The inflation part demonstrates a marked opening pressure of about 12 cm H_2O, the compliance in P_1 is almost zero.

The deflation part is characterized by a great tendency for atelectasis. At P_2 ($\Delta p \cong 6.3$ cm H_2O) and P_3 ($\Delta p \cong 3.2$ cm H_2O) there is much less retained air relatively to ΔV_s than in the intact lung. The stability index in Table XI is nearly twice as great for the lung with surfactant as for the rinsed lung.

Figure 41: Example of stationary loops of a lung with peanut oil in the right part

Note: The slope at P_1 is bigger for the lung with peanut oil (smaller compliance) than for the control lung. The "peanut oil lung" retains less air at P_3, in the deflation phase, than the normal lung.

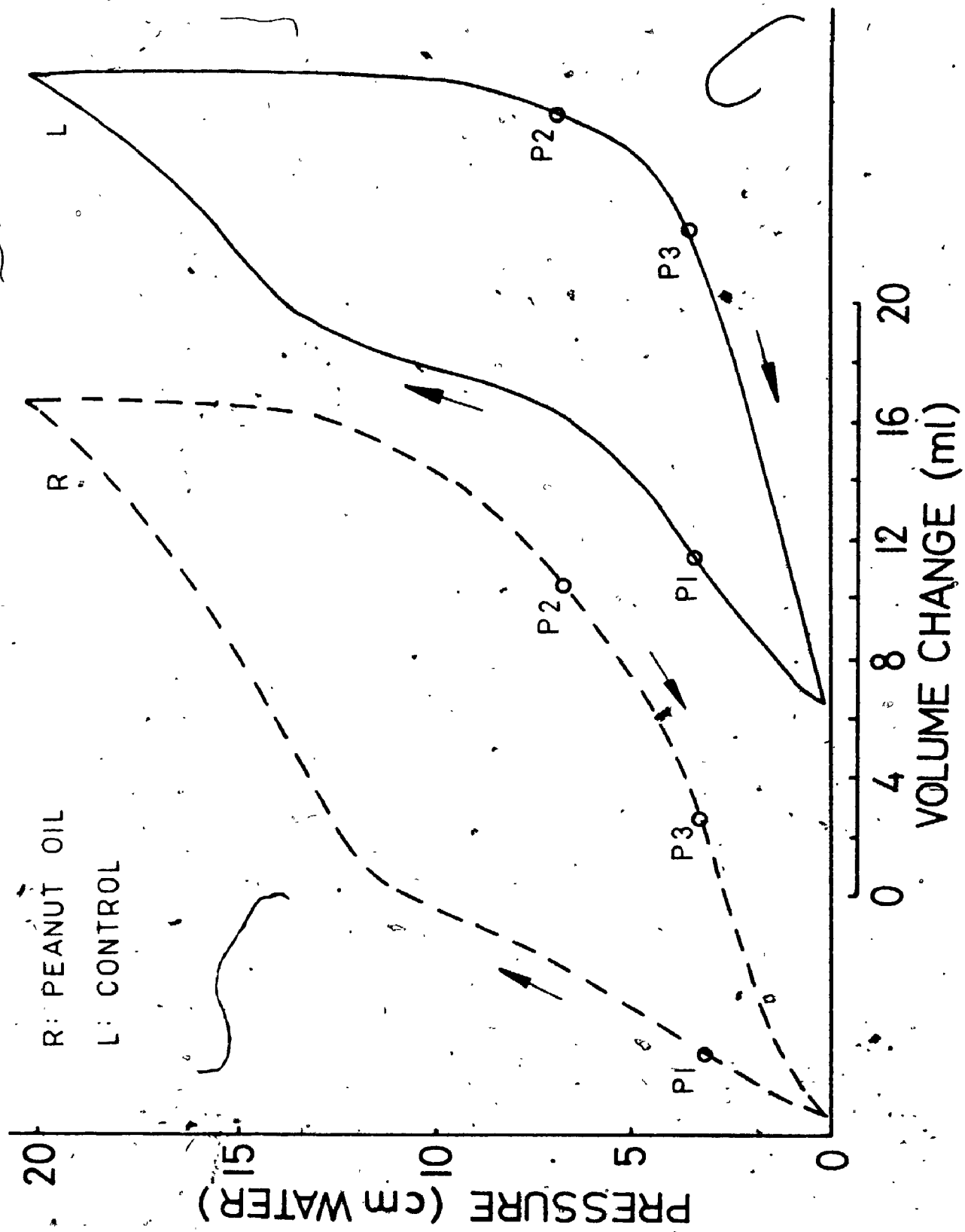
R: PEANUT OIL
L: CONTROL
L
R
P1
P2
P3
PRESSURE (cm WATER)
VOLUME CHANGE (ml)
0
5
10
15
20
0
4
8
12
16
20

Figure 42: Lung rinsed with 0.9% NaCl solution

The photograph demonstrates stationary loops of the same right lung. The control curve represents the p-V characteristic prior to the rinsing process. The loop labelled "washed out" is the diagram obtained after surfactant had been removed by rinsing.

Note: The rinsed lung (washed out) shows an opening pressure at about 12 cm H_2O.
The compliance in P_1 is zero.
At P_3, in the deflation part, there is much less air retained than in the normal lung (control).

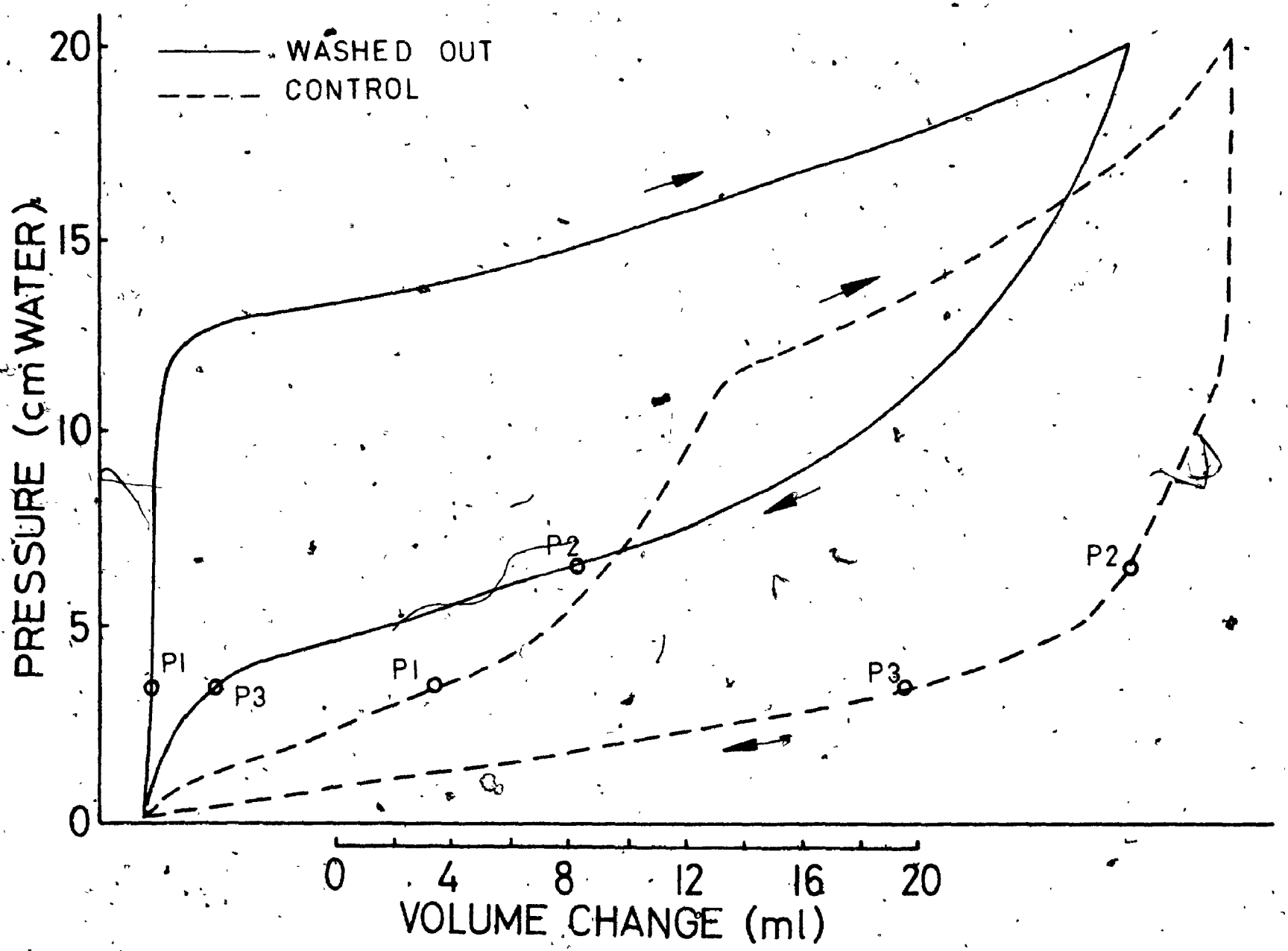
WASHED OUT
CONTROL
PRESSURE (cm WATER)
20
15
10
5
0
P1
P2
P3
P1
P2
P3
0
4
8
12
16
20
VOLUME CHANGE (ml)

142-(2)

The quantities $C_l/\Delta V_s$ are all close to zero. It is interesting to note that the p-V loops of rinsed lungs show a great hysteresis effect. Figure 43 demonstrates an irregular pattern on the rinsed lung (see arrow).

e) Statistical analysis (see Table XII)

The statistical investigation was done using a paired variate analysis with small sampling theory. The results show, that the $C_l/\Delta V_s$-values and the stability indices "L" are significantly lower for the lungs with Dionosil Oily and peanut oil than for the control lungs. The level of significance is 0.5% except for the peanut oil "L", where the level of significance was 1%.

The rinsed lungs show a greatly altered behaviour in the inflation part. $C_l/\Delta V_s$ is usually more than ten times lower for the rinsed lung than for the normal one. The stability indices "L" are also significantly different, at the level of significance of 1%.

10.3.2 X-rays and histological sections

a) X-rays with Dionosil Oily

X-rays were taken at various time intervals post injection of the agent. Dionosil Oily seems to spread out almost immediately. There is not much difference between pictures taken within 90 min after introduction of the contrast medium (Figure 44).

Figure 43: Right lung rinsed with 0.9% NaCl solution

The photograph shows the total lung at p = 5 cm H_2O, in the deflation phase.

The arrow indicates the irregular pattern which appears in the right lung.

TABLE XI

LUNGS WITH SALINE RINSED RIGHT LOBES

THE CONTROL PART IS THE SAME RIGHT LUNG, TESTED PRIOR TO RINSING

		ΔV_s	S_1	$C_1 = \frac{1}{S_1}$	$C_1/\Delta V_s$	ΔV_2	ΔV_3	L
1	Normal	20.0	0.650	1.54	0.077	17.4	12.5	1.06
	Washed out	18.0	7.14	0.140	0.0078	11.8	4.30	0.572
2	N	28.0	0.520	1.92	0.068	24.0	14.6	0.950
	W	26.0	> 20	< 0.05	< 0.001	13.8	3.80	0.412
3	N	17.0	1.16	0.862	0.051	14.0	8.20	0.894
	W	15.0	> 20	< 0.05	< 0.003	7.90	3.20	0.477
4	N	24.0	0.560	1.78	0.74	20.6	12.7	0.958
	W	18.5	0.100	0.0649	0.035	14.8	6.50	0.751
5	N	36.0	0.340	2.94	0.082	33.0	26.0	1.18
	W	31.0	> 20	< 0.05	< 0.001	18.8	8.80	0.587
R.E.(%)		7.0			15.0			15.0

N: Normal lung; W: Washed out lung (rinsed lungs); R.E.: Relative error

b) Histological sections of lungs with Dionosil Oily and peanut oil (Figures 45 - 47)

By checking the x-rays, the location of the contrast medium could be determined. In about 90% of the experiments, the Dionosil Oily had entered the lower lobe of the right lung which is biggest. The histological sections were taken accordingly. Three tissue specimens, about 1 cm apart, were taken from the right lower lobe and one or two from the two smaller upper lobes. Two specimens were processed from the control lung. In about 70 - 80% of the Dionosil sections, we found either crystals or peanut oil or both.

Control sections revealed the light network of the terminal bronchioles, the alveolar ducts, and the alveoli unless spillage occurred which was checked by x-ray.

Sections with crystals and/or peanut oil revealed definite areas of atelectasis spread diffusely throughout the section. This is called "microatelectasis". In sections with both, normal alveolar structure and microatelectasis in 90% of the cases, crystals and/or peanut oil could be identified in the collapsed regions.

c) Lungs with peanut oil only

These sections demonstrate microatelectasis almost like the "Dionosil Oily lungs". However, the sections with both, crystals and oil, seem to show more compactly col-

TABLE XII

DIONOSIL OILY - PEANUT OIL - AND WASHED OUT LUNGS

LUNGS WITH DIONOSIL OILY

	$C_l/\Delta V_s$ (1/cm H_2O)			L		
	Control	Dionosil		Control	Dionosil	
1	0.043	0.022		0.84	0.58	
2	0.052	0.023		1.0	0.46	
3	0.086	0.044		1.1	0.89	
4	0.062	0.041		1.1	0.71	
5	0.026	0.034		0.82	0.86	
6	0.057	0.019		1.1	0.49	
7	0.048	0.035		1.0	0.75	
8	0.061	0.043		1.0	0.68	
MEAN	0.054	0.033	0.5%	1.0	0.68	0.5%
S.E.	0.0126	0.0100		0.121	0.0158	

LUNGS WITH PEANUT OIL

	$C_l/\Delta V_s$ (1/cm H_2O)			L		
	Control	Peanut		Control	Peanut	
1	0.054	0.027		1.2	0.86	
2	0.056	0.016		0.97	0.68	
3	0.073	0.028		1.2	0.78	
4	0.052	0.021		1.2	0.76	
MEAN	0.059	0.032	0.5%	1.2	0.77	1.0%
S.E.	0.00963	0.00559		0.130	0.0739	

TABLE XII (continued)

RINSED LUNGS (WASHED OUT)

	$C_l/\Delta V_s$ (l/cm H_2O)		L		
	Control	Rinsed	Control	Rinsed	
1	0.077	0.0078	1.1	0.57	
2	0.068	< 0.001	0.95	0.41	
3	0.051	< 0.003	0.89	0.48	
4	0.74	0.035	0.95	0.75	
5	0.082	< 0.001	1.1	0.59	
MEAN			1.0	0.56	1.0%
S.E.			0.113	0.128	

Figure 44: X-ray photographs with Dionosil Oily in the right lung

A relatively large amount of the 0.8 ml of the contrast medium was injected into the upper right lobe and some into the lower lobes.

Figure 44a: Twenty min post injection

Figure 44b: Thirty min post injection

Figure 44c: Sixty min post injection

Figure 44d: Ninety min post injection

149 (2)

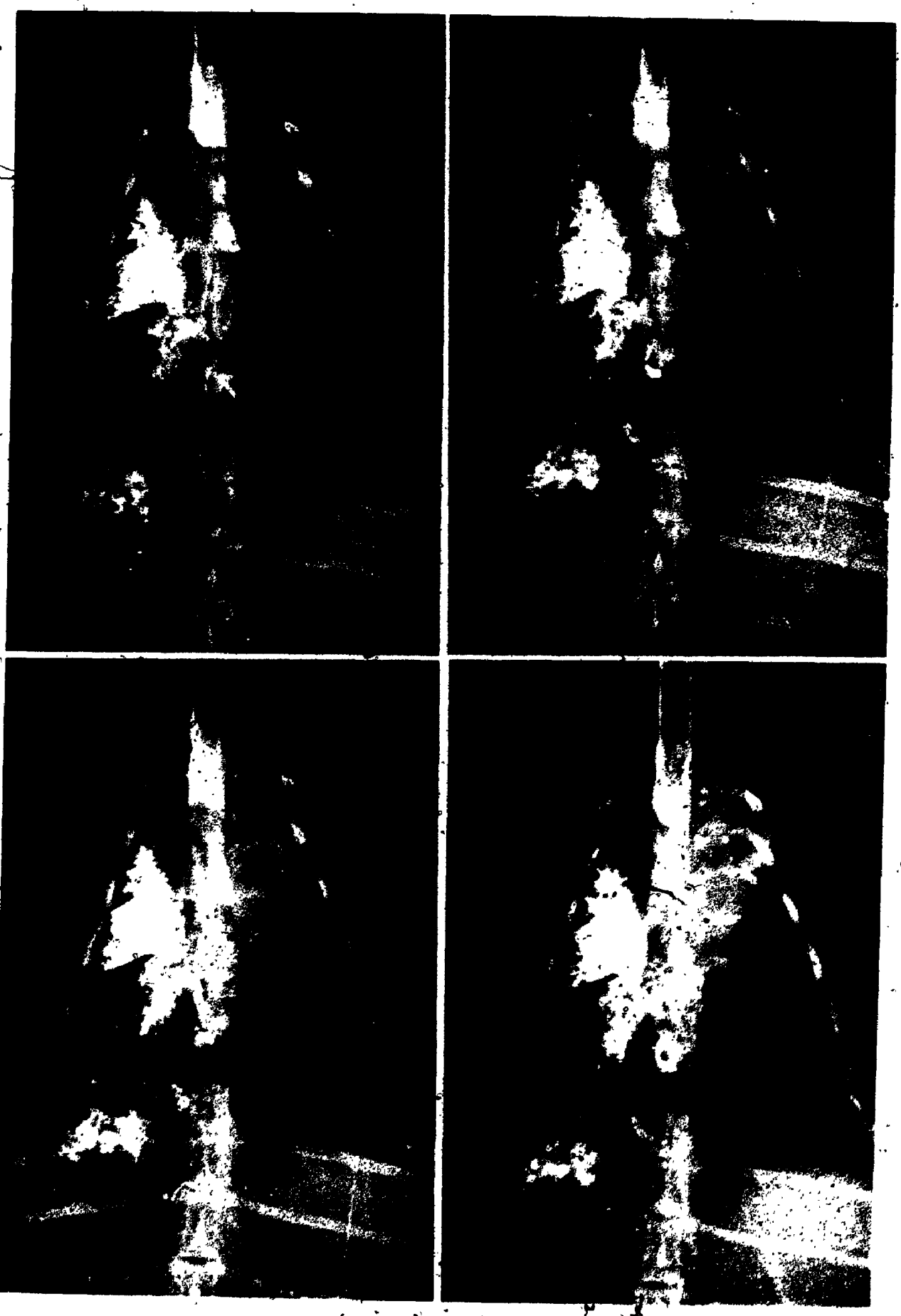

Figure 45: Frozen sections: 10 - 15 µm thick
Dionosil Oily, Toluidine blue stain

Figure 45a, 45b: Both photographs show microatelectasis where the Dionosil crystals are found. The peanut oil cannot be identified at this magnification. The left lower parts have normal appearance, see 45c, control. The distribution and size of the alveolar spaces seem to be altered in areas with Dionosil crystals.

Figure 45c: Control section of the same lung

Figure 45d: This section, at the higher magnification shows marked microatelectasis with crystals and peanut oil droplets.

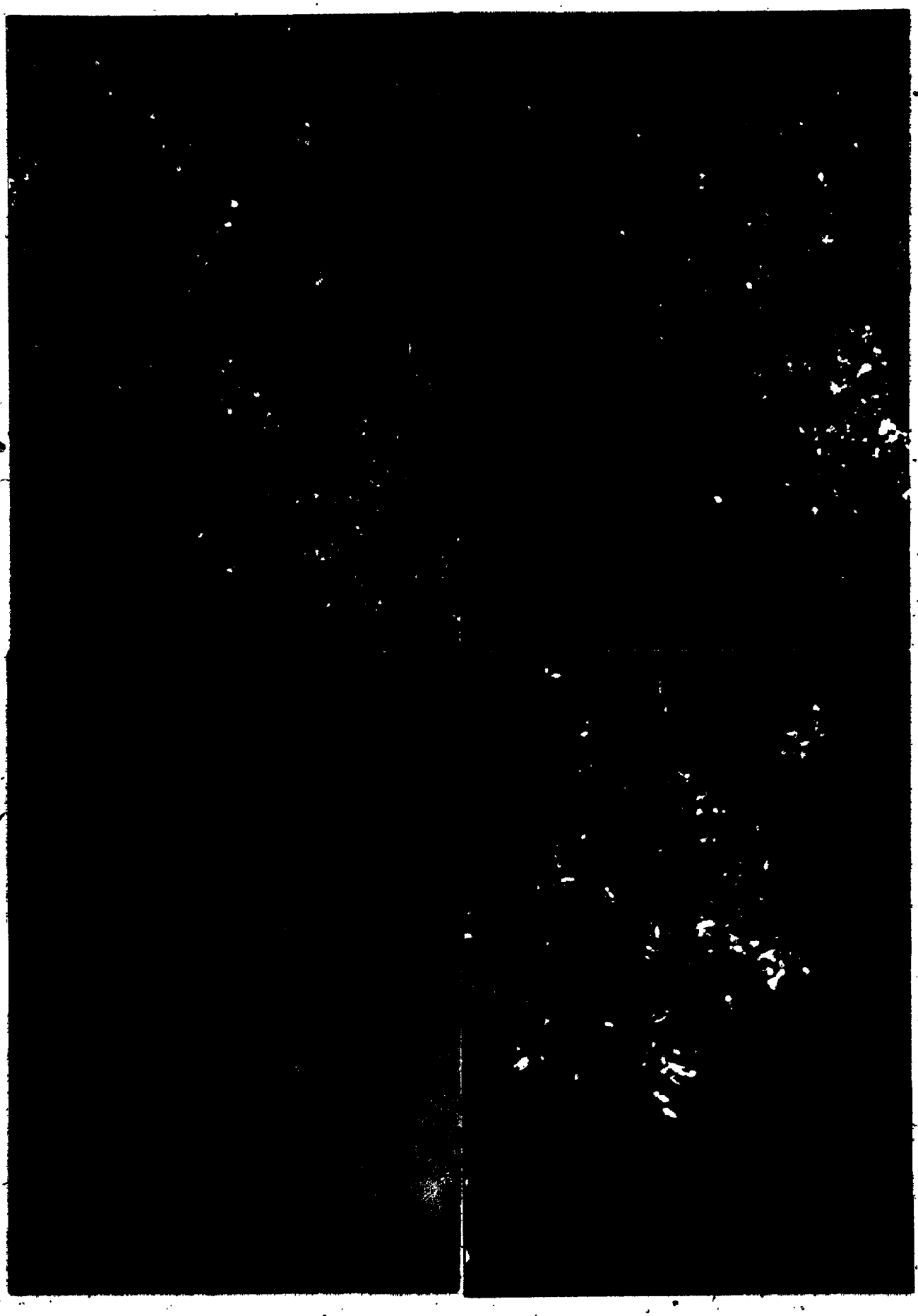

Figure 46: Frozen sections: 10 - 15 µm thick
Dionosil Oily, Toluidine blue stain

Figure 46a: The degree of microatelectasis seems to be dependent on the density of the Dionosil material. There are more crystals (and peanut oil droplets) per unit area than in Figures 45a and 45b.

Figure 46b: From the same section as 46a, at a four times higher magnification.

Figure 46c: From a lung with Dionosil Oily. There are only peanut oil droplets in sections 46c and 46d.

Figure 46d: A section of 46c, at a four times higher magnification

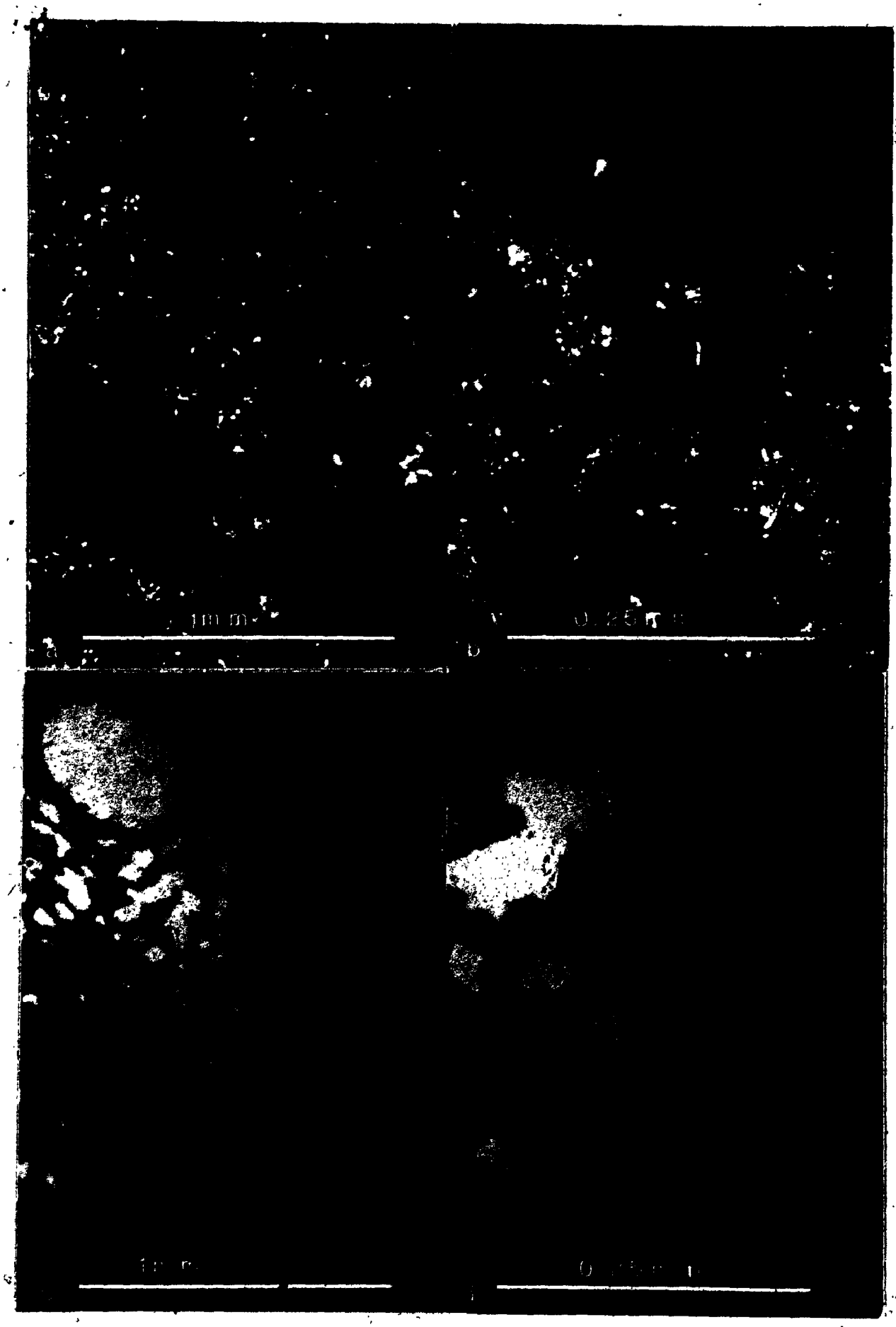

Figure 47: Frozen sections: 10 - 15 µm thick peanut oil, Toluidine blue stain

Figure 47a: The degree of microatelectasis seems to be related to the density of the peanut oil droplets. The upper left part with less peanut oil shows a pattern very close to normal.

Figure 47b: A section of 47a, at a four times higher magnification.

Figure 47c: Control section of the same lung.

152-(2)

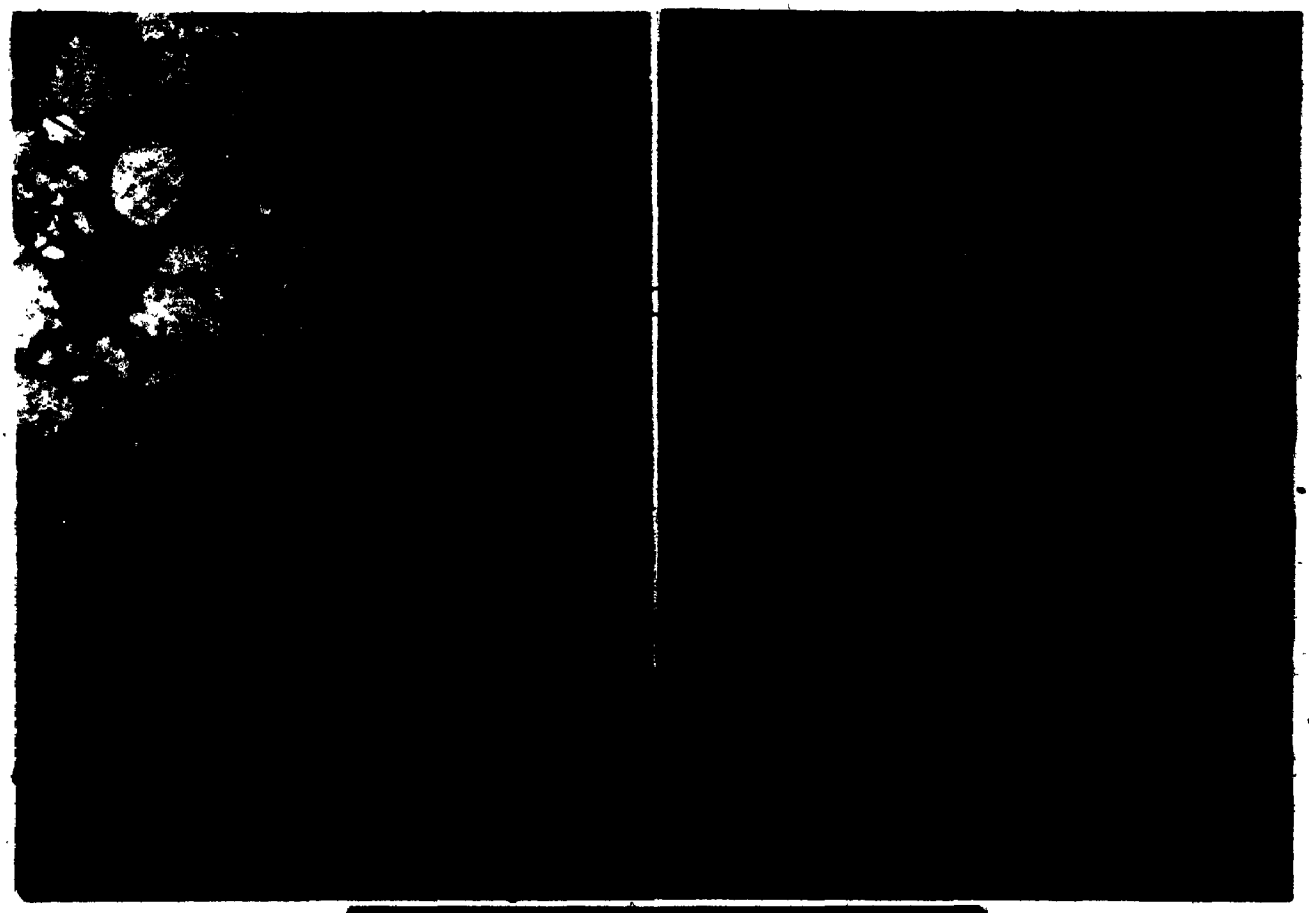

a

b

c

4 5

OF/DE

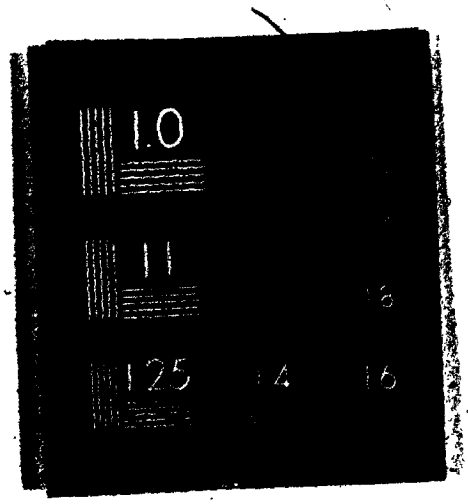

lapsed areas than pure oil sections.

10.4 Lungs with Hytrast and Dionosil Aqueous

The common characteristics of these bronchographic agents are:

1. They contain crystals with iodine, as contrast material.

2. The crystals are suspended in water

3. Carboxy-methyl cellulose is added to maintain the viscosity above 2 poise at 37°C. For further details see Appendix IV.

10.4.1 X-rays

The x-ray photographs (Figure 48 or 49) demonstrate the radiopaque material in the bronchial tree. No diffuse pattern, characteristic for bronchograms with Dionosil Oily, could be observed.

10.4.2 Gross pathology

a) Dionosil Aqueous

Six lungs out of eight demonstrated depressed areas (Figure 50a). If one of the upper lobes of the right lung showed collapse, the x-ray revealed blockage of the airways leading to this particular lobe.

b) Hytrast

Six lungs out of ten showed gross pathology (Figure 50b), the rest had normal appearance.

Figure 48: Hytrast in right lungs

The photographs were taken from two different rabbits, Figures 48a and 48b from the one, Figures 48c and 48d from the other.

Figure 48a: Ten min post injection

Figure 48b: Thirty min post injection

Figure 48c: Ten min post injection

Figure 48d: Sixty min post injection

14282

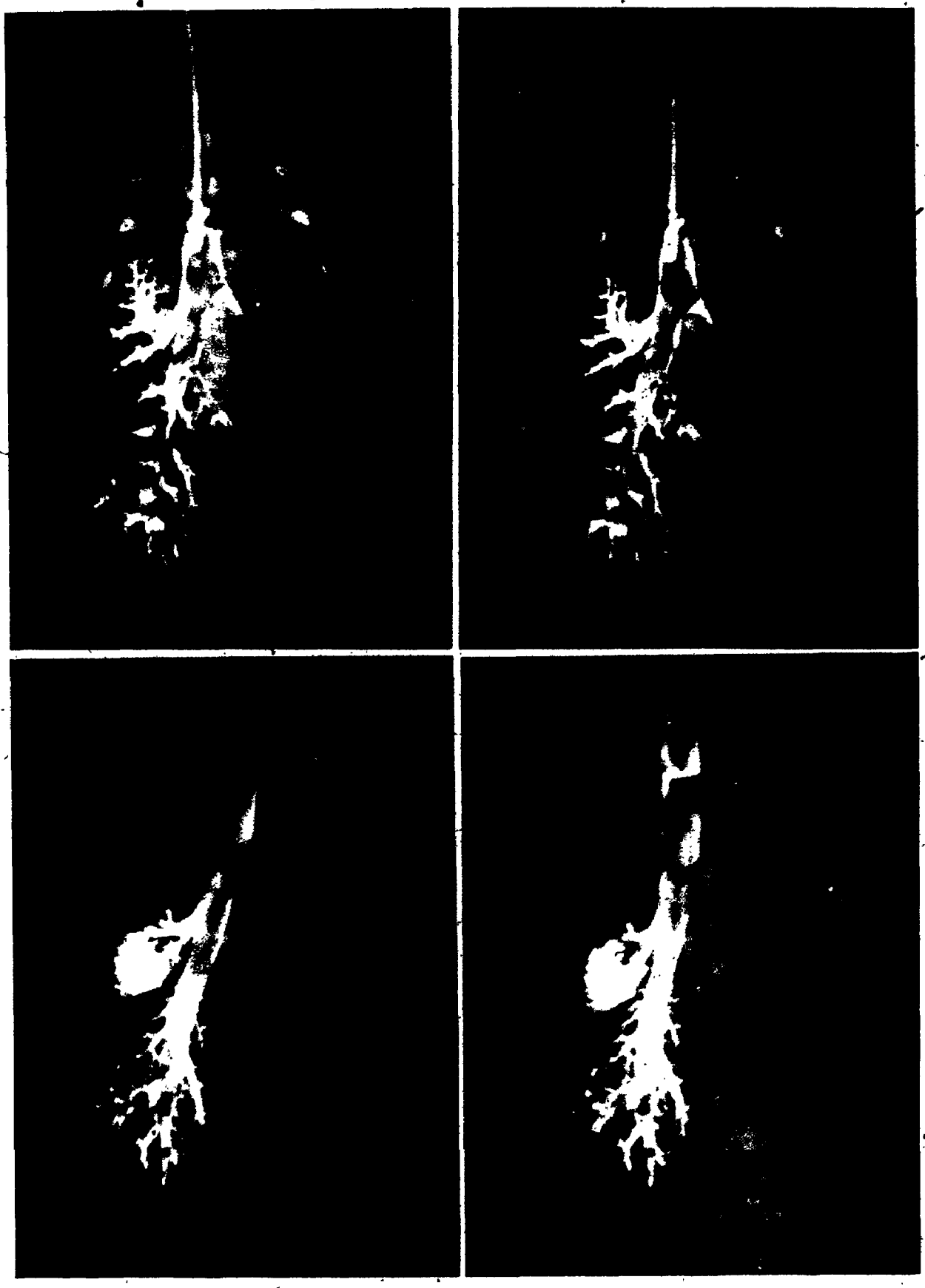

Figure 49: Dionosil Aqueous in right lungs

Figure 49a: Twelve sec post injection of an amount of approximately 0.6 ml

Figure 49b: Twelve sec post injection of an additional amount of about 0.5 ml

Figure 49c: This photograph was taken fifty min after the one of 49b.

Note: The x-rays are from the same rabbit.

155-(2)

Figure 50: Lungs with Dionosil Aqueous and Hytrast

Figure 50a: Lung with Dionosil Aqueous in right part

The photograph was taken immediately after removing it from the animal.

Figure 50b: Lung with Hytrast in right part

The photograph was taken during inflation, at about 15 cm H_2O. The left lung is inflated normally. The right lung shows clearly a depressed area in the lower lobe.

Figure 50c: This photograph demonstrates the "Hytrast lung" of 50b after the collapsed section was "opened up" completely. Several runs with pressures up to 35 cm H_2O were necessary.

156-(2)


a
b
c

10.4.3 Pressure-volume tests

Without exception, blockage of the airways was the major problem. Lungs without grossly collapsed sections would not inflate smoothly, even after several successive runs. Collapsed areas could be opened up occasionally by applying relatively high pressures up to 35 cm H_2O. Usually the lungs started to leak before the depressed regions disappeared completely. Therefore, we could not investigate the characteristics of the p-V diagrams in lungs with Hytrast or Dionosil Aqueous (Figure 51).

10.4.4 Histological sections

Hytrast crystals do spread out into the alveoli occasionally (Figure 52). But the density of particles found in any section was not even close to the one found in some sections with Dionosil Oily. No microatelectasis could be attributed clearly to the presence of crystals.

Dionosil Aqueous: Almost no particles could be found in the alveoli (Figure 53). The material seems to be stuck in the airways.

10.5 Lungs with tantalum powder as contrast medium

10.5.1 X-rays (Figure 54)

As mentioned before, the main problem was to produce an aerosol and inject it into the small rabbit lung. In a series of nine experiments, six were successful. In the first three trials there was not enough tantalum

Figure 51: The photograph demonstrates three successive loops of a right lung with Hytrast as contrast medium.

During inflation, parts of the lung opened up suddenly, the pressure fell instantly a little.
This irregular "opening up" of blocked airways is the reason for the peaks in the inflation part of the curve.

For comparison, the loop from the left (control) lung is shown (broken line).

This behaviour is typical for Hytrast and for Dionosil Aqueous.

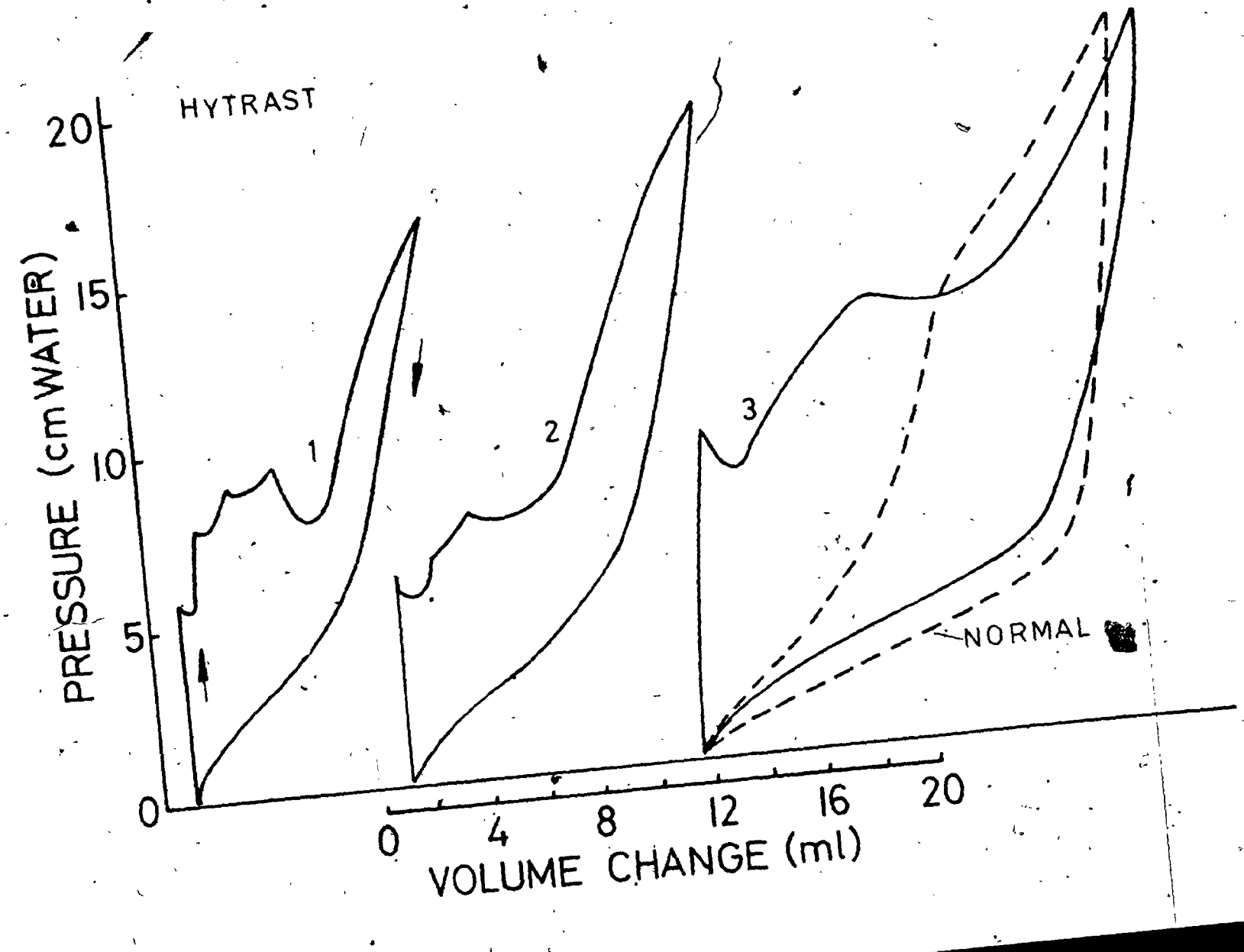
HYTRAST
PRESSURE (cm WATER)
20
15
10
5
0
1
2
3
NORMAL
0
4
8
12
16
20
VOLUME CHANGE (ml)

Figure 52: Normally processed microsections of "Hytrast lungs"

(Ethanol dehydrated and embedding in paraffin)

10 µm, Toluidine blue stain

Figure 52a: The greatest accumulation of Hytrast crystals found in any section. The tissue was obtained from the upper right lobe of the lung whose x-ray is Figure 48c, respectively 48d.

Figure 52b: Section of 52a at a four times higher magnification.

Figure 52c: Control section

Figure 52d: The crystals do not seem to stick firmly to the alveolar walls.

159-(2)

Figure 53: Dionosil Aqueous

Frozen sections: 10 - 15 µm, Toluidine blue stain

Figure 53a: Plugged airways might have caused micro-atelectasis by lack of aeration.

Figures 53b and 53c: From the same specimen as 53a, the alveolar network appears normal.

Figure 53d: Control section.

160-(2)

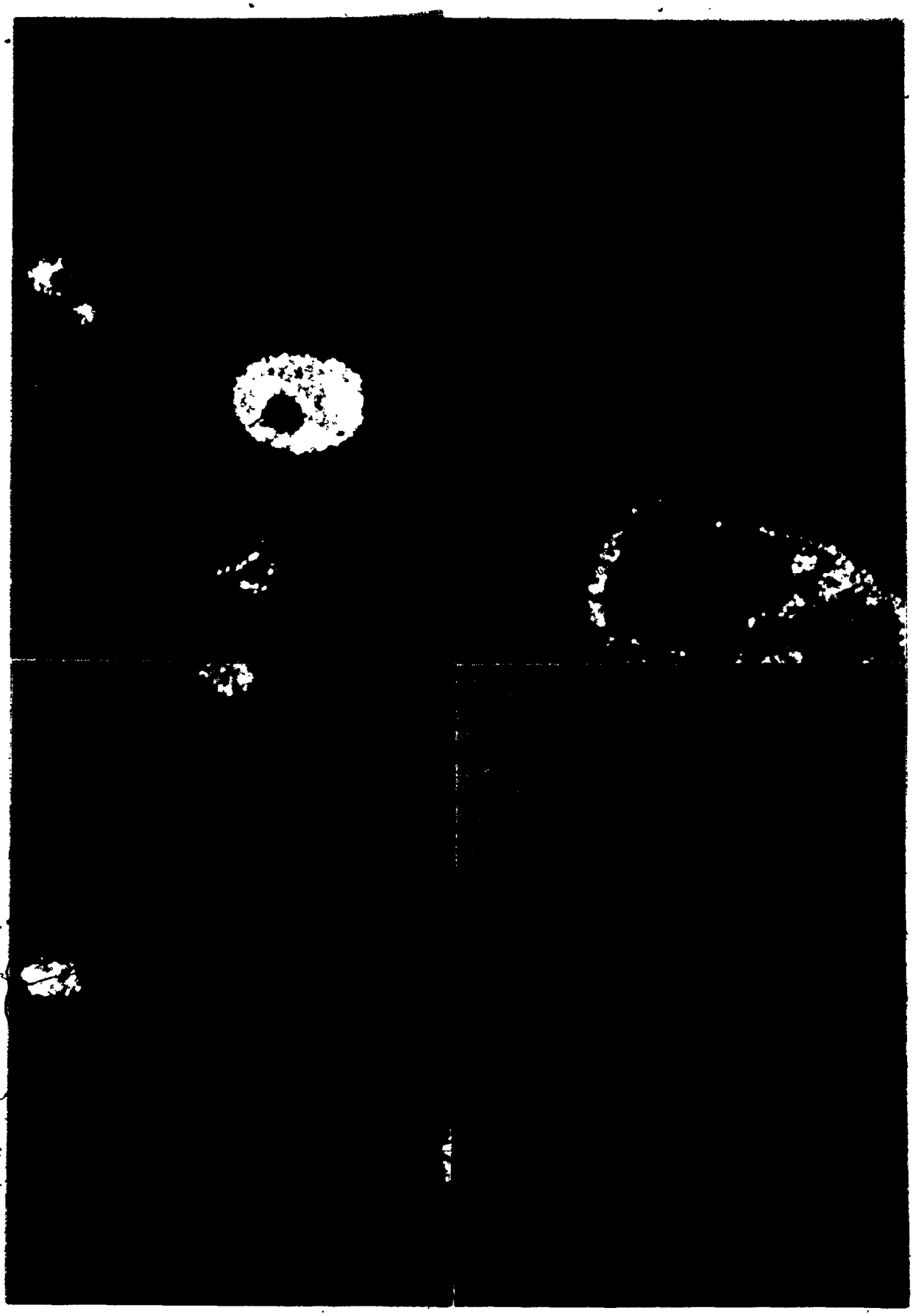

Figure 54: Bronchogram with tantalum powder

Approximately 1.0 g of tantalum particles were injected into the right lobe. Since the rabbit was breathing, some of the dust entered the left bronchus.

This photograph was taken about 30 sec post injection. Six more pictures were taken in intervals of about 12 min.

No time dependent re-distribution could be observed.

161-(2)

Figure 55: Histological sections of a lung with tantalum particles as a contrast medium.
The tissue was dehydrated with ethanol and paraffin embedded. The thickness of the sections is 8 µm - 10 µm. Toluidine blue was used as a stain.

Figure 55a: In the upper left corner an airway of about 0.8 mm across shows some tantalum powder sticking to the wall. Parts of the wall were detached from the adjacent tissue by the cutting process.

Figure 55b: Section of 55a, at a four times higher magnification.

Figure 55c: The tantalum particles are hardly visible on this magnification.

Figure 55d: Section of 55c, at a four times higher magnification. The particles outline parts of the airway nicely.

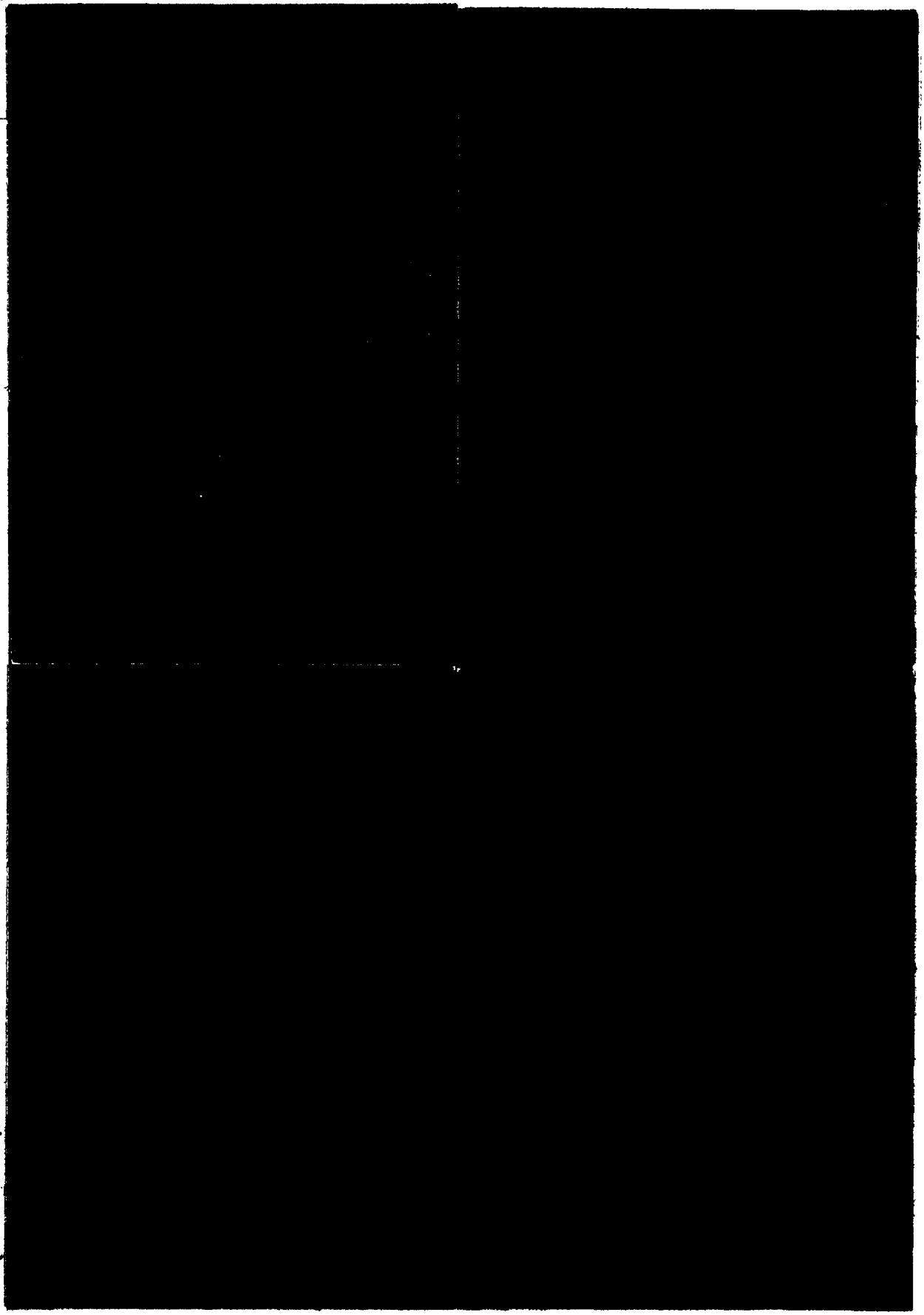

in the lungs to produce a satisfactory bronchogram. The 1 µm tantalum particles seem to stick firmly to the airways. The photographs give a better three dimensional picture of the bronchial tree. There was no diffuse pattern as it was found with Dionosil Oily (Figure 44).

10.5.2 Histological sections

Generally, tantalum dust was found in the airways, sticking to the walls (Figure 55). The smallest airways coated with particles had a diameter of 0.1 - 0.2 mm. There, single particles could be identified, but not conglomerations. Only in one section could we find some tantalum in alveolar ducts (Figure 56a and 56b).

Bigger airways from about 0.5 mm diameter and up showed a relatively heavy coating with conglomerations of particles (Figure 56c).

Figure 56: Histological sections of a lung with tantalum powder as contrast medium.
Thickness: 8 - 10 µm, Toluidine blue stain

Figure 56a: This is the only section in which tantalum could be found in the alveoli or terminal bronchioles.

Figure 56b: Section of 56a at a four times higher magnification

Figure 56c: Wall of an airway coated with tantalum. The coating seems to be detached by the cutting procedure.

Figure 56d: Tantalum particles on a microslide. Conglomerations are clearly visible.

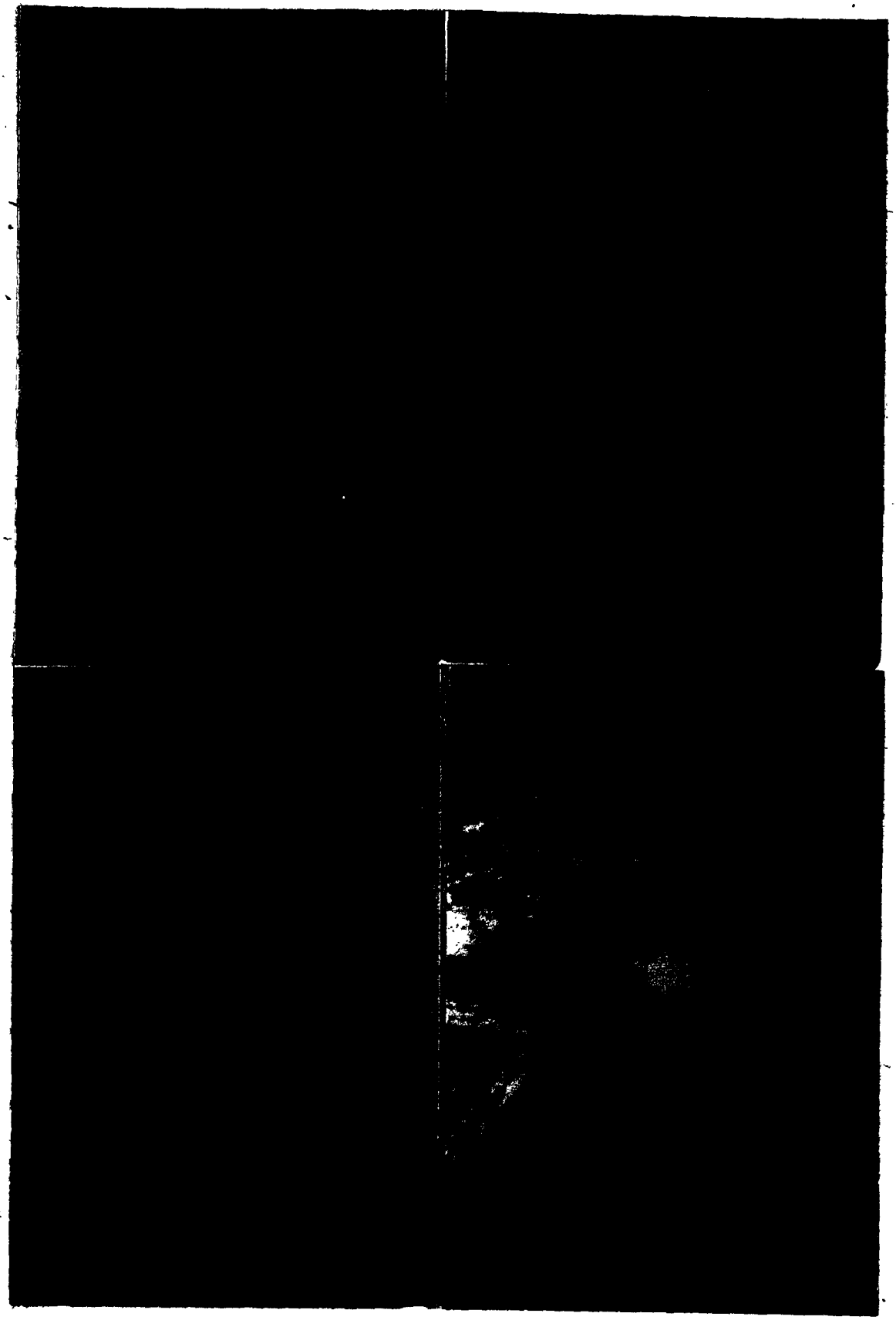

CHAPTER 11

DISCUSSION

11.1 Introduction

According to Johnson et al. (1960), an ideal bronchographic medium should have the following characteristics:

1. High radiopacity and the ability to coat bronchial walls uniformly and rapidly.

2. It must not penetrate to the alveolar ducts and to the alveoli.

3. It must undergo prompt and complete expulsion from the lungs after bronchography.

4. It must be physiologically and pharmalogically inert.

In our study, we are concerned only with short term effects, up to three hours post bronchography and only with physiological aspects regarding interference of contrast media or their suspension vehicle with the surfactant system of the lung.

There is wide agreement among radiologists that "alveolarization" of bronchographic agents should be avoided. Alveolar filling is recognized as one of the most

important causes of fever and the severity of this reaction appears to be related to the degree of "alveolarization". (Lang, 1964, Björk et al., 1957, Rayl, 1965).

Robinson et al. (1971, I) noted a 45% incidence of segmental or lobar collapse in pediatric patients, during bronchographic examination. Aqueous and oily suspensions were used in their study.

Obstruction of the airways was recognized among other factors related to gradual pulmonary collapse during the x-ray procedure. The possibility of interaction of the bronchographic agents with the surfactant was not considered,however.

11.2 Lungs with Dionosil Oily, peanut oil and "washed out lungs"

In our investigation, there was a much higher degree of alveolar filling with Dionosil Oily than with the other agents.

Within a few seconds post injection, the x-rays showed a diffuse pattern of the spread out agent, indicating penetration into the lung parenchyma. At the time of the second bronchogram, about 12 min later, the bronchi were hardly recognizable in the cloudy pattern (Figure 44). The histological sections demonstrate alveolar filling with crystals and peanut oil or with peanut oil only.

Microatelectasis found in over 90% of the sections could be clearly related to the presence of Dionosil Oily. Plugging of the airways was no problem with Dionosil Oily.

In the pressure-volume tests, on inflation, there is a significant decrease of the compliance $\frac{dV}{dp}$ at relatively low pressures (1 cm H_2O < Δp < 10 cm H_2O), for the lungs with Dionosil Oily or peanut oil. On deflation, there is less air retained at about 4 cm H_2O with a significantly lower stability index "L".

Saline rinsed lungs demonstrate similar tendencies to lungs with the oily agent. This abnormal behaviour can certainly be related to the damaged surfactant system.

Examination of the histological sections did not allow us to relate the presence of crystals to microatelectasis. However, there is good evidence that peanut oil causes microatelectasis. In the following surface tray experiments we will see, that peanut oil affects the minimum surface tension of surfactant and lecithin films. Particles, if present in sufficient density, may decrease the surface activity of a film.

11.3 Dionosil Aqueous and Hytrast

These agents contain carboxy methyl cellulose (see Appendix IV). It is added to adjust the viscosity to a relatively high value, 2.4 - 2.8 poise, for Hytrast at 37°C, (Morley, 1969). In a study with Dionosil Oily and

Dionosil Aqueous in rabbits, Björk et al. (1957) concluded that the oily suspension should be abandoned in favour of the aqueous suspension. These authors showed that the oily component is retained in the lungs even after six months with areas of pathological changes.

In a comparative study with Hytrast, Dionosil Aqueous and Dionosil Oily, Lang (1964) stated that Hytrast was least likely to fill alveoli. In a similar study, Le Roux et al. (1964) preferred Hytrast to Dionosil Oily because of better radiopacity and less alveolar filling.

Our study confirms these findings at least as far as the time period of about three hours post bronchography is concerned. Hytrast could be found in only one lung out of ten, possibly due to direct injection into a smaller, lateral bronchus, see Figure 48c. Dionosil Aqueous could not be found in the alveoli.

The common characteristic of Hytrast and propyliodone aqueous was obstruction of airways. Plugging of airways was most probably the cause for gross collapse of some of these lungs. Almost all lungs with Hytrast and Dionosil Aqueous revealed plugged airways, making our method of investigation (p-V tests) worthless, even after complete "opening" of the collapsed regions.

There was also microatelectasis due to blockage of bronchioles, see Figure 53a. Apparently, "opening up" of the grossly depressed regions does not guarantee normal appearance of the lung parenchyma.

Christoforidis et al. (1962) observed that bronchography, reduced lung capacity and interfered with alveolar aeration and intrapulmonary gas exchange. It was concluded that these effects were due to partial blockage and interference with air distribution within the lung.

11.4 Tantalum bronchography

According to Friedmann et al. (1972), and Nadel et al. (1970), tantalum or any other chemically inert metal powders have the following advantages compared to conventional contrast media:

1. the absence of airway obstruction

2. no inflammations following administration

3. a substantially smaller volume is required because no fluid medium is necessary and the medium has a relatively high radiopacity.

4. finely divided particles adhere firmly to the airway walls.

Nadel et al. (1970) noticed retention of tantalum particles in small numbers in airways less than 1 mm in

diameter and within the alveoli. Friedman et al. (1972) point out that "alveolarization" would be unlikely with controlled insufflation of powder of known particle size.

In our study, tantalum particles could not be found generally in airways smaller than (0.1 - 0.2) mm diameter. Only in one section some agglomerations of particles were found in the lung parenchyma (Figure 56a, 56b). The x-rays revealed a clearly outlined bronchial tree and no diffuse pattern, typical for Dionosil Oily. The deposition of particles in the parenchyma, especially beyond the region of effective muco-ciliary clearance is affected by many factors, e:g.: (Friedman et al., 1972)

- size of the particles
- method of administration
- aerodynamics of the aerosol entering the lungs
- position of the subject under bronchography and
- degree of anaesthesia.

Two methods of administration of the powder are described:

a) With the method described by Nadel and his co-workers (1970), the particles are blown into the lung with a certain applied pressure.

b) Kammler et al. (1971) reported tantalum administration by spontaneous breathing.

With our method (see Appendix V) the particles

were blown through small tubing into the lung. The tantalum dust left the catheter in short bursts. No continuous pressure was applied.

By using fluoroscopic control, this method could be developed for selective bronchography. Kammler et al. (1971) noted, that 1 µm tantalum particles did not produce satisfactory x-rays, due to spontaneous aggregation. These authors preferred 5 µm tantalum particles. We observed extremely little alveolarization in rabbit lungs. Whether this is due to the specific characteristic of the rabbit lung or due to our technique of using 1 µm size particles is not known. The possibility that 1 µm particles migrate less distally and with a shorter sedimentation time than larger particles, can not be excluded.

11.5 Summary

Propyliodone oily (Dionosil Oily), enters the alveoli readily. Microatelectasis in sections of the entered lung is related to the presence of peanut oil, which reduces the surface activity of the lung alveolar surfactant. Interaction of particles with the surfactant can not be excluded, especially if many particles enter the alveoli.

The "high viscosity" media, Hytrast and aqueous propyliodone obstruct the airways. Plugged airways can cause gross collapse and to a smaller extent microatelectasis.

Only negligible quantities of Hytrast or Dionosil Aqueous, compared with Dionosil Oily, entered the terminal bronchioles and the alveoli. Tantalum powder was the least likely to enter the alveoli. There is no obstruction of the airways with this powder method.

Interaction of tantalum particles with the surfactant cannot be excluded, but it was found to be highly unlikely, since these particles never entered the alveoli in a sufficient large number.

CHAPTER 12

SURFACE TRAY STUDIES

12.1 Introduction

In this chapter we will gather further evidence for the postulate that bronchographic media interfere with lung surfactant. The nature of interaction of these agents with surfactant and dipalmitoyl lecithin at the air-liquid interface will be discussed.

12.2 Material and methods

12.2.1 Propyliodone

Ten ml of Dionosil Oily were diluted with about 300 ml of light petroleum (petroleum ether) and then filtered. This procedure was repeated about four times. When the remaining propyliodone powder was dry, a small sample was tested on the surface tray on a water subphase for complete extraction of the oil. The pure propyliodone particles were then suspended in air by the "fluidized bed" technique (see Appendix V), and blown gently on surface films from rabbit surfactant or DPPC.

Some propyliodone was dissolved in acetone and recrystallized and the blown on the surface films.

Some substance was dissolved in chloroform and mixed with a solution of DPPC in chloroform. The mixture

was made up to produce a ratio of the number of molecules, DPPC/propyliodone such as 1 : 1, 1 : 2 ..., up to 8 : 1. The mixed solutions which had a DPPC concentration of approximately 2 to 4 mg/ml, were then spread on a surface of 0.9% NaCl.

12.2.2 Dionosil Aqueous, Hytrast and tantalum powder

In order to remove the water from Dionosil Aqueous and Hytrast, these two substances were dried at about 60°C, and then ground in a mortar to produce a light powder. The powder was blown either directly onto the surface films or again suspended in water to make up a concentration of about 20 mg/ml. The tantalum particles were blown directly onto the surface films.

12.2.3 Peanut oil

This was obtained from the top of a bottle of Dionosil Oily, which had been left standing upright for several weeks. The white substance had settled on the bottom of the flask. The oil was dissolved in n-hexane : propanol (10 : 1, by vol.), to make solutions from 2mg/ml up to 20 mg/ml((2, 4, 10, 20)mg/ml).

12.2.4 Dose

a) Peanut oil

The high dose was approximately 0.01 mg/cm^2, at maximum trough area, the low dose about 0.003 mg/cm^2. The order of magniture of these doses were estimated by

using the data of De Burgh Daly et al. (1966), p. 21, who suggested that the alveolar surface area of rabbit is about 6 m^2 or 3 m^2 per lung. Assuming 1 ml of Dionosil Oily for bronchography, of which about 30% is peanut oil, we have approximately 0.3 g of peanut oil per 3 m^2 of alveolar surface, or about 0.01 mg/cm^2.

b) Particles

Particles were blown on a water surface in the trough. If the density of particles at 100% trough area did not exceed a certain maximum value, the surface tension was not measurably influenced on compression of the area to 25%. This critical density was about 0.5 mg/cm^2 ± 20% for tantalum powder and approximately 0.3 mg/cm^2 ± 20% for the pure propyliodone crystals. The high dose for tantalum was twice this critical value or 1.0 mg/cm^2 ± 20%, the low dose was equal to the critical value of 0.5 mg/cm^2 ± 20%.

The amount of powder used in the surface tray studies was calibrated by dusting paper sheets of areas equal to 100% trough area and then by measuring the mass.

12.3 Results

12.3.1 Particles on a water surface

Figure 57a represents the surface tension-area characteristics of "films" from tantalum powder of four different concentrations. For the solid line, the con-

centration at 100% trough area was 0.5 mg/cm^2 ± 20%. For the second curve, the concentration was 1.0 mg/cm^2. Upon concentration, the surface tension begins to fall at a relative area below 50%.

For the third curve from top, the concentration of tantalum powder at 100% film area was 2.0 mg/cm^2 ± 20%. The surface tension begins to fall just below 100% relative area. For the last curve, the density of tantalum powder at 100% area was about 4.0 mg/cm^2. The surface tension at maximum film area is lower than the one of the subphase. The particles are very likely almost closely packed and are interacting with each other. Therefore, the surface energy is smaller than the one of a clean water-air interface.

Figure 57b demonstrates the surface potential-area characteristics of the corresponding curves of Figure 57a. (The solid line corresponds to the solid line etc.). The curve for which the initial concentration was about 2 mg/cm^2, shows a maximum surface potential at an area where the surface tension diagram demonstrates a plateau. There, the "film" is probably folding up, the particles begin to form conglomerations. Water penetration is likely, since the surface potential is falling upon further concentration.

The behaviour of tantalum dust on a water surface is typical for any kind of particles investigated in this

Figure 57: Behaviour of a "film" of tantalum particles ("1 μm particles") at the air-water interface

Figure 57a:

——— Surface tension-area characteristic of a "low dose" tantalum "film". The density at 100% trough area was 0.5 mg/cm^2 ± 20%.

-------- "High dose" tantalum "film"

The concentration of tantalum powder at 100% area was 1.0 mg/cm^2 ± 20%. The surface tension begins to fall below about 50% area.

—·—·—·— The density of tantalum particles was about 2.0 mg/cm^2.

—··—··—··— The density of tantalum particles at 100% trough area was about 4.0 mg/cm^2. The surface tension at 100% area is approximately 10 mN/m below the one of the pure water surface.

Figure 57b: Surface potential-area characteristics. The solid line corresponds to the solid line of Figure 57a etc. For comment see text.

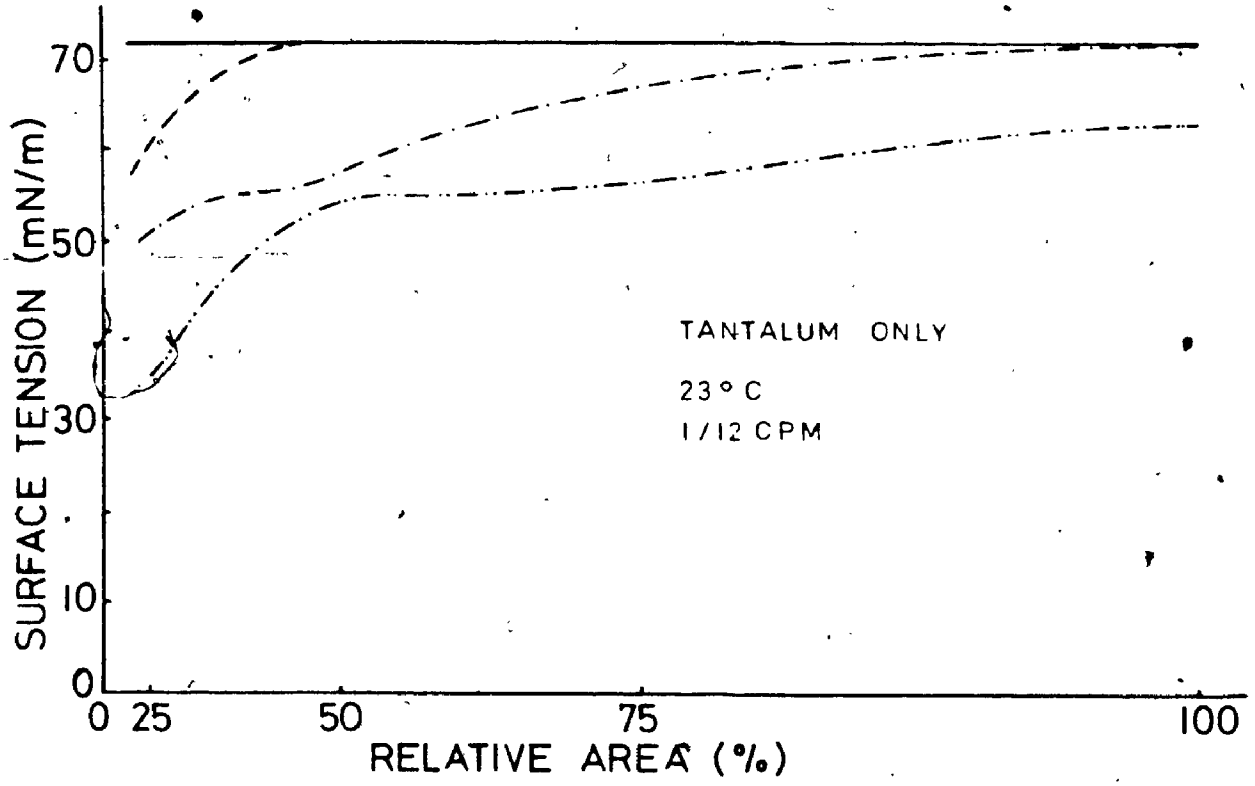
SURFACE TENSION (mN/m)
70
50
30
10
0
0 25
50
75
100
RELATIVE AREA (%)
TANTALUM ONLY
23° C
1/12 CPM

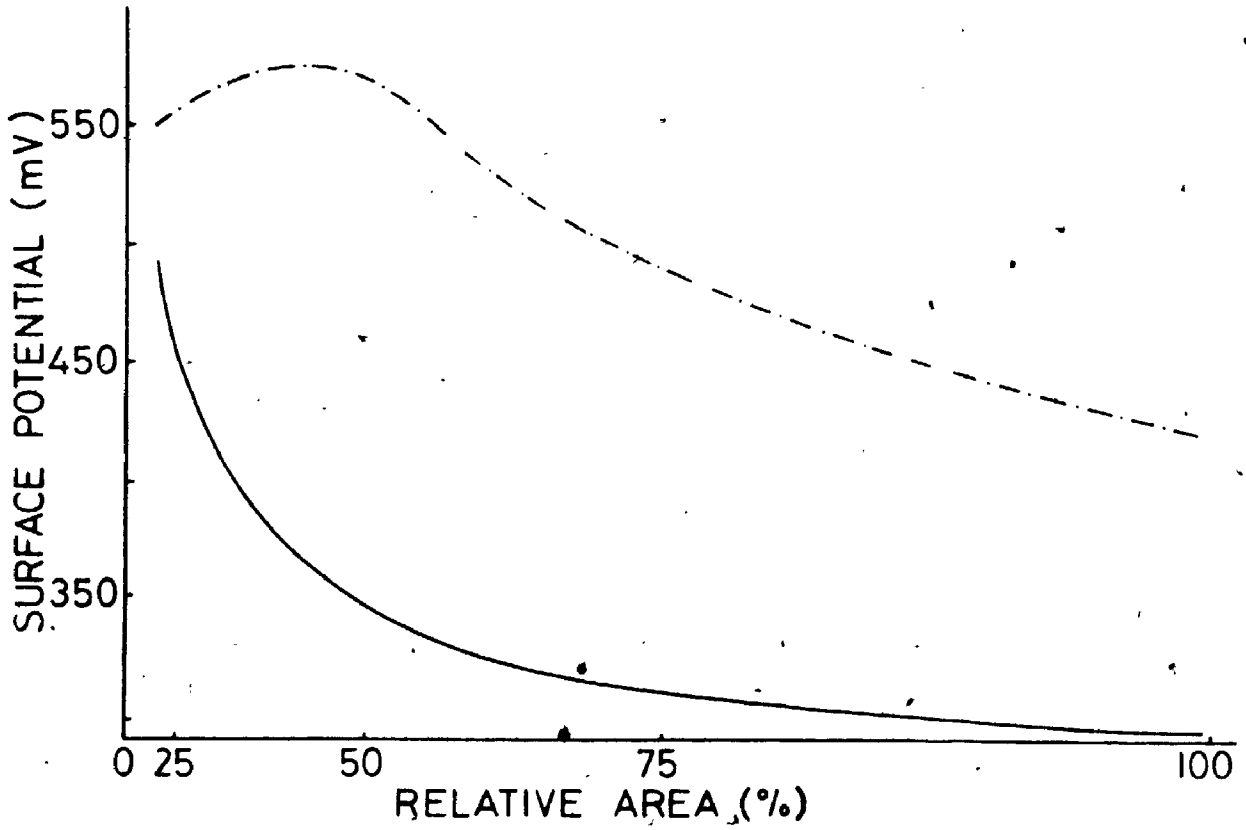
SURFACE POTENTIAL (mV)
550
450
350
0 25
50
75
100
RELATIVE AREA (%)

study. Most of the particles of the bronchographic agents have an optical diameter between 1 μm and about 20 μm (see Appendix IV).

Propyliodone crystals probably up to ten times bigger than tantalum particles did not demonstrate a different behaviour than tantalum particles at the air-water interface.

Figure 58 shows photographs of films from tantalum powder. Glass microslides were dipped into the surface trough at 25% area. The pictures, all at the same magnification, give an idea about the density of the particles.

12.3.2 Particles on a DPPC monolayer

The results shown in Figure 59 are typical for any kind of particles investigated in this study, propyliodone, Hytrast or tantalum. No effect due to the different chemical nature could be observed. As long as the amount of particles (mg/cm^2), was about the same, identical results were produced (within the error range of 20%).

In Figure 59, propyliodone particles were dusted onto the surfaces. The low dose was about 0.3 mg/cm^2, the high dose approximately 0.6 mg/cm^2. The DPPC film without the crystals produced the typical minimum surface tension of about 1 mN/m. With the particles on the film, the minimum surface tension was higher. The low dose increased the

Figure 58: Photographs of "films" from tantalum powder. Glass microslides were dipped into the trough at 25% film area.

Figure 58a: "low dose": 0.5 mg/cm^2 at 100% area, which corresponds to 2.0 mg/cm^2 at 25% area.

Figure 58b: "high dose": 1.0 mg/cm^2, at 100% area, which corresponds to 4 mg/cm^2, here at 25% area. The particles are closely packed.

Figure 58c: 2.0 mg/cm^2 at 100% area, which corresponds to 8 mg/cm^2 at 25% area (picture). Conglomerates of particles were formed with water gaps between.

Figure 59: DPPC monolayers with particles added

Low dose propyliodone crystals, about 0.3 mg/cm^2 at 100% area, on the saline surface.

High dose propyliodone crystals, approximately 0.6 mg/cm^2 at 100% area.

———— Surface tension-area characteristic of a DPPC film, without particles.

-------- DPPC film with low dose propyliodone crystals

—·—·— DPPC film with high dose propyliodone particles

The curves were drawn on the basis of at least ten independent experiments for each dose.

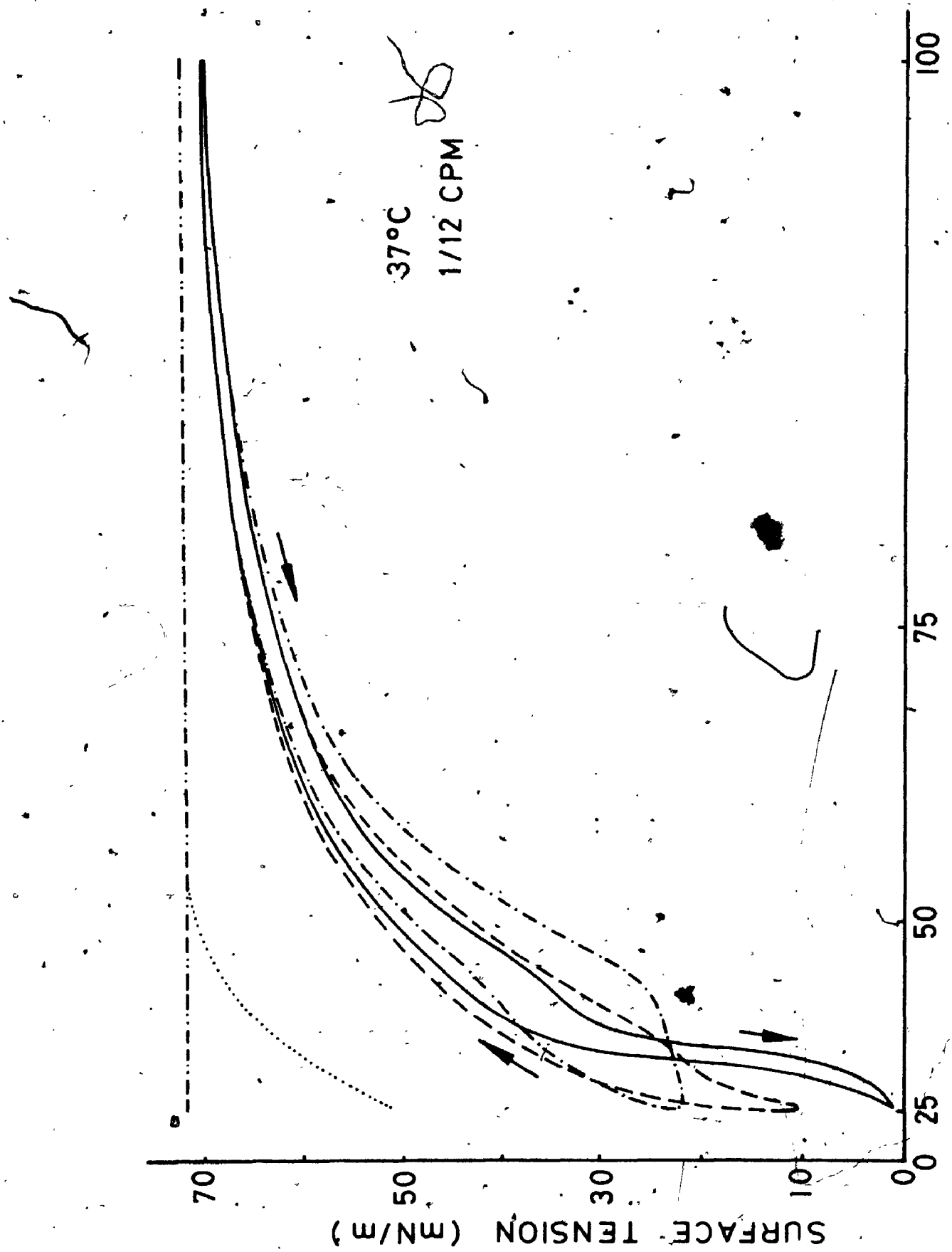
37°C
1/12 CPM
SURFACE TENSION (mN/m)
70
50
30
10
0
0
25
50
75
100
RELATIVE AREA. (%)

minimum surface tension from 1 mN/m to about 10 mN/m, the high dose from 1 mN/m to more than 20 mN/m. The original near zero minimum surface tension produced by the clean DPPC film could be restored, when additional lecithin was spread at 100% area. The lecithin swept the surface clean and pushed the particles to the trough walls. Upon reduction of the film area, some of the crystals sank to the bottom of the trough. Five experiments per dose and kind of particles were done.

12.3.3 Particles on a film from lung surfactant

Surfactant from six rabbits was obtained according to 4.1.1. The cell-free surfactant was then fractionated in a column and the preparation of foam no. 1 spread on 0.9% NaCl surfaces (see 4.1.2 c) and 4.2.1).

Since we obtained about four surface tray preparations from each rabbit, a total number of twenty experiments were done, a group of ten with tantalum powder, the other ten with propyliodone crystals. Half of the preparations from each group was used for high dose experiments. Loop no. 10 of ten successive curves was chosen as the control loop (4.2.1). As response to the agents, again ten successive loops were recorded, and no. 10 was drawn. All the experiments were done at 37°C and 8 cycles/min. At least eight preparations out of ten of each group produced a minimum surface tension lower than 5 mN/m (loop no. 10).

Figure 60a is typical for the influence of particles dusted on films of surfactant, foam fraction no. I. As long as about the same amount of particles (mg/cm^2) was added at 100% area, the effects were equal within the error range of 20%, regardless of the different nature of the substances.

The high dose increased the minimum surface tension from about 5 mN/m to the plateau level at approximately 23 mN/m. The low dose increased the minimum surface tension from 5 mN/m to 12 - 15 mN/m. If an amount equal to about twice the high dose was added, the minimum surface tension rose from 5 mN/m to 26 - 30 mN/m.

12.3.4 Peanut oil spread on a film from lung surfactant

Foam fractions no. 1 from three rabbits were obtained (4.1.2 c). From ten surface tray preparations the minimum surface tension of loop no. 10 were below 5 mN/m, for 37°C and 8 cycles/min.

Figure 60b is typical for the influence of peanut oil on lung surfactant films. The low dose of about 0.003 mg/cm^2 increased the minimum surface tension of the control loop from 5 mN/m to about 15 mN/m, the high dose, of 0.01 mg/cm^2 (12.2.4 a) increased the minimum surface tension from about 5 mN/m to the plateau level at approximately 23 mN/m. As response to the agent, again ten successive curves were recorded and no. 10 is drawn.

Figure 60: Influence of particles and peanut oil on surfactant films from foam fraction no. 1

Figure 60a:

-------- low dose particles, 0.3 - 0.5 mg/cm^2, dusted on the films at 100% area. The minimum surface tension rose from 5 mN/m to 12 - 15 mN/m.

—·—·—·— high dose particles, 0.8 - 1.0 mg/cm^2, the minimum surface tension rose from 5 mN/m to the plateau level, at about 23 mN/m.

Figure 60b:

—·—·—·— low dose peanut oil, 0.03 mg/cm^2 ± 10%, at 100% area. The minimum surface tension rose from 5 mN/m to about 15 mN/m.

— — — — high dose peanut oil, 0.01 mg/cm^2 ± 6%. The minimum surface tension rose to the plateau level of about 23 mN/m.

Note: The control loops are the curves no. 10 at a series of ten successive loops. As response to the agents, again ten curves were recorded and no. 10 is drawn.

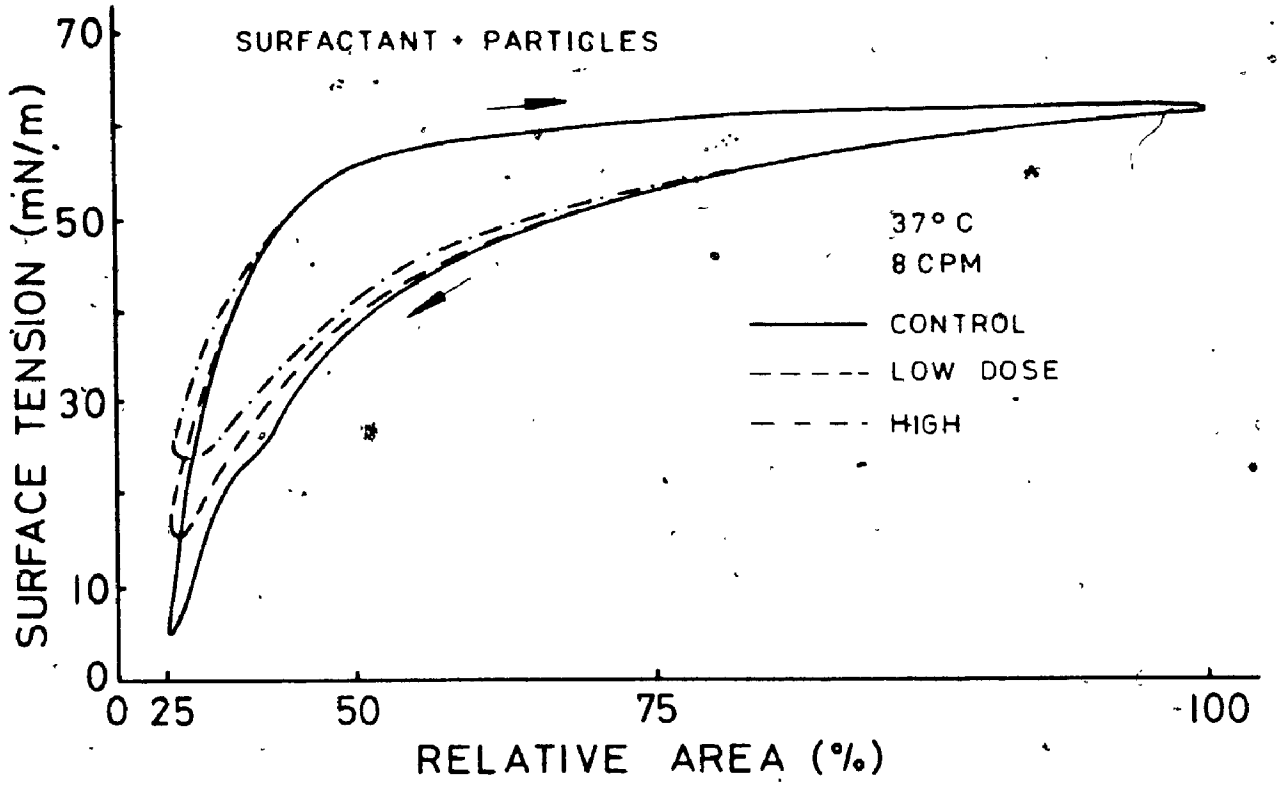
SURFACTANT + PARTICLES
SURFACE TENSION (mN/m)
70
50
30
10
0
0 25
50
75
100
RELATIVE AREA (%)
37° C
8 CPM
CONTROL
LOW DOSE
HIGH

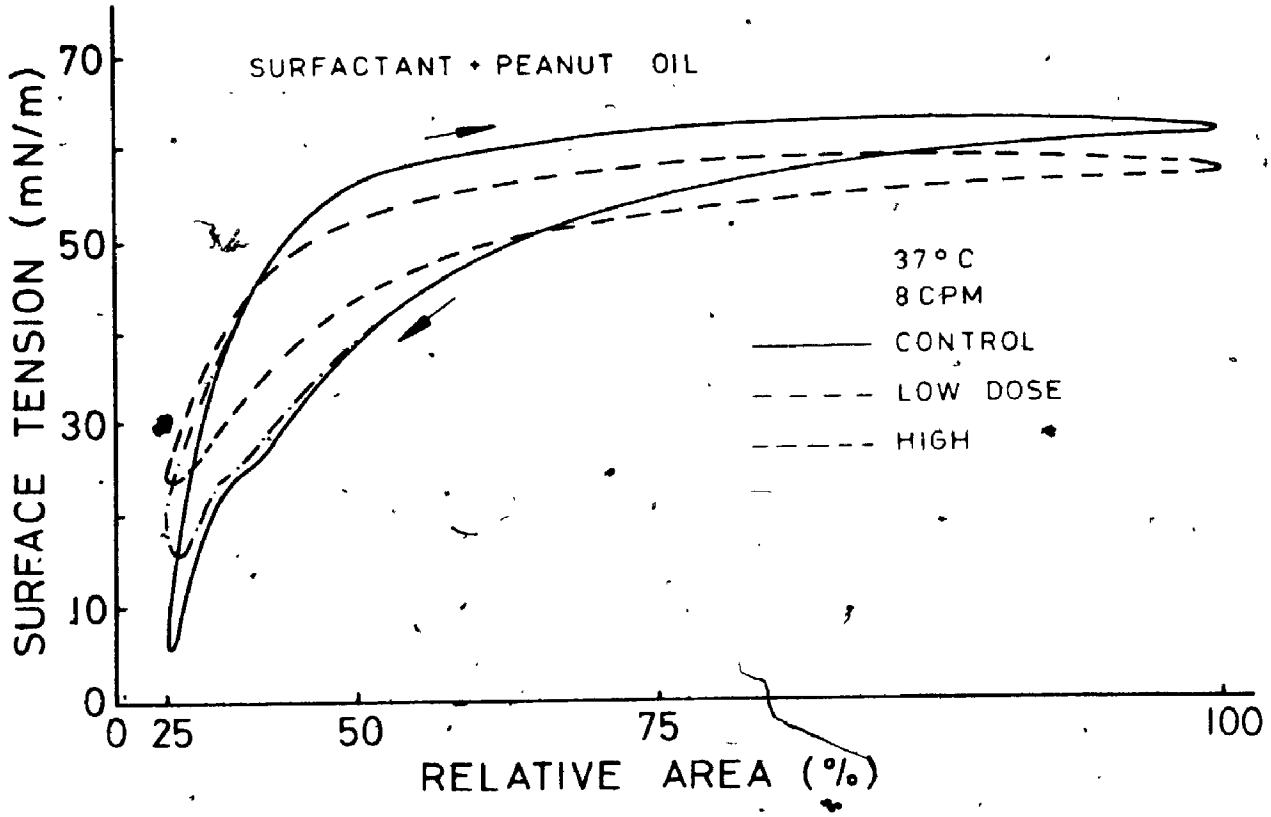
SURFACTANT + PEANUT OIL
SURFACE TENSION (mN/m)
70
50
30
10
0
0 25
50
75
100
RELATIVE AREA (%)
37° C
8 CPM
CONTROL
LOW DOSE
HIGH

12.3.5 Development of the curves as response to the added agents

The unbroken lines of Figure 61 represent loop no. 10 (control loop) of a series of ten curves from surfactant from fraction 1. For Figure 61a, a high dose of peanut oil was spread at 100% area after completion of the control loop. The broken lines represent no. 1 and no. 10 of a series of fifty successive curves.

Curve no. 1 demonstrates a minimum surface tension not much higher than the one of the control loop. With each cycle the minimum surface tension increases and reaches finally at about loop no. 10 the plateau level of approximately 23 mN/m. This level was maintained on further successive cycles.

In additional experiments we placed a drop of peanut oil on a surfactant film. On successive cycling we observed that this drop was divided in smaller and smaller drops in the expansion phase of the cycles. This is very likely the explanation for the gradually increasing surface tension in Figure 61a.

For Figure 61b, a high dose of tantalum powder was dusted after completion of the control loop. About fifty successive cycles did not reveal much difference between the minimum surface tension.

Figure 61: Development of loops from surfactant films with particles or peanut oil added

Figure 61a:

———— Control loop no. 10 of ten consecutive curves

-------- Loop no. 1, after a high dose of peanut oil had been added on the film.

—·—·— Loop no. 10 of ten consecutive curves, which started with loop no. 1 (--------).

Figure 61b:

———— Control loop no. 10 of ten consecutive curves

-------- Loop no. 2, after a high dose of tantalum-powder had been added to the film.

—·—·—·· Loop no. 10 of ten consecutive curves of which no. 2. (--------) is shown.

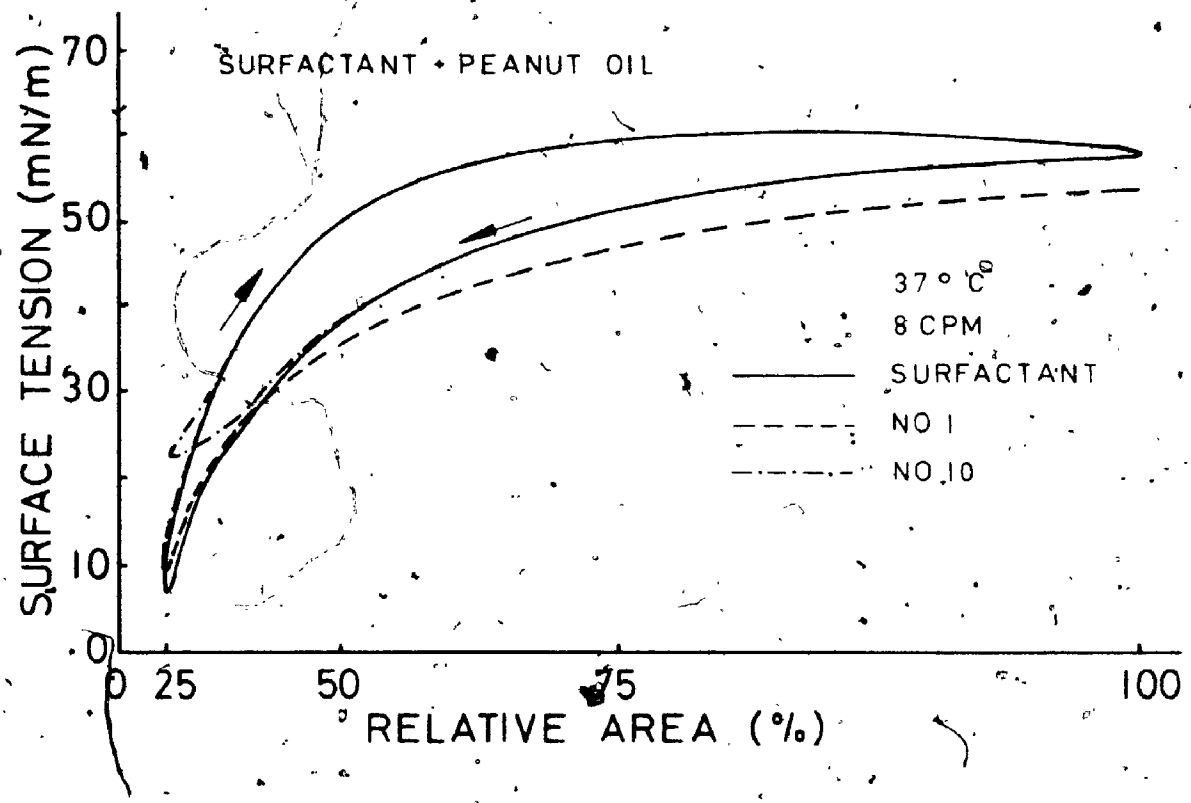
SURFACTANT + PEANUT OIL
SURFACE TENSION (mN/m)
70
50
30
10
0
0
25
50
75
100
RELATIVE AREA (%)
37° C
8 CPM
SURFACTANT
NO 1
NO 10

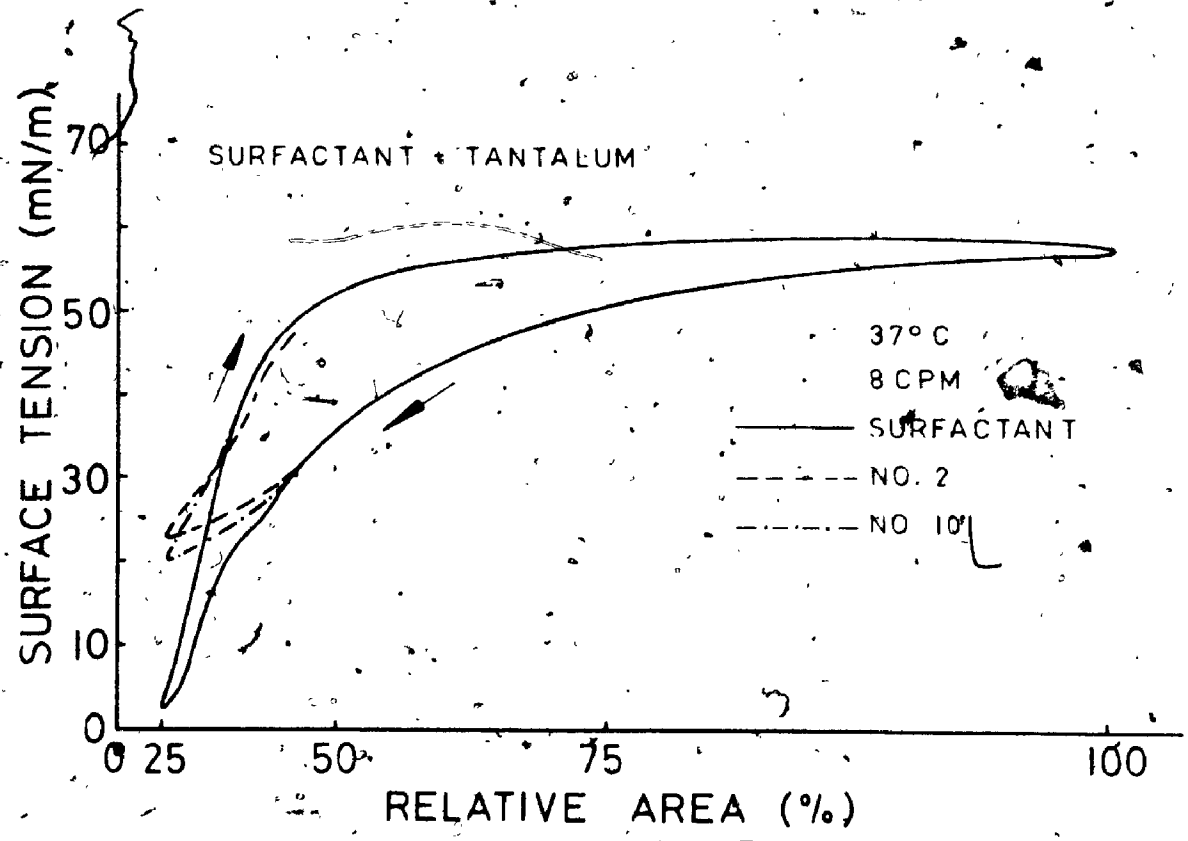
SURFACTANT + TANTALUM
SURFACE TENSION (mN/m)
70
50
30
10
0
0
25
50
75
100
RELATIVE AREA (%)
37° C
8 CPM
SURFACTANT
NO. 2
NO 10

12.3.6 Dionosil Oily on lung surfactant films

a) Methods

Lung surfactant from ten rabbits was extracted and prepared according to 4.1.2 a). A series of ten successive loops were recorded at 37°C and 8 cycles/min. Loop no. 10 was the control curve. Since the lavage material per rabbit was 150 - 160 ml and one trough filling required about 100 ml, we could only do ten experiments.

The control loops of two preparations showed a minimum surface tension below 5 mN/m, four control loops demonstrated minimum surface tensions between 5 and 10 mN/m and four of them showed minimum surface tensions from 10 - 15 mN/m.

Dionosil Oily was diluted with light petroleum (petroleum ether), 30°C to 60°C (does not dissolve propyliodone crystals) to make up a spreading solution of 50 mg/ml. We found that spreading agents like light petroleum did not influence film properties of surfactant and DPPC.

After completion of the control loop, 100 µl of the Dionosil Oily solution was spread on the surfactant film at 100% area. Spreading was done drop by drop all over the surface area and sufficient time was allowed for evaporation of the light petroleum. The density of

Dionosil Oily at 100% trough area (~50 cm^2), was approximately 0.1 mg/cm^2. This corresponds to a concentration of peanut oil of about 0.04 mg/cm^2, and to a concentration of propyliodone particles of about 0.06 mg/cm^2. The portion of peanut oil of the amount spread corresponds approximately to the low dose (0.03 mg/cm^2), see 12.2.4. The portion of particles, 0.06 mg/cm^2, is only one sixth of a low dose particles (3.2.4 b).

b) Results

The effect of 0.1 mg/cm^2 of Dionosil Oily is identical to the one obtained by a high dose peanut oil (0.01 mg/cm^2) or a high dose of particles (~ 1.0 mg/cm^2), Figure 60. The minimum surface tension rose from about 5 mN/m to approximately 23 mN/m for the two preparations with the lowest minimum surface tension. The effect on the films of the other preparations with initially higher minimum surface tensions was also to increase this minimum up to the plateau level at about 23 mN/m. In some additional experiments, higher concentrations of Dionosil Oily were spread, e.g. 0.2 mg/cm^2 and 0.4 mg/cm^2. The minimum surface tension did not increase much more. It was generally between 25 and 30 mN/m.

12.4 Surface pressure-area isotherms of DPPC- and DPPC/peanut oil films

12.4.1 Experimental

In a series of experiments, surface pressure-area isotherms were obtained for pure DPPC monolayers and for mixed monolayers from DPPC and peanut oil. The temperature range was from 22°C up to 40°C and the conditions for the "quasi equilibrium state" (7.2.3 b), were maintained. For each of the isotherms of Figure 62 an individual monolayer was spread and the isotherm at a particular temperature was plotted at least three times. Each curve was then drawn on the basis of these readings. In order to compensate for the temperature effect on the surface tension of the 0.9% NaCl subphase (pH 6.6 - 7.1), the signal from the electrobalance was calibrated, to produce a reading of zero surface tension at each temperature. Therefore, the surface pressure $\pi = \gamma_o - \gamma$ could be recorded directly. (γ_o: surface tension of the subphase, γ: surface tension of the monolayer system.

DPPC monolayers

At 100% trough area, the area per DPPC molecule was assumed to be 100×10^{-20} m^2 or 100 A^2. The amount of substance required was calculated accordingly. The error range for the area/molecule was $\pm$ 3×10^{-20} m^2.

DPPC/peanut oil monolayers

A mixed solution was made up of DPPC/peanut oil (2 : 1, by mass). The amount to be spread at 100% area was chosen so that the same number of lecithin molecules were in the mixed film as in the pure DPPC monolayer.

Figure 62 demonstrates the isotherms for the pure DPPC monolayers (unbroken lines) and the isotherms for the mixed monolayers (broken lines). Initially, the surface pressure of the mixed films is higher, but below about 70×10^{-20} m^2/molecule, it is lower than the one for the pure DPPC monolayer.

12.4.2 Theory

According to equation (3.4), in 3.7, the change of the Helmholtz free energy of an insoluble monolayer is:

$$dF = - SdT - \pi dA$$

For T = constant, the change of the free energy between the film areas A_1 and A_2 is then:

$$\Delta F = - \int_{A_2}^{A_1} \pi dA \qquad (12.1)$$

Our aim is to calculate the change of entropy for the pure DPPC monolayer and for the mixed film, and to compare the values.

The temperature range is from 22°C to 40°C. The surface pressure-area isotherms, are recorded from the

Figure 62: Surface pressure-area isotherms of pure DPPC monolayers (unbroken lines) and mixed films of DPPC/peanut oil = 27 : 1, by mass.

The temperatures from top to bottom are:

40°C ± 0.5°C

37°C

31°C

27°C

22°C

The entropy change was calculated for the film area between

$A_2 = (43 \pm 2) \times 10^{-20} m^2$/molecule, the limiting area of the DPPC monolayer

$A_1 = (75 \pm 2) \times 10^{-20} m^2$/molecule

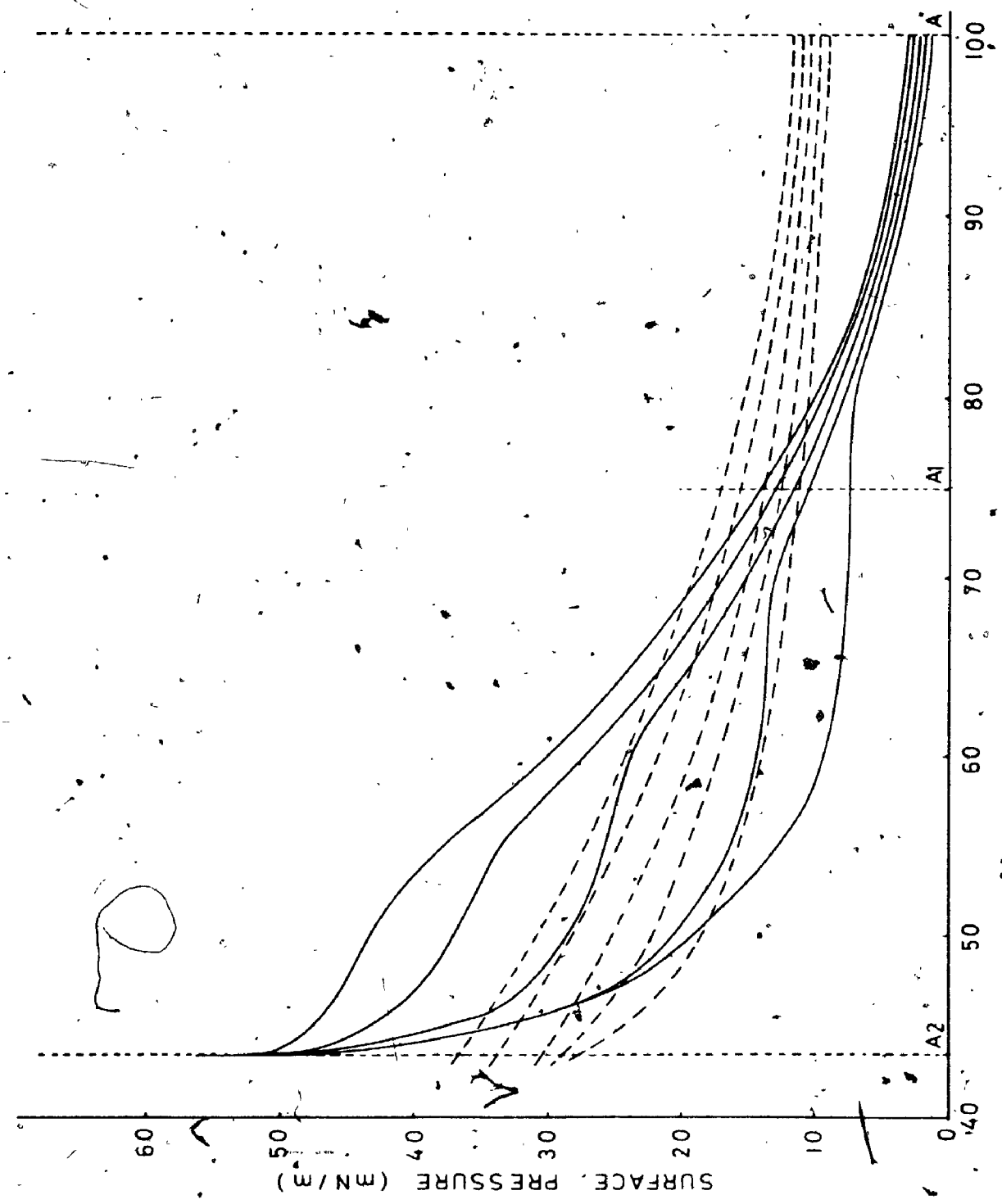
SURFACE PRESSURE (mN/m)
60
50
40
30
20
10
0
A2
A1
A
40
50
60
70
80
90
100
10^{20} × AREA / MOLECULE (m²)

area $A^* = 100 \times 10^{-20}$ m^2/molecule till the limiting area of the DPPC molecule in the monolayer, $A_2 = 43 \times 10^{-20}$ m^2/molecule (Figure 62). The isotherms reveal that the condensation occurs below $A_1 = 75 \times 10^{-20}$ m^2/molecule. Since we suspect that the oil is interfering with the condensation and ordering process, we determine the change of the entropy between A_1 and A_2. From (3.4) and for A = constant, we get:

$$-\Delta S = \left(\frac{\partial F}{\partial T}\right)_A \qquad (12.2)$$

$$T_1 : I_1 = \int_{A_2}^{A^*} \pi dA \; ; \quad I_1' = \int_{A_1}^{A^*} \pi dA \qquad (12.3)$$

$$T_2 : I_2 = \int_{A_2}^{A^*} \pi dA \; ; \quad I_2' \quad \int_{A_1}^{A^*} \pi dA$$

and so on for each temperature, and for both series of isotherms. (Pure DPPC monolayers, and mixed films).

I_1, I_1', I_2, I_2' etc. were then plotted vs. temperature. The numerical values and an example for the graphs can be found in Appendix VIII. The change of the free energy (absolute value) between A_1 and A_2 is:

$$|\Delta F \Big|_{A_1}^{A_2}| = |I_2 - I_1|$$

12.4.3 Results

From Table XIII in Appendix VIII and from the graphs of I vs. T we obtained for the DPPC monolayers:

$$\left| \frac{\Delta S}{\text{DPPC}} \right| = \frac{\partial}{\partial T} (\Delta F)_A \qquad \text{with } A = A_1 - A_2$$

$$= 1.8 \times 10^5 \pm 15\% \text{ (J/kmole·degree)}$$

For the mixed films:

$$\left| \frac{\Delta S}{\text{mixed}} \right| = \frac{\partial}{\partial T} (\Delta F)_A \qquad \text{with } A = A_1 - A_2$$

$$= 1.1 \times 10^5 \pm 15\% \text{ (J/kmole·degree)}$$

For the film area between A_1 and A_2 (Figure 62), the entropy of the DPPC monolayer decreases over 60% more than the entropy of the mixed film.

Less decrease of the entropy means less orientation and order. Therefore, we conclude that the peanut oil is preventing the DPPC molecules from becoming oriented and aligned at the interface.

12.5 Summary

1) Any kind of particles investigated here, propyliodone crystals from Dionosil Oily or Aqueous, crystals from Hytrast, and tantalum particles, affect the minimum surface tensions of lung surfactant and DPPC films. An amount of particles of about 1 mg/cm^2 added on a surfactant film increases the minimum surface tension from 5 mN/m to the plateau level at 23 mN/m.

2) Peanut oil, the suspension medium in Dionosil Oily,

when spread in a concentration of 0.01 mg/cm^2, increases the minimum surface tension from about 5 mN/m to values above 20 mN/m, and also lowers the maximum surface tension.

3) The effect of Dionosil Oily is stronger than the one produced by the single components (peanut oil and propyliodone). Relatively small amounts increase the minimum surface tensions of surfactant films up to the plateau level ($\sim$ 23 mN/m).

CHAPTER 13

GENERAL DISCUSSION AND CONCLUSIONS

13.1 Introduction

The objective of this thesis was to investigate whether bronchographic agents interfere with lung surfactant in situ. There is no method yet to evaluate surface properties of surfactant in the living lung. Therefore, we approached the problem with two indirect methods. One was by surface tray experiments with extracts of lung surfactant, the other was by investigating properties of pressure-volume characteristics of excised rabbit lungs.

13.2 Surface tray experiments with surfactant

The most direct way to a system of reference would have been to use established and standardized methods for the extraction of surfactant and for the tray experiments. However, a great variety of methods can be found in the literature. As already mentioned, Scarpelli (1968), p. 63, points out, that standardization is an empirical process for a particular laboratory. Therefore, we developed our own scheme. We started with crude lung lavage, which was followed by foam fractionation, then by the lipid extract and finally, by synthetic dipalmitoyl lecithin (DPPC). Dipalmitoyl lecithin is the most surface active component of the surfactant phospholipids. With each step the system became more defined and easier to investigate.

Films from cell-free lung extract demonstrated the characteristics of "normal" lung surfactant at room temperature (2.1), but no longer at 37°C. We found that by increasing the cycling speed closer to physiological frequencies, e.g. 8 cycles/min, the criteria for "normal surfactant" could be met again. However, the results were not consistent. Out of fifteen tray experiments from the same number of rabbits, only four showed a minimum surface tension below 10 mN/m at 37°C and 8 cycles/min. These four samples had a relatively high lecithin (PC) content. There was a good correlation between the amount of PC and the minimum surface tension (Figure 5).

In order to produce a minimum surface tension below 2 mN/m at 25% trough area, a monolayer of synthetic DPPC required about 0.03 mg substance, spread at 100% area ($\sim$200 cm^2). This amount is far below the one found in the fifteen samples, even if we assume only about half of the total lecithin to be saturated. There, the range of the lecithin, relative to the trough content was from 1.5 mg to approximately 13 mg. Because there was enough lecithin in each sample to produce near zero surface tension at 37°C, we concluded there must be factors which reduced the surface activity of saturated PC.

13.3 Properties of mixed monolayers from synthetic phospholipids

The analysis of the fatty acid composition of

surfactant phospholipids revealed substantial amounts of unsaturated compounds, see 7.1.3.

Our experiments with unsaturated PC and with mixtures of saturated and unsaturated PC demonstrated that the minimum surface tension was higher, due to unsaturation. At the same time we learned that unsaturation is mainly responsible for dynamic effects, such as lower minimum surface tension at higher speeds.

The minimum surface tension of mixed films is also dependent on the mixing ratio. The bigger the ratio of saturated PC to unsaturated PC or PG (we studied saturated PC only), the lower is the minimum surface tension at a given temperature and speed. (Figure 23 and 25).

13.4 Aging of lung surfactant films and foam fractionation

Surfactant preparations had to age about three hours before cycling was started. Adsorption of saturated PC at the air-liquid interface is favoured energetically compared to the adsorption of unsaturated components or lipids other than DPPC (stronger mutual interactions). Therefore, we concluded that a relatively large amount of PC (saturated and unsaturated) in a sample produces a surface film with a bigger ratio of saturated PC to unsaturated PC than the one in the lung extract.

The next step was then to improve separation of the

most surface active molecules from the less surface active ones (not just by aging). This was done by foam fractionation in a column (4.1.2 e). The results demonstrated that foam from the top of the column (foam fraction no. 1), produced more consistent results with minimum surface tensions as low as the "best" values from the cell-free surfactant (4.1.2 a). Films obtained from fractionated surfactant may be more similar to the film of the surfactant lining layer in the alveoli. There is no reason why the surface layer in the alveolus should not be covered by a film of the most surface active molecules.

13.5 Function of protein

The third step was to extract the lipids from surfactant preparations, to exclude proteins. Lipid layers from crude lung extract showed inconsistent results. The lipid extract from foam fraction no. 1, produced hysteresis loops with characteristics identical to the ones from the foam itself. Relatively large amounts of bovine albumin in the subphase (Figures 9, 28 and 29) did not measurably influence properties of DPPC films or layers from the lipid extract. Therefore, we conclude that protein has no function in the surface film. This statement does not exclude a possible role in the surface lining layer, below the film.

13.6. Hysteresis

Films from synthetic DPPC meet the criteria such as near zero surface tension and hysteresis. However,

hysteresis of successive curves from DPPC films disappear quickly. The material is squeezed out at near zero surface tension and does not respread upon re-expansion. (Figures 15 and 16). Mixed films from DPPC and PG demonstrate more hysteresis on prolonged cycling. This suggests an exchange mechanism between the subphase and the top layer. Lipid structures of DPPC and other phospholipids in the subphase, might release components more easily on re-expansion than structures of DPPC alone (Figure 26).

13.7 Plateau

Hysteresis loops from lung surfactant show a plateau between 22 and 25 mN/m. Plateaux can be reproduced by mixed films from DPPC and other phospholipids (Figures 22, 25 and 26). The plateau level (surfactant or mixed films) does not measurably depend on speed or temperature. Plateaux of pure DPPC monolayers are due to phase transitions and are temperature dependent (Figure 11). We conclude that surfactant plateaux do not represent primarily a condensation process in the surfactant film. They are due to separation and squeezing out of molecules other than DPPC. Surface tensions of surfactant below the plateau level ($\sim$ 23 mN/m) are almost certainly produced by DPPC.

13.8 System of referen

From our studies of various surfactant preparations and their properties at the air-liquid interface and from the experiments with synthetic phospholipids we

concluded that films from foam fraction no. 1 and DPPC monolayers are good and valid models for the surfactant system of the lung. Therefore, we used these films as system of reference for studying the influence of bronchographic agents. Since we concluded DPPC to be responsible for the surface tension of surfactant below the plateau level, the results supported the findings from the surfactant films.

13.9 Surface tray experiments with bronchographic agents

From surface tray experiments with surfactant and DPPC, and added agents, we concluded that there is interaction between surfactant and these bronchographic media. Minimum surface tensions, especially the ones below the plateau level (~23 mN/m) were increased by the agents. The fluid media are suspensions of particles in either water or peanut oil. The contrast medium tantalum consists of pure metal particles. The effect of particles and the suspension material peanut oil was investigated separately. Particles on a water surface decrease the surface tension if they are closely packed. The "high dose" particles were the amount of material necessary to produce a closely packed film at 50% trough area (Figure 57). At 100% area, the high dose was about 1.0 mg/cm^2. In response to the high dose, minimum surface tensions of surfactant and DPPC films rose from below 5 mN/m to the plateau level at about 23 mN/m.

Bianco et al. (1974) suggested that more than 10 mg/cm^2 of "1 µm tantalum powder" was required to produce a satisfactory x-ray from a calibrated tape in the chest of a dog. This density is ten times higher than our "high dose" density. If "alveolarization" of particles occurs we cannot exclude interaction with the surfactant. The amount necessary to rise the minimum surface tension from about 5 mN/m to 15 - 25 mN/m is 0.5 to 1.0 mg/cm^2. This behaviour is typical for all kinds of particles investigated (Figure 60).

We estimated the number of tantalum particles on the surface of an alveolus of 100 µm diameter. The density corresponds to the high dose of 1 mg/cm^2. Assuming a diameter of 5 µm for a spherical tantalum particle, and with the density of 16 g/cm^3, we get approximately 100 particles per alveolus for the high dose and about 50 for the low dose.

Peanut oil, the suspension medium of Dionosil Oily increased the minimum surface tensions of surfactant or DPPC films from about 5 mN/m to 15 - 25 mN/m. The dose was calculated according to the amount of Dionosil Oily used in bronchography (12.2.4 a). A drop of peanut oil, when placed on a film of surfactant or DPPC, does not spread spontaneously. But it splits into smaller drops in the expansion phase of a cycle, when the surface tension rises up to 50 - 70 mN/m. A substance spreads on a subphase

if the energy of mutual interaction between the molecules to be spread is smaller than the energy of interaction between the substance and the subphase.

Surface pressure-area experiments with pure DPPC and mixed monolayers of peanut oil and DPPC revealed that the entropy change (decrease) is smaller in the mixed film than in the pure DPPC film. This means, molecules in the mixed films are less ordered, the mutual interaction is smaller and the molecules are less oriented (12.4.3).

13.10 Pressure-volume tests, gross pathology and histological sections of rabbit lungs

Dionosil Oily and its suspension medium, peanut oil, reached the alveoli (Figures 45, 46 and 47). The other media, Hytrast, Dionosil Aqueous and tantalum dust could not be found generally in the alveoli or in the alveolar ducts. Therefore, only Dionosil Oily and peanut oil could produce results which support our final conclusion that bronchographic media decrease the surface activity of lung surfactant in situ.

By rinsing the lungs with 0.9% NaCl solution, we removed lung surfactant. The stationary loop (Figure 32) of the p-V diagrams revealed opening pressures above 10 cm H_2O (Figure 42). Stationary loops of control lungs demonstrated an "opening pressure" of 1 cm H_2O at the most. The stability index "L" ((10.1) and Figure 32) was significantly lower for the rinsed lungs than for the

normal ones. There are still air-liquid interfaces in rinsed lungs, but the alveolar lining layer and its surface film is replaced to a great extent by saline. Therefore, the surface tension will be relatively high and constant.

Lungs with Dionosil Oily and peanut oil demonstrate tendencies similar to rinsed lungs. The compliance in the inflation part with a pressure between 3 and 4 cm H_2O is significantly reduced compared with the one of a normal lung. The stability index, a measure for retention of air at relatively low pressures (3 - 4 cm H_2O) is significantly lower. The significantly smaller values of both parameters indicate a higher surface tension (at 3 - 4 cm H_2O) in the lungs with peanut oil or Dionosil Oily, compared to the one in a normal lung.

Histological sections from lungs with Dionosil Oily and peanut oil demonstrate microatelectasis (Figures 45, 46 and 47).

Evidently, peanut oil causes microatelectasis and changes characteristics of the p-V loop significantly. From these studies it is not clear whether the propyliodone crystals cause microatelectasis or not. We could not find any section from a lung with Dionosil Oily, with particles only. There was always peanut oil present,

sometimes without particles.

Gross pathology demonstrated depressed areas in freshly excised lungs, with all the agents except for tantalum (Figures 36, 40, 50a and 50b). In lungs with Dionosil Aqueous and Hytrast these depressed areas were almost certainly due to plugged airways, since generally, these agents did not reach the alveoli. In lungs with Dionosil Oily or peanut oil interaction with surfactant or plugged airways or both might have been the reason for the depressed regions.

13.11 Interaction of bronchographic agents with lung surfactant (Final conclusions)

Dionosil Oily reduces the surface activity of lung surfactant in situ. There is strong evidence that the suspension medium peanut oil is responsible for the interaction with surfactant, although an effect of propyliodone crystals cannot be excluded.

If particles are added in sufficient quantities to surface layers from lung surfactant or synthetic dipalmitoyl lecithin, the surface properties of these films are altered. Particles prevent the minimum surface tension from reaching relatively low values.

Finally, we suggest that bronchographic agents should be prevented from entering the terminal airways and the alveoli. Liquid media are either obstructing the

airways (Hytrast, Dionosil Aqueous) or flooding the alveoli (Dionosil Oily). They should be abandoned. If surfactant is altered, the atelectatic zone reappears each time the lung is deflated; while in the atelectatic regions due to partial bronchial obstruction, the atelectasis does not reappear after full expansion.

SUGGESTIONS FOR FUTURE RESEARCH

Surfactant

The main problem is to find an answer to the question: What is surfactant?

1) Chemistry

a) Better extraction techniques should be developed to exclude factors from the blood system which might leak into the alveolar spaces during the lavage process. Alternate methods have already been suggested by Hurst et al. (1973). These authors recommend rinsing the vascular system of the lung prior to extraction of the surfactant.

b) The ratio of unsaturated to saturated lecithins determines the minimum surface tension of mixed monolayers for a given temperature and cycling speed. Therefore, an analysis of the fatty acids of the surfactant phospholipids should be done and correlated with surface tension studies.

c) More monolayer experiments with synthetic lipids which are related to surfactant components could be done. The influence of chain length and unsaturation on the film stability should be further studied.

2) Structure

a) It would be interesting to produce phospholipid-water systems, possibly by sonication (liquid crystalline

systems). The influence of various saturated and unsaturated components on lecithin structures could be investigated, e.g. by studying adsorption at the air-liquid interface in function of time.

b) High resolution nuclear magnetic resonance studies of lecithin dispersion in D_2O could be done. By adding various amounts of unsaturated components or other phospholipids, e.g. phosphatidyl glycerol, the influence on the structure of lipid aggregates might be investigated. Variations of the relaxations time should give information on the structure, e.g. liquid or closely packed and solid.

Bronchography

More bronchographic agents could be tested on surfactant or DPPC films. Especially the fluid media with a relatively low viscosity should be investigated. However, the fluid agents may be abandoned in the future, since the high viscosity ones, like Hytrast or Dionosil Aqueous are obstructing the airways, the low viscosity ones, like Dionosil Oily are flooding the alveoli.

It would be interesting to find a reliable method to inject tantalum powder or other suitable particles just into the airways without deposition in the terminal bronchioles or in the alveoli.

APPENDIX I

THE RHOMBIC SURFACE TROUGH

In the early part of the experiments, a rectangular teflon trough was used. The surface layers were compressed by two teflon blades. Leakage between the teflon blades and the trough walls was a problem, and hence the rhombic trough, illustrated in Figure 63, was developed. With the rhombus-shaped trough, leaks are eliminated completely. The surface layers are confined by an endless teflon ribbon, which is supported by a metal frame.

The area is changed by changing the shape of the rhombus. The displacement-area relationship is nonlinear (Figure 63).

Figure 63: Area change of the rhombic surface trough

The thick curve represents the displacement vs. area characteristic.

At $x = 1/2\sqrt{2}$, the rhombus has its maximum area, equal to a square of the side 1.

Since the rate of the area change is initially low, we chose as 100% trough area the one corresponding to point P.

For x_1, the trough area is 100%: P

x_2, 75%: Q

x_3, 50%: R

x_4, 25%: S

These divisions were transferred proportionally to our graphs. Therefore, the area coordinates are nonlinear.

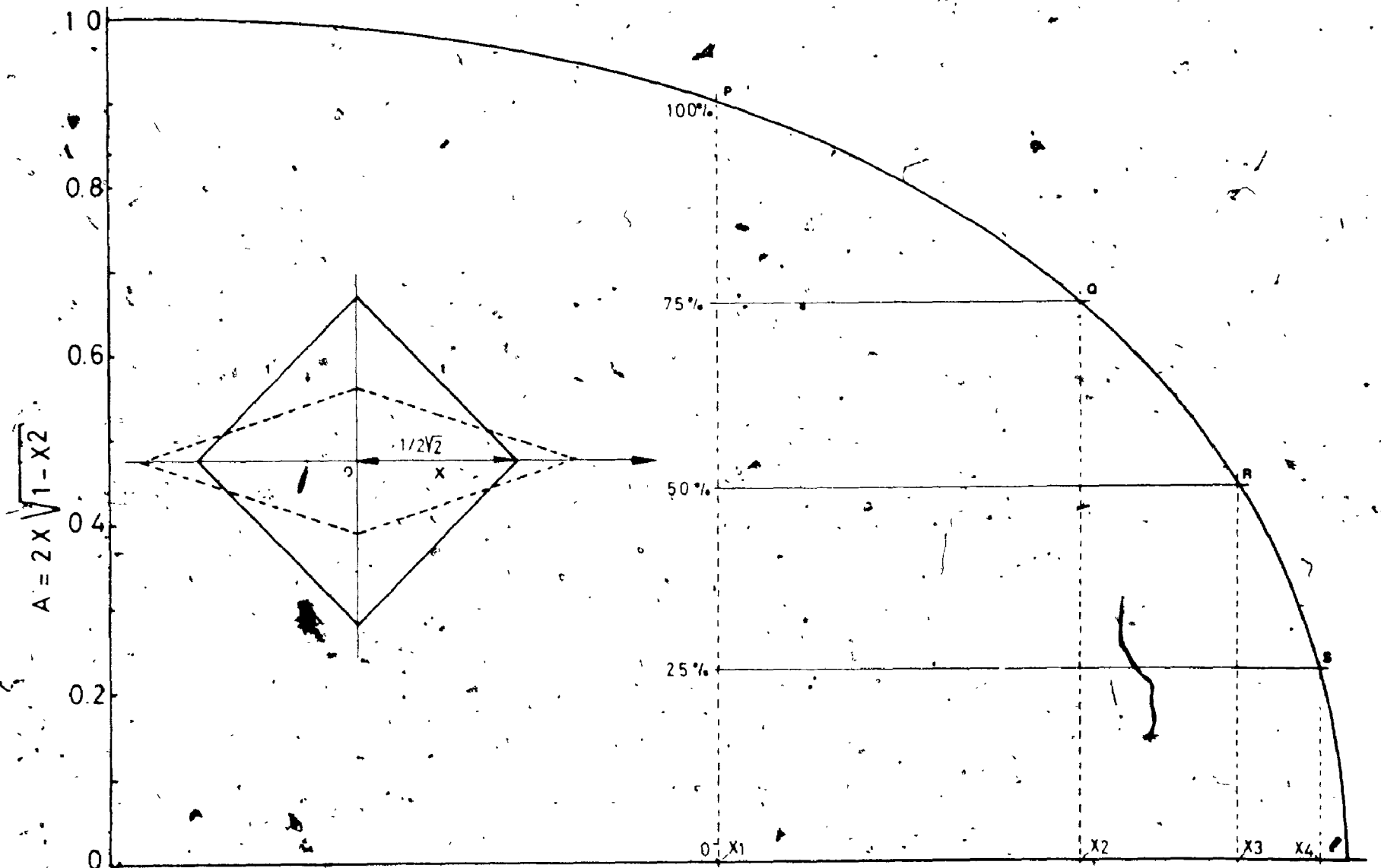
1.0
0.8
0.6
0.4
0.2
0
A = 2X√(1-X2)
100%
75%
50%
25%
P
Q
R
S
1/2√2
O
X
0
X1
X2
X3
X4
1
1/2√2
DISPLACEMENT X

5 5

OF/DE

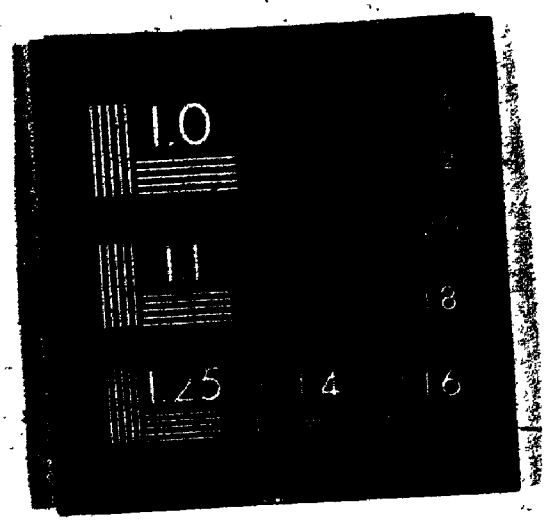

APPENDIX II

CALCULATION OF THE POTENTIAL OF A DIPOLE LAYER

In surface chemistry the surface potential due to a dipole layer is usually described by the parallel plate capacitor model. The capacitor consists of two plates with free electric charges.

A dipole is not a system of free charges. It is a system of two opposite charges + q and - q which are separated by the distance a.

Here we are calculating the potential of a dipole layer without using the capacitor model. The assumptions are:

1. continuity for the dipole layer
2. $a \ll r$
3. no mutual interaction between the dipoles
4. axial symmetry of the dipole orientation with respect to the z axis

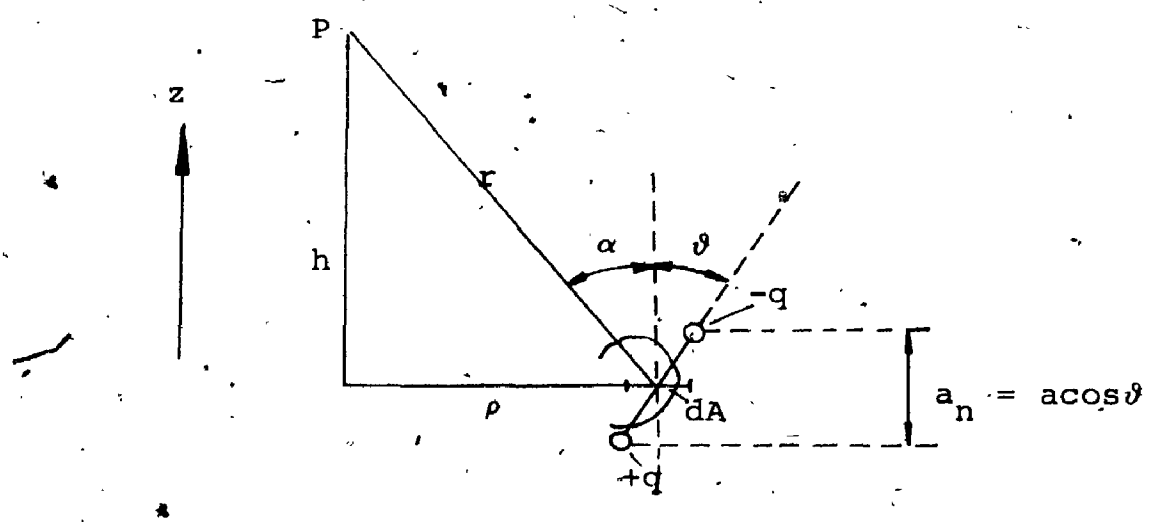

The potential in point P due to a dipole moment $qa\cos\theta = p_n$ is

$$V = \frac{1}{4\pi\varepsilon_o} \frac{p_n \cos\alpha}{r^2} \qquad \text{(II.1)}$$

If σ is the charge density in (C/m^2) and dA is the unit area, then

$$dV = \frac{1}{4\pi\varepsilon_o} \frac{dA a_n \cdot \cos\alpha}{r^2} \qquad \text{with } a_n = a\cos\theta$$

$$dV = \frac{\sigma a_n}{4\pi\varepsilon_o} \frac{\rho d\phi d\rho \cdot \cos\alpha}{r^2} \qquad \text{where } dA = \rho d\phi d\rho$$

For a circular unit area we get

$$dV_C = \frac{\sigma a_n}{4\pi\varepsilon_o} \frac{\rho d\rho \cdot \cos\alpha}{r^2} \int_{\phi=0}^{\phi=2\pi} d\phi$$

$$= \frac{\sigma a_n}{2\varepsilon_o} \frac{\rho d\rho \cdot \cos\alpha}{r^2}$$

and with $\rho = r\sin\alpha$

$$d\rho = r\cos\alpha d\alpha$$

we have

$$dV_C = \frac{\sigma a_n}{2\varepsilon_o} \cos^2\alpha \sin\alpha d\alpha$$

Now we are integrating over the circular area from $\alpha = 0$ to $\alpha = \alpha_1$

$$V_P = \frac{\sigma a_n}{2\varepsilon_o} \int_{\alpha = 0}^{\alpha = \alpha_1} \cos^2\alpha \cdot \sin\alpha d\alpha \qquad \text{(II.2)}$$

(II.2) can be solved easily with the substitution

$\cos\alpha = u$

$$V_P = \frac{\sigma a_n}{2\varepsilon_o} \left[-\frac{1}{3} \cos^3\alpha \right]_{\alpha = 0}^{\alpha = \alpha_1} \qquad \text{(II.3)}$$

By integrating over the whole plane ($\alpha_1 = \pi/2$) we get

$$V_P = \frac{\sigma a_n}{2\varepsilon_o} \cdot \frac{1}{3} = \frac{\sigma a_n}{6\varepsilon_o} \qquad \text{(II.4)}$$

The charge density σ can be written as

$$\sigma = \frac{mq}{A} = Nq,$$

where q is a unit charge, m is the number of unit charges and $N = m/A$ is the number of unit charges or dipoles per unit area.

The potential in P due to the plane dipole layer is then

$$V_P = \frac{1}{6\varepsilon_o} Nq\, a_n$$

$$= \frac{1}{6\varepsilon_o} Np_n \qquad \text{(II.5)}$$

where $p_n = qa_n$, the normal component of the dipole moment.

Since the integration was done from $\alpha = 0$ to $\alpha = \pi/2$, we assumed the dipole layer to be infinitely

extended, or in other words, h is negligible relatively to the dimensions of the layer.

From (I.5) follows that the surface potential can be written as

$$\Delta V = \frac{1}{6\varepsilon_o} \Delta(Np_n) \qquad \text{(II.6)}$$

where N = number of dipoles per unit area ($1/m^2$)

p_n = $p\cos\theta$, the normal component of the dipole moment (Cm)

ε_o = vacuum permittivity

= $8.854 \times 10^{-12}\ C^2/Nm^2$

(II.6) is very similar to the expression obtained by the capacitor model, where

$$\Delta V = \frac{1}{\varepsilon_o} \Delta(Np_n), \qquad \text{see (3.9).}$$

In both cases, dipole-dipole interactions are neglected and ε is assumed to be equal to ε_o, the vacuum permittivity.

APPENDIX III

PHOSPHOLIPID EXTRACTION AND SEPARATION BY THIN LAYER CHROMATOGRAPHY

Lung lavage, 0.9% NaCl, 150 - 160 ml

Centrifugation, 800 g, 20 min, 3°C

Freeze drying

White powder extracted with $CHCl_3$: CH_3OH =
(1 : 1, by vol.)

Washed with 0.9% NaCl solution (2-phase system)

Dried in N_2

Dissolved in 500 µl $CHCl_3$

Aliquots of 80 - 100 µl spotted on TLC plate
(Silica gel H)

Developed in $CHCl_3$: CH_3OH : HCOOH : H_2O
(100 : 60 : 4 : 2, by vol.)

APPENDIX IV

BRONCHOGRAPHIC MEDIA

1. *Dionosil Oily, Dionosil Aqueous are the brand names of an oily and an aqueous suspension of propyliodone.

Chemical composition of propyliodone: normal propylester of 3 : 5-di-iodo-4-pyridone-N-acetic acid.

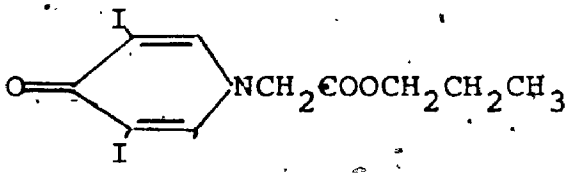

Before blending, the ester is milled so that the size of the vast majority of the crystals is in the range of 5 to 14 μm. The material contains about 30% iodine. (Holden et al., 1953).

Dionosil Aqueous is the aqueous suspension, 50 per cent w/v of the compound. Carboxy-methyl-cellulose is added and a suitable wetting agent.

Dionosil Oily is the oily suspension, 60 per cent w/v, of the compound. The suspension medium is arachis oil (peanut oil).

The properties of the two agents were first described by Tomich at al. (1952)

---

*Glaxo Laboratories Ltd., Greenford, Middlesex, England

2. *Hytrast was introduced as a bronchographic medium in 1962. It is a neutral suspension of crystals of N (propyl-2 : 3-diol)-3 : 5 di-iodo-4pyridone, and 3-5 di-iodo-4 pyridone in a hypertonic aqueous solution of sodium carboxy-methyl-cellulose. The latter compound was added to maintain the viscosity at 2.4 - 2.8 poise at 37°C and the pH at 7.1.

The crystals are 2 - 5 μm across. The iodine content is 0.5 g/ml (Morley, 1969).

3.**Tantalum powder

The particles were nominally 1 μm in size.

---

*Laboratoires Andre Guerbet, 22 Rue du Landy, Saint-Ouen, (Seine) France

**Fansteel, Inc., Number one Tantalum Place, North Chicago, Illinois, 60064 U.S.A.

APPENDIX V

FLUIDIZED BED TECHNIQUE

A method to inject tantalum dust into rabbit lungs had to be found. Prior to the injection, the tantalum particles had to be suspended in air. To do this, we have chosen the "fluidized bed technique", used by chemical engineers.

In Figure 64 a glass pipe of about 20 cm length and 3 cm diameter is mounted on top of a loudspeaker. A mixture of tantalum (1 µm size), powder and sand (~ 0.5 mm diameter) is put on the membrane in the middle of the glass pipe. The tantalum/sand mixture is about 1 : 1, by volume. Dry air from a steel cylinder flows from below through the membrane and through a T-tube on top of the cylinder. Both flows are adjusted so that the mixture of particles starts to "boil". The loudspeaker is fed from a variable oscillator and a 30 - 40 W power supply. The frequency of the loudspeaker is adjusted to optimize fluidization. A second T-tube is mounted on top of the glass cylinder and connected at one end with a rubber ball, at the other end to a plastic tube, inside diameter 0.12 cm, the catheter. The catheter was placed into the rabbit trachea. By pressing the rubber ball, small thrusts of tantalum dust could be blown into the lung. The sand particles did not leave the glass tube.

217-(2)


8
7
6
1
5
4
3
2
9

Figure 64: "Fluidized bed technique"

1	Steel cylinder with dry air
2	Loudspeaker (30 - 40 W)
3	Tube, inside diameter 0.12 cm, to blow particles into the trachea (catheter)
4	Overflow
5	Rubber ball to push air through the second T-tube no. 7.
6	Membrane with about 8 ml of a tantalum/sand mixture, 1 : 1, by vol., on top
7	T-tube connected to rubber ball and catheter
8	T-tube with adjustable air flow
9	Tube for an adjustable air from the steel cylinder flowing from bottom to top of the glass column

APPENDIX VI

MEASUREMENT OF THE VOLUME CHANGE

As illustrated in Figure 31, the air flow caused by the expanding (or shrinking) rabbit lung was recorded by a hot wire (constant temperature) anemometer.

In order to produce an output signal proportional to the volume of the displaced air, the air flow had to be integrated over a certain time interval. Figure 65 demonstrates the electronic circuit of the integrater.

The function of the integrater can be expressed mathematically as

$$\int_{t=0}^{t=t_1} \dot{V} dt = \Delta V$$

where $\dot{V}$ is the flow rate and

ΔV is the volume change for the time interval 0 to t_1.

5 5

OF/DE

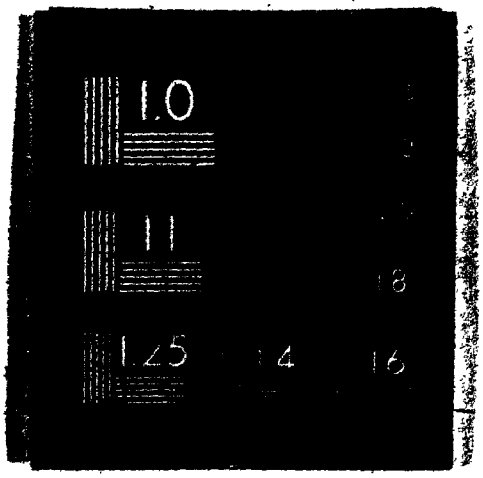

Figure 65. Circuit of the integrater used with the pressure-volume apparatus (Figure 31)

S1 SWITCH FUNCTION
1 OFF
2 INFUSION
3 WITHDRAWAL

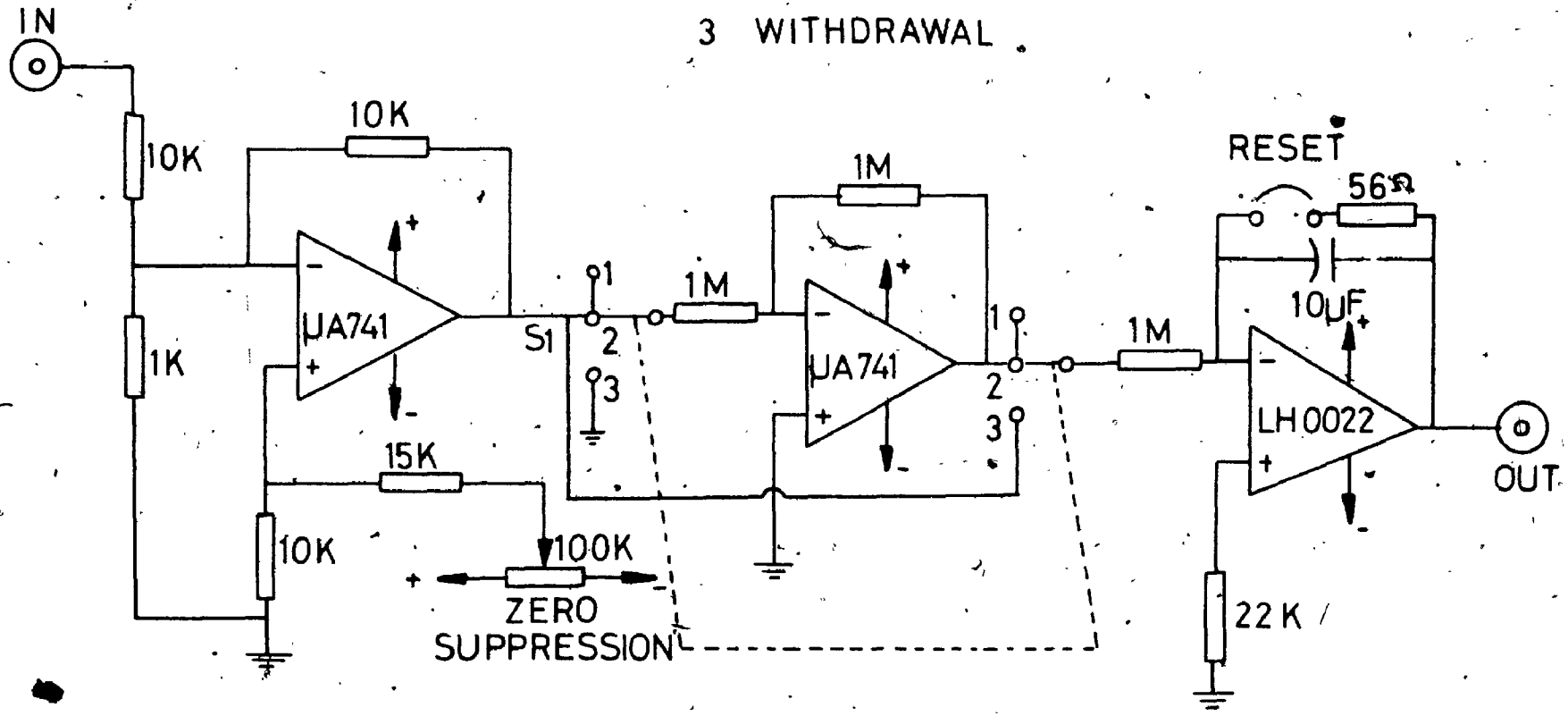

POWER SUPPLY
±8.4V 2 E/R MERCURY BATTERIES

219-(2)

APPENDIX VII

ERROR ESTIMATION

The principle is to calculate the error range of functions if the error range of measured data is known or estimated.

For a function of three variables, f (x, y, z), x, y, z are the "true" values, and a, b, c the approximate values for x, y, z. The error range for the approximate values is:

$$\Delta a,\ \Delta b,\ \Delta c.$$

The range for the relative error for the function f is then:

$$\frac{\Delta f}{|f|} \quad \frac{\Delta a\left|\frac{\partial}{\partial_x}\left(f\ (x,y,z)\right)\right| + \Delta b\left|\frac{\partial}{\partial_x}\left(f\ (x,y,z)\right)\right| + \Delta c..}{|f\ (x,y,z)|}$$

at $x = a,\ y = b,\ z = c$ (VII.1)

This formula was used to calculate the relative error for a function when the error range of the variables were known.

1. Pressure-volume characteristics

a) Mass of the lungs: m

The mass of the lung was determined with a Mettler balance after the fixation process in formalin. We would have had to take in account the absorbed preservative. But we are mainly interested in relative quantities and each lung was prepared the same way; we neglected the influence of formalin on the mass of the lung. The relative error was:

$$\frac{\Delta m}{m} = \pm 0.5\%$$

b) The volume change ΔV

Calibration of the Harvard pump

The pump was calibrated with a Fisher flowmeter kit, Fisher Scientific, Cat. no. 11-164. The relative error of the flow rate at gear position 3 and for a 500 ml syringe was about 5%, 23.5 $\pm$ 1.2 m/min. Since we used the pump to calibrate the flowmeter-integrater set-up, we had to take a relatively high error for the volume measurements.

The linearity of the flowmeter-integrater set-up was tested for the flow rates of 12 ml/min, 24 ml/min and 48 ml/min, according to the gear positions 4, 3, 2, respectively. The linearity could be optimized by varying the bridge output and the current in the probe (probe resistance). The error introduced by deviation from linearity was small relatively to the error of the pump

flow rate.

Drift of the integrater output

For the integrater see Figure 65. The zero suppression had to be adjusted carefully prior to each experiment. The error introduced to the volume measurement by the drift of the output voltage was 1 to 2% for the time concerned.

The relative error for the volume was:

$$\frac{\Delta V}{V} \cong 7\%$$

c) Pressure

The pressure output was calibrated with a water manometer prior to the experiments. The absolute error was:

$$p \sim 0.1 \text{ cm } H_2O$$

d) Quotient of mass (m) and the stationary volume change (ΔV_s)

$$Q = \frac{m}{\Delta V_s}$$

$$\frac{\Delta Q}{Q} \sim 8\%$$

e) Slope S_1 at P_1 ($p \cong 3$ cm H_2O)

$$\frac{\Delta S_1}{S_1} \simeq 10\%$$

f) Quotient of compliance and the stationary volume change

$$\frac{C_1}{\Delta V_s} = C'$$

$$\frac{\Delta C'}{C'} \sim 15\%$$

g) Stationary volume change

$$\frac{\Delta(\Delta V_s)}{\Delta V_s} \sim 5\%$$

h) Factor "L"

$$L \equiv \frac{2\Delta V_1 + \Delta V_2}{2\Delta V_s}$$

$$\frac{\Delta L}{L} \sim 15\%$$

APPENDIX VIII

ENTROPY CHANGE OF A PURE DPPC MONOLAYER AND OF A MIXED FILM FROM DPPC/PEANUT OIL, (2 : 1, BY MASS)

In Table XIII, the results of the graphic integrations, see (12.3) in 12.4.2, can be found. The values represent the change of the Helmholtz free energy for the film areas between A_1 and A* and between A_2 and A* (Figure 62).

In Figure 66, the change of the free energy I' between the film areas A_1 and A* is plotted vs. temperature. The entropy change is obtained by taking the slope of the graph, according to equation (12.2).

TABLE XIII

CHANGE OF THE FREE ENERGY

$10^{-6} \times |I| \pm 0.2$ (J/kmole)

Temperature ± 0.5 (°K)	DPPC	DPPC/peanut oil
313	7.1	6.9
310	6.3	6.2
304	5.3	5.5
300	4.1	4.9
295	3.4	4.2

$10^{-6} \times |I'| \pm 0.1$ (J/kmole)

Temperature ± 0.5 (°K)	DPPC	DPPC/peanut oil
313	0.99	2.0
310	0.91	1.8
304	0.80	1.6
300	0.71	1.5
295	0.59	1.4

Figure 66: Example of the graph $|I'|$ vs. temperature (Table XIII)

The entropy change was calculated by taking the slope of the graph, according to

$$\left|\Delta S\right|_{A_1}^{A^*} = \left|\frac{\partial}{\partial T} I\right|_{A_1}^{A^*}$$

Note: We used I as abbreviation for "integral". I represents the change of the Helmholtz free energy between A_1 and A* or between A_2 and A* (Figure 62).

The error range was estimated from the range of the slope.


1.00
0.90
0.80
0.70
0.60
0.50
290
295
300
305
310
315
TEMPERATURE (°K)
10⁻⁶ x I'(J/kmole)

APPENDIX IX

PROBLEMS WITH THE PLATINUM SENSOR

(surface tension recordings)

We observed frequently that the surface tension readings were too low in the expansion part of a surface tension-area loop. This was particularly true for films from synthetic phospholipids.

In the expansion phase, the surface tension increases. There is less and less interaction between the film molecules, but increasing interaction between the film and the metal plate of the sensor. In the case of phospholipid films, the platinum plate was probably coated with film material in the compression phase. Due to this contamination, the interaction between the platinum and the surface layer was reduced, which means the readings were wrong.

At low cycling speeds, e.g. 1/12 cycle/min, there was enough time to switch the electrobalance off and on several times. By switching off the electrobalance, the platinum plate was lowered about 3 mm into the liquid. By switching on, the plate was pulled up through the liquid. After this procedure, the readings were correct. (This was verified by measuring the surface tension by a freshly flamed plate at different levels in the expansion phase).

At higher cycling frequencies there was no time for switching the electrobalance on and off. For these frequencies, the platinum sensor was replaced by a stripe of filter paper. Prior to each experiment, the paper sensor was kept partly immersed in saline for about two hours, until it was completely saturated with the NaCl solution.

The recordings from the paper sensor were calibrated by the platinum sensor. It was interesting to note that the readings were correct for the compression and the expansion phases of a cycle.

In the case of films from lung surfactant, the platinum plate worked properly.

REFERENCES

ABRAMS, M. E. (1966). Isolation and quantitative estimation of pulmonary surface active lipoprotein. J. Appl. Physiol. 21, 718-720.

ADAM, N. K. (1968). The physics and chemistry of surfaces. Dover Publications Inc., New York; published in Canada by General Publishing Company Ltd., Don Mills, Toronto, Ont.

AVERY, M. E. and J. MEAD. (1959). Surface properties in relation to atelectasis and hyaline membrane disease. Amer. J. Dis. Child. 97, 517-523.

AVEYARD, R. and D. A. HAYDON. (1973). An introduction to the principles of surface chemistry. Cambridge at the University Press.

BECKER, R. (1964). Theorie der Wärme. Springer Verlag, Berlin.

BIANCO, A., F. R. GIBB, R. W. KILPPER, S. LANDMAN and P. E. MORROW. (1974). Studies of tantalum dust in the lungs. Radiology 112, 549-556.

BJÖRK, L. and H. LODIN. (1957). Pulmonary changes following bronchography with Dionosil Oily. (Animal experiments). Acta Radiol. 47, 177-180.

CADENHEAD, D.A. (1970). Monolayers of synthetic phospholipids. Recent Progress in Surface Science, vol.3 (Academic Press, New York).

CHRISTOFORIDIS, A. J. (1962). Effects of bronchography on pulmonary function. Amer. Rev. Resp. Dis. 85, 127-129.

CLEMENTS, J. A. (1957). Surface tension of lung extracts. Proc. Soc. Exptl. Biol. Med. 95, 170-172.

_____. (1962). Surface phenomena in relation to pulmonary function. Physiologist 5, 11-28.

_____. (1970). Pulmonary surfactant. Amer. Rev. Resp. Dis. 101, 984-990.

_____, E. S. BROWN and R. P. JOHNSON (1958). Pulmonary surface tension and the mucus lining of the lung. Some theoretical considerations. J. Appl. Physiol. 12, 262-268.

CLEMENTS, J. A., R. F. HUSTEAD, R. P. JOHNSON and I. GRIBETZ. (1961). Pulmonary surface tension and alveolar stability. J. Appl. Physiol. 16, 444-450.

COLACICCO, G. (1971). Lipid monolayers: surface potential of dipal mitoyllecithin with regard to ion sorption and Ca^{++} binding. Biochim. Biophys. Acta 266, 313-319.

_____; and E. M. SCARPELLI. (1973). Pulmonary surfactants: molecular structure and biological activity. Biological Horizons in Surface Science, ed. by L. M. Prince and D. F. Sears (Academic Press, New York and London), 367-425.

DE BURGH DALI, I. and C. HEBB. (1966). Pulmonary and bronchial vascular systems. Monographs of the Physiological Society. (Edward Arnold Ltd., London).

DERMER, G. B. (1969). The fixation of pulmonary surfactant for electron microscopy. I.: The alveolar lining layer. J. Ultrasfruct. Res. 27, 88-104.

FRIEDMAN, P. J. and G. M. TISI. (1972). "Alveolarization" of tantalum powder in experimental bronchography and the clearance of inhaled particles from the lung. Radiology 104, 523-535.

FROSOLONO, M. F., B. L. CHARMS, R. PAWLOWSKI and S. SLIVKA. (1970). Isolation, characterization, and surface chemistry of a surface-active fraction from dog lung. J. Lipid Research, II, 439-457.

_____, R. PAWLOWSKY, B. L. CHARMS, C. COPBUSIER, M. ABRAMS and J. JONES. (1973). Lung surface-active fraction as a model system for macromolecular ultrastructural studies with Crotalus atrox venom. J. Lipid Research 14, 110-120.

GAINES, G. L. JR. (1966). Insoluble monolayers at liquid-gas interfaces. Interscience Publishers, a division of John Wiley and Sons, New York, London, Sidney.

GALDSTON, M., D.O. SHAH and G. J. SHINOWARA. (1969). Isolation and characterization of lung lipoprotein surfactant. J. Colloid Interface Sci. 29, 319-334.

GAMSU, G., R. M. WEINTRAUB and J. A. NADEL. (1973). Clearance of tantalum from airways of different caliber in man evaluated by a roentgenographic method. Amer. Rev. Resp. Dis. 107, 214-224.

GHOSH, D., M. A. WILLIAMS and J. TINOCO. (1973). The influence of lecithin structure on their monolayer behavior and interactions with cholesterol. Biochim. Biophys. Acta 291, 351-362.

GRUENWALD, P. (1963). A numerical index of the stability of lung expansion. J. Appl. Physiol. 18, 665-667.

GUGGENHEIM, E. A. (1933). Modern thermodynamics by the method of Willard Gibbs. Methuen + Co. Ltd., London.

HAYASHI, M., T. MURAMATSU and I. HARA. (1972). Surface properties of synthetic phospholipids. Biochim. Biophys. Acta 255, 98-106.

HILDEBRANDT, J. and A. C. YOUNG. (1966). Physiology and Biophysics, ed. by T. C. Ruch and H. D. Patton (W. B. Saunders, Comp., Philadelphia and London), 733-760.

HOLDEN, W. S. and R. S. CRONE. (1953). Bronchography using Dionosil Oily. Brit. J. Radiol. 26, 317-322.

_____, and R. H. COWDELL. (1958). Late results of bronchography using Dionosil Oily. Acta radiol. 49, 105-112.

HURST, D. J., K. H. KILBURN and W. S. LYNN. (1973). Isolation and surface activity of soluble alveolar components. Resp. Physiol. 17, 72-80

IWAINSKY, H., H. REUTGEN and J. VOGEL. (1970). Bestimmung und Markierung der oberflächen aktiven Lipoproteide der Lunge. Acta Biol. Med. Germ., Band 24, 47-58.

JOHNSON, P. M., N. J. MONTCLAIR, W. R. BENSON, W. H. SPRUNT and W. A. DUNNAGAN. (1960). Toxicity of bronchographic contrast media. Ann. Otol., Rhin. Laryng. 69, 1102-1113.

KAMMLER, E. und W. T. ULMER. (1971). Ein neuer Weg in der Bronchographie. Pneumonologie 144, 344-351.

KEZDY, F. (1972). Lipid monolayers. Membrane Molecular Biology, ed. by C. F. Fox and A. D. Keith (Sinauer Associates Inc., Stamford, Conn.), 123-145.

KING, R. J. and J. A. CLEMENTS. (1972). Surface active materials from dog lung. II. Composition and physiological correlations. Amer. J. Physiol. 233, 715-726.

KLAUS, M. H., J. A. CLEMENTS and R. J. HAVEL. (1961). Composition of surface active material from beef lung. Proc. Nat. Acad. Sci. U.S. 47, 1858-1859.

LANG, E. K. (1964). Comparative study of febrile reactions to Hytrast, Aqueous Dionosil, and Oily Dionosil in bronchography. Radiology 83, 455-459.

LE ROUX, B. T. and J. G. DUNCAN. (1964). Bronchography with Hytrast. Thorax 19, 37-43.

MORLEY, A. R. (1969). Pulmonary reaction to Hytrast. Thorax 24, 353-357.

MOTOMURA, K. (1967). Thermodynamics and phase transitions in monolayers. J. Colloid Interface Sci. 23, 313-318.

MUNDEN, J. W. and J. SWARBRICK. (1973a). Effect of spreading solvent on monolayer characeristics of dipalmitoyl lecithin. J. Colloid Interface Sci. 42, 657-659.

_____, and J. SWARBRICK. (1973b). Time dependent surface behavior of dipalmitoyllecithin and lung alveolar surfactant monolayers. Biochim. Biophys. Acta 291, 344-350.

NADEL, J. A., W. G. WOLFE, P. D. GRAF, J. E. YONKER, N. ZARNEL, J. H. M. AUSTIN, W. A. HINCHCLIFFE, R. H. GREENSPAN and R. R. WRIGHT. (1970). Powdered tantalum. A new contrast medium for roentgenographic examination of human airways. New England J. Med. 283, 281-286.

PATTLE, R. E. (1955). Properties, function and origin of the alveolar lining layer. Nature 175, 1125-1126.

_____. (1965). Surface lining of lung alveoli. Physiol. Ref. 45, 48-79.

PFLEGER, R. C. and H. G. THOMAS. (1971). Beagle dog pulmonary surfactant lipids. Arch. Int. Med. 127, 863-872.

_____, R. F. HENDERSON and J. WAIDE. (1972). Phosphatidyl glycerol - a major component of pulmonary surfactant. Chem. Phys. Lipids 9, 51-68.

PHILLIPS, M. C. (1972). The physical state of phospholipids and cholesterol in monolayers, bilayers and membranes. Progress in Surface and Membrane Science, vol.5 (Academic Press, New York, London), 159-167.

PHILLIPS, M. C. and D. CHAPMAN. (1968). Monolayer characteristics of saturated 1, 2-diacyl phosphatidyl cholines (lecithins) and phosphatidyl ethanolamins at the air-water interface. Biochim. Biophys. Acta 163, 301-313.

RAYL, J. E. (1965). Clinical reactions following bronchography. Ann. Otol. Rhin. Laryng. 74, 1120-1132.

REIFENRATH, R. (1973). Chemical analysis of the lung alveolar surfactant obtained by alveolar micropuncture. Resp. Physiol. 19, 35-46.

_____, and I. ZIMMERMANN. (1973a). Blood plasma contamination of lung alveolar surfactant obtained by various sampling techniques. Resp. Physiol. 18, 238-248.

_____, and I. ZIMMERMANN. (1973b). Surface tension properties of lung alveolar surfactant obtained by alveolar micropuncture. Resp. Physiol. 19, 369-393.

ROBINSON, A. E., K. D. HALL, K. N. YOKOYAMA and M. P. CAPP. (1971). Pediatric bronchography: The problem of segmental pulmonary loss of volume. I. A retrospective study of 165 pediatric bronchograms. Invest. Radiol. 6, 89-94.

_____, K. D. HALL, K. N. YOKOYAMA and M. P. CAPP. (1971). Pediatric bronchography: The problem of segmental pulmonary loss of volume. II. An experimental investigation of the mechanism and prevention of pulmonary collapse during bronchography under general anesthesia. Invest. Radiol. 6, 95-100.

ROUSER, G., G. KRITCHEVSKY, D. HELLER and E. LIEBER. (1963). Lipid composition of beef brain, beef liver, and the sea anemone: Two approaches to quantitative fractionation of complex lipid mixtures. J. Amer. Oil. Chem. Soc. 40, 425-454.

SCARPELLI, E. M. (1968). The surfactant system of the lung. (Lea + Febiger, Philadelphia).

_____, B. C. CLUTARIO and F. A. TAYLOR. (1967). Preliminary identification of the lung surfactant system. J. Appl. Physiol. 23, 880-886.

_____, and G. COLACICCO. (1970). Absence of lipoprotein in pulmonary surfactants. Advan. Exp. Med. Biol. 7, 275-286.

SLAMA, H., W. SCHOEDEL and E. HANSEN. (1973). Lung surfactant: film kinetics at the surface of an air bubble during prolonged oscillation of its volume. Resp. Physiol. 19, 233-243.

STEIM, J. M. (1969). Isolation and characterization of lung surfactant. Biochem. Biophys. Research Communications 34, no. 4, 434-440.

TOMICH, E. G., B. BASIL and B. DAVIS. (1953). The properties of n-propyl 3:5-di-iodo-4-pyridone-n-acetate (propyliodone). Brit. J. Pharmacol. 8, 166-170.

TOSHIMA, N. and T. AKINO. (1972a). Alveolar and tissue phospholipids of rat lung. Tohoku J. Exp. Med. 108, 253-263.

_____, T. AKINO and K. OHNO. (1972b). Turnover time of lecithin in lung tissue and alveolar wash of rat. Tohoku J. Exp. Med. 108, 265-277.

VON NEERGAARD, K. (1929). Neue Auffassungen über einen Grundbegriff der Atemmechanik. Zeitschrift fur die gesamte experimentelle Medizin 66, 373-394.

VILALLONGA, F. (1968). Surface chemistry of L-α-dipalmitoyl lecithin at the air-water interface. Biochim. Biophys. Acta 163, 290-300.

_____, M. FERNANDEZ, C. ROTUNNO and M. CEREIJIDO. (1969). The interactions of L-α-dipalmitoyl lecithin monolayers with Na^+, K^+ or Li^+, and its possible role in membrane phenomena. Biochim. Biophys. Acta 183, 98-109.

WEIBEL, E. R. (1970/1971). Morphometric estimation of pulmonary diffusion capacity. Resp. Physiol. 11, 54-75.